USGS
science for a changing world

Rock Geochemistry in the Tuscarora Mountains, Northern Carlin Trend, Nevada

By Ted G. Theodore[1], Boris B. Kotlyar[1], Donald A. Singer[1], Vladimir I. Berger[1], Barry C. Moring[1], and J. Kelly Cluer[2]

Open-File Report 00–402

2000

U.S. DEPARTMENT OF THE INTERIOR
U.S. GEOLOGICAL SURVEY

[1] U.S. Geological Survey, 345 Middlefield Road, Menlo Park, CA 94025–3561
[2] Cameco (U.S.) Inc., 5450 Riggins Court, Suite 6 Reno, NV 89502

TABLE OF CONTENTS

LIST OF TABLES

ILLUSTRATIONS

Rock Geochemistry in the Tuscarora Mountains, Northern Carlin Trend, Nevada

By

Ted G. Theodore, Boris B. Kotlyar, Donald A. Singer, Vladimir I. Berger, Barry C. Moring, and J. Kelly Cluer

INTRODUCTION

Geochemical study of 286 rock samples—the main focus of the present report—is designed primarily to answer three fundamental questions ensuing from a previous stream-sediment investigation in the Santa Renia Fields (SRF) and Beaver Peak (BP) quadrangles: (1) What is the regional variation in rock geochemistry across the Carlin trend of Au deposits? (2) What specific rocks provided the major metal sources for widespread base-metal anomalies in stream sediments near the southeast corner of the BP quadrangle (Theodore and others, 1999, 2000)? (3) What is the geochemical signature of northeast-striking faults that parallel similar trending metallotects in the region? As a corollary to question (1), we further attempt to determine whether lithogeochemical signature(s) of the Carlin trend, if present, could be detected by means of a relatively widespread rock-sampling program. This overall geologic and geochemical investigation in the Tuscarora Mountains is directly supportive of ongoing regional geochemical studies in the Humboldt River Drainage Basin Project of the U.S. Geological Survey, also currently (2000) underway, as well the Mineral Resource Surveys Project of the USGS. Analytical data of 286 rock samples, as well as their geologic and geochemical implication, are included in this report.

Geochemical study of rocks reported herein was undertaken in the Tuscarora Mountains, Nev., in association with on-going geologic investigations by private industry and by the U.S. Geological Survey (USGS). This geochemical research is a natural outgrowth of recently completed stream-sediment studies by the USGS (Theodore and others, 1999, 2000). The stream-sediment studies were designed, on the one hand, to aid in evaluation and (or) recognition of subtle district-scale patterns in metal-distribution haloes that surround major loci of Carlin-type Au–mineralized rock. On the other hand, the stream-sediment studies were not intended to form the basis of an expansion of grass-roots exploration activities in this part of the Carlin trend. However, stream-sediment sampling is an old methodology that many now consider to have limited usefulness in a mature mining district. Nonetheless, stream-sediment sampling provides an appropriate and efficient technique for detecting elemental signatures of various types of deposits, and such sampling recently has enjoyed a comeback of sorts. This was demonstrated fully by Tingley and Castor (1999) who investigated a large area in southern Nevada that had been withdrawn from mineral entry for more than 50 years. Moreover, the number of National Uranium Resource Evaluation (NURE) stream-sediment sample sites (Hoffman and Buttleman, 1994) in the Humboldt River drainage basin near the north end of the Carlin trend of Au deposits—specifically in the SRF and BP 7–1/2 minute quadrangles (fig. 1)—clearly is deficient for adequate regional syntheses (Kotlyar and others, 1998). Partly to rectify this deficiency, approximately 440 additional stream-sediment samples were collected and analyzed from the SRF and BP quadrangles (Theodore and others, 1999, 2000). At roughly the same time, 78 rock samples were collected by Cameco (U.S.) Ltd. in the western part of the BP quadrangle as part of a regional evaluation program. Subsequently, another 208 rock samples were collected by the USGS for geochemical studies as site-specific followups of the previously completed stream-sediment-sampling program by the USGS.

GEOLOGIC FRAMEWORK OF THE SANTA RENIA FIELDS AND BEAVER PEAK QUADRANGLES

Recent geologic investigations in the SRF and BP quadrangles (fig. 2) have established the presence of a remarkably intact lower Paleozoic stratigraphic sequence of siliceous rocks in the upper plate of the Roberts Mountains thrust (RMT) (Theodore and others, 1998; Theodore, 1999; Theodore and others, 2000). The RMT was emplaced during the middle and late Paleozoic Antler orogeny (see also, Roberts and others, 1958; Saucier, 1997; Cluer, 1999). Prior to the above-listed investigations in the Tuscarora Mountains, the Antler orogeny was envisaged as having been completed by the Late Pennsylvanian (Roberts, 1964). The lower plate of the RMT crops out in the general area of the Capstone-Bootstrap and Tara Au mines as well as in and near the open pit of the Dee Mine (fig. 2). As pointed out by Saucier (1997), the largely carbonate rocks of the lower plate of the RMT regionally are cut in a number of places by thrust faults and also folded probably during the Antler orogeny thereby indicating that some lower plate rocks are themselves allochthonous. The siliceous stratigraphic sequence in the upper plate of the RMT in the area includes Upper Ordovician Vinini Formation of Merriam and Anderson (1942; see also, Finney and Perry, 1991), Silurian and Devonian Elder Sandstone of Gilluly and Gates (1965), and Devonian Slaven Chert of Gilluly and Gates (1965). Uppermost strata of the Elder Sandstone regionally are as young as early Early Devonian (Paula Noble, oral commun., 2000).

The Vinini Formation, Elder Sandstone, and Slaven Chert all are well exposed south of Beaver Peak where stratigraphic relations among the formations have been revealed by sharply incised deep canyons (fig. 2). As mapped in this part of the Tuscarora Mountains, strata of the three formations are remarkably devoid of altered basaltic rock (greenstone), a fact previously noted as well by Dubé (1987, 1988) in the Lake Mountain area of the Roberts Mountains allochthon. The Lake Mountain area is located approximately 10 km northeast of Beaver Peak. In the SRF and BP quadrangle, the three formations (1) generally dip homoclinally at shallow angles to the north, (2) apparently are in depositional contact with one another in many places, and (3) are structurally overlain by a Devonian chert mélange unit along the Little Jack thrust—a widespread intraformational fault (fig. 2). The Elder Sandstone at its base locally contains discontinuous, approximately 10–m-thick sequences of well-bedded knobby black and blue-green chert that probably are correlative with the Cherry Spring chert unit of Noble and others (1997), a unit exposed in the Adobe Range, approximately 50 km to the east (fig. 1). The Cherry Spring unit also forms the basal unit of the Elder Sandstone in the area and is well exposed in several places near the southeast corner of the area as well as southeast of the Dee Mine (fig. 2). South of Beaver Peak, these three formations comprise the lowest structural package of rocks exposed in the upper plate of the RMT.

All of these rocks are overlain structurally by a widespread Devonian sedimentologic and tectonic chert mélange unit in the upper plate of the Little Jack thrust (fig. 2). We are not using the term "mélange" to infer a body of rock that is tectonically disrupted as result of a consuming plate boundary as it commonly had been applied in the past (for example, see Hsü (1983) and Fox (1983), as well as many others). Rather, the term "mélange" is applied here in a descriptive sense as suggested by Raymond (1984)—

> "a body of rock mappable at a scale of 1:24,000 or smaller and characterized by both the lack of internal continuity of contacts or strata and by the inclusion of fragments and blocks of all sizes, both exotic and native, embedded in a fragmented matrix of finer-grained material."

The critical criterion diagnostic of the unit is (1) its lack of continuity of geologic contacts, and (2) bedding that commonly cannot be traced entirely through even a single exposure. Further, presence of exotic blocks in the unit cannot be demonstrated, although Raymond (1984) questioned whether presence of exotic blocks should constitute a defining criterion for his usage of the term "mélange." Typically, chert fragments of various sizes are cemented by similar appearing chert throughout the chert mélange unit yielding thereby a mottled, highly disrupted appearance to most outcrops. From a regional perspective, the chert mélange unit occupies roughly the same structural position as (1) an olistostromal unit above Devonian Scott Canyon Formation in the Battle Mountain Mining District, approximately 80 km to the southwest (Doebrich, 1994); and (2) a Late Devonian chert-breccia and barite-breccia unit stratigraphically high in the sequence of the Slaven Chert in the Shoshone Range, approximately 50 km to the southwest (C.T. Wrucke, oral commun., 1999) (fig. 1). On the basis of these regional relations and the presence of Late Devonian conodonts in the unit where it crops out in the SRF quadrangle (Theodore and others, 1998) as well as Devonian radiolaria in the BP quadrangle, the chert mélange unit also is assigned to the Slaven Chert. The chert mélange unit is interpreted to have originated as submarine sedimentary slide breccia in a basinal environment during onset of middle Paleozoic tectonism associated with initial emplacement of the Roberts Mountains allochthon. The unit subsequently also was deformed probably during the Mississippian and Pennsylvanian Periods as the Antler orogeny continued well into late Paleozoic (Permian) by reactivation of the allochthon (see below). Although this Devonian package of rocks is apparently quite thick, siliceous rocks of the Devonian Scott Canyon Formation—lowest rocks structurally in the upper plate of the RMT in the Battle Mountain Mining District (fig. 1)—are as much as 1,500 m thick (Theodore and Roberts, 1971). The upper plate rocks in that district have been inferred to have a structural thickness of approximately 6,000 m (Madrid, 1987).

The chert mélange unit, as well as the Little Jack thrust along which chert mélange was thrust into the area, crop out widely across a broad expanse that encompasses approximately two thirds of the area of exposure of lower Paleozoic rocks (fig. 2). The Little Jack thrust probably is a late Paleozoic contractional structure of relatively minor offset—most likely less than 10 km—because it places Late Devonian chert mélange of the Slaven Chert on less-deformed sequences of well-bedded chert also belonging to the Slaven as described above. In addition, rocks in the upper plate of the Little Jack thrust locally also override rocks of the Upper Pennsylvanian and Lower Permian Strathearn Formation of Dott (1955). The Little Jack thrust apparently forms the floor thrust to a late Paleozoic duplex or imbricate thrust with the roof thrust being the Coyote thrust (Cluer and others, 1997), which crops out widely across the SRF quadrangle (fig. 2).

All these rocks are overlain unconformably in numerous places by a variety of rocks belonging to the Strathearn Formation, which comprises the overlap assemblage of the Antler orogen in the area. In some places, basal strata of the Strathearn Formation—commonly chert-pebble conglomerate—are Late Pennsylvanian in age, whereas in other places the Strathearn displays basal dolomitic siltstone strata that may be as young as middle Early Permian. However, prominent sequences of chert- and quartzarenite-pebble conglomerate also form the stratigraphic highest outcrops in the stratigraphic succession of the Strathearn Formation. The chert- and quartzarenite-pebble conglomerate are well exposed on the high ridge approximately 3 km southwest of Beaver Peak. The regional extent of the Strathearn recently has been broadened into the area from its type section in Carlin Canyon approximately 20 km to the southeast (fig. 1). In addition, the Strathearn Formation also crops out extensively in the Snake Mountains approximately 100 km to the northeast where its undeformed basal strata rest unconformably on deformed sequences of rock in the upper plate of the RMT (McFarlane, 1997). The Strathearn Formation includes biofacies indicative of a normal marine depositional setting throughout its best-exposed stratigraphic sequences on the western slopes of Beaver Peak (fig. 2). The Strathearn Formation is roughly age equivalent to the Pennsylvanian and Permian Antler Peak Limestone, middle unit of the overlap assemblage present in the classic Antler orogenic relations at Battle Mountain (fig. 1) described by Roberts (1964). Dubé (1987) previously assigned similar rocks in the nearby Lake Mountain area to the Pennsylvanian and Permian Antler Peak Limestone.

Conglomeratic strata of the lower Strathearn Formation have been overridden widely along the Coyote thrust system by a thick, sedimentary-rock unit dominated by quartzarenite of the Vinini Formation—this latter package of rocks makes up the upper plate of the Coyote thrust (fig. 2). Previously, the quartzarenite unit, as well as chert-pebble conglomerate, was referred to informally as the Boulder Creek quartzite by Schull (1991). Basal beds of the allochthon are predominantly quartzarenite of the Vinini Formation and they crop out across broad areas in the BP quadrangle where the basal quartzarenite unit may be as much as 800 m thick on the basis of estimates of stratal thicknesses in cross sections through the area. Ordovician quartzarenite in the upper plate of the Coyote thrust in the BP quadrangle probably is roughly equivalent to quartzarenite in the upper unit of the Vinini Formation in the Roberts Mountains (Finney and Perry, 1991). However, quartzarenite in the upper plate of the Coyote thrust apparently belongs to graptolite Zone 11 of Berry (1960) whereas quartzarenite of the upper unit of the Vinini in the Roberts Mountains belongs to Zone 13. Quartzarenite crops out throughout the northern one-third of the BP quadrangle, where it holds up many high ridges, and across approximately the northernmost quarter of the SRF quadrangle. Although quartzarenite of the upper plate of the Coyote thrust is approximately 800 m thick northwest of Beaver Peak, it thins to as little as approximately 50 m to the west-northwest across the area. Ordovician quartzarenite also is present above Late Devonian rocks near Beaver Creek, approximately 5 km northeast of Beaver Peak (Dubé, 1987).

Jurassic (?) dikes are present in two localities southeast of the Boulder Creek fault and a number of similar dikes crop out in the general area of the Dee, Rossi, and Ren Mines (fig. 2). The two poorly exposed dikes southeast of the Boulder Creek fault intrude conglomeratic strata of the lower Strathearn Formation. These intensely altered alkali granite and monzonite dikes contain narrow seams of yellow limonite (jarosite?)±Fe–oxide mineral(s) as well as relatively abundant white mica. Many variably altered dikes in the general area of the Rossi, Dee, Queen, and Tara Mines show fabrics indicative of their emplacement as spessartite lamprophyres. All of these dikes presumably post date the previously described thrust faults.

Tertiary rocks and Tertiary and Quaternary unconsolidated deposits are present mostly in the SRF quadrangle (fig. 2). Miocene rhyolite flows that are approximately 15 Ma crop out in a 16–km^2 area near the west-central border of the SRF quadrangle—small bodies of intrusive rhyolite also intrude some of the flows west of Antelope Creek. Tertiary intrusive dikes apparently also are present in the Meikle Au deposit because they have petrographic similarities to a biotite-feldspar porphyry dike (39.3 Ma, Hofstra and others, 1999) in the Betze Au deposit (Poul Emsbo, oral commun., 1999). The Miocene Carlin Formation of Regnier (1960), moreover, crops out widely in the western part of the area, from which air-fall tuff yielded 14.4– to about 15.0–Ma ages by the Ar–Ar method (Fleck and others, 1998).

The geometry and structural relations of faults in the quadrangles have been used to unravel the age of regionally extensive geologic structures and events. The fault surfaces that comprise the Coyote thrust system generally strike east-west and dip at shallow angles to the north throughout the area (fig. 2). This thrust system probably is correlative with the Lander thrust in the Shoshone Range (fig. 1). The inferred roughly east-west strike of the Coyote thrust system the SRF and BP quadrangles appears to parellel generally the east-northeast trend of the Proterozoic continental margin which is inferred from relations farther to the north (S. Ludington, written commun., 2000; see also, Theodore, 2000, fig. 5). The basal or master surface of the Coyote thrust is inferred to bend northeast around the northwest flank of Beaver Peak (fig. 2).

The Little Jack thrust probably is an imbricate structure slightly older and structurally lower than the Coyote thrust—much of the fabric in the mélange unit of the Slaven Chert is tectonic, but an early fabric that resulted from soft sediment deformation may also be present. Some sedimentologic breccia in the mélange, composed of fragments of chert set in a matrix of similar-appearing chert, probably also owes its origins to early contractional tectonism of the Antler orogen during the Late Devonian. Much of the tectonic strain in upper parts of the underlying well-bedded unit of the Slaven Chert is confined to dark, pyrobitumin-rich sequences. Early Permian strata of the Strathearn Formation unequivocally onlap Ordovician quartzarenite in the upper plate of the Coyote thrust—they as well lap across the leading edge of the Coyote thrust where it crops out southwest of Beaver Peak (fig. 2). These relations constrain emplacement of the upper plate of the Coyote thrust to a relatively narrow time interval between late Virgilian (Late Pennsylvanian) to latest Sakmarian-earliest Artinskian (middle Early Permian) (Theodore and others, 1998). We envisage that various parts of the Strathearn also were involved structurally with a nearby belt of lower Paleozoic rocks that were advancing towards the southeast (present day coordinates) in a largely shallow marine environment. Thus, the lower Paleozoic rocks, in places, overrode their own detritus.

Regionally, shortening in the SRF and BP quadrangles suggests late Paleozoic reactivation of rocks previously emplaced along the RMT, because the shortening involved rocks of the

Strathearn Formation. We envision this tectonism as probably marking the final Humboldt phase (see also, Ketner, 1977) of the Antler orogeny whose onset has been well documented elsewhere as having occurred during Late Devonian and Early Mississippian (Roberts and others, 1958; Roberts, 1964). We suggest that the late Paleozoic thrust faults in the area most likely represent the culmination of protracted, episodic Antler-age shortening and uplift that spanned a time interval of approximately 100 m.y. from Late Devonian to Early Permian (see also, Saucier, 1997; Cluer, 1999). Previously, Burchfiel and Davis (1972) suggested an episodic eastward subduction of oceanic crust during the Antler orogeny. As described above, the Coyote thrust may be correlative with the Lander thrust in the Shoshone Range. Somewhat farther to the west in the Edna Mountains (fig. 1), Erickson and Marsh (1974) documented well the presence of deformation of Late Pennsylvanian or Early Permian age. Folded strata involving the Middle Pennsylvanian Battle Formation, the Late Pennsylvanian Highway Limestone, and the Pennsylvanian and Permian Antler Peak Limestone make up the upper plate of the Iron Point thrust (Erickson and Marsh, 1974). This deformation must have occurred prior to deposition of the Middle and (or) Late Permian Edna Mountain Formation. Elsewhere during the late Paleozoic, protracted shortening and uplift were marked by multiple unconformities of regional extent suggesting active tectonism throughout this period of time (Snyder and others, 2000).

Associated temporally with late Paleozoic thrusting in this part of the Tuscarora Mountains is transcurrent sinistral shear along several prominent northeast-striking, high-angle faults in the quadrangles—the Boulder Creek and Toro faults, as well as the Rossi fault system (fig. 2). These northeast-striking faults are major fault strands that form an integral part of the 90–km-long Crescent Valley-Independence lineament of Peters (1998, 2000; see also, Theodore and Peters, 1998). The northeast-striking faults provided the most important Au conduits in the Independence Mining District (Dewitt, 1999) and at The Bobs Flat quadrangle (Peters, 1998) (fig. 1). The pattern of faults in the area of the SRF and BP quadrangles has been reproduced below as a geologic frame of reference for geochemical plots of rock data reported herein that also utilize plots of some stream-sediment data from Theodore and others (1999, 2000) as a geochemical backdrop.

The western part of the area, the SRF quadrangle, includes a number of major sediment-hosted Au deposits that define the currently (2000) known northwest terminus of the Carlin trend of Au deposits (fig. 2; see also, Teal and Jackson, 1997). The Au deposits in the area include the Meikle, Banshee, Ren, Tara, Capstone-Bootstrap, Dee, and Rossi-Storm. Although farther to the southeast the alignment of Au deposits along the trend is decidedly northwest-southeast, in the SRF quadrangle the Au deposits assume a northerly trend possibly reflecting premineral structural control by a deep-seated oroclinal bend associated with late Paleozoic sinistral shear along the northeast-striking faults. A number of Paleozoic bedded-barite deposits and minor occurrences of barite also are present in the area, including the Rossi, Queen Lode, and Coyote deposits (Papke, 1984; see above). Several Au deposits and barite deposits were in production in 2000. The geology and geochemistry of the Coyote barite deposit are discussed in detail below.

SAMPLING PROCEDURES

Standard procedures were used to collect rock samples for geochemical study (Rose and others, 1979; see also, Peters, 1978; Evans, 1995). Commercially available hand-held global positioning system (GPS) instruments determined longitude and latitude, and locations were estimated, as well, by visual inspection on 1:24,000–scale topographic maps and subsequently digitized. A minimum of four satellites was used for the GPS determinations. One sample was collected from each of the 270 locations shown separately on figure 2 with the exception of two sites. At those two sites, two samples were collected. An added 14 samples were collected within the open pit of the Coyote barite deposit (fig. 2). Sampling of rocks for geochemistry involved collection of representative composite chip samples weighing as much as 3 kg from areas of outcrop approximately 10 m wide. Attempts generally were made at each sample site to collect rock chips at the corners as well as at the center of approximately 10–m-wide squares. However, because of irregular distribution of many areas of outcrop, we could not always adhere strictly to such a sampling scheme.

Our rock-sampling program comprises three groups of samples. Of the 286 rock samples collected (fig. 2), 115 (Group 1) are along an approximately east-west traverse across the entire area (table 1), 93 (Group 2) are located near the southeast corner of the area (table 2), and 78 (Group 3) were collected near the west-central part of the BP quadrangle in the Boulder Creek area (table 4) (fig. 2). The 14 rocks analyzed from the open pit at the Coyote barite deposit are included with Group 2 (sample nos. 99TT118–128, 99TT189–191, table 2). Although 78 samples comprise Group 3, a complete spectrum of analyses was not performed on all of these samples and this group of samples was treated separately from the others (see below).

ANALYTICAL PROCEDURES

Rock samples from the east-west traverse and from near the southeast corner of the area (tables 1 and 2) were submitted in several batches for sample preparation to Minerals Exploration & Environmental Geochemistry, Reno, Nev., during the course of the field investigations. All rock-chip samples obtained from these areas were crushed and pulverized following standard procedures. A two-step crushing operation was followed wherein a jaw crusher first was used to reduce the rock-chip samples to less than one-quarter-inch diameters and the resulting material then was crushed further using a Bico Badger flat plate (Shea C. Smith, oral commun., 2000). Roughly 50–60 volume percent of the original material, generally 200 g, achieved a size reduction to –10 mesh (approximately 2 mm opening) which was finally pulverized to –150 mesh (1.05 µm opening) and split into two aliquots at the laboratories of Minerals Exploration & Environmental Geochemistry. The prepared aliquots were sent to two commercial analytical laboratories (see below), where an adequate number of internal standards, whose chemical compositions are well established, also were analyzed as part of the batch submittals. Samples from the Boulder Creek area (Group 3) were collected separately from the above-described sampling program, but generally followed the same sampling and preparation procedures (table 3).

Samples from the east-west traverse (Group 1) and from the southeast corner of the area (Group 2) were analyzed using the same laboratories (tables 1 and 2). The predominantly Fe– and Mn–oxide fraction from one aliquot of these two groups of samples was analyzed by U.S. Mineral Laboratories Inc. (USML), Auburn, Calif., by inductively-coupled plasmas, atomic emission spectroscopy (ICP–AES) methods after using mixed-acid partial digestion techniques involving hydrochloric acid and hydrogen peroxide whereby selective extraction of metals not bound in silicates could be obtained (see also, O'Leary and Viets (1986) and Church and others (1987) for a description of the method used to analyze the solubilized metals). For further review of selective extraction techniques see Çagatay (1984) and Hall (1998). Gold was analyzed by graphite furnace atomic adsorption methods (GFAA) by USML at detection levels of 2 parts per billion (ppb). This procedure yields low detection levels for many metals (Ag, As, Bi, Cd, Cu, Ga, Mo, Pb, Sb, Se, Te, Tl, and Zn) because of sparse interference by unwanted elements, particularly Fe. Thus, the concentration of metals in hydromorphic compounds and sulfide minerals is enhanced relative to minerals bound in silicates (Church and others, 1987). The preferred lower determination limits for these elements are shown in table 3. However, raw data for elements reported under column heading "Partial" in tables 1 and 2 include values less than the lower detection limit for some elements. In order to have a completely filled matrix among elemental analyses for the statistical calculations to be described below, values that are 50 percent of the lowest reported determinations were substituted for all elemental analyses reported as "less thans." Table 5 shows the number of analyses for each element for which such substitutions were made. We strongly emphasize, nevertheless, that variances corresponding to such extremely low elemental concentrations are quite high (W.B. Henderson, oral commun., 1999; see also below). These reported low concentrations are probably not reproducible to the number of significant figures reported. Nonetheless, the data provide additional low-level geochemical "noise"—either real or instrumental—over broad areas that one would expect to be present in a geologically complex region. None of the samples, however, from all three sample groups contain concentrations of elements higher than their respective upper limits of determination by the various analytical techniques employed.

A strong four-acid (HNO_3, $HClO_4$, HF, HCl) digestion that effectively dissolves most minerals—total digestion—was thereupon applied to a second 5-g aliquot that was obtained from samples collected from the east-west profile and from the southeast corner of the area (sample Groups 1 and 2, see above). These aliquots were submitted to Acme Analytical Laboratories Ltd., Vancouver, British Columbia, together with an adequate number of internal standards (elements reported under column heading "Total" in tables 1 and 2). For statistical calculations, values that are 50 percent of the lowest reported determinations were substituted for all analyses noted as "less thans" for the aliquots analyzed by total digestion methods (table 5). The dissolved material was analyzed for 35 elements by ICP–AES methods (see also, Crock and Lichte, 1982; Lichte and others, 1987; Motooka, 1988).

Samples collected from the Boulder Creek area in the west-central part of the BP quadrangle, 78 in all, make up Group 3, and they were analyzed for various numbers of elements (table 4). Seventy-eight samples were analyzed for 10 elements (Au, Ag, As, Sb, Hg, Cu, Pb, Zn, Mo, and Bi); 71 of the 78 samples also were analyzed for Te and Tl; and 30 of the 78 samples were analyzed for Ga, Se, and Cd. As with the preceding two groups of samples, values that are 50 percent of the lowest reported determinations also were substituted for all elemental analyses reported as "less thans" for the 78 samples that comprise Group 3 (table 5).

For the various plots described below and the accompanying discussion, raw analytical data of element concentrations in the three groups of rock samples first were log transformed. With trace-element geochemistry, small but important variation may be compressed into a relatively narrow range while other variation may be spread out over a range wider than their importance justifies (Masters, 1993). Another reason to transform the data is that tests of significance of correlation coefficients are not valid for skewed distributions. For these reasons, we have used a logarithmic (base 10) transformation on the data prior to all our subsequent statistical and graphical handling of the data. Selected Group 1 data plotted using results from partial versus total digestion techniques for the same element further demonstrate some lower-limit-of-detection problems (fig. 3). Because of high detection levels, no concentrations were detected by total digestion for some elements as exemplified by plots of Bi and Au (fig. 3*A*, *D*). Thus, analytical results by the total digestion method for eight elements (Au, U, Ag, Sb, Bi, W, Sn, and Be) only are discussed incidentally in the calculations and (or) comparative plots presented below. Because all of an element measured by the partial extraction method should also be included in the total extraction of that element, there should be a positive correlation between the measurements by the two methods for most elements. Exceptions would be elements that are almost exclusively bound to silicate structures. Tests of the correlations and associated regressions are shown in figure 3. Samples reported at the lower limit of detection were excluded from the calculations.

Some comparative plots show an excellent correspondence in elemental concentrations reported by the two methods, particularly Zn, Cu, and Mo which have coefficients of determination (R^2) respectively equal to 0.95, 0.95, and 0.86 (fig. 3*G*, *I*, *J*). At the other extreme, the coefficient of determination for Sb (fig. 3*B*) is not significantly different from zero. The presence of only three distinct values of Sb reported by the total digestion method suggests that not too much weight should be placed on these results. Comparative plots of As (fig. 3*E*), Cd (fig. 3*C*), Ag (fig. 3*F*), and Pb (fig. 3*H*), demonstrate significant correlations—but in each case the correlations drop to near zero as the lower limit of detection is approached. This means that at least one of the two methods is producing meaningless numbers near the lower limit of detection. In other words, the lower limit of detection for these elements is really higher than stated for at least one of the methods. It is not possible from these data to determine which method has the problem.

ELEMENT DISTRIBUTIONS FOR GROUPS 1 AND 2 COMBINED

Frequency distributions and box plots of elements aggregated from Groups 1 and 2 show significant variability of metal concentrations in the area. Such variability results from two major influences: (1) syngenetic variables among major rock units in the area, and (2) superposition of epigenetic overprints onto the rock units together with their accompanying geochemical signatures (fig. 4). Because samples that comprise Group 3 were not analyzed for as many elements as the other two groups, analytical data from it have not been combined with that from Groups 1 and 2 for this part of the study. All manipulations of data were done after log transformation of the respective raw data—the latter including numerical values substituted for indeterminate results as described above. A fixed 20–class interval was used for all histograms. We first discuss the results of histograms showing elemental distributions in a data set combined from Group 1 (table 1) and Group 2 (table 2). However, we emphasize that the reported distributions are the result of a combination of disparate metal concentrations in a number of widely diverse geologic environments that range from lower Paleozoic deep sea basins (represented by Ordovician Vinini Formation and Devonian Slaven Chert) to middle Tertiary lake beds that have incorporated significant stratal thicknesses of air-fall tuff (Miocene Carlin Formation). Contributions to overall metal distributions from each geologic environment will be examined in detail below in sections that follow.

Frequency distributions for all elements analyzed in the combined Group 1 and Group 2 data set do not extend beyond any respective upper limits of determination (fig. 4). However, the number of analyses below detection limits for each element by both partial and total digestion methods is listed in table 5. For some elements (for example U, Au, and Bi by total digestion), almost all of the 208 analyses that comprise Groups 1 and 2 report concentrations below detection. The number of analyses for Au by the GFAA method that are below detection—28 of 208 analyses (approximately 13 percent)—is higher than any of the 14 metals analyzed by partial digestion methods.

After log transformation, histograms for almost all elements are unimodal (fig. 4). Some elements (for example, Ag, Cd, and Zn by partial digestion) show distributions that must extend well below their lower detection limits. Nonetheless, a surprising number of elements have symmetrical distributions that approach lognormal distributions, particularly among those elements that have been analyzed by partial digestion. In addition, Bi, Cd, and Zn (partial) appear to have distributions that are slightly skewed positively, whereas Ga and Se (partial) are slightly skewed negatively. Among all 35 elements analyzed by total digestion methods, Zn, Ag, Ni, Co, Mn, Sr, Ca, La, Mg, and Na appear to have slightly positive skewed distributions (fig. 4). Certainly, not all distributions result from some type of superposed effect of mineralization. In fact, the positive skewed distributions for some rock-forming elements (for example, Mn, Sr, Ca, and Mg) simply result from inclusion in the data of small numbers of carbonate-rich rocks of the Strathearn Formation. This relation is in contrast to predominantly siliceous rocks in the remainder of the data.

Examination of the combined data by linear regression and correlation reveals that Au has a weakly positive association with all 14 elements (Ag, As, Bi, Cu, Ga, Hg, Mo, Pb, Sb, Se, Te, and Zn) analyzed by partial digestion (fig. 5). However, all of these positive associations are quite weak. Gold has the highest values of R^2 (coefficient of determination) with Ag and Sb, respectively 0.27 and 0.22 (fig. 5*A*, *J*). Initially, these metal associations do not appear surprising because of the well-established relationship among the three elements in many Au deposits along the Carlin trend. The numerical values determined suggest that approximately 27 and 22 percent respectively of the variability of Au in the dataset could be accounted for by the variation of Ag and Sb contents of the rocks. The association between Au and As in the combined dataset also is extremely weak ($R^2 = 0.079$, fig. 5*B*). Despite such a low value, one cannot assume an unimportant relationship between Au and As in the area. Arsenic concentrations in stream sediments from the area are, in part, elevated in the general area of the Carlin trend (Theodore and others, 1999, 2000). As we discuss below, the distribution and associations of As with mineralized rock are important and were quickly established by our sampling irrespective of the apparently low contents of As in the mineralized halo surrounding the Carlin trend. The relative contributions of various rock types that make up the database that have been composited from sample Groups 1 and 2 now will be examined individually in somewhat more detail.

ELEMENT DISTRIBUTIONS FOR GROUPS 1 AND 2 INDIVIDUALLY

For comparative purposes, lognormal frequency distributions also were prepared separately for sample Groups 1 and 2 (figs. 6 and 7). Group 1 data (115 samples) represent rocks from all formations that crop out in the area, including significant numbers of samples from the quartzarenite unit of the Ordovician Vinini Formation, a small number of samples from the Pennsylvanian and Permian Strathearn Formation, and a significant number of samples from the Miocene Carlin Formation (table 1). Group 2 data (93 samples) represent only rocks from the chert and shale unit of the Vinini Formation, the mostly siltstone Silurian and Devonian Elder Sandstone, and mostly chert and chert mélange of the Devonian Slaven Chert—all from the southeast part of the BP quadrangle (table 2). Many samples included within Group 2 are from the immediate area of the Coyote barite mine and 14 samples are from the mine itself. This tract also is part of an area that has exceptionally high base-metal contents in the stream sediments (fig. 8*D*, *E*; see also, Theodore and others, 1999, 2000). As a result, major contrasts are present in histograms of some elements when Groups 1 and 2 are compared. Among the minor elements, As, Bi, Cd (partial and total), Cu (partial), Mo, Tl, Zn, Fe, Cr, Zr, and Y show significant shifts of their modes to higher values (compare figs. 6 and 7). Surprisingly, Ba histograms in the two datasets do not differ substantially. The 14 samples from the Coyote Mine, however, have a range in compositions from 231 to 7,766 ppm Ba and an average Ba content of approximately 2,200 ppm (table 2). This value is about twice the median value for Ba in the Group 1 dataset. More will be discussed below about analytical data and areal distributions of elements surrounding the Coyote barite mine.

RELATIONS AMONG ELEMENTS ALONG PROFILE AA' (GROUP 1)

Geochemical relations along the east-west traverse (Group 1 data; profile AA', fig. 2) are examined in this section by point plots, line plots, box plots, and corresponding statistics primarily to compare overall metal distributions in the rocks with stream sediments previously sampled from the area. In addition, a number of other geochemical factors are addressed including: (1) geochemical variability among the various Paleozoic units, as well as those that host stratiform base-metal accumulations elsewhere in the area; (2) epigenetically altered Paleozoic rocks near the Carlin Au trend; and (3) largely unconsolidated deposits of the Miocene Carlin Formation. Table 6 includes summary statistics of the analyses reported in table 1 whose "less than" values below detection have (1) been substituted by an appropriate value (see above), and (2) then been log transformed. All plots along the profile were prepared using the substituted and log-transformed database.

Point plots of rock geochemical data (Ag, As, Au, Cu, and Zn, all by partial digestion) along the traverse indicate a strong correspondence between presence of As in stream sediments (Theodore and others, 1999) and As in rock in the general area of the Carlin trend of Au deposits (fig. 8). The presence of high As in stream sediments in the Dee segment of the Carlin trend has been confirmed by reoccupation and reanalysis of 16 sampling sites (T.G. Theodore and others, unpub. data, 2000). On the one hand, the highest value of As in the stream sediments near the Carlin trend is 54 ppm (Theodore and others, 1999). On the other hand, the highest content of As in the rocks sampled near the Carlin trend is about 90 ppm (sample no. 99–TT–82, table 1). Additional specifics concerning As contents, as well as many other elements in the general area of the Carlin trend, are included below in discussion of plots of elements along profile AA'. Point plots of As in rock farther to the east along profile AA' commonly are at background levels in those areas where the stream-sediment data also indicate low normalized levels of As (fig. 8). Unfortunately, much of the eastern third of the geochemical traverse is in an area where the stream-sediment data were not contoured because of the presence of expansive topographically high ridges. Of the remaining comparative plots showing superposed stream-sediment and rock data for Ag, Au, Cu, and Zn, those for Cu and Zn (fig. 8*D*, *E*) appear to confirm presence of elevated concentrations of these elements in rock near the Carlin trend. Weak halos of Cu and Zn in this general area were alluded to on the basis of the stream-sediment data alone (Theodore and others, 1999). Despite several of the Au deposits near the northern end of the Carlin trend in the SRF quadrangle being characterized by unusually high Ag:Au ratios, Ag does not appear to provide a useful pathfinder element for these deposits (fig. 8*A*). On the basis of these plots, we suggest that As distribution maps of both rock data and stream-sediment data provide the best pathfinders to mineralized haloes surrounding Carlin-type deposits. From our stream-sediment (Theodore and others, 1999) and rock data, the breadth of the As halo surrounding the Carlin trend appears to be approximately 4 km in this area (fig. 8*B*). Radtke and others (1972) reported that primary unoxidized Au ore hosted by the Silurian and Devonian Roberts Mountains Formation at the Carlin Au deposit contains, on average, 480 ppm As—an approximate 50–fold increase over local background. In addition, Albino (1994) found that haloes of As and Hg extend 80 m beyond Au–mineralized rock that is between 380 and 500 m below the surface at the Ren deposit (fig. 2). However, anomalous concentrations of Au are more widespread than the As and Hg haloes at Ren. At the Meikle deposit (fig. 2), Emsbo and others (1997) note a strong down-hole association of the Carlin-suite of elements (As, Hg, Sb, Ag, Tl, Te, and W) with Au. Bettles and Lauha (2000) report that composited assay contents of mineralized rock from the Betze/Post Au deposit have the following ranges: 0.23–0.33 oz Au/t, 336–850 ppm As, 12–114 ppm Sb, and 0.34–6.7 ppm Hg.

Concentrations of Ag, As, Cu, Hg, Pb, Sb, and Zn in partially digested rock from the Carlin trend apparently all show variably developed local anomaly contrasts with adjoining Paleozoic bedrock along profile AA' (fig. 9). Near the profile, mineralized fractures comprise the halo and extend to depths of about 1,000 m where significant mineralized rock is present (fig. 9). Unaltered, well-bedded chert of the Devonian Slaven Chert crops out extensively near the intersection of the Carlin trend with profile AA'. The intersection is present west of a gap in sampling sites along the profile because of presence of the fanglomerate unit of the Carlin Formation as well as other unconsolidated Quaternary deposits (fig. 2). Abundance of As in the air-fall tuff unit of the Miocene Carlin Formation near the west end of the profile shows an exceptionally well-developed progressive increase to about 30 ppm As as altered rock surrounding the Carlin trend is approached from the west (fig. 9*B*). This increase certainly implies that elevated abundance of As in the Carlin Formation owes its origins to immediately adjacent rock comprising the altered halo of the Carlin trend. Similar relations have been reported elsewhere along the Carlin trend. At the Gold Quarry and at the Betze/Post deposits, tuffaceous gravel of the Carlin Formation present in local grabens is enriched in Au by presence of of Au–bearing clastic material derived from exposed, nearby mineralized bedrock (J.B. Harlan and E. Lauha, oral communs., 2000). Some parts of the Carlin Formation also are silicified near these two deposits. The enrichments in Au locally achieve leach-grade concentrations.

Lead and Bi in the western part of the Carlin Formation along the profile show much higher concentrations—respectively > 10 ppm and approximately 0.3 ppm—than mineralized rocks from the adjoining Carlin trend (fig. 9*D*, *I*). Lead and Mn (see below) apparently have been introduced epigenetically into the Carlin Formation near the western end of the profile. More is discussed below about other abnormally high metal contents of the air-fall tuff unit of the Carlin Formation. Although several closely-spaced samples were collected along the profile near the low-temperature silica that locally is present in some unconsolidated deposits of the Carlin Formation (figs. 10 and 11), the only metal in silica-flooded samples that might be demonstrated by our analytical data to be present in concentrations elevated above local background is Se. Silica-flooded samples approach roughly 1 ppm Se (fig. 9*K*). It would be surprising if Hg also is not partly enriched in these silica-altered samples. However, the lower detection level for Hg by the analytical technique employed is a relatively high 0.1 ppm Hg (table 3). As described previously, low-temperature silica in this area includes cross fiber-textured chalcedonic quartz and opal as well as some adularia (fig. 12; Fleck and others, 1998). Examination by scanning electron microscope of a selected number of samples of the low-temperature silica indicates that well-formed adularia crystals, approximately 5–10 µm wide, are intimately intergrown with Mn–oxide minerals (fig. 13*A*). In addition, narrow, 2–µm-wide layers of barite mantle botryoidal-shaped low-temperature silica (fig. 13*B*).

Plots of abundances of 31 metals along profile AA' analyzed by total digestion methods also show a high number of metals that are especially elevated in the air-fall tuff unit of the Carlin Formation. The metals are elevated relative to the adjoining lower Paleozoic bedrock, including that bedrock forming part of the altered halo that surrounds the Au deposits in the northern part of the Carlin trend (figs. 14 and 15). Arsenic certainly is high in bedrock of the western part of the profile in the general area of the Carlin trend as well as in the adjoining Carlin Formation as we discussed above (fig. 14*J*). The metals that are elevated in the air-fall tuff unit include the following with the approximate value of their contents shown paranthetically : Co (7 ppm), Mn (500 ppm), Zn (80 ppm), Fe (2.5 weight percent), Th (10 ppm), Sr (200 ppm), Ca (> 1 weight percent), La (50 ppm), Mg (0.8 weight percent), Al (6 weight percent), Na (1 weight percent), K (2 weight percent), Zr (100 ppm), Y (20 ppm), Nb (20 ppm), Be (2.5 ppm), and Sc (6 ppm). Tin contents also are elevated ($\geq$ 2 ppm) for a number of samples analyzed from the Carlin Formation (fig. 15*P*). Most of the increased presence of these metals is directly attributable to the high magmatic content—exemplified by abundant alkali feldspar and abundant glass shards—throughout much of the unit (Fleck and others, 1998). As pointed out by Fleck and others (1998), comparative plots of Al_2O_3 versus SiO_2 contents of glass shards in the Carlin Formation suggest that the eruptive center(s) from which the tuffs in the formation were derived must be peralkaline. In addition, the alkali feldspars described by Fleck and others (1998) are either Na–rich sanidine or anorthoclase. Of the remaining metals, Ni also shows a progressive increase in the air-fall tuff unit near the west edge of the profile towards exposed altered bedrock surrounding the Au deposits (fig. 14*K*).

The abundance plots along profile AA' identify additional variations in metal concentrations among the various units in the area. Some contrasts in major rock-forming elements and their geochemically associated elements (for example Ca, Mg, Al, Sr, and K) result primarily from fundamental differences in depositional environments of the units. High Mg content in rock belonging to the Strathearn Formation reflects diagenetic conversion of many of these rocks to dolomite in a shallow near-shore, saline environment (Theodore and others, 1998). However, care must be exercised because many geochemical anomalies along the profile also result from introduction of some metals by epigenetic processes along mineralized faults near the eastern end of the profile. Silver, Cd and Zn contents are anomalous along a number of mineralized faults near Beaver Peak (figs. 14 and 15). Also, the chert and shale unit of the Ordovician Vinini Formation near the Carlin trend has higher contents of K, Al, Na, V, Ni, and Mg than the largely quartzarenite unit of the same formation that crops out near Beaver Peak (figs. 14, 15). Much of the contrast shown by these elements probably results from the higher amounts of clay minerals in the former rather than in the latter unit. The Devonian Slaven Chert, including the uniformly well-bedded chert and shale unit below the Little Jack thrust and the mélange unit above the thrust, have generally similar minor element geochemical signatures. However, La, V, and P appear to be slightly less abundant in the well-bedded unit than in the mélange unit (fig. 15). In addition, Al also appears to be less abundant in the well-bedded unit of the Slaven than in the mélange unit.

Box plots graphically illustrate major geochemical differences among the units encountered along the east-west geochemical profile (fig. 16). The box plots show graphically 10^{th}, 25^{th}, 50^{th} (median), 75^{th}, and 90^{th} percentiles of element distributions for eight classes or categories of rock that we delineated along the profile: Carlin Formation, dike rock, Elder Sandstone, Elder Sandstone (?), well-bedded Slaven Chert, mélange unit of the Slaven Chert, Strathearn Formation, and Vinini Formation. Analytical results either above the 90^{th} percentile or below the 10^{th} percentile are plotted as individual data points on the individual box plots. Two of the eight categories of rock—those reported as dike rock or Elder Sandstone (?)—include only one rock sample that was analyzed from its respective category. The analyzed sample reported as Elder Sandstone (?) probably represents some material from the Carlin Formation as will be discussed below. In addition, as we described above, two distinct varieties of rocks belonging to the Vinini Formation are present along the profile. Near the western end of the profile, the Vinini Formation includes mostly chert and shale, whereas near the east end of the profile, Vinini includes mostly quartzarenite (see also, fig. 2).

The most significant contrasts in element concentrations are conveyed by geochemistry of the Carlin Formation versus all Paleozoic formations in the area (fig. 16). Present-day metal concentrations in the Carlin Formation are derived from a wide variety of sources of different ages—unmineralized Paleozoic bedrock; mineralized Paleozoic bedrock; Miocene Craig rhyolite; post 14.4–Ma hydrothermal fluids that deposited chalcedony, opal, and adularia in the formation; and 15.1– to 14.4–Ma sanidine-rich air-fall tuff. These complexly mixed sources result in elevated concentrations for a number of elements. The elements elevated relative to adjoining Paleozoic bedrock include the following: Bi, Ga, Pb, Co, Mn, Fe, La, Ti, Tl, Al, Na, K, Zr, Y, Nb, and Sc. In addition, some elements such as Se, Mo, and Cr are much lower in the Carlin Formation than in the Paleozoic bedrock. Lead and Mn appear to have been introduced into the Carlin Formation near the western end of the profile together with low-temperature silica (see above). Further, from the box plots, the sample categorized as Elder? apparently has a geochemical signature that is much more closely allied with analyzed samples of the Carlin Formation than with the analyzed samples of certain Elder Sandstone (fig. 16). The single sample of altered igneous rock analyzed along the profile also has a significant geochemical contrast with the other rocks, exemplified by elevated As, Pb, Se, Tl, Zn, Ni, Co, Mn, Sr, V, P, La, Ba, Ti, Al, Na, K, Zr, and Sc (fig. 16). In fact, the Zr content of the dike is higher than any other sample analyzed along the profile (225 ppm Zr, sample no. 99-VB-13, table 1). However, one sample of igneous rock analyzed does not represent an adequate sample size for further discussion of comparative geochemistry.

GEOCHEMICAL DATA FROM SOUTHEAST PART OF AREA (GROUP 2)

Distribution of Metals in General Area of Coyote Barite Mine

The primary purpose of focusing our geochemical sampling on rocks in the southeast part of the area is to determine bedrock sources for the extremely high base- and precious-metal stream-sediment anomaly previously detected here (Theodore and others, 1999). This area of mostly high base metals is approximately 16 km^2. A total of 93 samples were analyzed in the present report (table 2) from the southeast part of the area (figs. 17 and 18). Fifty-eight samples are from the general area of the Coyote Mine, and 14 of the 58 are from within the outer pit perimeter at the mine. Collection of samples especially converged on the Coyote Mine because of extremely high Zn contents and other base metals in two stream drainages below the mine (fig. 8*E*) —one of these catchment basins includes the actual mine site (Theodore and others, 1999). The two stream-sediment samples, approximately 1 km east of the mine and at the bottom of steep catchment basins immediately to the east and topographically below the mine, contain approximately 5,000 and 1,200 ppm Zn. However, the latter stream-sediment sample represents a catchment basin that does not include the Coyote Mine itself—this specific catchment basin is adjacent, on the south, to the one hosting the Coyote Mine. The remaining 35 samples were collected near the south edge of the area in an ancillary effort to add to our understanding of background-metal distributions in the upper plate of the RMT, specifically where the Vinini Formation, Elder Sandstone, and Slaven Chert form a well-exposed, coherent stratigraphic package of rocks in the area. Surface distributions of 15 elements determined by partial digestion methods are shown in figure 17, and a selected number of elements analyzed by total digestion methods are shown in figure 18.

The rock sampling traverses near the Coyote Mine primarily were designed to test strata of the Devonian Slaven Chert stratigraphically and (or) structurally below the main barite horizons at the Coyote deposit. Of all rocks examined along the traverses, the following are, in order of probable declining importance, the most likely candidates to have contributed significantly to major base-metal stream-sediment anomalies in the catchment basins: (1) gossanous <3–m-wide sequences of lower Paleozoic stratiform-mineralized rock present in Slaven Chert at the Coyote barite deposit; (2) 20– to 30–m-wide, presumably minor, intensely brecciated Paleozoic thrust zones in Slaven Chert; (3) widespread mm–scale concentrations of stratiform sulfide minerals, mostly pyrite, along parting surfaces in rhythmically bedded chert of the Slaven Chert; and (4) contamination from dumps at the Coyote deposit (Theodore and others, 2000). In addition, some Fe–oxide-stained calcareous siltstone of the Silurian and Devonian Elder Sandstone, in fault slivers near the Coyote Mine, contains as much as 3,600 ppm Zn and 189 ppm Cd (sample no. 99-TT-175, table 2). Precious-metal contents are low in the 42 rocks sampled from the two catchment areas below the Coyote deposit—no more than 1.84 ppm Ag and 25 ppb Au. Although material derived from the dump at the Coyote deposit extends approximately 0.4 km downstream in the drainage immediately below the deposit, careful examination of stream bottoms upstream from the two stream-sediment sites that yielded the 5,000– and 1,200–ppm-Zn concentrations revealed no obvious presence of dump material.

Metal concentrations are generally low outside the open pit and distribution patterns for most elements, including Zn, do not show a strong preferred metal concentration by formation (fig. 17). Of the 14 elements analyzed by partial methods, Ag and Ga apparently show a weak preferred clustering of samples that contain respectively more than 1.0 and 1.6 ppm in the Elder Sandstone (fig. 17*A* and *G*). Thallium may have a slightly higher local background in the well-bedded chert unit of the Slaven Chert than the chert and shale unit of the Vinini Formation (fig. 17*N*). However, these high local background contents in the Slaven Chert unit outside the open pit of the Coyote Mine are in the range 0.32 to approximately 1.0 ppm Tl (table 2).

Distributions of seven elements (Ba, Sr, P, V, Cr, La, and Nb) in rock near the Coyote Mine analyzed by total digestion methods show a variety of relations with their surrounding geology and their respective enclosing formations (fig. 18). Barium shows a clustering of values higher than 2,500 ppm in a relatively broad, north-south belt of rocks in the immediate area of the Coyote Mine (fig. 18*A*). Such high Ba concentrations, when compared to geology of the Slaven Chert in this area, suggest a strong stratigraphic component to the elevated Ba contents because bedding attitudes of the Slaven commonly strike north-south. Chromium in some parts of the chert and shale unit of the Vinini Formation near the southeast corner of the area commonly is marked by widespread contents higher than 400 ppm as opposed to less than 400 ppm Cr in most of the immediately overlying Elder Sandstone and the well-bedded unit of the Slaven Chert (fig. 18*E*). Lanthanum and Nb commonly have concentrations respectively higher than 10 and 3.5 ppm in the Elder Sandstone (fig. 18*F*, *G*).

Distribution of Metals within the Coyote Barite Mine

The geology and locations of 14 rock samples analyzed from the Coyote barite mine, a Devonian bedded barite deposit (Papke, 1984), are shown on figures 19–22. Late Devonian, probably Famennian, radiolaria have been obtained from chert interbedded with massive barite at the Coyote barite mine (Dubé, 1988). The small open pit at the mine is located within NW 1/4 sec. 7, T. 36 N., R. 51 E. (unsurveyed), and originally was included in the Patsy Ann 1, 2, and 4 (located May 17, 1961) as well as the Unichem 1 and 2 lode claims. The underlying owner of the property at the time was The Milchem Co., and the operator was Unichem Minerals Inc., Oklahoma City, Oklahoma. Concentration of the ore was accomplished in Maggie Creek, approximately 15 km southeast of the mine. Mining operations were shut down in 1982 (D. McFarlane, oral commun., 2000). The mine also has been referred to as the Patsy Ann Mine in some informal company reports (D. McFarlane, oral commun., 2000). As noted by Papke (1984), between 1,000 and 25,000 tons barite were produced from the Coyote Mine in 1979–1980.

The complete analyses of the 14 samples analyzed from within the open cut at the mine are listed in table 2 (sample nos. 99–TT–118 to –128; 99–TT–189 to –191). Papke (1984) also noted high organic content of the barite-enclosing strata, pointing out that a sample analyzed from the Coyote Mine contained 6.1 weight percent organic C. Ten samples analyzed for the present report are representative chip samples collected from an intensely sheared black and dark gray chert and shale subunit of the well-bedded unit of the Devonian Slaven Chert.

Geology of the Coyote Mine is relatively straightforward. The strata exposed in the pit dip gently to the west, and they strike roughly due north. Tectonic shearing present in rocks throughout this part of the district reflects a culmination of a district-wide increase in overall intensity of penetrative both brittle and ductile styles of deformation up section towards the projection of the overlying sole of the Little Jack thrust. At one time, the Little Jack thrust probably passed within several hundred meters above the present mine site as evidenced by a nearby klippe made up of the mélange unit of the Slaven Chert in the upper plate of the Little Jack thrust. The klippe crops out roughly 500 m south of the mine (fig. 2). This late Paleozoic thrust is inferred to have overlain the Coyote Mine prior to being eroded back to its present trace. The most common rock in the Coyote Mine is black and dark gray chert, although some interbedded light gray chert and shale are well exposed near the northeast corner of the open cut (figs. 21 and 22). In addition, a number of west-dipping minor intraformational thrust faults related to the Little Jack thrust (fig. 2) crop out prominently in the Coyote Mine, particularly near the north end of the mine (fig. 22). Steeply dipping, presumably normal faults that have minor displacements, also crop out in the mine. The generally carbonaceous character of the sampled subunit also is indicated by the overall dark color of rocks in the pit (figs. 19 and 20). The only sulfide mineral reported by Papke (1984) at the Coyote barite deposit is pyrite, and examination by scanning electron microscope of a limited number of polished specimens of pyrite-bearing rock from this deposit failed to reveal the presence of sphalerite (Theodore and others, 2000).

The bedded barite remaining in the open pit—as of this writing (2000)—is outlined roughly on figure 19. Bedded barite exposed in the bottom of the pit has a stratigraphic thickness of approximately 2 m. In places, black highly carbonaceous, Fe–oxide-stained shale is healed tightly to underlying individual beds of brownish-gray well-layered barite. Although the underlying barite locally is schistose, probably as a result of strain associated with late Paleozoic shortening, much of the strain close to the barite horizon appears to have been concentrated immediately above the Fe–oxide-stained shale where a tectonic breccia and shaly phyllonite is exposed. The shaly phyllonite includes lenticular phacoids made up of red-brown Fe–oxide minerals and light lime-green weathering fragments of chert. Furthermore, prominent zones of gossan—various shades of red brown, dark brown, and reddish black, some as much as 2 m thick—are present in conformable relations with barite. This gossanous material is interpreted to mark the former presence of stratiform-mineralized horizons on the Devonian seafloor.

Four determinations of $\delta^{34}S$ relative to Cañon Diablo Troilite (CDT) in three samples of barite collected by Keith Papke (sample nos. 41–2–A, –B, –C, and –D) from the Coyote Mine have been determined: 19.3, 18.4, 40.9 and 50.0 (S.S. Howe, written commun., 1996). The variability in the isotopic values of these samples may result from periodic fluctuations in the "openness" of the isotopic system during diagenesis and not from an epigenetic overprint. The following in this paragraph has been modified from S.S. Howe (written commun., 2000). Hand-sample descriptions indicate that the type of barite sampled and analyzed isotopically for determinations 41–2–A and –B was somewhat different from that determined for 41–2–C and –D. The material comprises three separate pieces. The first piece is fine-grained to sugary textured, brownish medium-gray barite that contains porous ochre Fe–oxide mineral(s) and recrystallized(?) dark-gray barite in a pod to 2.1 cm long and 8 mm wide, as well as several irregular to subhedral (approximately cubic) masses of fine-grained, soft, powdery chocolate brown to charcoal gray, possibly mixed Fe–oxide and Mn–oxide minerals. The latter are mostly 0.5 mm to 1.0 cm wide. Minor ochre Fe–oxide staining is present on some outer surfaces. Isotopic determination "A" was drilled into a freshly broken edge or surface of brownish-gray barite away from Fe–oxide minerals on the surfaces. Clean up was accomplished using an ion-exchange procedure prior to isotopic analysis. The second piece is quite similar to first piece but with a smaller porous ochre Fe–oxide pod and only one dark mass that is harder than the Fe–oxide masses in the first piece—the dark mass actually may be a shale and (or) chert fragment rather than a mixed Fe–oxide and Mn–oxide fragment. Trace subhedral crystals of pyrite as much as 1 mm wide are locally surrounded by Fe–oxide-stained halos as much as 1 cm wide. Determination "B" drilled into a broken corner of the piece and clean up was accomplished using an ion-exchange procedure prior to isotopic analysis. The third and largest piece consists of coarse-grained, locally bladed, dark gray barite cut by coarsely crystalline white barite—possibly recrystallized—in locally vuggy veins as much as 6 mm thick. A few hairline fractures cutting both the dark gray barite and the white barite fizz with HCl, so the piece is likely to contain some calcite. In addition, a pale emerald green crust locally is associated with the white barite veins. Determination "C" drilled into freshly broken surface of dark gray barite. Clean up was accomplished by using an ion-exchange procedure prior to isotopic analysis. Determination "D" drilled into a white barite vein, at least 2 mm away from dark gray barite walls. The third sample probably was clean enough to burn as is for isotopic analysis, but nonetheless was cleaned up as the others prior to isotopic analysis.

As further noted by S.S. Howe (written commun., 2000), it is clear that bedded barite from the Coyote deposit is associated with variable amounts of syngenetic or diagenetic pyrite, and that this pyrite likely formed by bacterial reduction of seawater sulfate. In sytems closed with respect to sulfate, the rate of sulfate reduction exceeds sulfate supply so that all sulfate is eventually consumed. Initial sulfur isotopic values of the sulfate reflect that of Late Devonian seawater sulfate (+23 ± 2 per mil) but become progressively more enriched due to Rayleigh fractionation as the concentration of sulfate decreases. Examples of systems partially closed with respect to sulfate include sediments beneath the bioturbation zone under oxic seawater and sediments underlying the anoxic water column in euxinic basins (Ohmoto and Goldhaber, 1997). All barite formed from this sulfate would have a bulk isotopic composition similar to Late Devonian seawater sulfate, but some barite would have slightly more depleted isotopic compositions (+19 per mil, shown by 41–2–A and –B) while other barite would have considerably more enriched isotopic compositions (+40 to +50 per mil, shown by 41–2–C and –D), perhaps as high as +70 per mil. Variations in the degree of "openness" of a system lead to wide variations in sulfide and sulfate sulfur isotopic compositions (see also, Rye and others, 1978; Claypool and others, 1980; Goodfellow and Jonasson, 1984; Howe, 1988).

Analyses of select samples of gossanous material from the Coyote Mine indicate that it contains as much as 7,400 ppm Zn, 181 ppm Cu, 1,800 ppm Ni, 77 ppm Cd, 491 ppm Co, 67,000 ppm Mn, as well as roughly 5 ppm As and 20 ppm Mo (sample no. 99-TT-189, table 2; see also, fig. 19 for location of this sample). Another rock sample from minor workings just west of the northernmost pit perimeter contains approximately 1,200 ppm Zn and >10,000 ppm Mn (Roy Owen, oral commun., 2000). Dubé (1988) also noted the presence of Mn– and Fe–oxide-rich lenses of rock in association with bedded barite deposits in the Tuscarora Mountains. It is likely that at one time additional base-metal-rich zones cropped out in the general area of the Coyote deposit, but they have since been removed during mining operations to exploit the narrow barite horizons.

Foulk (1991) previously described 2.5– to 8–cm-thick, discontinuous beds of gossanous mudstone in his section A1 near the base of the Slaven Chert, approximately 400 m south of Hill 7521 near the southeast corner of the BP quadrangle. The gossanous mudstone is oxidized completely—approximately 20 volume percent of it is made up of Fe–oxide minerals that have, in large part, been derived from Fe–sulfide minerals. Further, the gossanous mudstone is conformable with enclosing chert and shale of the Slaven Chert and is interpreted by Foulk (1991) to represent synsedimentary exhalative horizons in the Devonian basin. Chemical analyses of seven samples of the gossanous mudstone showed them to contain approximately 1,200 ppm Zn, 11 ppm Cd, 200 ppm Ni, 66 ppm Cr, 200 ppm V, 4,300 ppm Mn, and 3,000 ppm P, as well as roughly 10 ppm As and 14 ppm Mo (Foulk, 1991).

Many elements in stream sediments previously were reported to be in significantly elevated concentrations across a broad area near the southeast corner of the BP quadrangle (Theodore and others, 1999). These elements include Zn, Cd, Mn, Ni, P, Sb, Te, and V. Analytical results of rock samples in the present report and in Foulk (1991) have documented that all of these elements with the exception of perhaps Sb and Te are present in high concentrations in stratiform-mineralized horizons in lower Paleozoic formations, mostly confined to the Slaven Chert. Thus, stratiform bedrock sources in the Slaven Chert and the Vinini Formation are inferred to have provided the bulk of the geochemically anomalous stream sediments near the southeast corner of the area.

GEOCHEMICAL DATA FROM BOULDER CREEK AREA (GROUP 3)

In this section we briefly discuss geochemical results obtained from chemical analysis of 78 composite rock samples collected during 1999 from localities in the general area of Boulder Creek in the west-central part of the BP quadrangle (fig. 2). Analytical data for the 78 samples are listed in table 4 and their log-frequency distributions are shown in figure 23. The primary purpose of this part of the sampling program is to determine the amount of metal(s), if any, concentrated along (1) the trace of the northeast-striking Boulder Creek fault, (2) along the trace of the Coyote thrust in this area, and (3) in strata of the Strathearn Formation chemically favorable for development of replacement deposits near the two faults (fig. 2). Both structures are considered to have had a significant part of their initial displacement during the late Paleozoic in association with north-south shortening (Theodore and others, 1998). Contoured Z-score values of stream-sediment data—that is, values normalized to standard deviations—suggested previously that the Boulder Creek fault may have formed a weakly developed geochemical boundary for a number of elements, including Ag, As, Au, Bi, Cu, Hg, Ni, and possibly Zn (Theodore and others, 1999). Generally, these metals show extended increases in stream-sediment concentrations to the southeast more or less parallel to the trace of the Boulder Creek fault, and some metals (Zn, for example) also show elevated concentrations broadly centered on the Toro fault, another northeast-striking fault (fig. 2). The Toro fault is considered to be roughly the same age and to have the same structural history as the Boulder Creek fault. These two faults are prominent splays of the CVIL (Peters, 1998) in the area.

After log transformation, histograms for most elements in the Boulder Creek area tend toward unimodal distributions (fig. 23). Some elements (for example, Mo, Bi, Te, and Tl) show distributions that must extend well below their lower detection limits. However, most elements do not have symmetrical distributions that approach lognormal distributions—this partly may be a result of the relatively small numbers of samples that comprise the database. In addition, Au, As, Zn, and Cd appear to have distributions that visually appear to be slightly skewed positively, whereas Cu is skewed negatively (fig. 23). In the Boulder Creek area, as opposed to distributions along profile AA', the positively skewed histograms probably reflect a weak superposed epigenetic mineralization event because of visible alteration that locally affects some siliceous rocks. Various statistics of the database are shown in table 7, including calculations of the skewness shown by the observed distributions.

Concentrations of various numbers (see above) of 15 metals analyzed in 78 rocks from the Boulder Creek area generally are low (fig. 24). Class intervals for the elemental spot maps were determined on the basis of the distributions shown by histograms of the data (fig. 23). The presence of any possible anomalous concentrations along the main Boulder Creek fault in this area was determined by analytical results of two suites of samples whose sites were specifically designed to test the fault trace. The first suite comprises 10 samples collected along a traverse approximately at right angles to the main splay of the Boulder Creek fault, and the second comprises eight samples collected along the main splay near the bottom of Boulder Creek (fig. 24). At the actual trace of the fault splay, only one sample shows an elevated concentration to between 0.01 and 0.03 ppm Au (fig. 24*A*). Silver also is elevated slightly in this one sample to between 0.06 and 0.2 ppm (fig. 24*B*). In addition, two other samples—obtained from the second suite of eight samples collected along an approximate 1–km-long strike length of the fault—contain more than 0.2 ppm Ag. Certainly these contents of Ag are not very exciting from an exploration standpoint, but they nonetheless are above local geochemical background in both walls of the fault where background appears to be < 0.06 ppm Ag. Arsenic and Sb show no anomalous concentrations along the fault (fig. 24*C*, *D*), whereas Hg, Pb, and Zn show some elevated abundances near the trace of the fault (fig. 24*E*, *G*, *H*). Again, absolute values of all these local anomalies near the Boulder Creek fault are not that extraordinary, and, in fact, for some elements (Zn, for example) appear to be less than local background in unmineralized mélange unit of the Slaven Chert southeast of the Boulder Creek fault (fig. 24*H*). Metal abundances along the Boulder Creek fault certainly do not show levels comparable to the CVIL elsewhere, particularly that segment of the CVIL in The Bobs Flat quadrangle (fig. 1) approximately 45 km south of Boulder Creek (S.G. Peters, written commun., 1999). However, the general area of Boulder Creek examined in the present report might be significantly damped because of great depths to site(s) of significant mineralized rock if such mineralized rock is present.

The potential of mineralized rock along the trace of the Coyote thrust also was evaluated by a suite of eight samples collected near its trace southeast of Boulder Creek (fig. 24). This suite of samples only shows slightly elevated concentrations of Cu, Pb, and Zn relative to local background near the trace of the thrust (fig. 24*F*–*H*). In addition, rocks of the Strathearn Formation do not show any elevated metal concentrations in samples near Boulder Creek from which we would infer presence of significant mineralized rock.

DISCUSSION

The broad area of high metal concentrations (Ag, As, Au, Cd, Co, Cu, Mn, Ni, P, Sb, Sc, Te, V, and especially Zn; Theodore and others, 1999) present in stream-sediments near the southeast corner of the BP quadrangle may primarily be the result of their being derived from lower Paleozoic sediment-hosted or stratiform-mineralized rock as we describe above. Elevated contents of Ni and V in these rocks may be a function of rapid burial of siliciclastic rocks in an anaerobic environment combined with ready availability of metals from an overlying lower Paleozoic water body in a chemically open system (Lewan and Maynard, 1982). Chert and shale of the Ordovician Vinini Formation and mostly chert of the Devonian Slaven Chert crop out across the anomalous area of approximately 15 km^2 near the southeast corner of the area. These formations are known to be likely hosts for stratiform-mineralized rocks elsewhere in Nevada (Cox and others, 1991; Emsbo, 1993; Cox and others, 1996; Peters and others, 1996; Young-Mitchell and Titley, 1996a, b). Shales at the base of the uppermost unit of the Vinini Formation recognized by Emsbo (1993) in the Roberts Mountains (fig. 1) contain elevated abundances of Cu, Au, and Hg; those in the upper member at the type section contain elevated abundances of Mo, Ag, Zn, Cd, Se, V, Tl, and Cu. A sample from his unit 2 contains about 2,100 ppm Zn, 400 ppm Cu, and 37 ppm Cd (Emsbo, 1993, Appendix B). Foulk (1991) documented that organic-rich black shale in the Slaven Chert—containing as much as 9 weight percent organic C—is enriched in Ag, Mo, V, Cr, Se, Zn, Cd, Ni, Tl, and Hg. Young-Mitchell and Titley (1996a, b) found that unmineralized organic-rich strata of the Vinini Formation are enriched to approximately 7 ppb Au—a value higher than crustal abundance—primarily because of weathering of the Au-enriched Precambrian craton combined with hydrothermal activity along early Paleozoic spreading centers and (or) ridges. In addition, a suite of samples of gossanous mudstone representing synsedimentary-exhalative horizons in Devonian strata near the southeast corner of the BP quadrangle contains as much as 2,500 ppm Zn, 100 ppm Cu, and 15 ppm Cd (Foulk, 1991). We have shown above, as well, that some base-metal-enriched horizons are present in the Coyote bedded barite deposit.

Although we suggested previously (Theodore and others, 1999) that the multi-element anomaly in the southeast corner of the area may owe its origin(s) to a number of temporally widespread but superposed geologic events, the rock geochemistry of the present report suggests otherwise. The breadth of the multi-element anomaly—approximately 4– to 6–km—certainly is the best evidence that it is related to synsedimentary-exhalative events in lower Paleozoic rocks that comprise this lowest exposed structural package in the upper plate of the RMT (see above). Further, our confirmation of the presence of base-metal-enriched horizons in the Coyote deposit suggests strongly that stratiform-mineralized rock is the primary contributor to the anomaly.

Some relatively recently completed geochemical studies of massive sulfide deposits at the sediment-covered Escanaba Trough, southern Gorda Ridge spreading center, and submarine hot springs along basaltic mid-ocean ridges shed light on the association of Ag, As, Au, and Sb with base metals near the southeast corner of the BP quadrangle. The two environments—upper plate of the RMT near the Carlin trend versus submarine spreading centers—are not analogous primarily because of the absence of widespread basalt in the upper plate of the RMT. Nonetheless, precious metals can form a significant geochemical signature of some nonvolcanic sedimentary submarine exhalative environments. For example, at Escanaba Trough, fundamental controls on elevated presence of Ag, As, Au, and Sb, as well as many other metals, have been exerted by source-rock composition of surrounding turbidites and hemipelagic sediments (Zierenberg and others, 1993; Koski and others, 1994). There, high concentrations of Pb, Bi, As, and Sb are inferred to have resulted from the leaching of surrounding continentally-derived turbidites by NaCl–rich waters (Koski and others, 1994). The metals, in effect, have been recycled from their turbiditic host rocks as heated, highly pressurized fluids associated with the spreading center circulated through the sediments. Although average Ag and Au contents of 23 pyrrhotite-rich samples analyzed by Koski and others (1994) from Escanaba Trough are approximately 52 and 2 ppm respectively, no contents of Ag and Au as high as these were detected during our studies of rock geochemistry (Group 2 data, table 2) from the southeast corner of the BP quadrangle. Also, clastic components in the Slaven Chert are absent or rare—basinal chert is the predominant rock. In addition, Au contents in pyrite- and chalcopyrite-bearing chimneys from a hydrothermal field along the Mid-Atlantic Ridge are in the range 0.2– to 1.0–ppm Au (Hannington and others, 1991). High temperature hydrothermal fluids (350 °C) in such environments may transport as much as 1,000 g Au/yr, most of which is dispersed into surrounding seawater and eventually is deposited over widespread areas of the seafloor (Hannington and Scott, 1989). Such fine-grained sediments with low precious metal contents may have been incorporated in the siliceous sediments deposited in the basin. Further, the association of elevated contents of Au with high organic content in siliciclastic strata in the upper plate of the RMT suggested to Young-Mitchell and Titley (1996a, b) that fixing of Au by plankton and algae might have contributed to relatively high contents of Au in these rocks. Thus, we infer that the association of Ag, As, Au, and Sb with base metals near the southeast corner of the BP quadrangle is most likely the result of their introduction penecontemporaneous with stratiform mineralization at or near the Devonian seafloor. Moreover, we found no strong evidence near the southeast corner of the BP quadrangle to suggest presence of widespread mineralized faults or veins that are highly discordant to bedding below the Coyote barite deposit.

Nonetheless, the possibility of epigenetically mineralized rock at depth near the southeast corner of the BP quadrangle cannot be discounted completely. The trace of the Lynn fault, a northeast-striking structure that is mineralized locally near the Carlin Au mine, approximately 12 km to the south-southwest, projects towards the southeast corner of the quadrangle (Evans and Peterson, 1984; Teal and Jackson, 1997). A north-northeast striking, apparently steeply dipping fault crops out near the southeast corner of the BP quadrangle (fig. 2). The Lynn fault is one of the fault strands that make up the Crescent Valley-Independence lineament farther to the south. Evans and Peterson (1984) show in the Rodeo Creek NE quadrangle, which is immediately south of the BP quadrangle, a number of rock samples near the trace of the Lynn fault that contain 1,000 to 5,000 ppm Zn, 1 to 5 ppm Ag, and 1 to 5 ppm Hg. In addition, a weak positive aeromagnetic anomaly is present near the southeast corner of the BP quadrangle, as we described above, suggesting presence of a buried intrusion. The Mike Au–Cu deposit, approximately 16 km southeast of Meikle, contains overlapping Au– and Cu–enriched zones largely coincident with rock flooded by secondary K–feldspar and quartz thereby suggesting genetic association with a buried intrusion (Branham and Arkell, 1995). The Mike deposit also hosts a 1998 drill-indicated mineral inventory of 813 million lbs Zn, all as sphalerite (Norby and Orobono, 2000). Furthermore, some steeply dipping north-striking faults approximately 1 km northwest of Beaver Peak contain as much as 1,000 ppm Zn and Fe–oxide-strained conglomerate of the Strathearn Formation approximately 3 km southwest of Beaver Peak contains as much as 5.6 ppm Ag (fig. 14*F*). These occurrences demonstrate that some epigenetic-mineralized rock in the eastern part of the area contains anomalous concentrations of base and precious metals and a similar origin cannot be eliminated entirely for the broad anomaly near the southeast corner of the BP quadrangle.

REFERENCES

Albino, G.V., 1994, Geology and lithogeochemistry of the Ren gold prospect, Elko County, Nevada; the role of rock sampling in exploration for deep Carlin-type deposits: Journal of Geochemical Exploration, v. 51, no. 1, p. 37–58.

Bartlett, M.W., Enders, M.S., and Hruska, D.C., 1991, Geology of the Hollister gold deposit, Ivanhoe district, Elko County, Nevada, *in* Raines, G.L., Lisle, R.E., Schafer, R.W., and Wilkinson, W.H., eds., Geology and ore deposits of the Great Basin, Symposium Proceedings: Reno, Nevada, Geological Society of Nevada, p. 957–978.

Berry, W.B.N., 1960, Graptolite faunas of the Marathon region, west Texas: Texas University, Bureau of Economic Geology, Publication 6005, 179 p.

Berry, W.B.N., and Murphy, M.A., 1975, Silurian and Devonian graptolites of central Nevada: Berkeley, California, University of California, Publications in Geological Sciences no. 110, 109 p.

Bettles, K.H., and Lauha, Eric, 2000, Mineralization, geology, geochemistry, and geophysics of the Goldstrike Mine, Carlin trend, Nevada, *in* Griffin, Lane, ed., Giant sedimentary rock-hosted mineral systems of the Carlin trend: Gold Quarry and Betze/Post deposits: Reno, Nevada, Geological Society of Nevada, Geology and Ore Deposits 2000: The Great basin and Beyond, Field Trip 7, p. 129–142.

Branham, Alan, and Arkell, Brian, 1995, The Mike gold-copper deposit, Carlin trend, Nevada, *in* Hagni, R.D., ed., Process mineralogy XIII: Applications to beneficiation problems, pyrometallurigical products, advanced mineralogical techniques, precious metals, environmental concerns, ceramic materials, hydrometallurgy, and minerals exploration: Warrendale, Pennsylvania, The Minerals, Metals, & Materials Society, p. 203–211.

Burchfiel, B.C., and Davis, G.A., 1972, Structural framework and evolution of the southern part of the Cordilleran orogen, western United States: American Journal of Science, v. 272, no. 2, p. 97–118.

Çagatay, M.N., 1984, Selective extraction techniques in exploration for volcanogenic sulphide deposits, eastern Black Sea region, Turkey, *in* Bjorkland, A.J., ed., Geochemical exploration 1983: Journal of Geochemical Exploration, v. 21, no. 1–3, p. 273–290.

Church, S.E., Mosier, E.L., and Motooka, J.M., 1987, Mineralogical basis for the interpretation of multi-element (ICP–AES), oxalic acid, and aqua regia partial digestions of stream sediments for reconnaissance exploration geochemistry, *in* Garrett, R.G., ed., Geochemical exploration 1985, Part II: Journal of Geochemical Exploration, v. 29, no. 1–3, p. 207–233.

Claypool, G. E., Holser, W. T., Kaplan, I. R., Sakai, Hitoshi, and Zak, Israel, 1980, The age curves of sulfur and oxygen isotopes in marine sulfates and their mutual interpretation: Chemical Geology, v. 28, p. 199–260.

Cluer, J.K., 1999, Future of gold exploration in the Roberts Mountains allochthon, Nevada: Role of structural geology and biostratigraphy [abs.]: Geological Society America, Abstracts with Programs, v. 31, no. 4, March, 1999, p. A–7.

Cluer, J.K., Cellura, B.R., Keith, S.B., Finney, S.C., and Bellert, S.J., 1997, Stratigraphy and structure of the Bell Creek nappe (Antler orogen), Ren property, northern Carlin trend, Nevada: Reno, Nevada, Nevada Petroleum Society, 1997 Fall Field Trip Guide, p. 41–54.

Cox, D. P., Berger, B.R., Ludington, Steve, Moring, B.C., Sherlock, M.G., Singer, D.A., and Tingley, J.V., 1996, Delineation of mineral resource assessment tracts and estimation of number of undiscovered deposits in Nevada, *in* Singer, D.A., ed., An analysis of Nevada's metal-bearing mineral resources: Nevada Bureau of Mines and Geology Open-File Report 96–2, Chapter 12, p.12.1–12.25, 3 sheets, scale 1:1,000,000.

Cox, D.P., Ludington, Steve, Sherlock, M.J., Singer, D.A., Berger, B.R., and Tingley, J.V., 1991, Mineralization patterns in time and space in the Great Basin of Nevada, *in* Raines, G.L., Lisle, R.E., Schafer, R.W., and Wilkinson, W.H., eds., Geology and ore deposits of the Great Basin: Reno, Nevada, Geological Society of Nevada, Symposium Proceedings, p. 193–198.

Crock, J.G., and Lichte, F.E., 1982, Determination of rare earth elements in geological materials by inductively coupled argon plasma/atomic emission spectrometry: Analytical Chemistry, v. 54, no. 8, p. 1,329–1,332.

Dewitt, Alexander, 1999, Alteration, geochemical dispersion, and ore controls at the SSX mine, Jerritt Canyon district, NV [abs.]: SEG Newsletter, October 1999, no. 39, p. 7.

Doebrich, J.L., 1994, Preliminary geologic map of the Galena Canyon 7-1/2 minute quadrangle, Lander County, Nevada: U.S. Geological Survey Open-File Report 94–664, 14 p.

Dott, R.H., Jr., 1955, Pennsylvanian stratigraphy of Elko and northern Diamond Ranges, northeastern Nevada: American Association of Petroleum Geologists Bulletin, v. 39, no. 11, p. 2,211–2,305.

Dubé, T.E., 1987, Setting and origin of exhalative bedded barite and associated rocks of the Roberts Mountains allochthon in north-central Nevada: Seattle, Washington, University of Washington, M.S. Thesis, 76 p.

———1988, Tectonic significance of Upper Devonian igneous rocks and bedded barite, Roberts Mountains allochthon, Nevada, U.S.A., *in* McMillan, N.J., Embry, A.F., and Glass, D.J., eds., Devonian of the world—Volume II: Sedimentation: Calgary, Alberta, Proceedings of the Second International Symposium on the Devonian System, Canadian Society of Petroleum Geologists Memoir, p. 235–249.

Emsbo, Poul, 1993, Geology and geochemistry of the Ordovician Vinini Formation, Roberts Mountains, Nevada: Golden, Colorado, Colorado School of Mines, M.S. Thesis, 145 p.

Emsbo, Poul, Hutchinson, R.W., Hofstra, A.H., Volk, J.A., Bettles, K.H., Baschuk, G.J., Collins, T.M., Lauha, E.A., and Borhauer, J.L., 1997, Newly discovered Devonian sedex-type base and precious metal mineralization, northern Carlin trend, Nevada, *in* Vikre, Peter, Thompson, T.B., Bettles, Keith, Christensen, Odin, and Parratt, Ron, eds., Carlin-type gold deposits field conference: Society of Economic Geologists, Guidebook Series, v. 28., p. 109–117.

Erickson, R.L., and Marsh, S.P., 1974, Paleozoic tectonics in the Edna Mountain quadrangle, Nevada: U.S. Geological Survey, Journal of Research, v. 2, no. 3, p. 331–337.

Evans, A.M., 1995, ed., Introduction to mineral exploration: Oxford, Blackwell Science Ltd., 396 p.

Evans, J.G., and Peterson, J.A., 1984, Distribution of minor elements in the Rodeo Creek NE and Welches Canyon quadrangles, Eureka County, Nevada: U.S. Geological Survey Bulletin 1657, 65 p.

Finney, S.C., and Perry, B.D., 1991, Depositional setting and paleogeography of

Ordovician Vinini Formation, central Nevada, *in* Cooper, J.D., and Stephens, C.H., eds., Paleozoic paleogeography of the western United States–II: Los Angeles, California, Pacific Section Society Economic Paleontologists and Mineralogists, v. 67, p. 747–766.

Fleck, R.J., Theodore, T.G., Sarna-Wojcicki, Andrei, and Meyer, C.E., 1998, Age and possible source of air-fall tuffs of the Miocene Carlin Formation, northern Nevada, *in* Tosdal, R.M., ed., Contributions to the gold metallogeny of the northern Great Basin: U.S. Geological Survey Open-File Report 98–338, p. 176–192.

Foulk, C.L., 1991, Geology, geochemistry and metal enrichments of the allochthonous siliceous assemblage rocks, central Tuscarora Mountains, Nevada: Golden, Colorado, Colorado School of Mines, M.S. Thesis, 182 p.

Fox, K.F., Jr., 1983, Melanges and their bearing on late Mesozoic and Tertiary subduction and interplate translation at the west edge of the North American plate: U.S. Geological Survey Professional Paper 1198, 40 p.

Gilluly, James, and Gates, Olcott, 1965, Tectonic and igneous geology of the northern Shoshone Range, Nevada: U.S. Geological Survey Professional Paper 465, 153 p.

Goodfellow, W. D. and Jonasson, I. R., 1984, Ocean stagnation and ventilation defined by $\delta^{34}S$ values in pyrite and barite, Selwyn Basin, Yukon: Geology, v. 12, p. 583-586.

Hall, G.E.M., 1998, Analytical perspective on trace element species of interest in exploration, *in* Hall, G.E.M., and Bonham-Carter, G.F., eds., Selective extractions: Journal of Geochemical Exploration, v. 61, no. 1–3, p. 1–19.

Hannington, M.D., Herzig, P.M., and Scott, S.D., 1991, Auriferous hydrothermal precipitates on the modern seafloor, *in* Foster, R.P., ed., Gold metallogeny and exploration: Glasgow and London, Blackie and Son Ltd., p. 249–282.

Hannington, M.D., and Scott, S.D., 1989, Gold mineralization in volcanogenic massive sulfides: Implications of data from active hydrothermal vents on the modern sea floor, *in* Keays, R.R., Ramsay, W.R.H., and Groves, D.I., eds., The geology of gold deposits: The perspective in 1988: Economic Geology Monograph 6, p. 491–507.

Hoffman, J.D., and Buttleman, Kim, 1994, National geochemical data base: National uranium resource evaluation for the conterminous United States: U.S. Geological Survey Digital Data Series DDS–18–A, 1 CD.

Hofstra, A.H., Snee, L.W., Rye, R.O., Folger, H.W., Phinisey, J.D., Loranger, R.J., Dahl, A.R., Naeser, C.W., Stein, H.J., and Lewchuk, M., 1999, Age constraints on Jerritt Canyon and other Carlin-type gold deposits in the western United States—Relationship to mid-Tertiary extension and magmatism: Economic Geology, v. 94, no. 6, p. 769–802.

Howe, S. S., 1988, Sulfur isotope characteristics of bedded and vein barite deposits, north-central Nevada [abs.], *in* Schindler, K. S., ed., USGS research on mineral resources—1989, Program and Abstracts, Fifth annual V.E. McKelvey Forum on mineral and energy resources: U.S. Geological Survey Circular 1035, p. 33, 35.

Hsü, K.J., 1983, Geosynclines in plate-tectonic settings: Sediments in mountains, *in* Hsü, K.J., ed., Mountain building processes: London, Academic Press, p. 3–12.

Ketner, K.B., 1977, Deposition and deformation of lower Paleozoic western facies rocks, northern Nevada, *in* Stewart, J.H., Stevens, C.H., and Fritsche, A.E., eds., Paleozoic paleogeography of the western United States: Pacific Coast Paleogeography Symposium 1: Los Angeles, Society of Economic Paleontologists and Mineralogists, Pacific Section, p. 251–258.

Koski, R.A., Benninger, L.M., Zierenberg, R.A., and Jonasson, I.R., 1994, Composition and growth history of hydrothermal deposits in Escanaba Trough, southern Gorda Ridge, *in* Morton, J.L., Zierenberg, R.A., and Reiss, C.A., eds., Geologic, hydrothermal, and biologic studies at Escanaba Trough, Gorda Ridge, offshore northern California: U.S. Geological Survey Bulletin 2022, p. 293–324.

Kotlyar, B.B., Singer, D.A., Jachens, R.C., and Theodore, T.G., 1998, Regional analysis of the distribution of gold deposits in northeast Nevada using NURE arsenic data and geophysical data, *in* Tosdal, R.M., ed., Contributions to the gold metallogeny of the northern Great Basin: U.S. Geological Survey Open-File Report 98–338, p. 234–242.

Lewan, M.D., and Maynard, J.B., 1982, Factors controlling enrichment of vanadium and nickel in the bitumen of organic sedimentary rocks: Geochimica et Cosmochimica Acta, v. 46, p. 2,547–2,560.

Lichte, F.E., Golightly, D.W., and Lamothe, P.J., 1987, Inductively coupled plasma—atomic emission spectrometry, *in* Baedecker, P.A., ed., Methods for geochemical analysis: U.S. Geological Survey Bulletin 1770, p. B1–B10.

Madrid, R.J., 1987, Stratigraphy of the Roberts Mountains allochthon in north-central Nevada: Stanford, California, Stanford University, Ph.D. dissertation, 341 p.

Masters, T., 1993, Practical neural network recipes in C++: San Diego, California, Academic Press, Inc., 493 p.

McFarlane, M.J., 1997, The Roberts Mountains thrust in the northern Snake Mountains, Elko County, Nevada, *in* Perry, A.J., and Abbott, E.W., eds., The Roberts Mountains thrust, Elko and Eureka Counties, Nevada: Reno, Nevada, Nevada Petroleum Society, 1997 Field Trip Guidebook, p. 17–34.

Merriam, C.W., and Anderson, C.A., 1942, Reconnaissance survey of the Roberts Mountains, Nevada: Geological Society of America Bulletin, v. 53, p. 1,675–1,728.

Motooka, J.M., 1988, An exploration geochemical technique for the determination of preconcentrated organometallic halides by ICP–AES: Applied Spectroscopy, v. 42, no. 7, p. 1,293–1,296.

Noble, P.J., Ketner, K.B., and McClellan, W., 1997, Early Silurian radiolaria from northern Nevada: Marine Micropaleontology, v. 30, p. 215–223.

Norby, J.W., and Orobono, M.J.T., 2000, Contact metamorphic, epithermal, and supergene mineralization at the Mike deposit, Eureka County, Nevada, in Griffin, Lane, ed., Giant sedimentary rock-hosted mineral systems of the Carlin trend: Gold Quarry and Betze/Post deposits: Geological Society of Nevada Symposium 2000, Guidebook Fieldtrip 7, p. 107–108.

Ohmoto, H., and Goldhaber, M., 1997, Sulfur and carbon isotopes, *in* Barnes, H. L., ed., Geochemistry of hydrothermal ore deposits, 3rd ed.: New York, John Wiley and Sons, p. 517–612.

O'Leary, R.M., and Viets, J.G., 1986, Determination of antimony, arsenic, bismuth, cadmium, copper, lead, molybdenum, silver, and zinc in geologic materials by atomic absorption spectrometry using a hydrochloric acid-hydrogen peroxide digestion: Atomic Spectroscopy, v. 7, no. 1, p. 4–8.

Papke, K. G., 1984, Barite in Nevada: Nevada Bureau of Mines and Geology Bulletin 98, 125 p.

Peters, S.G., 1998, Evidence for the Crescent Valley-Independence Lineament, north-central, Nevada, *in* Tosdal, R.M., ed., Contributions to the gold metallogeny of northern Nevada: U.S. Geological Survey Open-File Report 98–338, p. 106–118.

———2000, Regional- and district-scale dissolution, deformation, and fluid flow in sedimentary rock-hosted Au deposits of northern Nevada, *in* Cluer, J.K., Price, J.G., Struhsacker, E.M., Hardyman, R.D., and Morris, C.L., eds., Geology and ore deposits 2000: The Great Basin and beyond: Reno, Nevada, Geological Society of Nevada, Symposium Proceedings, p. 661–681.

Peters, S.G., Nash, J.T., John, D.A., Spanski, G.T., King, H.D., Connors, K.A., Moring, B.C., Doebrich, J.L., McGuire, D.J., Albino, G.V., Dunn, V.C., Theodore, T.G., and Ludington, Steve, 1996, Metallic mineral resources in the U.S. Bureau of Land Management's Winnemucca District and Surprise Resource Area, northwest Nevada and northeast California: U.S. Geological Survey Open-File Report 96–712, 147 p.

Peters, W.C., 1978, Exploration and mining geology: New York, John Wiley and Sons., 696 p.

Radtke, A.S., Heropoulos, Chris, Fabbi, B.P., Scheiner, B.J., and Essington, Mel, 1972, data on major and minor elements in host rocks and ores, Carlin gold deposit, Nevada: Economic Geology, v. 67, no. 7, p. 975–978.

Raymond, L.A., 1984, Classification of mélanges, *in* Raymond, L.A., ed., Mélanges: Their nature, origin, and significance: Geological Society of America Special Paper 198, p. 7–20.

Regnier, Jerome, 1960, Cenozoic geology in the vicinity of Carlin, Nevada: Geological Society of America Bulletin, v. 71., no. 8, p. 1,191–1,199.

Roberts, R.J., 1964, Stratigraphy and structure of the Antler Peak quadrangle, Humboldt and Lander Counties, Nevada: U.S. Geological Survey Professional Paper 459–A, 93 p.

Roberts, R.J., Hotz, P.E., Gilluly, James, and Ferguson, H.G., 1958, Paleozoic rocks in north-central Nevada: American Association of Petroleum Geologists Bulletin, v. 42, no. 12, p. 2,813–2,857.

Rose, A.W., Hawkes, H.E., and Webb, J.S., 1979, Geochemistry in mineral exploration: London, Academic Press Ltd., 657 p.

Rye, R. O., Shawe, D. R., and Poole, F. G., 1978, Stable isotope studies of bedded barite at East Northumberland Canyon in Toquima Range, central Nevada: Journal of Research of the U.S. Geological Survey, v. 6, p. 221–229.

Saucier, A.E., 1997, The Antler thrust system in northern Nevada, *in* Perry, A.J., and Abbott, E.W., eds., The Roberts Mountains thrust, Elko and Eureka Counties, Nevada: Reno, Nevada, Nevada Petroleum Society, 1997 Field Trip Guidebook, p. 1–16.

Schull, H.W., 1991, The lithostratigraphy and sedimentology of the contact/transition between the Roberts Mountains Formation and the western facies rocks in the Carlin Mining District, Eureka and Elko Counties, Nevada, *in* Raines, G.L., Lisle, R.E., Schafer, R.W., and Wilkinson, W.H., eds., Geology and ore deposits of the Great Basin, Symposium Proceedings: Reno, Nevada, Geological Society of Nevada, p. 705–712.

Snyder, W.S., Trexler, J.H., Jr., Cashman, P.H., Schlappa, T.A., and Davydov, V.I., 2000, Tectonostratigraphic framework of the upper Paleozoic continental margin of Nevada and southeastern California, *in* Geology and ore deposits 2000: The Great Basin and beyond, Program with Abstracts, Geological Society of Nevada Symposium 2000, Reno/Sparks, May, 2000, p. 76–77.

Teal, Lewis, and Jackson, Mac, 1997, Geologic overview of the Carlin trend gold deposits and descriptions of recent deep discoveries, *in* Vikre, Peter, Thompson, T.B., Bettles, Keith, Christensen, Odin, and Parratt, Ron, eds., Carlin-type gold deposits field conference: Society of Economic Geologists Guidebook Series, v. 28, p. 3–37.

Theodore, T.G., 1999, Implications of regional geology and geochemistry in the northern Carlin trend, southern Tuscarora Mountains, Nevada [Extended abs.]: Ralph J. Roberts Sixth Distinguished Lecture in Economic Geology, Program, Mackay School of Mines, 4 p.

——— 2000, Geology of pluton-related gold mineralization at Battle Mountain, Nevada, *with a section on* Potassium-argon chronology of Cretaceous and Cenozoic igneous activity, hydrothermal alteration, and mineralization *by* E.H. McKee, *and a* *section on* Lone Tree gold deposit *by* E.I. Bloomstein, B.L. Braginton, R.W. Owen, R.L. Parrrat, K.C. Raabe, and W.F. Thompson, *and a section on* Geology of the Marigold Mine area *by* D.H. McGibbon and A.B. Wallace, *and a section on* Geology, mineralization, and exploration history of the Trenton Canyon project *by* R.P. Felder: Tucson, Arizona, University of Arizona and U.S. Geological Survey Center for Mineral Resources, Monograph 2, 271 p.

Theodore, T.G., Armstrong, A.K., Harris, A.G., Stevens, C.H., and Tosdal, R.M., 1998, Geology of the northern terminus of the Carlin trend, Nevada: Links between crustal shortening during the late Paleozoic Humboldt orogeny and northeast-striking faults, *in* Tosdal, R.M., ed., Contributions to the gold metallogeny of northern Nevada: U.S. Geological Survey Open-File Report 98–338, p. 69–105.

Theodore, T.G., Kotlyar, B.B., Berger, V.I., Moring, B.C., and Singer, D.A., 2000, Implications of stream-sediment geochemistry in the northern Carlin trend, Nevada, *in* Cluer, J.K., Price, J.G., Struhsacker, E.M., Hardyman, R.F., and Morris, C.L., eds, Geology and ore deposits 2000: The Great Basin and beyond: Reno, Nevada, Geological Society of Nevada Symposium Proceedings, p. 929–958.

Theodore, T.G., Kotlyar, B.B., Berger, V.I., Moring, B.C., Singer, D.A., and Edstrom, S.A., 1999, Geochemistry of stream-sediment samples from the Santa Renia Fields and Beaver Peak quadrangles, northern Carlin trend, Nevada: U.S. Geological Survey Open-File Report 99–341, 103 p.

Theodore, T.G., and Peters, S.G., 1998, Links between crustal shortening during the late Paleozoic Humboldt orogeny, northeast striking faults, and Carlin-type gold deposits in Nevada [abs.]: Geological Society America, Abstracts with Programs, v. 30, no. 7, October, 1998, p. A–76.

Theodore, T. G., and Roberts, R. J., 1971, Geochemistry and geology of deep drill holes at Iron Canyon, Lander County, Nevada, *with a section on* Geophysical logs of DDH–2, by C. J. Zablocki: U.S. Geological Survey Bulletin 1318, 32 p.

Tingley, J.V., and Castor, S.B., 1999, Stream sediment exploration for gold and silver in Nevada—application of an old prospecting method using modern analytical techniques: Journal of Geochemical Exploration, v. 66, p. 1–16.

Young-Mitchell, M.N., and Titley, S.R., 1996a, Gold enrichments and carbon compositions of lower Paleozoic marine strata of Nevada [abs.]: Geological Society of America, Abstracts with Programs, v. 28, no. 5, p. 128.

———1996b, Origins and consequences of gold enrichments in lower Paleozoic organic-rich strata [abs.]: Geological Society of America, Abstracts with Programs, v. 28, no. 7, p. 86.

Zeegers, H., Al Shanfari, S.M., Al Muflehi, Y.A., and Letalenet, J., 1985, Aspects of regional geochemical prospecting in desert conditions, *in* Prospecting in desert terrains: Institution of Mining and Metallurgy, p. 131–139.

Zierenberg, R.A., Koski, R.A., Morton, J.L., Bouse, R.M., and Shanks, W.C., III, 1993, Genesis of massive sulfide deposits on a sediment-covered spreading center, Escanaba Trough, southern Gorda Ridge: Economic Geology, v. 88, no. 8, p. 2,069–2,098.

TABLE 1—ANALYTICAL DATA FOR 40 ELEMENTS FROM 115 ROCKS ALONG TRAVERSE AA' (SAMPLE GROUP 1) FROM THE SANTA RENIA FIELDS AND BEAVER PEAK QUADRANGLES, NEV.

[ppm, parts per million; wt. percent, weight percent; partial, analysis by partial digestion methods; total, analysis by total digestion methods (see text)]

Sample	Latitude	Longitude	Ag partial ppm	As partial ppm	Au partial ppm	Bi partial ppm	Cd partial ppm	Cu partial ppm	Ga partial ppm	Hg partial ppm	Mo partial ppm	Pb partial ppm	Sb partial ppm	Se partial ppm	Te partial ppm	Tl partial ppm	Zn partial ppm	Mo total ppm	Cu total ppm	Pb total ppm	Zn total ppm
99-TT-72	41.04333	-116.49874	0.029	2.68	0.0007	0.324	0.187	11.4	3.67	0.015	0.645	7.83	0.583	0	0.135	0.425	33.6	2	14	15	68
99-TT-71	41.04207	-116.49693	0.021	0.745	0	0.164	0.046	3.04	0.56	0.007	0.652	1.91	0.239	0.006	0.092	0.308	6.19	3	5	20	31
99-TT-70	41.04092	-116.49337	0.033	2.67	0.0007	0.322	0.187	10.2	3.81	0.005	0.596	8.16	0.471	0.035	0.101	0.403	32.4	2	12	21	69
99-TT-69	41.04079	-116.49048	0.068	4.15	0.0003	0.28	0.224	12.6	3.37	0.036	1.45	10.5	0.944	0.38	0.097	0.628	41.7	<2	15	16	66
99-TT-68	41.03876	-116.48751	0.117	5.15	0.0005	0.186	0.211	16.3	1.26	0.048	1.96	4.66	1.05	0.624	0.154	0.307	30.3	2	21	6	42
99-VB-1	41.03975	-116.48328	0.196	6.07	0.005	0.355	0.198	11.7	4.64	0.013	0.835	13.6	1.43	0	0.115	0.762	36.6	<2	19	24	71
99-VB-2	41.04224	-116.47969	0.066	15.7	0.001	0.351	0.143	11.3	4.72	0.055	1.63	18.6	1.03	0.235	0.074	0.61	31.6	2	21	26	68
99-VB-3	41.04361	-116.47678	0.14	4.82	0.0008	0.167	0.123	10.4	0.85	0.075	1.71	3.93	1.12	0.391	0.113	0.238	18.3	3	17	9	30
99-VB-4	41.04605	-116.47502	0.097	9.58	0.001	0.28	0.278	18.3	4.35	0.029	0.862	9.98	1.09	0.021	0.074	0.644	44.6	<2	24	15	71
99-VB-5	41.04842	-116.47177	0.034	8.46	0.0003	0.373	0.17	8.59	5.78	0.043	0.824	15.7	0.844	0.054	0.125	0.467	34.6	2	16	25	67
99-VB-6	41.05016	-116.46894	0.07	10.4	0.0006	0.27	0.133	9.4	2.2	0.046	2.14	9.76	0.955	0	0.134	0.459	42.5	3	12	25	54
99-VB-7	41.05341	-116.46879	0.083	9.99	0.0007	0.282	0.328	16.2	4.18	0.04	1.62	14.8	1.84	0.168	0.156	0.412	46.1	3	23	22	71
99-VB-8	41.05497	-116.46402	0.061	5.04	0.003	0.169	0.095	5.69	1.67	0.016	1.34	4.85	0.595	0.072	0.095	0.175	17.3	2	8	14	30
99-TT-73	41.05577	-116.46103	0.021	4.3	0.0004	0.304	0.103	9.96	8.36	0.021	0.549	17.1	0.556	0.167	0.134	0.573	41.9	<2	11	18	61
99-TT-74	41.05582	-116.45953	0.077	13.1	0.0007	0.372	0.291	17.3	5.93	0.015	5.53	16.8	2.32	0.17	0.127	0.406	45.1	6	19	24	67
99-TT-75	41.05519	-116.45689	0.054	22.7	0.002	0.412	1.22	16.2	4.99	0.038	1.46	19	1.47	0.06	0.136	0.428	46.5	2	23	20	82
99-TT-76	41.05379	-116.45284	0.071	31	0.004	0.392	1.28	17.8	4.87	0.059	1.49	18.7	1.34	0.079	0.144	0.366	57.5	2	25	24	103
99-TT-87	41.05508	-116.44844	0.08	87.4	0	0.128	0.216	5.14	0.197	0.28	0.977	3.9	0.985	0.427	0.097	0.253	16.6	2	5	6	18
99-TT-86	41.05514	-116.44719	0.057	6.2	0	0.111	0.092	5.14	0	0.069	1.18	3.08	0.277	0.362	0.108	0.268	14.7	<2	5	<5	15
99-TT-85	41.05532	-116.44528	0.051	1.92	0	0.145	0.422	3.64	0	0.023	1.22	3.72	0.351	0.149	0.078	0.305	23.6	<2	3	8	23
99-TT-84	41.05531	-116.44404	0.036	11.2	0.0003	0.139	0.051	4.31	0.109	0.081	0.704	5.1	0.399	0.404	0.115	0.179	9.65	<2	4	<5	12
99-TT-83	41.05574	-116.4423	0.055	22	0.0003	0.158	0.104	18	0.19	0.115	1.62	2.3	0.732	0.506	0.139	0.159	21.6	2	19	<5	29
99-TT-82	41.05636	-116.44039	0.092	89.1	0	0.146	0.052	21.3	0.213	1.38	1.54	3.56	1.47	0.711	0.076	0.586	3.9	2	23	6	8
99-TT-81	41.05698	-116.43872	0.071	125	0.0004	0.122	0.259	11.2	0.308	2.47	2.64	2.72	2.33	2.64	0.142	0.386	6.82	3	12	<5	10
99-TT-80	41.05666	-116.43666	0.313	7.75	0.0003	0.152	0.425	23.8	0.423	0.34	4.63	2.4	1.08	6.75	0.297	0.332	9.79	6	27	<5	14
99-TT-79	41.05677	-116.43475	0.219	28.8	0.002	0.172	1.05	41.8	0.601	0.334	3.23	2.67	1.05	3.88	0.152	0.262	89.7	5	46	5	102
99-TT-78	41.05507	-116.43377	0.4	8.45	0.0008	0.174	0.391	41.7	0.563	0.127	2.69	2.81	0.856	3.82	0.202	0.169	65.8	3	49	<5	82
99-TT-77	41.05407	-116.43436	0.459	11.6	0.004	0.158	0.369	42.1	0.538	0.12	4.52	3.08	1.02	4.77	0.175	0.237	59.4	6	47	5	71
99-VB-9	41.05363	-116.43223	0.078	3.98	0.001	0.159	0.025	14	0.303	0.045	1.83	1.5	0.609	0.397	0.155	0.202	2.42	3	18	8	6
99-VB-10	41.05351	-116.42985	0.055	2.58	0.0004	0.162	0.047	13.4	0.338	0.123	1.75	1.36	0.474	0.002	0.097	0.251	7.39	2	18	<5	10
99-VB-11	41.05243	-116.4282	0.042	1.97	0.0008	0.112	0.026	14	0	0.318	1.48	0.924	0.272	0	0.046	0.123	5.53	2	16	<5	8
99-VB-12	41.05143	-116.42714	0.432	4.59	0.0006	0.205	0.048	10.6	0.666	0.354	4.54	9.52	1.32	0.873	0.146	0.337	6.56	9	16	20	13
99-VB-13	41.05135	-116.42685	0.035	48.7	0.0003	0.203	1.38	6.71	0.876	0.102	0.935	15.1	0.124	4.51	0.117	1.24	99.8	<2	9	27	126
99-VB-14	41.05183	-116.42539	0.582	11.9	0.001	0.283	0.246	30.4	0.937	0.476	15.4	4.63	1.53	2.68	0.168	0.439	46.8	21	36	9	58
99-VB-15	41.05138	-116.42466	0.869	6.18	0.003	0.214	0.214	32.4	0.353	0.386	6.33	14.4	4.45	1.78	0.188	0.234	24.3	9	48	19	32
99-VB-16	41.05126	-116.42271	0.083	31.1	0.0004	0.247	0.382	21.8	0.641	0.171	3.14	6.83	1.72	0.954	0.245	0.239	25.5	3	23	8	31
99-VB-17	41.05148	-116.42184	1.28	16.6	0.0005	0.183	0.533	75.3	1.69	0.45	4.61	9.66	5.6	0.481	0.153	0.298	8.69	7	93	12	14
99-VB-18	41.05166	-116.42106	0.893	53.8	0.004	0.153	7.24	91.6	1.46	1.4	7.82	7.79	11.6	4.87	0.162	0.369	211	9	97	7	213
99-VB-19	41.05091	-116.41897	0.065	5.64	0.0003	0.217	0.354	32.6	1.04	0.066	3.95	2.18	0.728	0.074	0.108	0.203	38	6	35	5	43
99-VB-20	41.05075	-116.41717	0.15	5.9	0	0.181	0.324	25	0.212	0.076	1.41	1.97	1.07	0.415	0.09	0.326	39.4	2	30	<5	45
99-VB-21	41.05071	-116.41542	0.218	2.41	0.0005	0.15	0.255	16.4	0.219	0.117	6.31	3.1	1.28	0.745	0.073	0.199	20.6	10	23	8	31
99-TT-98	41.04961	-116.39157	0.159	3.83	0.005	0.168	0.083	13.8	0.295	0.109	4.25	3.23	1.37	7.13	0.162	0.272	6.49	5	22	7	13
99-TT-99	41.05041	-116.38971	0.124	1.69	0.004	0.207	0.038	16.3	0.646	0.092	7.86	2.87	0.654	2.15	0.119	0.136	3.75	10	22	5	8
99-TT-100	41.0518	-116.38736	0.113	2.02	0.007	0.179	0.147	15.9	0.469	0.374	3.79	4.52	0.798	1.37	0.182	0.246	7.22	5	19	7	11
99-TT-101	41.05289	-116.38502	0.086	1.99	0.007	0.181	0.152	14.6	0.382	0.123	12.2	2.58	0.99	9.84	0.255	0.205	5.91	18	19	6	11
99-TT-102	41.05368	-116.3818	0.156	1.91	0.008	0.13	0.218	18.1	0.429	0.151	4.34	4.73	0.742	4.24	0.213	0.209	21.8	5	23	7	32
99-TT-103	41.05581	-116.38129	0.03	0.897	0.0002	0.185	0.087	26.2	0.309	0.053	4.59	2.83	0.386	0.248	0.253	0.137	12.5	6	34	<5	21
99-TT-104	41.05683	-116.37895	0.147	2.36	0.0004	0.176	0.374	27.7	0.337	0.122	3.78	2.96	0.552	1.93	0.183	0.157	10.9	4	34	5	18
99-TT-105	41.05807	-116.3784	0.085	1.69	0.002	0.156	0.391	29.6	0.248	0.163	5.89	2.53	0.824	1.92	0.131	0.169	25.7	8	37	<5	41
99-TT-97	41.05874	-116.37479	0.041	2.52	0.0004	0.192	0.26	27	0.392	0.156	2.21	2.95	0.489	0.275	0.136	0.237	21.2	3	27	<5	30
99-TT-96	41.05924	-116.37187	0.045	2.15	0.002	0.198	0.089	26.8	0.555	0.182	1.57	3.92	0.511	0.449	0.187	0.207	15.2	2	25	9	21
99-TT-95	41.0594	-116.36971	0.061	1.56	0.0007	0.192	0.026	12.4	0.345	0.076	2.33	2.39	0.596	0.342	0.088	0.094	3.22	2	12	<5	8
99-TT-94	41.05994	-116.36649	0.021	1.09	0	0.17	0.036	14.3	0.244	0.056	1.51	1.66	0.343	0.342	0.102	0.178	20.5	<2	15	<5	24
99-TT-93	41.05971	-116.36507	0.046	1.11	0.0002	0.114	0.228	12.7	0.147	0.087	1.8	1.61	0.21	0.218	0.127	0.153	121	2	12	<5	124
99-TT-92	41.05942	-116.36366	0.035	0.731	0.0006	0.191	0.11	24	0.22	0.073	1.44	1.6	0.451	0.194	0.143	0.03	6.84	<2	23	<5	11
99-TT-91	41.05813	-116.3609	0.018	1.19	0	0.203	0.194	14.9	0.717	0.09	1.4	4.55	0.359	0.742	0.146	0.129	7.11	2	15	<5	13
99-TT-90	41.05747	-116.3587	0.042	1.42	0.001	0.216	0.378	14.8	0.57	0.173	1.78	3.9	0.463	0.703	0.166	0.232	8.13	2	15	7	14
99-TT-89	41.05831	-116.35725	0.024	1.09	0	0.175	0.064	19	0.228	0.037	1.72	2.04	0.307	0.458	0.182	0.198	4.56	2	20	5	10
99-TT-88	41.05841	-116.35471	0.042	1.84	0.0005	0.193	0.416	22.4	0.217	0.097	1.66	2.79	0.614	1.78	0.169	0.309	13.2	2	24	<5	19
99-VB-22	41.05923	-116.34985	0.185	1.06	0.0002	0.148	0.112	20.4	0.239	0.103	2.93	2.86	0.632	1.74	0.033	0.398	2.5	4	25	8	5
99-VB-23	41.06057	-116.3476	0.029	1.85	0.0006	0.131	0.172	18.1	0.337	0.2	3.86	2.54	0.67	0.583	0.183	0.254	3.94	6	22	<5	7
99-VB-24	41.05891	-116.34433	0.029	0.777	0	0.159	0.099	31	0.237	0.077	1.73	1.72	0.5	1.09	0.132	0.211	2.59	3	43	5	9
99-VB-25	41.05884	-116.34201	0.751	2.13	0.004	0.136	0.437	33.3	0.913	0.324	8.97	2.51	1.46	6.31	0.109	0.298	11.9	11	39	<5	14

TABLE I—CONT'D.

Sample	Ag total ppm	Ni total ppm	Co total ppm	Mn total ppm	Fe total wt percent	As total ppm	U total ppm	Au total ppm	Th total ppm	Sr total ppm	Cd total ppm	Sb total ppm	Bi total ppm	V total ppm	Ca total wt percent	P total wt percent	La total ppm	Cr total ppm
99-TT-72	<.5	9	6	466	2 53	<5	<10	<4	13	210	< 4	<5	<5	34	1 32	0.024	41	44
99-TT-71	<.5	5	2	186	0.78	<5	16	<4	16	50	<.4	<5	<5	7	0.45	0.02	44	62
99-TT-70	<.5	8	5	407	2.43	<5	<10	<4	15	191	0.5	<5	<5	35	1 14	0.038	41	34
99-TT-69	0.6	11	5	477	2.09	<5	<10	<4	13	156	<.4	<5	<5	62	1.04	0.047	41	91
99-TT-68	1.2	14	4	222	1 28	6	12	<4	4	121	<.4	<5	<5	98	0.45	0.085	18	228
99-VB-1	0.6	14	6	451	2 44	11	<10	<4	21	275	<.4	5	<5	61	4.13	0.06	55	51
99-VB-2	0.5	10	8	488	2.31	30	<10	<4	16	465	<.4	<5	<5	57	0.92	0.066	45	73
99-VB-3	1.1	15	3	144	1 13	9	<10	<4	4	112	<.4	<5	<5	102	0.7	0.044	24	159
99-VB-4	<.5	15	8	531	2.4	20	<10	<4	11	270	<.4	<5	<5	63	4.79	0.1	33	77
99-VB-5	<.5	8	6	726	2.32	14	<10	<4	15	225	< 4	<5	<5	65	3.89	0.056	42	25
99-VB-6	0.6	10	4	288	2.06	18	<10	<4	15	231	<.4	<5	<5	57	0.71	0.059	52	100
99-VB-7	0.5	16	7	706	2.12	14	<10	<4	12	320	<.4	<5	<5	70	4.2	0.101	39	122
99-VB-8	<.5	7	7	191	1 08	6	<10	<4	13	478	< 4	<5	<5	25	0.78	0.026	40	215
99-TT-73	<.5	7	8	625	2.2	5	<10	<4	13	1091	<.4	<5	<5	49	1.51	0.042	41	25
99-TT-74	0.8	10	6	587	2.23	19	<10	<4	12	226	<.4	5	<5	105	1.12	0.04	38	108
99-TT-75	<.5	18	8	535	2.45	27	<10	<4	18	172	1.2	5	<5	88	1 08	0.065	49	65
99-TT-76	<.5	19	8	626	2.88	32	<10	<4	17	177	1.7	<5	<5	88	1 2	0.081	49	67
99-TT-87	0.7	9	3	200	0.77	88	<10	<4	5	47	<.4	<5	<5	33	2.85	0.036	13	102
99-TT-86	< 5	8	2	191	0 82	10	<10	<4	<2	91	< 4	<5	<5	26	7.5	0.024	7	130
99-TT-85	<.5	6	2	248	0.61	<5	<10	<4	3	76	<.4	<5	<5	16	4.73	0.023	10	154
99-TT-84	<.5	7	2	301	0.77	12	<10	<4	5	93	<.4	<5	<5	24	6.81	0.033	11	52
99-TT-63	<.5	16	4	96	0.89	29	<10	<4	2	60	<.4	<5	<5	53	0.1	0.036	5	199
99-TT-62	<.5	10	3	47	0.86	104	<10	<4	2	84	<.4	<5	<5	45	0.06	0.019	5	182
99-TT-81	<.5	10	2	50	0.9	137	<10	<4	2	46	<.4	<5	<5	51	0.04	0.02	5	167
99-TT-80	1.3	15	2	49	0 77	11	<10	<4	3	54	0.4	<5	<5	155	0 08	0.048	6	166
99-TT-79	1.5	29	2	53	0 96	27	<10	<4	2	108	1.2	<5	<5	145	0.38	0.197	7	196
99-TT-78	2	29	2	56	1.06	12	<10	<4	3	131	< 4	<5	<5	149	0.58	0.255	11	308
99-TT-77	2.2	30	2	65	1.29	13	<10	<4	3	84	< 4	<5	<5	142	0.3	0 148	8	333
99-VB-9	<.5	11	3	51	0.66	<5	<10	<4	2	34	<.4	<5	<5	31	0.04	0.013	6	182
99-VB-10	<.5	14	5	65	0.77	<5	<10	<4	3	59	<.4	<5	<5	24	0.14	0.013	6	174
99-VB-11	<.5	13	3	82	0.64	<5	<10	<4	2	30	<.4	<5	<5	16	0.03	0.009	4	184
99-VB-12	2.6	20	2	96	0.65	6	<10	<4	4	67	<.4	<5	<5	233	0.04	0.017	16	146
99-VB-13	<.5	42	22	976	5.38	68	<10	<4	31	326	1.9	6	<5	227	0.65	0.226	88	51
99-VB-14	2.4	29	4	41	0.93	21	<10	<4	4	103	<.4	<5	<5	302	0.06	0.054	18	107
99-VB-15	4	19	3	46	0.68	9	<10	<4	<2	73	<.4	5	<5	337	0.08	0.028	10	224
99-VB-16	0.5	17	4	99	1.21	42	<10	<4	6	51	< 4	<5	<5	75	0.05	0.031	13	147
99-VB-17	9.3	19	2	81	0.82	24	<10	<4	<2	162	0.5	8	<5	849	2.28	0.947	11	317
99-VB-18	5.5	39	<2	38	0.69	65	<10	<4	<2	227	7.2	10	<5	1003	2.27	0.92	11	256
99-VB-19	<.5	33	9	86	1.12	5	<10	<4	2	36	<.4	<5	<5	45	0.06	0.02	5	191
99-VB-20	0.7	18	3	60	0.91	6	<10	<4	3	35	<.4	<5	<5	87	0.04	0.017	9	177
99-VB-21	1.1	19	3	49	0.8	<5	<10	<4	3	35	<.4	<5	<5	202	0.04	0.009	9	189
99-TT-98	0.5	20	3	63	0.92	7	<10	<4	2	78	<.4	<5	<5	53	0.08	0.032	7	207
99-TT-99	0.8	16	2	53	0.8	5	<10	<4	3	60	<.4	<5	<5	83	0.05	0.027	11	236
99-TT-100	<.5	18	2	62	0 92	7	<10	<4	2	73	< 4	<5	<5	61	0.05	0.031	6	233
99-TT-101	<.5	17	2	62	0.82	5	<10	<4	2	48	<.4	<5	<5	55	0.04	0.014	4	260
99-TT-102	0.8	19	2	53	0.89	6	<10	<4	2	69	< 4	<5	<5	107	0 05	0.033	7	188
99-TT-103	<.5	23	5	68	0.92	<5	<10	<4	2	73	<.4	<5	<5	35	0.05	0.008	7	214
99-TT-104	<.5	21	4	40	0.91	6	<10	<4	<2	602	0 4	<5	<5	48	0.05	0.019	3	165
99-TT-105	<.5	24	5	173	0.79	7	<10	<4	2	98	0.5	<5	<5	52	0 08	0.021	5	197
99-TT-97	<.5	17	5	59	0.81	5	<10	<4	3	98	< 4	<5	<5	29	0.06	0.011	5	148
99-TT-96	<.5	15	5	126	0.9	5	<10	<4	2	93	< 4	<5	<5	33	0.06	0.015	5	131
99-TT-95	<.5	15	3	44	0.7	6	<10	<4	2	51	< 4	<5	<5	20	0.03	0.011	4	164
99-TT-94	<.5	12	3	164	0 83	<5	<10	<4	<2	39	< 4	<5	<5	16	0.03	0.008	4	158
99-TT-93	<.5	20	2	155	0.79	5	<10	<4	<2	34	<.4	<5	<5	26	0.05	0.012	4	196
99-TT-92	<.5	10	2	60	0 6	<5	<10	<4	2	36	<.4	<5	<5	34	0.05	0 007	5	238
99-TT-91	<.5	11	2	34	0.7	5	<10	<4	3	35	< 4	<5	<5	41	0 04	0.015	8	118
99-TT-90	<.5	11	3	31	0.78	8	<10	<4	2	51	< 4	<5	<5	61	0 05	0 028	10	121
99-TT-89	<.5	12	4	49	0.75	<5	<10	<4	2	47	< 4	<5	<5	25	0 07	0 034	6	157
99-TT-88	<.5	13	3	50	0.75	<5	<10	<4	2	67	< 4	<5	<5	46	0 11	0 029	7	134
99-VB-22	0.9	16	<2	45	0.6	7	<10	<4	2	92	< 4	<5	<5	127	0 14	0.027	8	278
99-VB-23	0.5	12	2	46	0.84	<5	<10	<4	3	49	< 4	<5	<5	46	0 06	0.026	6	188
99-VB-24	<.5	6	2	45	0.61	<5	<10	<4	3	66	< 4	<5	<5	65	0 07	0 03	7	127
99-VB-25	3.5	15	3	46	0.95	<5	<10	<4	2	125	< 4	<5	<5	161	0 06	0 037	9	334

TABLE I—CONT'D.

Sample	Mg total wt. percent	Ba total ppm	Ti total wt percent	Al total wt. percent	Na total wt. percent	K total wt percent	W total ppm	Zr total ppm	Sn total ppm	Y total ppm	Nb total ppm	Be total ppm	Sc total ppm
99-TT-72	0.6	793	0.27	6.26	1.14	2.71	<4	151	<2	32	18	3	6
99-TT-71	0.16	829	0.08	2.66	0.56	2.19	<4	92	2	29	23	2	1
99-TT-70	0.42	1102	0.27	5.95	0.75	2.79	<4	200	<2	37	21	3	6
99-TT-69	0.7	753	0.24	5.04	0.7	1.85	<4	131	2	33	17	3	5
99-TT-68	0.28	1240	0.11	1.79	0.13	0.87	<4	42	<2	16	6	1	3
99-VB-1	1.53	843	0.3	6.76	0.82	1.27	<4	132	<2	35	20	2	6
99-VB-2	1.24	598	0.27	6.18	1.03	1.58	<4	145	4	32	18	3	6
99-VB-3	0.29	872	0.09	1.85	0.11	0.8	<4	34	<2	16	4	1	3
99-VB-4	1.09	862	0.28	5.85	1.04	1.68	<4	88	<2	21	9	2	6
99-VB-5	1.86	686	0.28	6.24	0.47	0.8	<4	144	<2	30	16	2	6
99-VB-6	0.34	1374	0.2	4.03	0.94	2.13	<4	86	<2	33	15	2	4
99-VB-7	1.03	1176	0.24	5.17	0.7	1.41	<4	97	<2	28	11	2	5
99-VB-8	0.29	6357	0.09	2.84	0.35	1.65	<4	83	2	20	12	2	2
99-TT-73	0.8	4030	0.26	5.29	0.23	2.82	4	180	<2	36	20	3	6
99-TT-74	1.3	876	0.25	5.63	0.59	1.24	<4	127	2	31	16	3	6
99-TT-75	1.82	844	0.28	8.94	0.3	1.04	<4	148	<2	35	19	3	6
99-TT-76	1.3	822	0.36	7.4	0.5	1.24	<4	173	<2	36	19	3	7
99-TT-87	1.51	959	0.1	2.11	0.04	1.31	<4	31	<2	7	4	1	1
99-TT-88	4.2	839	0.03	1.05	0.05	0.81	<4	12	<2	7	2	<1	<1
99-TT-85	2.57	1499	0.07	1.8	0.52	1.02	<4	30	<2	9	5	<1	1
99-TT-84	3.6	873	0.09	2.04	0.19	0.77	<4	23	<2	8	4	<1	2
99-TT-83	0.12	1390	0.05	0.86	0.02	0.4	<4	12	<2	4	3	1	2
99-TT-82	0.1	1553	0.05	0.84	0.03	0.41	<4	13	<2	3	3	1	2
99-TT-81	0.12	1288	0.06	0.88	0.02	0.4	<4	14	<2	3	3	1	2
99-TT-80	0.16	1089	0.07	0.99	0.03	0.41	<4	20	<2	6	3	1	2
99-TT-79	0.14	1236	0.05	1	0.02	0.33	<4	17	<2	11	3	1	2
99-TT-78	0.18	1566	0.06	1.14	0.03	0.49	<4	14	<2	14	3	1	2
99-TT-77	0.19	1491	0.07	1.09	0.04	0.48	<4	28	<2	8	3	1	2
99-VB-9	0.13	2294	0.06	1.23	0.03	0.53	<4	14	<2	3	2	1	2
99-VB-10	0.12	4323	0.05	1.11	0.04	0.37	<4	14	<2	3	2	1	2
99-VB-11	0.06	1509	0.03	0.6	0.02	0.22	<4	8	<2	2	2	<1	1
99-VB-12	0.18	957	0.11	1.53	0.04	0.64	<4	25	<2	8	2	1	3
99-VB-13	0.36	3774	0.59	9.06	0.86	3.85	5	225	<2	23	15	2	15
99-VB-14	0.18	2252	0.11	1.91	0.04	0.83	<4	24	<2	9	3	1	4
99-VB-15	0.06	1672	0.03	0.58	0.02	0.23	<4	14	<2	12	<2	1	1
99-VB-16	0.29	1299	0.12	2.22	0.03	1.15	<4	32	<2	8	4	1	4
99-VB-17	0.11	743	0.06	1.14	0.03	0.41	<4	5	<2	38	<2	1	2
99-VB-18	0.06	422	0.05	0.88	0.02	0.33	<4	4	<2	27	<2	1	2
99-VB-19	0.33	6867	0.06	1.3	0.04	0.52	<4	12	2	3	3	1	2
99-VB-20	0.19	1816	0.08	1.48	0.03	0.67	<4	19	<2	5	3	1	3
99-VB-21	0.17	1391	0.08	1.46	0.07	0.66	<4	19	<2	8	2	1	2
99-TT-98	0.05	2031	0.04	0.59	0.03	0.24	<4	33	<2	4	2	<1	2
99-TT-99	0.05	1105	0.04	0.57	0.02	0.23	<4	21	<2	5	<2	<1	3
99-TT-100	0.06	1615	0.04	0.66	0.04	0.25	<4	26	<2	6	2	<1	3
99-TT-101	0.03	827	0.02	0.4	0.03	0.17	<4	14	<2	2	<2	<1	2
99-TT-102	0.07	1276	0.04	0.72	0.03	0.28	<4	24	<2	5	2	<1	3
99-TT-103	0.16	4280	0.05	1.23	0.06	0.57	<4	17	<2	6	2	1	3
99-TT-104	0.13	2503	0.04	0.94	0.07	0.39	<4	14	<2	4	<2	1	2
99-TT-105	0.07	3003	0.04	0.55	0.05	0.25	<4	19	<2	5	2	<1	3
99-TT-97	0.13	3511	0.04	0.81	0.06	0.39	<4	13	<2	4	3	1	2
99-TT-96	0.15	3667	0.06	0.95	0.05	0.49	<4	29	<2	4	3	1	2
99-TT-95	0.09	2195	0.04	0.74	0.04	0.42	<4	16	<2	4	3	1	2
99-TT-94	0.09	1928	0.04	0.71	0.04	0.34	<4	12	<2	3	4	1	1
99-TT-93	0.09	1117	0.04	0.77	0.04	0.37	<4	12	<2	3	2	1	1
99-TT-92	0.12	1436	0.05	0.98	0.05	0.52	<4	15	<2	3	3	1	2
99-TT-91	0.19	1046	0.06	1.27	0.05	0.64	<4	20	<2	4	4	1	3
99-TT-90	0.18	2481	0.08	1.32	0.06	0.69	<4	23	<2	6	4	1	3
99-TT-69	0.11	2991	0.05	0.93	0.06	0.49	<4	15	<2	3	3	1	2
99-TT-68	0.13	2458	0.06	1.01	0.05	0.5	<4	16	<2	6	3	1	2
99-VB-22	0.07	920	0.08	1	0.05	0.4	<4	19	<2	6	2	<1	2
99-VB-23	0.09	1239	0.06	1.14	0.05	0.42	<4	15	<2	7	2	<1	2
99-VB-24	0.11	993	0.07	1.34	0.04	0.6	<4	19	<2	6	2	1	2
99-VB-25	0.04	2058	0.04	0.55	0.02	0.24	<4	19	<2	7	2	<1	2

TABLE 1—CONT'D.

Sample	Latitude	Longitude	Ag partial ppm	As partial ppm	Au partial ppm	Bi partial ppm	Cd partial ppm	Cu partial ppm	Ga partial ppm	Hg partial ppm	Mo partial ppm	Pb partial ppm	Sb partial ppm	Se partial ppm	Te partial ppm	Tl partial ppm	Zn partial ppm	Mo total ppm	Cu total ppm	Pb total ppm	Zn total ppm
99-VB-26	41.05974	-116.33961	0.722	2.66	0	0.172	1.32	37.6	0.259	0.182	2.18	2.75	1.38	1.62	0.233	0.24	27.6	4	44	5	38
99-VB-27	41.05927	-116.33719	0.107	2.62	0.007	0.152	0.211	25.3	0.245	0.141	3.82	1.65	0.959	1.69	0.192	0.252	35.2	6	28	<5	45
99-VB-28	41.05779	-116.33559	0.126	2.33	0.003	0.161	1.32	30.4	0.365	0.18	2.26	3.38	1.01	1.41	0.161	0.2	22.3	2	36	6	28
99-VB-29	41.05855	-116.33354	0.98	3.54	0.0008	0.193	0.123	46.6	0.442	0.176	9.81	2.03	3.19	2.41	0.11	0.199	9.6	12	53	<5	12
99-VB-30	41.05783	-116.33075	0.82	3.15	0.006	0.134	0.234	11.1	0.185	0.374	5.77	2.74	0.98	11.9	0.146	0.217	15	7	12	<5	17
99-VB-31	41.05717	-116.3282	0.401	3.56	0.0003	0.183	0.064	20.2	0.509	0.175	6.87	2.54	1.42	3.35	0.162	0.389	2.64	7	21	<5	5
99-VB-32	41.056	-116.32567	0.078	1.65	0.0003	0.126	0.038	19.2	0.492	0.133	2.52	1.98	0.434	1.69	0.116	0.213	2.11	4	21	<5	7
99-VB-33	41.05463	-116.32339	0.035	0.832	0	0.157	0.042	12.7	0.221	0.09	1.15	3.05	0.505	0.52	0.141	0.353	4.52	2	16	6	11
99-VB-34	41.05429	-116.32155	0.102	4.78	0.0008	0.182	0.116	18.9	0.572	0.113	3.96	3.48	0.952	1.45	0.073	0.518	2.64	5	21	6	5
99-TT-113	41.05367	-116.31921	0.046	1.08	0.0002	0.185	0.037	20.2	0.293	0.078	3.36	2.34	0.493	0.845	0.151	0.523	4.62	5	25	17	25
99-TT-112	41.05426	-116.31678	0.142	18.8	0.01	0.242	0.402	46.4	1.09	0.397	15.2	4.65	2.01	3.78	0.282	0.349	563	16	58	6	600
99-TT-111	41.0553	-116.31588	0.444	3.01	0.01	0.232	0.065	41.5	1.1	0.45	8.12	4.32	2.11	12.1	0.122	0.384	2.57	10	48	6	9
99-TT-110	41.05492	-116.3141	0.028	1.02	0.0005	0.2	0.034	9.12	0.41	0.068	2.65	3.9	0.387	0.556	0.132	0.329	1.91	3	12	<5	7
99-TT-109	41.05473	-116.31241	0.073	2.54	0.0004	0.268	0.083	19.7	1.37	0.191	6.84	8.43	0.886	0.668	0.114	0.574	3.31	8	23	5	9
99-TT-108	41.05447	-116.31063	0.067	1.49	0.0006	0.192	0.113	16	0.482	0.098	3.78	3.08	0.533	0.959	0.152	0.174	3.26	4	18	<5	7
99-TT-107	41.05177	-116.30848	0.028	0.707	0.0002	0.165	0.044	8.95	0.53	0.077	4.99	3.74	0.342	0.334	0.124	0.235	2.38	6	11	11	8
99-TT-106	41.05279	-116.30588	0.127	13.8	0.003	0.213	1.02	72.6	0.789	0.035	14.3	4.72	3.3	0.821	0.166	0.523	111	15	71	<5	116
99-VB-35	41.05351	-116.3024	0.312	2.93	0.005	0.206	0.032	14.8	0.521	0.662	5	4.88	2.44	1.51	0.181	0.448	2.19	7	20	10	5
99-VB-36	41.05423	-116.30078	0.194	4.15	0.018	0.241	0.031	8.5	1.11	0.154	7.29	5.58	1.47	11.4	0.204	0.387	2.16	14	13	10	7
99-VB-37	41.05489	-116.29859	0.279	1.73	0.0003	0.199	0.022	18.8	0.571	0.219	3.86	2.56	0.78	5.49	0.216	0.286	1.79	5	23	7	6
99-VB-38	41.05514	-116.29899	0.844	1.38	0.007	0.164	0.029	7.85	0.112	0.091	4.4	1.69	0.855	0.539	0.189	0.262	2.18	5	11	<5	5
99-VB-39	41.05587	-116.29817	0.14	0.956	0.0003	0.214	0.023	10.5	0.586	0.162	5.01	1.36	0.855	1.64	0.091	0.14	1.7	7	15	<5	6
99-VB-40	41.05616	-116.29696	0.272	1.73	0.008	0.211	0.039	15	0.313	0.285	5.32	3.78	0.97	2.75	0.262	0.177	3.02	7	19	7	7
99-VB-41	41.0569	-116.29679	0.268	4.46	0.01	0.265	0.074	11.7	1.95	0.259	9.54	7.4	1.78	8.18	0.196	0.554	5.34	12	15	7	9
99-VB-42	41.05787	-116.29629	0.107	7.98	0.002	0.209	0.035	7.62	1.29	0.106	6.87	6.87	2.22	6.62	0.183	0.754	3.46	10	12	11	7
99-VB-43	41.0589	-116.2945	0.836	0.94	0.001	0.141	0.079	6.08	0	0.096	3.06	0.69	0.142	0.212	0.153	0.164	29.9	4	7	<5	40
99-VB-44	41.05938	-116.29312	5.6	2.05	0.002	0.168	0.536	13.3	0	0.128	2.83	2.68	0.438	1.48	0.173	0.244	135	3	16	9	182
99-VB-45	41.0606	-116.29117	0.137	0.655	0	0.157	0.092	15.4	0.046	0.079	4.79	1.55	0.182	1.02	0.144	0.19	5.75	7	18	<5	10
99-VB-46	41.06095	-116.28947	0.384	1.97	0	0.16	0.492	7.51	0.275	0.044	0.54	2.22	0.338	0.859	0.133	0.36	53.5	<2	8	8	57
99-VB-47	41.06265	-116.28719	0.058	3.4	0	0.208	0.291	11.8	0.493	0.059	5.45	4.6	0.362	0.398	0.166	0.319	46.1	7	13	10	51
99-TT-114	41.06515	-116.28611	0.15	3.92	0.001	0.161	0.159	25.3	0.307	0.085	2.48	4.34	1.01	0.767	0.165	0.121	20.6	3	31	9	30
99-TT-115	41.06705	-116.28625	0.104	1.08	0.003	0.152	0.098	7	0	0.036	2.91	0.974	0.242	0.235	0.121	0.138	10.9	4	9	<5	15
99-TT-116	41.06987	-118.28743	0.152	2.31	0	0.171	0.131	18.5	0.101	0.079	4.34	1.71	0.403	0.231	0.128	0.072	33.6	5	22	<5	45
99-TT-117	41.07177	-116.28814	0.041	0.821	0	0.157	0.055	11.7	0.053	0.114	2.8	1.63	0.192	0.169	0.116	0.025	4.24	3	14	5	9
99-TT-146	41.07387	-116.29014	0.084	0.783	0	0.151	0.046	6.92	0.114	0.048	2.96	1.2	0.214	0.045	0.151	0.236	3.31	5	9	<5	7
99-TT-145	41.07726	-116.29015	0.221	18.3	0.0002	0.17	0.367	21.2	0.595	0.461	4.88	7.36	2.16	9.32	0.187	1.6	63	7	27	12	72
99-TT-144	41.07826	-116.28697	0.046	1.27	0.0004	0.174	0.021	6.93	0.159	0.07	2.85	1.53	0.242	0.141	0.086	0.226	3.84	3	8	<5	5
99-TT-143	41.07916	-116.28462	0.046	0.321	0	0.151	0.028	5.71	0.083	0.039	3.27	0.889	0.223	0.027	0.131	0.3	1.65	4	7	<5	4
99-TT-142	41.08275	-116.28391	0.059	0.511	0	0.12	0.055	6.72	0.007	0.05	2.72	0.792	0.204	0	0.106	0.267	4.06	4	9	<5	6
99-TT-141	41.08552	-116.27965	0.036	0.762	0	0.141	0.022	6.26	0.018	0.033	3.03	0.877	0.135	0.237	0.113	0.253	1.69	4	8	<5	4
99-TT-140	41.08356	-116.2759	0.048	0.582	0	0.141	0.07	5.21	0.054	0.077	2.06	1.13	0.153	0.144	0.151	0.228	3.39	4	8	<5	6
99-TT-139	41.08165	-116.272	0.058	0.909	0.0002	0.162	0.055	29.2	0.294	0.08	2.42	2.69	0.318	0.276	0.18	0.201	5.53	3	32	12	12
99-TT-138	41.08157	-116.26838	0.255	6.88	0.004	0.22	0.912	129	1.17	0.197	4.44	4.28	1.75	2.15	0.336	0.259	1040	6	138	6	1033
99-TT-137	41.08242	-116.26739	0.547	1.24	0.003	0.179	0.115	21	0.717	0.153	2.68	3.57	1.04	4.63	0.201	0.16	6.63	3	28	8	12
99-TT-136	41.082	-116.26453	0.056	0.589	0.0003	0.16	0.032	4.98	0.071	0.049	3.72	1.25	0.157	0.29	0.17	0.128	5.92	3	7	<5	11
99-TT-135	41.08096	-116.26266	1.86	6.78	0.005	0.171	0.153	37.5	0.927	0.395	12.1	2.85	3.84	26.4	0.315	0.242	6.14	15	47	5	11
99-TT-134	41.08078	-116.26093	0.108	2.29	0.011	0.199	0.472	19.9	0.671	0.053	2.49	5.66	0.374	0.533	0.139	0.228	25.3	3	30	10	35
99-TT-133	41.08071	-116.25927	0.496	5.25	0	0.196	0.043	36.7	1.09	0.154	4.56	5.2	2.12	2.06	0.251	0.265	2.71	7	68	11	6
99-TT-132	41.08082	-116.25799	0.201	5.49	0	0.196	0.917	31.7	0.782	0.099	2.5	6.96	2.02	1.38	0.19	0.298	49.7	4	41	8	67
99-TT-131	41.08047	-116.25603	0.296	2.45	0.007	0.152	0.261	9.02	0.234	0.056	2.27	3.13	0.347	1.69	0.097	0.14	37.4	2	11	5	42
99-TT-130	41.07999	-116.25355	0.226	1.52	0.0002	0.175	0.274	4.05	0.082	0.02	1.47	1.38	0.282	0.953	0.136	0.019	37.3	<2	6	<5	43
99-TT-129	41.07651	-116.25321	0.203	1.69	0.0002	0.141	0.341	6.88	0.226	0.032	2.75	2.21	0.286	0.781	0.147	0.031	32.3	3	9	6	35

TABLE 1—CONT'D.

Sample	Ag total ppm	Ni total ppm	Co total ppm	Mn total ppm	Fe total wt.percent	As total ppm	U total ppm	Au total ppm	Th total ppm	Sr total ppm	Cd total ppm	Sb total ppm	Bi total ppm	V total ppm	Ca total wt percent	P total wt.percent	La total ppm	Cr total ppm
99-VB-26	2.9	17	5	79	0.69	<5	<10	<4	2	71	1 5	<5	<5	102	0 08	0.02	9	277
99-VB-27	0.8	24	4	56	0 88	5	<10	<4	2	347	< 4	<5	<5	96	0 12	0 061	8	199
99-VB-28	0 8	16	3	46	0 96	<5	<10	<4	3	85	1.6	<5	<5	85	0 07	0.022	6	187
99-VB-29	3 5	14	2	45	0.81	<5	<10	<4	2	68	< 4	5	<5	133	0.07	0.03	7	203
99-VB-30	1 6	10	2	44	1.09	<5	<10	<4	<2	37	<.4	<5	<5	46	0.06	0.086	4	276
99-VB-31	1 8	13	<2	50	0.81	<5	<10	<4	2	62	<.4	<5	<5	97	0.09	0.032	8	288
99-VB-32	<.5	8	2	48	0 89	<5	<10	<4	2	63	<.4	<5	<5	47	0.06	0.016	6	221
99-VB-33	<.5	10	2	47	0 71	<5	<10	<4	3	70	<.4	<5	<5	45	0.07	0.026	7	165
99-VB-34	< 5	15	2	45	1.89	<5	<10	<4	3	50	<.4	<5	<5	79	0.07	0.069	8	210
99-TT-113	<.5	17	2	38	1.2	<5	<10	<4	3	41	<.4	<5	<5	60	0.07	0.063	9	380
99-TT-112	0.9	40	4	71	10.51	25	<10	<4	3	60	<.4	5	<5	196	0.14	0.384	10	245
99-TT-111	2.1	24	2	24	1.2	6	<10	<4	5	53	<.4	<5	<5	193	0 16	0.225	15	179
99-TT-110	<.5	12	3	31	0.83	5	<10	<4	2	53	0 4	<5	<5	43	0.08	0.018	8	113
99-TT-109	<.5	10	<2	42	2.51	8	<10	<4	4	68	<.4	<5	<5	90	0 08	0.05	13	153
99-TT-108	< 5	16	4	46	0.86	<5	<10	<4	3	61	< 4	<5	<5	43	0 07	0 017	7	148
99-TT-107	<.5	11	2	47	0.87	7	<10	<4	3	66	<.4	<5	<5	41	0 06	0.013	9	142
99-TT-106	<.5	32	2	67	5.13	18	<10	<4	3	72	0.6	<5	<5	154	0 08	0.123	7	234
99-VB-35	0.6	16	3	43	1 22	<5	<10	<4	4	58	< 4	5	<5	81	0.07	0 028	9	410
99-VB-36	<.5	14	3	59	2.11	8	<10	<4	3	491	<.4	<5	<5	100	0.06	0.093	12	298
99-VB-37	0.6	14	2	45	1.04	<5	<10	<4	3	64	<.4	<5	<5	45	0.07	0.017	8	230
99-VB-38	2.6	13	2	57	0 64	<5	<10	<4	<2	27	<.4	<5	<5	45	0.13	0.037	3	229
99-VB-39	0.8	17	5	39	0.78	<5	<10	<4	3	484	<.4	5	<5	208	0.06	0.034	11	195
99-VB-40	0.6	11	3	29	0.83	<5	<10	<4	6	168	<.4	<5	<5	117	0.04	0.033	15	143
99-VB-41	0.5	8	<2	35	4.08	<5	<10	<4	4	638	< 4	5	<5	108	0.13	0 181	16	275
99-VB-42	0.5	7	<2	30	3.55	9	<10	<4	5	495	<.4	6	<5	214	0.06	0.184	17	225
99-VB-43	1.7	13	3	37	0.61	<5	<10	<4	2	87	< 4	<5	<5	12	0 04	0 015	6	162
99-VB-44	8	35	7	248	1.21	<5	<10	<4	2	264	0.7	<5	<5	26	0.09	0 027	8	181
99-VB-45	<.5	15	5	54	0.52	<5	<10	<4	2	91	<.4	<5	<5	17	0.04	0.015	9	158
99-VB-46	<.5	19	2	178	0.58	6	<10	<4	3	92	0.5	<5	<5	32	13.5	0.081	17	94
99-VB-47	<.5	21	2	71	1.16	7	<10	<4	2	119	< 4	<5	<5	36	0.29	0 124	20	263
99-TT-114	1.1	15	2	51	0.86	7	<10	<4	3	56	<.4	<5	<5	101	0.07	0.032	9	160
99-TT-115	<.5	11	<2	40	0 53	7	<10	<4	2	106	<.4	<5	<5	14	0.04	0.015	5	103
99-TT-116	0.5	22	2	55	2.26	6	<10	<4	2	88	< 4	<5	<5	19	0.15	0.271	8	237
99-TT-117	<.5	9	<2	56	0.77	<5	<10	<4	3	42	< 4	<5	<5	6	0.03	0.016	9	156
99-TT-146	0.5	12	<2	54	0.67	5	<10	<4	2	40	<.4	<5	<5	11	0.08	0.013	7	154
99-TT-145	0.9	28	3	47	4.35	20	<10	<4	4	56	<.4	<5	<5	205	0.09	0.061	10	272
99-TT-144	<.5	11	<2	46	0 58	<5	<10	<4	2	30	<.4	<5	<5	16	0.05	0.009	7	144
99-TT-143	<.5	9	<2	45	0.48	<5	<10	<4	2	20	<.4	<5	<5	7	0.03	0.006	6	139
99-TT-142	<.5	13	2	57	0.71	<5	<10	<4	<2	37	<.4	<5	<5	8	0.09	0.027	6	204
99-TT-141	<.5	10	<2	61	0.54	<5	<10	<4	<2	22	<.4	<5	<5	5	0.08	0.01	7	188
99-TT-140	<.5	10	2	69	0.49	<5	<10	<4	2	39	< 4	<5	<5	5	0.18	0.026	7	171
99-TT-139	<.5	12	<2	45	0.69	5	<10	<4	4	98	<.4	<5	<5	21	0.07	0.036	11	231
99-TT-138	0.8	212	13	100	9.83	<5	<10	<4	4	63	0.7	<5	<5	118	0.18	0 329	11	309
99-TT-137	1	19	2	39	0.78	6	<10	<4	4	87	<.4	<5	<5	98	0.14	0.025	12	344
99-TT-136	<.5	12	3	57	0.66	<5	<10	<4	2	37	<.4	<5	<5	10	0.05	0.042	7	190
99-TT-135	6.3	19	2	46	1 86	8	<10	<4	3	68	<.4	<5	<5	245	0.18	0 137	9	512
99-TT-134	0.8	15	4	42	0.67	5	<10	<4	3	460	<.4	<5	<5	222	0.36	0.139	13	198
99-TT-133	3.8	12	4	37	1.32	5	<10	<4	5	944	<.4	<5	<5	323	0.29	0.334	14	407
99-TT-132	0.8	39	11	68	1 59	<5	<10	<4	4	139	1.1	6	<5	179	0.18	0.057	15	193
99-TT-131	0.5	19	2	165	0.73	6	<10	<4	3	61	<.4	<5	<5	35	5.55	0.103	13	380
99-TT-130	0 7	11	<2	143	0.33	<5	<10	<4	2	58	<.4	<5	<5	18	13.79	0.083	15	144
99-TT-129	<.5	19	2	103	0.65	<5	<10	<4	3	70	<.4	<5	<5	23	5 96	0 153	14	258

TABLE 1—CONT'D.

Sample	Mg total wt. percent	Ba total ppm	Ti total wt. percent	Al total wt percent	Na total wt. percent	K total wt percent	W total ppm	Zr total ppm	Sn total ppm	Y total ppm	Nb total ppm	Be total ppm	Sc total ppm
99-VB-26	0.06	3478	0.04	0.76	0.03	0.35	<4	17	<2	15	2	1	1
99-VB-27	0.1	966	0.06	1.24	0.03	0.47	<4	17	<2	8	2	1	2
99-VB-26	0.12	1454	0.07	1.42	0.04	0.59	<4	18	<2	9	3	1	2
99-VB-29	0.04	970	0.03	0.48	0.01	0.19	<4	14	<2	7	<2	<1	1
99-VB-30	0.05	541	0.03	0.77	0.03	0.27	<4	23	<2	3	2	<1	1
99-VB-31	0.09	605	0.06	1.12	0.03	0.47	<4	26	<2	5	2	<1	2
99-VB-32	0.06	679	0.06	1.06	0.03	0.4	<4	16	<2	4	3	<1	2
99-VB-33	0.11	721	0.06	1.32	0.04	0.55	<4	16	<2	7	2	1	2
99-VB-34	0.09	1934	0.06	1.09	0.04	0.54	<4	15	<2	3	<2	1	3
99-TT-113	0.16	1124	0.08	1.54	0.05	0.73	<4	22	<2	5	3	1	3
99-TT-112	0.14	1432	0.09	1.65	0.05	0.72	<4	21	<2	7	2	2	3
99-TT-111	0.24	1753	0.12	2.33	0.09	1.01	<4	36	<2	7	3	1	6
99-TT-110	0.15	2959	0.08	1.44	0.05	0.66	<4	20	<2	4	3	1	3
99-TT-109	0.21	1323	0.12	1.94	0.06	1.16	<4	32	<2	5	4	1	4
99-TT-108	0.12	3298	0.07	1.23	0.04	0.57	<4	19	<2	4	3	1	3
99-TT-107	0.14	1069	0.08	1.45	0.04	0.7	<4	20	<2	4	3	1	3
99-TT-106	0.17	1500	0.06	1.71	0.05	0.61	<4	24	<2	4	2	1	3
99-VB-35	0.14	2096	0.08	1.34	0.04	0.68	<4	21	<2	3	3	<1	2
99-VB-36	0.12	2239	0.09	1.37	0.04	0.74	<4	24	<2	4	3	<1	3
99-VB-37	0.14	1040	0.09	1.33	0.04	0.61	<4	21	<2	3	3	<1	2
99-VB-38	0.02	622	0.02	0.24	0.01	0.09	<4	5	<2	3	<2	<1	<1
99-VB-39	0.12	4674	0.09	1.4	0.04	0.62	<4	26	<2	3	2	1	3
99-VB-40	0.13	1530	0.11	1.64	0.02	0.83	<4	42	<2	6	4	1	3
99-VB-41	0.13	234	0.12	1.3	0.07	1.11	<4	37	<2	6	4	1	3
99-VB-42	0.12	287	0.1	1.47	0.03	1.26	<4	36	<2	4	3	<1	3
99-VB-43	0.02	2458	0.02	0.21	0.01	0.12	<4	17	<2	2	2	<1	<1
99-VB-44	0.07	4860	0.02	0.3	0.01	0.19	<4	17	<2	4	<2	<1	<1
99-VB-45	0.05	4274	0.03	0.4	0.01	0.24	<4	18	<2	2	3	<1	<1
99-VB-46	8.84	1596	0.06	0.99	0.06	0.73	<4	20	<2	10	2	<1	2
99-VB-47	0.14	964	0.06	1.01	0.03	0.4	<4	24	<2	33	2	1	2
99-TT-114	0.1	923	0.06	1.21	0.02	0.46	<4	26	<2	13	3	1	3
99-TT-115	0.02	254	0.02	0.25	0.01	0.12	<4	20	<2	2	2	<1	<1
99-TT-116	0.03	1225	0.02	0.66	0.01	0.13	<4	11	<2	10	3	1	<1
99-TT-117	0.04	461	0.03	0.49	0.01	0.29	<4	25	<2	3	2	<1	<1
99-TT-146	0.03	226	0.02	0.33	<.01	0.11	<4	15	<2	2	2	<1	<1
99-TT-145	0.11	1609	0.09	1.12	0.03	0.62	<4	34	<2	6	2	1	3
99-TT-144	0.06	269	0.03	0.45	0.01	0.25	<4	24	<2	2	4	<1	<1
99-TT-143	0.03	327	0.02	0.32	0.01	0.13	<4	17	<2	<2	2	<1	<1
99-TT-142	0.02	807	0.02	0.21	0.01	0.1	<4	14	<2	3	2	<1	<1
99-TT-141	0.02	132	0.01	0.2	0.01	0.07	<4	13	<2	3	<2	<1	<1
99-TT-140	0.02	361	0.02	0.23	0.01	0.14	<4	17	<2	2	2	<1	<1
99-TT-139	0.09	1169	0.1	2.12	0.05	1.66	<4	67	<2	6	4	<1	1
99-TT-138	0.16	671	0.09	1.65	0.04	0.84	<4	36	<2	16	4	2	4
99-TT-137	0.21	630	0.11	1.79	0.04	0.94	<4	36	<2	7	5	1	3
99-TT-136	0.03	2079	0.02	0.31	<.01	0.14	<4	20	<2	2	2	<1	<1
99-TT-135	0.15	653	0.09	1.52	0.04	0.65	<4	33	<2	7	3	1	4
99-TT-134	0.12	3832	0.12	1.71	0.04	0.78	<4	32	<2	9	4	1	4
99-TT-133	0.1	4192	0.13	2.38	0.04	1.03	<4	41	<2	14	5	1	5
99-TT-132	0.25	8697	0.11	2.04	0.04	0.99	<4	29	<2	9	4	1	3
99-TT-131	3.39	339	0.08	1.49	0.05	0.97	<4	33	<2	13	3	<1	2
99-TT-130	8.78	171	0.04	0.6	0.05	0.45	<4	12	<2	12	2	<1	<1
99-TT-129	3.59	643	0.06	1.11	0.06	0.76	<4	17	<2	14	2	<1	1

TABLE 2—ANALYTICAL DATA FOR 40 ELEMENTS FROM 93 ROCKS IN THE SOUTHEAST PART OF THE BEAVER PEAK QUADRANGLE, NEV.

[ppm, parts per million; wt. percent, weight percent; partial, analysis by partial digestion methods; total, analysis by total digestion methods (see text); Coyote Mine, sample location at Coyote barite mine (see figs. 2, 19, 21, 22)]

Sample	Formation	Rock type	Latitude	Longitude	Ag partial ppm	As partial ppm	Au partial ppm	Bi partial ppm	Cd partial ppm	Cu partial ppm	Ga partial ppm	Hg partial ppm	Mo partial ppm	Pb partial ppm	Sb partial ppm	Se partial ppm	Te partial ppm	Tl partial ppm	Zn partial ppm
99-TT-152	Slaven	fault bx	41.028	-116.284	0.213	22.5	0.006	0.273	5.03	86.7	0.495	0.246	29.4	3.54	4.04	2	0.399	0.728	887
99-TT-153	Slaven	bx	41.028	-116.283	1.06	32.8	0.014	0.34	1.25	180	1.03	0.364	46.5	5.61	3.48	7.47	0.411	0.473	782
99-TT-154	Slaven	blk chert	41.029	-116.280	0.247	2.73	0.004	0.171	0.209	27.3	0.671	0.149	4.02	3.8	0.708	1.07	0.215	0.276	41.4
99-TT-155	Slaven	blk chert	41.029	-116.280	0.152	1.88	0.005	0.173	0.056	35.8	0.538	0.222	2.93	3.31	0.659	2.66	0.173	0.138	5.8
99-TT-156	Slaven	blk chert	41.029	-116.279	0.095	4.98	0	0.182	0.346	8.38	0.174	0.018	6.62	1.22	1	0.027	0.151	0.32	22.4
99-TT-157	Slaven	blk chert	41.029	-116.279	0.261	11.8	0.001	0.229	0.077	10.2	0.329	0.095	20.5	2.28	3.13	0.741	0.107	0.104	23.9
99-TT-158	Slaven	dk gy chert	41.029	-116.278	1.34	3.92	0.007	0.217	0.049	26	0.351	0.112	13.4	4.08	2.41	4.46	0.172	0.352	10.8
99-TT-159	Slaven	blk cherty sh	41.028	-116.276	0.556	4.69	0.002	0.16	0.325	20.5	0.575	0.071	10.4	4.07	2.04	2.58	0.156	0.532	11.4
99-TT-160	Slaven	blk shaley ch	41.028	-116.275	1.56	7.54	0	0.239	0.645	22.7	0.574	0.145	29	4.92	5.42	8.65	0.184	0.499	19.8
99-TT-161	Slaven	blk cherty sh	41.028	-116.273	1.7	7.03	0.0007	0.204	0.06	44.6	0.473	0.231	24	2.28	4.28	14.8	0.178	0.418	16.4
99-TT-162	Slaven	blk chert	41.027	-116.272	0.165	1.6	0.002	0.215	0.148	23.2	0.456	0.073	6.27	3.34	0.44	0.821	0.158	0.1	21.4
99-TT-163	Slaven	shaley ch	41.028	-116.272	0.623	3.2	0.003	0.213	0.789	46	0.672	0.177	9.49	3.02	1.88	2.74	0.147	0.183	44.7
99-TT-164	Slaven	blk chert	41.029	-116.273	0.736	2.65	0.004	0.203	0.982	32.4	0.64	0.202	8.11	3.73	0.876	2.17	0.2	0.391	68.2
99-TT-166	Slaven	shaley ch	41.038	-116.287	0.105	3.85	0	0.204	0.257	26.7	0.643	0.14	5.37	5.88	1.52	1.35	0.101	0.261	112
99-TT-167	Slaven	shaley ch	41.037	-116.286	0.113	4.73	0.003	0.232	0.052	23.8	1.46	0.087	7.75	8.27	0.671	0.471	0.143	0.219	20.7
99-TT-168	Slaven	gossan	41.037	-116.285	0.07	12.5	0	0.257	2.62	39.5	1.74	0.146	23.3	7.36	0.559	0.542	0.153	0.292	150
99-TT-169	Slaven	chert bx	41.037	-116.284	0.033	0.856	0	0.19	0.075	30.4	0.663	0.155	3.48	4.6	0.36	0.201	0.151	0.162	7.28
99-TT-170	Slaven	cherty sh	41.036	-116.283	0.171	6.21	0.025	0.207	0.064	45.1	0.889	1.95	6.16	7.83	0.991	2.28	0.099	0.409	18
99-TT-171	Slaven	gy chert	41.038	-116.282	0.026	0.567	0.01	0.211	0.039	13.9	0.817	0.029	2.44	4.02	0.357	0.343	0.16	0.216	6.28
99-TT-172	Slaven	shale	41.036	-116.281	1.84	8.5	0.0008	0.242	0.478	35.9	0.727	0.253	23.8	6.1	9.41	12.3	0.184	0.448	33.5
99-TT-173	Elder	shaley silt	41.035	-116.279	0.018	0.675	0	0.192	189	60.7	4.19	0	0.463	2.57	0.241	0.277	0.236	0.194	3832
99-TT-174	Elder	chert	41.034	-116.276	0.189	4.06	0.001	0.237	0.926	34.7	1.09	0.038	7.92	10.4	1.6	1.43	0.203	0.458	72.9
99-TT-175	Elder	siltstone	41.033	-116.276	0.025	0.649	0	0.238	0.762	14.9	3.67	0	0.343	1.71	0.366	0.203	0.127	0.329	34.7
99-TT-176	Elder	siltstone	41.033	-116.275	0.028	1.28	0	0.239	0.036	11	2.52	0.02	0.8	6.24	0.252	0.205	0.069	0.268	22.3
99-TT-177	Slaven	chert	41.032	-116.274	0.43	6.26	0.006	0.198	0.62	18.8	0.515	0.055	5.72	2.5	3.9	6.71	0.136	0.341	31.4
99-VB-48	Vinini	gy chert	41.006	-116.268	0.339	3.25	0.008	0.223	0.521	81.1	0.847	0.33	4.21	9.01	1.61	3.84	0.276	0.184	79.6
99-VB-49	Vinini	shaley ch	41.005	-116.267	0.857	4.31	0.004	0.166	0.754	49.1	0.607	0.13	12.2	2.75	3.02	9.35	0.18	0.41	75.4
99-VB-50	Vinini	shaley ch	41.004	-116.267	0.257	3.65	0.0008	0.191	1.97	29.1	1.16	0.122	5.92	4.89	1.18	3.07	0.16	0.261	133
99-VB-51	Vinini	shaley ch	41.003	-116.267	0.071	1.38	0.0003	0.173	0.1	46.6	1.05	0.038	3.41	4.91	0.47	0.736	0.143	0.12	24.5
99-VB-52	Vinini	blk shaley	41.002	-116.267	2.07	13.9	0.004	0.231	0.76	45.3	1.26	0.279	14.8	8.67	3.36	5.53	0.141	0.393	26.2
99-VB-53	Vinini	blk shale	41.001	-116.267	0.214	3.82	0.001	0.189	0.916	26.6	0.361	0.056	3.77	2.34	1.21	1.83	0.141	0.341	68.5
99-TT-178	Slaven	shaley ch	41.031	-116.272	0.558	4.64	0.003	0.24	1.43	45.3	0.579	0.263	26.1	5.1	1.93	3.12	0.181	0.474	55.1
99-TT-179	Slaven	blk chert	41.032	-116.286	0.042	0.831	0	0.209	0.112	45.7	1.29	0.062	2.82	1.84	0.402	0.247	0.142	0.25	21.6
99-TT-180	Slaven	fault bx	41.031	-116.286	0.257	4.23	0.005	0.215	0.43	30.6	1.07	0.203	6.9	3.19	1.15	1.86	0.22	0.247	77.7
99-TT-181	Slaven	fault bx	41.031	-116.285	0.894	27.2	0.013	0.242	0.556	79.3	1.13	0.468	14.7	4.54	3.81	3.21	0.298	0.553	189
99-TT-182	Slaven	blk chert	41.031	-116.283	0.412	3.09	0.009	0.213	0.148	56.1	1.05	0.38	6.24	5.25	2.11	4.69	0.234	0.224	25.5
99-TT-183	Slaven	blk chert	41.032	-116.283	0.211	1.97	0.007	0.205	0.134	28.2	0.84	0.307	3.68	4.55	0.795	2.52	0.26	0.254	35.2
99-TT-184	Slaven	chert	41.033	-116.281	0.133	1.82	0.003	0.178	0.033	21.9	0.488	0.173	3.6	2.01	1.31	1.01	0.213	0.157	11.7
99-TT-185	Slaven	blk chert	41.033	-116.283	0.415	1.98	0.007	0.206	0.079	47.2	0.736	0.266	6.77	4.9	0.905	2.36	0.184	0.175	50.7
99-TT-186	Slaven	grn chert	41.034	-116.283	0.025	1.15	0	0.186	0.083	18.7	0.873	0.099	2.4	2.83	0.288	0.996	0.111	0.068	13.8
99-TT-187	Slaven	brn chert	41.034	-116.285	0.022	0.607	0	0.204	0.124	22.3	0.852	0.034	5.59	2	0.311	0	0.177	0.191	14.9
99-TT-188	Slaven	blk chert	41.034	-116.287	0.066	1.51	0.001	0.239	0.06	28.5	1.08	0.125	2.59	4.93	0.359	0.338	0.17	0.225	19.3
99-TT-192	Slaven	blk chert	41.025	-116.280	0.325	1.18	0.004	0.153	0.055	24.6	0.609	0.18	3.82	2.99	0.625	0.978	0.172	0.236	7.01
99-TT-193	Slaven	chert	41.026	-116.279	0.198	3.07	0.004	0.216	0.321	37.7	0.87	0.185	4.58	2.72	1.05	2.39	0.247	0.229	99.3
99-TT-194	Elder	grn chert	41.026	-116.278	0.04	0.503	0.001	0.19	0.351	85.7	4.1	0.043	0.651	10.5	0.429	0.116	0.13	0.31	57.4
99-TT-195	Slaven	blk chert	41.027	-116.276	1.52	3.55	0.005	0.173	0.862	27.8	0.539	0.131	4.98	3.4	2.33	3	0.23	0.211	75.3
99-TT-196	Slaven	blk chert	41.027	-116.276	1.16	3.36	0.005	0.188	0.1	28.3	0.893	0.189	6.72	3	1.59	3.52	0.185	0.427	22
99-TT-197	Slaven	chert	41.025	-116.275	0.757	4.22	0.008	0.228	0.287	38.4	1.04	0.398	9.39	3.22	1.61	3.38	0.228	0.385	63.2
99-TT-198	Slaven	blk shale	41.025	-116.275	1.33	4.82	0.006	0.196	0.118	41.9	0.739	0.276	6.74	2.7	1.92	6.48	0.178	0.272	22.6
99-TT-199	Slaven	blk chert	41.024	-116.275	0.886	7.26	0.003	0.198	0.767	22.8	0.582	0.161	8.4	3.02	3.19	8.57	0.209	0.4	57.9
99-TT-200	Slaven	chert	41.022	-116.275	0.126	3.7	0.0006	0.279	0.41	61.1	2.39	0.104	4.29	7.21	0.726	1.09	0.268	0.27	101
99-TT-201	Elder	chert	41.007	-116.268	0.021	1.33	0	0.284	0.044	21.8	0.371	0.016	4.08	11.1	0.553	0	0.189	0.057	8.59
99-TT-202	Elder	cherty silt	41.008	-116.269	0.024	0.186	0.0002	0.188	0.093	14.5	3.06	0.055	1.77	3.72	0.251	0	0.084	0.169	25.4
99-TT-203	Slaven	chert	41.009	-116.269	0.048	1.01	0.0007	0.26	0.233	46	1.06	0.082	4.27	3.19	0.509	0.088	0.238	0.11	56.2
99-TT-204	Slaven	gossan	41.011	-116.269	0.707	56.3	0.006	0.309	1.8	70.8	1.36	0.292	42.3	4.82	4	4.93	0.437	0.138	1531
99-TT-205	Slaven	shale	41.012	-116.269	0.922	7.43	0.003	0.466	0.295	81.5	2.23	0.479	35.9	13.3	7.26	9.8	0.175	0.832	17.9
99-TT-206	Vinini	cherty sh	41.004	-116.260	0.04	5.56	0.009	0.171	0.17	25.8	0.898	0.187	9.91	1.87	1.35	17.8	0.164	0.345	30.2
99-TT-207	Vinini	cherty mudst	41.003	-116.260	0.817	6.28	0.004	0.253	0.129	83	0.87	0.378	21.9	3.24	3.18	7.73	0.165	0.292	7.77
99-TT-208	Vinini	cherty sh	41.003	-116.260	0.313	4.06	0.005	0.204	0.162	48.1	0.65	0.263	11.9	2.63	1.22	2.49	0.206	0.24	9.61
99-TT-209	Vinini	cherty sh	41.002	-116.260	0.673	4.84	0.0008	0.213	0.112	69.2	0.754	0.341	20.8	2.52	4.57	6.14	0.187	0.42	14
99-TT-210	Vinini	cherty sh	41.001	-116.258	0.08	2.04	0.002	0.183	0.033	35.3	0.417	0.177	4.31	2.81	0.822	1.04	0.134	0.27	3.38
99-TT-211	Vinini	cherty sh	41.000	-116.257	0.095	2.96	0.006	0.192	0.064	26.4	0.627	0.207	5.12	3.87	1.32	0.943	0.213	0.329	3.33
99-TT-212	Elder	calc siltstone	41.006	-116.260	0.053	11	0	0.194	0.057	21.5	3.32	0.08	1.28	6.19	0.355	0	0.124	0.36	28.6
99-TT-213	Elder	chert	41.000	-116.284	0.038	0.687	0.0006	0.222	0.098	19.5	0.201	0.041	2.86	4.63	0.565	0	0.229	0.136	15.4

TABLE 2—CONT'D.

Sample	Mo total ppm	Cu total ppm	Pb total ppm	Zn total ppm	Ag total ppm	Ni total ppm	Co total ppm	Mn total ppm	Fe total wt percent	As total ppm	U total ppm	Au total ppm	Th total ppm	Sr total ppm	Cd total ppm	Sb total ppm	Bi total ppm	V total ppm	Ca total wt. percent
99-TT-152	31	95	5	965	<.5	304	109	6521	4.84	31	<10	<4	2	80	5.6	<5	<5	245	0.12
99-TT-153	49	204	10	870	2.3	289	186	8285	5.47	40	<10	<4	3	88	1.1	<5	<5	599	0.08
99-TT-154	6	33	<5	44	0.7	22	7	125	0.93	6	<10	<4	2	163	<.4	<5	<5	69	0.79
99-TT-155	3	38	<5	7	0.6	12	3	52	0.85	6	<10	<4	2	47	<.4	<5	<5	54	0.05
99-TT-156	8	9	<5	26	<.5	13	7	132	1.61	10	<10	<4	<2	27	<.4	<5	<5	36	0.02
99-TT-157	20	11	<5	26	<.5	12	2	57	2.21	16	<10	<4	<2	31	<.4	<5	<5	83	0.05
99-TT-158	14	26	<5	15	2.1	18	3	49	1.36	7	<10	<4	2	34	<.4	<5	<5	61	0.13
99-TT-159	9	20	<5	14	0.9	13	4	44	1.23	7	<10	<4	3	48	<.4	<5	<5	59	0.16
99-TT-160	28	23	5	21	2.3	36	3	40	1.04	6	<10	<4	2	58	0.4	6	<5	227	0.33
99-TT-161	22	45	<5	16	2.7	31	2	44	0.95	10	<10	<4	<2	19	<.4	<5	<5	358	0.03
99-TT-162	8	25	<5	22	<.5	20	3	117	0.92	<5	<10	<4	2	37	<.4	<5	<5	36	0.04
99-TT-163	10	50	<5	48	1.3	29	3	54	0.89	7	<10	<4	<2	81	0.5	<5	<5	189	0.25
99-TT-164	13	34	<5	69	1.6	27	3	96	1.01	7	<10	<4	<2	53	0.6	<5	<5	72	0.06
99-TT-166	7	32	6	122	<.5	30	11	152	2.32	6	<10	<4	2	85	<.4	<5	<5	128	0.1
99-TT-167	9	25	7	24	<.5	24	5	87	1.49	8	<10	<4	2	55	<.4	<5	<5	49	0.07
99-TT-168	21	41	6	146	<.5	432	64	4657	3.84	18	<10	<4	2	65	2.3	<5	<5	32	0.07
99-TT-169	3	30	<5	9	<.5	22	7	327	1.3	<5	<10	<4	<2	208	<.4	<5	<5	29	0.06
99-TT-170	6	45	<5	21	<.5	22	4	150	1.99	9	<10	<4	2	195	<.4	<5	<5	103	0.12
99-TT-171	2	14	<5	10	<.5	14	5	48	0.87	8	<10	<4	2	64	<.4	<5	<5	24	0.04
99-TT-172	23	38	<5	41	2.7	48	3	52	1.19	14	<10	<4	4	43	0.5	10	<5	433	0.08
99-TT-173	<2	48	<5	2815	<.5	248	4	322	1.64	<5	<10	<4	7	59	164.6	<5	<5	38	1.59
99-TT-174	8	35	9	79	0.7	52	7	91	0.92	5	<10	<4	2	108	1.3	<5	<5	284	0.5
99-TT-175	<2	12	<5	34	<.5	15	5	1345	1.82	<5	<10	<4	5	50	0.7	<5	<5	45	2.8
99-TT-176	<2	9	<5	22	<.5	9	4	1023	1.6	6	<10	<4	5	146	<.4	<5	<5	25	9.07
99-TT-177	5	18	<5	33	1	18	3	71	1.1	8	<10	<4	2	47	0.4	<5	<5	73	0.15
99-VB-48	4	88	9	66	1.2	40	4	221	1.57	5	<10	<4	3	56	<.4	<5	<5	120	0.09
99-VB-49	13	54	6	82	2.9	45	4	113	1.09	<5	<10	<4	3	62	1	8	<5	185	0.23
99-VB-50	5	31	5	136	<.5	41	7	65	1.23	8	<10	<4	4	86	2	<5	<5	110	0.5
99-VB-51	6	48	<5	26	<.5	31	7	123	1.12	5	<10	<4	3	35	<.4	<5	<5	81	0.14
99-VB-52	12	43	7	32	3.4	24	2	39	1.91	18	<10	<4	4	49	0.7	6	<5	148	0.1
99-VB-53	3	29	<5	68	<.5	25	2	77	0.88	5	<10	<4	<2	28	0.9	<5	<5	128	0.07
99-TT-178	29	51	<5	56	1.6	54	5	221	0.86	<5	<10	<4	<2	46	1.4	<5	<5	175	0.09
99-TT-179	2	46	<5	23	<.5	25	5	136	1.03	5	<10	<4	<2	49	<.4	<5	<5	29	0.05
99-TT-180	7	31	5	81	0.6	26	6	189	1.59	5	<10	<4	3	119	0.4	<5	<5	74	0.1
99-TT-181	14	78	<5	183	2	41	9	370	5.34	32	<10	<4	2	46	<.4	<5	<5	246	0.05
99-TT-182	6	56	7	27	0.7	18	2	62	1.82	<5	<10	<4	3	40	<.4	<5	<5	77	0.05
99-TT-183	3	29	8	41	<.5	17	2	66	1.58	5	<10	<4	2	33	<.4	<5	<5	43	0.03
99-TT-184	3	23	<5	14	<.5	10	2	60	0.87	<5	<10	<4	<2	25	<.4	<5	<5	44	0.03
99-TT-185	7	50	<5	58	0.8	21	3	59	1.89	6	<10	<4	3	58	<.4	<5	<5	82	0.05
99-TT-186	2	20	7	20	<.5	14	7	69	1.06	<5	<10	<4	3	84	<.4	<5	<5	29	0.05
99-TT-187	8	23	<5	18	<.5	24	4	218	1.08	<5	<10	<4	2	47	<.4	<5	<5	26	0.04
99-TT-188	3	28	8	22	<.5	18	5	63	1.18	<5	<10	<4	2	65	<.4	<5	<5	38	0.07
99-TT-192	4	26	7	10	<.5	19	4	110	0.99	<5	<10	<4	2	43	<.4	<5	<5	35	0.06
99-TT-193	4	37	5	104	<.5	27	3	80	1.84	<5	<10	<4	2	50	<.4	<5	<5	66	0.04
99-TT-194	<2	56	13	55	<.5	34	7	281	1.79	<5	<10	<4	7	47	<.4	<5	<5	63	1.79
99-TT-195	5	29	8	84	1.9	26	4	81	1.05	9	<10	<4	2	64	1	5	<5	52	0.12
99-TT-196	7	29	8	28	1.6	25	4	63	1.29	5	<10	<4	2	48	<.4	<5	<5	56	0.2
99-TT-197	13	42	7	71	1.5	33	3	93	1.26	5	<10	<4	<2	60	<.4	<5	<5	103	0.27
99-TT-198	7	44	<5	26	2.5	27	3	61	1.43	5	<10	<4	2	41	<.4	<5	<5	79	0.04
99-TT-199	8	26	5	67	1.2	24	4	54	1.54	8	<10	<4	2	67	0.8	6	5	99	0.13
99-TT-200	3	58	11	108	<.5	30	6	81	1.47	11	<10	<4	6	65	0.6	<5	<5	64	0.1
99-TT-201	10	25	14	11	<.5	25	8	867	1.09	<5	<10	<4	<2	26	<.4	<5	<5	55	0.15
99-TT-202	<2	14	7	28	<.5	18	5	92	1.48	<5	<10	<4	3	30	<.4	<5	<5	61	0.16
99-TT-203	3	45	<5	62	<.5	29	5	141	0.96	6	<10	<4	3	68	<.4	<5	<5	36	0.06
99-TT-204	40	74	11	1669	2.3	273	10	812	18.02	63	<10	<4	4	261	<.4	13	<5	162	0.14
99-TT-205	31	74	19	26	1.5	41	2	34	1.57	<5	<10	<4	7	66	<.4	8	<5	737	0.05
99-TT-206	11	26	5	34	<.5	19	3	252	2.25	10	<10	<4	<2	43	<.4	<5	<5	86	0.04
99-TT-207	23	83	<5	10	3.3	22	2	45	0.91	8	<10	<4	<2	42	<.4	5	<5	210	0.11
99-TT-208	12	51	5	14	1.5	18	2	84	0.9	6	<10	<4	2	57	<.4	<5	<5	99	0.06
99-TT-209	22	81	<5	18	3.5	24	2	49	0.72	5	<10	<4	<2	40	<.4	7	<5	366	0.08
99-TT-210	5	39	6	8	<.5	17	2	66	0.81	6	<10	<4	<2	40	<.4	<5	<5	39	0.04
99-TT-211	5	27	<5	6	<.5	12	2	56	0.85	5	<10	<4	2	35	<.4	<5	<5	45	0.03
99-TT-212	<2	19	13	31	<.5	16	6	889	1.92	<5	<10	<4	6	82	<.4	<5	<5	37	6.07
99-TT-213	3	25	9	18	<.5	16	5	716	0.71	<5	<10	<4	2	24	<.4	<5	<5	38	0.16

TABLE 2—CONT'D.

Sample	P total wt. percent	La total ppm	Cr total ppm	Mg total wt. percent	Ba total ppm	Ti total wt. percent	Al total wt percent	Na total wt. percent	K total wt percent	W total ppm	Zr total ppm	Sn total ppm	Y total ppm	Nb total ppm	Be total ppm	Sc total ppm
99-TT-152	0.181	5	405	0.1	1341	0.03	0.63	0.05	0.29	<4	22	2	4	<2	1	2
99-TT-153	0.329	9	489	0.18	2594	0.08	1.3	0.06	0.7	<4	40	<2	10	2	2	4
99-TT-154	0.328	7	532	0.09	5563	0.04	0.6	0.06	0.34	<4	6	<2	9	<2	<1	2
99-TT-155	0.021	6	555	0.09	2192	0.04	0.68	0.05	0.33	<4	19	<2	4	3	<1	3
99-TT-156	0.348	5	275	0.11	1600	0.05	0.89	0.04	0.33	<4	12	<2	6	2	<1	2
99-TT-157	0.404	7	340	0.15	1626	0.06	1.1	0.04	0.43	<4	15	<2	5	2	<1	2
99-TT-158	0.168	6	322	0.09	1118	0.05	0.85	0.05	0.44	<4	16	<2	3	3	<1	1
99-TT-159	0.378	6	303	0.15	3269	0.06	1.15	0.04	0.49	<4	18	<2	6	2	<1	2
99-TT-160	0.227	6	461	0.12	1537	0.05	0.89	0.05	0.44	<4	14	<2	10	<2	<1	2
99-TT-161	0.093	4	494	0.06	1552	0.03	0.46	0.03	0.19	<4	16	<2	5	<2	<1	<1
99-TT-162	0.012	5	317	0.1	1301	0.04	0.7	0.05	0.36	<4	18	<2	4	3	<1	2
99-TT-163	0.101	7	521	0.13	2075	0.04	0.77	0.04	0.4	<4	20	<2	10	2	<1	2
99-TT-164	0.021	7	277	0.11	1825	0.05	0.73	0.05	0.39	<4	24	<2	5	2	<1	3
99-TT-166	0.038	5	501	0.16	5896	0.06	1.11	0.06	0.54	<4	16	<2	4	2	<1	2
99-TT-167	0.027	8	249	0.28	2957	0.08	1.57	0.07	0.71	<4	19	<2	5	3	<1	3
99-TT-168	0.057	7	264	0.35	4073	0.07	1.46	0.06	0.58	<4	18	<2	7	3	<1	3
99-TT-169	0.014	5	259	0.15	3131	0.06	1.14	0.06	0.55	<4	14	<2	6	3	<1	2
99-TT-170	0.095	7	295	0.22	1158	0.07	1.3	0.08	0.72	<4	19	<2	7	3	<1	3
99-TT-171	0.013	6	372	0.21	3290	0.07	1.3	0.06	0.71	<4	16	<2	4	3	<1	2
99-TT-172	0.138	7	386	0.2	1564	0.08	1.32	0.06	0.68	<4	22	<2	5	2	<1	2
99-TT-173	0.028	20	63	1.84	986	0.19	3.31	0.36	1.89	<4	43	<2	10	5	<1	5
99-TT-174	0.148	8	373	0.37	1975	0.06	0.94	0.07	0.48	<4	12	<2	10	<2	<1	2
99-TT-175	0.024	16	25	2.85	751	0.17	3.31	0.27	1.75	<4	29	<2	9	6	<1	5
99-TT-176	0.033	20	44	5.86	1432	0.12	2.39	0.59	1.2	<4	23	<2	14	5	<1	3
99-TT-177	0.04	5	243	0.17	1583	0.06	0.92	0.08	0.41	<4	15	<2	2	2	<1	2
99-VB-48	0.034	9	471	0.18	1028	0.07	1.14	0.06	0.63	<4	33	<2	9	3	<1	4
99-VB-49	0.069	9	535	0.2	1274	0.07	1.12	0.07	0.53	<4	20	<2	8	2	<1	2
99-VB-50	0.201	12	435	0.3	1404	0.1	1.49	0.06	0.82	<4	27	<2	14	4	<1	3
99-VB-51	0.033	7	484	0.3	990	0.08	1.27	0.06	0.64	<4	18	<2	5	3	<1	2
99-VB-52	0.507	9	400	0.28	792	0.11	1.87	0.05	0.96	<4	26	<2	24	4	<1	4
99-VB-53	0.008	3	600	0.06	651	0.03	0.54	0.03	0.24	<4	10	<2	2	<2	<1	1
99-TT-178	0.036	5	313	0.05	957	0.02	0.37	0.03	0.18	<4	13	<2	7	<2	<1	2
99-TT-179	0.008	6	248	0.25	2580	0.05	1.07	0.06	0.48	<4	15	<2	4	3	<1	3
99-TT-180	0.197	12	477	0.26	3833	0.08	1.5	0.07	0.75	<4	24	<2	8	4	<1	3
99-TT-181	0.603	8	490	0.18	2993	0.05	1.02	0.04	0.41	<4	7	<2	9	<2	1	4
99-TT-182	0.04	8	329	0.14	1524	0.07	0.96	0.05	0.54	<4	33	<2	5	4	<1	4
99-TT-183	0.022	6	342	0.09	1340	0.05	0.7	0.05	0.37	<4	24	<2	3	3	<1	3
99-TT-184	0.018	4	297	0.05	930	0.03	0.47	0.04	0.21	<4	17	<2	2	2	<1	2
99-TT-185	0.05	8	347	0.15	1979	0.07	1.07	0.06	0.58	<4	36	<2	5	5	<1	5
99-TT-186	0.013	7	205	0.24	6038	0.08	1.49	0.07	0.84	<4	22	<2	6	3	<1	3
99-TT-187	0.009	5	250	0.19	1995	0.05	1.02	0.07	0.49	<4	15	<2	4	3	<1	3
99-TT-188	0.013	5	290	0.17	3162	0.06	1.1	0.06	0.51	<4	17	<2	4	3	<1	3
99-TT-192	0.016	4	325	0.07	2672	0.03	0.47	0.05	0.25	<4	17	<2	2	2	<1	2
99-TT-193	0.047	6	371	0.12	1602	0.05	0.85	0.05	0.45	<4	26	<2	4	3	<1	3
99-TT-194	0.031	17	51	2.23	759	0.19	3.66	0.26	1.98	<4	44	<2	10	6	1	6
99-TT-195	0.033	4	293	0.13	2210	0.06	1.01	0.07	0.56	<4	23	<2	2	3	<1	2
99-TT-196	0.097	7	263	0.15	1427	0.06	1.12	0.06	0.61	<4	27	<2	5	3	<1	3
99-TT-197	0.125	7	341	0.09	1252	0.05	0.67	0.05	0.36	<4	24	<2	7	3	<1	3
99-TT-198	0.052	5	620	0.08	1563	0.04	0.6	0.05	0.32	<4	29	<2	6	2	<1	2
99-TT-199	0.096	5	452	0.14	2151	0.06	1.07	0.06	0.57	<4	24	<2	3	2	<1	2
99-TT-200	0.044	14	121	0.53	1933	0.14	2.32	0.06	1.35	<4	51	<2	10	7	1	7
99-TT-201	0.045	8	484	0.15	671	0.03	0.84	0.05	0.56	<4	13	<2	8	2	<1	3
99-TT-202	0.034	12	75	1.29	933	0.11	1.98	0.06	1.02	<4	27	<2	10	6	<1	4
99-TT-203	0.021	8	201	0.2	1449	0.07	1.13	0.05	0.6	<4	27	<2	6	4	<1	4
99-TT-204	0.989	15	174	0.17	1381	0.07	1.34	0.04	0.86	<4	2	<2	15	<2	1	4
99-TT-205	0.178	21	226	0.46	816	0.21	3.55	0.07	1.92	<4	59	<2	14	6	1	9
99-TT-206	0.042	5	350	0.06	664	0.03	0.45	0.04	0.21	<4	17	<2	2	2	<1	2
99-TT-207	0.099	4	554	0.05	552	0.03	0.46	0.03	0.21	<4	15	<2	10	<2	<1	1
99-TT-208	0.039	4	371	0.05	645	0.03	0.49	0.05	0.21	<4	20	<2	6	2	<1	2
99-TT-209	0.037	4	299	0.04	775	0.03	0.41	0.03	0.18	<4	15	<2	7	<2	<1	1
99-TT-210	0.017	4	274	0.04	556	0.03	0.43	0.04	0.22	<4	14	<2	2	<2	<1	2
99-TT-211	0.065	5	269	0.05	744	0.03	0.49	0.03	0.24	<4	19	<2	3	2	<1	2
99-TT-212	0.032	20	34	4.42	1290	0.18	3.46	0.49	1.86	<4	44	<2	11	4	<1	5
99-TT-213	0.024	6	557	0.1	790	0.04	0.69	0.04	0.4	<4	11	<2	4	2	<1	2

TABLE 2—CONT'D.

Sample	Formation	Rock type	Latitude	Longitude	Ag	As	Au	Bi	Cd	Cu	Ga	Hg	Mo	Pb	Sb	Se	Te	Tl	Zn
					partial ppm	partial ppm	partial ppm	partial ppm	partial ppm	partial ppm	partial ppm	partial ppm	partial ppm	partial ppm	partial ppm	partial ppm	partial ppm	partial ppm	partial ppm
99-TT-214	Slaven	blk chert	41 001	-116 285	0 842	6.18	0.005	0.157	0.511	35.9	1.09	0.225	6.62	6.94	2 18	27.5	0.697	0.282	26.3
99-TT-215	Slaven	shaley ch	41 002	-116 287	1 32	5 54	0.002	0.2	2.58	112	0.6	0.39	10.3	5.29	2.87	8 06	0.217	0.324	33.3
99-TT-216	Slaven	blk chert	41 003	-116 288	1.38	5.96	0.005	0 203	0 471	40.6	0.563	0.149	8.09	2.93	3.68	9.28	0.184	0.379	24.5
99-TT-217	Vinini	blk chert	41 003	-116 289	0 07	0 913	0.0002	0 151	0.231	38.1	1 09	0.024	3.19	5.73	0.517	0.839	0 172	0.25	30.2
99-TT-218	Vinini	chert	41.004	-116 29	0 055	2 04	0 008	0 176	0.177	15.8	0.645	0.073	4.18	1.77	0.465	1.79	0.139	0.232	11.2
99-TT-219	Vinini	blk chert	41.005	-116 291	0.225	2.39	0 0007	0 263	0.247	57.4	0.836	0.208	11.8	5.32	1.01	1 27	0.322	0.298	65.9
99-TT-220	Vinini	blk chert	41.006	-116.292	0.08	0.925	0 0007	0.182	0 09	25.2	1.29	0.077	2.44	2.79	0 767	0.411	0.18	0.274	17.5
99-TT-221	Vinini	blk limestone	41.007	-116.294	0.101	2 58	0.0004	0.095	1.31	4.57	0	0.017	1.41	1.65	1.07	0 2	0 112	0.192	60.1
99-TT-222	Vinini	blk chert	41.007	-116.296	0.412	2 25	0.005	0 144	0.558	50 3	1.16	0.203	3.91	3.71	0.942	3.19	0.156	0 285	56.3
99-TT-223	Elder	shaly silt	41 007	-116.297	0.02	0 204	0.0006	0 22	0.067	17.9	2.81	0.026	1.01	3.27	0.159	0	0.129	0 327	27 3
99-TT-224	Vinini	cherty sh	41.006	-116.298	0.027	3.13	0.0005	0.226	0.05	18	0.18	0.073	5.66	14.9	1.66	0.2	0.159	0 239	15.2
99-TT-225	Vinini	blk chert	41.005	-116.299	0.144	1.53	0.011	0.198	0.04	32 4	0.87	0.119	2.81	3.7	0.635	1.17	0.141	0.092	12 7
99-TT-226	Vinini	fault bx	41.004	-116.3	0.078	25.8	0.001	0.417	1.55	101	3.06	0 148	9.68	50 3	9.46	22.8	0.58	0 255	162
99-TT-227	Vinini	shaley ch	41.003	-116.3	0.043	2.73	0 0003	0.253	0 223	34.2	0.367	0.021	2.66	19.8	0.718	0.17	0.297	0.155	45 5
99-TT-228	Vinini	cherty sh	41.001	-116.301	1.01	7.81	0.003	0.182	3.19	46	0.66	0.14	8.89	3.92	3.9	4.27	0.163	0.323	83.7
99-TT-118	Slaven	blk chert	Coyote Mine	Coyote Mine	0.735	9.48	0.002	0.241	2	35.2	0.564	0.426	17.8	5.48	3.6	15	0.26	0.495	191
99-TT-119	Slaven	shaley ch	Coyote Mine	Coyote Mine	0.267	5.28	0.0003	0.277	[illegible]	17.3	0.617	0.447	22.6	7.41	2 83	5.13	0.171	0.749	98.6
99-TT-120	Slaven	gossan	Coyote Mine	Coyote Mine	0 411	23 2	0.014	0.522	0.703	22.3	0.581	0.123	48.1	5 9	2.95	25.5	0.402	0.371	60.7
99-TT-121	Slaven	brn chert	Coyote Mine	Coyote Mine	0.707	9.54	0.009	0.191	0 751	38.2	0.469	0.3	10.4	4.44	1.55	17.6	0.351	0.114	213
99-TT-122	Slaven	blk chert	Coyote Mine	Coyote Mine	0.514	4.73	0.003	0.286	2.01	28.8	0.871	0.182	15.5	5 32	1.29	5.61	0.239	0.49	74.9
99-TT-123	Slaven	brn chert	Coyote Mine	Coyote Mine	0.134	2.8	0.0001	0.274	0.576	39.5	0.869	0.129	12.4	2.73	0.535	0.992	0.133	0.462	154
99-TT-124	Slaven	blk shale	Coyote Mine	Coyote Mine	0.361	2.79	0.002	0 173	0 438	21.1	0.099	0.289	5.71	3.25	1.65	2.6	0.112	0.409	64.4
99-TT-125	Slaven	shaly argill	Coyote Mine	Coyote Mine	0.046	0.295	0.0007	0.119	0.147	7.06	0.025	0.194	0.563	0.726	0.267	0.017	0.15	0.174	16.6
99-TT-126	Slaven	blk shale	Coyote Mine	Coyote Mine	0.614	7.89	0.0003	0.297	0 717	28.4	0.605	0.553	15.8	10.8	6.97	10.2	0.188	0.786	47.9
99-TT-127	Slaven	shaley ch	Coyote Mine	Coyote Mine	0.867	7.75	0.002	0 343	0.766	37.9	0.833	0.601	25.8	8.16	7.96	15.3	0.169	0.505	23.9
99-TT-128	Slaven	shale	Coyote Mine	Coyote Mine	0.62	8 23	0.032	0.356	1.01	76.2	1 58	0.735	11.9	9.27	2.47	5.25	0.222	0.591	105
99-TT-189	Slaven	gossan	Coyote Mine	Coyote Mine	0.22	5 29	0.001	0.107	76.8	200	0.654	0.595	20.4	2 62	2.09	1.98	0	3.36	6448
99-TT-190	Slaven	gossan	Coyote Mine	Coyote Mine	0.219	3.53	0.0009	0.181	0.852	49.1	0.403	0.253	5.02	9 67	1.75	1.36	0.172	0.064	137
99-TT-191	Slaven	gossan	Coyote Mine	Coyote Mine	0.178	1.84	0 002	0.153	4.21	46.4	0.051	0.304	11.4	2.19	0.453	1.55	0.167	1.14	263

TABLE 2—CONT'D.

Sample	Mo	Cu	Pb	Zn	Ag	Ni	Co	Mn	Fe	As	U	Au	Th	Sr	Cd	Sb	Bi	V	Ca
	total	total	total	total	total	total	total	total	total	total	total	total	total	total	total	total	total	total	total
	ppm	ppm	ppm	ppm	ppm	ppm	ppm	ppm	wt percent	ppm	ppm	ppm	ppm	ppm	ppm	ppm	ppm	ppm	wt. percent
99-TT-214	7	41	11	29	2 5	20	2	56	1.63	15	<10	<4	3	61	<.4	6	<5	116	0.12
99-TT-215	15	142	9	36	4.3	58	2	58	0 69	9	<10	<4	<2	57	3	<5	<5	307	0.15
99-TT-216	10	50	6	29	3.2	35	3	58	1 09	9	<10	<4	2	64	0 4	7	<5	191	0.09
99-TT-217	3	43	10	30	<.5	30	7	82	1.04	5	<10	<4	2	48	< 4	<5	<5	90	0.14
99-TT-218	5	18	<5	12	< 5	15	2	54	0 79	<5	<10	<4	2	42	<.4	<5	<5	32	0.03
99-TT-219	14	70	6	67	1	36	5	201	0 96	5	<10	<4	2	63	<.4	<5	<5	58	0.48
99-TT-220	2	26	9	17	<.5	8	2	31	0 88	7	<10	<4	2	23	< 4	<5	<5	38	0.02
99-TT-221	<2	5	<5	51	< 5	5	<2	458	0 23	5	<10	<4	<2	328	1	<5	<5	75	33.61
99-TT-222	4	57	6	58	1 1	30	3	55	0.97	7	<10	<4	2	119	0.8	<5	<5	93	0.5
99-TT-223	<2	19	8	27	<.5	15	5	650	1.62	<5	<10	<4	4	38	<.4	9	<5	40	1.74
99-TT-224	6	22	19	16	<.5	27	12	2701	1.63	6	<10	<4	<2	37	<.4	5	<5	27	0.08
99-TT-225	6	41	17	15	0.6	20	4	77	0 94	6	<10	<4	2	32	< 4	<5	<5	41	0.07
99-TT-226	10	113	55	156	0.5	36	5	566	11.04	35	<10	<4	3	44	< 4	18	<5	127	0.17
99-TT-227	3	40	26	46	< 5	27	24	1375	0.97	<5	<10	<4	<2	30	< 4	<5	<5	64	0.14
99-TT-228	12	60	6	99	3.1	43	3	162	0.73	9	<10	<4	<2	59	3 9	5	<5	375	0.28
99-TT-118	24	46	8	269	1.2	69	4	64	1.78	12	5	2	3	84	2 5	5	2.5	356	0.13
99-TT-119	33	25	10	121	0 25	71	4	56	0 85	2.5	5	2	2	38	1 7	<5	2.5	391	0 07
99-TT-120	51	26	9	76	0.25	23	4	49	4.4	33	5	2	4	56	0.2	5	2.5	63	0.04
99-TT-121	14	47	9	247	1	71	6	63	2.89	9	5	2	4	143	0.7	<5	2.5	113	0 27
99-TT-122	18	35	8	96	0.25	40	6	71	1 63	6	5	2	4	144	2.4	<5	2.5	84	0.33
99-TT-123	13	45	2.5	178	0 25	72	44	5474	2 88	6	5	2	3	82	0.2	<5	2.5	34	0.03
99-TT-124	8	27	2.5	86	0 25	33	6	480	1.05	2 5	5	2	1	921	0.7	2.5	2.5	104	0.08
99-TT-125	1	10	2.5	24	0.25	5	3	63	0.21	2.5	5	2	1	1869	0.4	2.5	2.5	15	0 02
99-TT-126	21	36	12	69	0 8	42	3	67	1.55	2 5	5	2	5	79	1.1	10	2.5	240	0 04
99-TT-127	34	49	9	41	1.2	47	4	47	1.21	2.5	5	2	3	46	1	9	2 5	505	0.03
99-TT-128	14	80	14	118	0.6	49	4	106	1.46	8	5	2	4	54	1 3	<5	2.5	249	0.1
99-TT-189	2	181	<5	7371	<.5	1776	491	67090	22.54	<5	<10	<4	2	125	62.1	<5	<5	21	0.03
99-TT-190	4	52	10	154	0.5	43	9	608	2 86	9	<10	<4	3	88	<.4	5	<5	46	0.04
99-TT-191	9	43	<5	254	<.5	165	19	5714	6.15	5	<10	<4	<2	1136	2.9	<5	<5	15	1 68

TABLE 2—CONT'D.

Sample	P	La	Cr	Mg	Ba	Ti	Al	Na	K	W	Zr	Sn	Y	Nb	Be	Sc
	total	total	total	total	total	total	total	total	total	total	total	total	total	total	total	total
	wt. percent	ppm	ppm	wt. percent	ppm	wt percent	wt percent	wt. percent	wt. percent	ppm	ppm	ppm	ppm	ppm	ppm	ppm
99-TT-214	0.073	8	433	0.23	1171	0.1	1.58	0.06	0.88	<4	37	<2	6	4	1	4
99-TT-215	0.016	4	566	0.04	708	0.03	0.46	0.04	0.22	<4	32	<2	9	<2	1	1
99-TT-216	0.083	4	581	0.09	899	0.05	0.81	0.06	0.44	<4	30	<2	3	2	1	2
99-TT-217	0.046	7	449	0.29	1044	0.08	1.31	0.07	0.71	<4	19	<2	6	3	1	3
99-TT-218	0.013	4	277	0.06	641	0.03	0.5	0.05	0.25	<4	21	<2	2	2	<1	3
99-TT-219	0.212	7	465	0.12	960	0.05	0.85	0.05	0.45	<4	17	<2	10	2	1	3
99-TT-220	0.005	8	296	0.19	1147	0.07	1.37	0.03	0.68	<4	24	<2	3	4	1	3
99-TT-221	0.076	3	16	0.33	547	0.02	0.25	0.02	0.12	<4	4	<2	5	<2	<1	<1
99-TT-222	0.178	9	257	0.16	1233	0.07	1.16	0.07	0.57	<4	28	<2	10	3	1	3
99-TT-223	0.02	15	49	1.76	642	0.14	2.72	0.26	1.39	<4	35	<2	7	5	1	6
99-TT-224	0.017	5	501	0.08	661	0.03	0.68	0.05	0.42	<4	14	<2	5	2	1	2
99-TT-225	0.022	6	314	0.13	1280	0.06	0.82	0.05	0.4	<4	24	<2	6	2	1	3
99-TT-226	0.205	16	313	0.17	566	0.09	1.35	0.04	0.58	<4	10	2	12	3	2	5
99-TT-227	0.04	9	388	0.1	692	0.03	0.77	0.06	0.48	<4	14	<2	9	<2	1	2
99-TT-228	0.084	3	492	0.03	737	0.03	0.39	0.04	0.16	<4	8	<2	7	<2	1	<1
99-TT-118	0.192	12	446	0.27	371	0.09	1.75	0.07	0.69	2	25	1	37	2	1	4
99-TT-119	0.023	8	424	0.16	1304	0.08	1.29	0.12	0.56	2	22	1	10	1	1	3
99-TT-120	0.285	7	452	0.26	2141	0.07	1.51	0.07	0.83	2	21	1	6	2	1	3
99-TT-121	0.203	8	437	0.22	2446	0.09	1.57	0.06	0.78	2	27	1	10	3	2	4
99-TT-122	0.164	12	365	0.35	930	0.11	2.35	0.08	1.11	2	31	1	10	4	1	5
99-TT-123	0.167	8	407	0.27	2392	0.07	1.67	0.07	0.73	2	21	1	7	3	1	4
99-TT-124	0.094	3	77	0.16	1188	0.06	1.07	0.03	0.4	2	18	1	5	2	1	2
99-TT-125	0.012	1	14	0.03	2646	0.01	0.19	0.01	0.04	2	4	1	1	2	0.5	0.5
99-TT-126	0.054	11	330	0.4	231	0.15	2.45	0.06	1.33	2	43	1	7	4	1	5
99-TT-127	0.028	8	372	0.2	2954	0.09	1.43	0.05	0.67	2	31	1	6	1	1	3
99-TT-128	0.072	19	235	0.48	1628	0.14	2.71	0.06	1.3	2	40	3	16	5	1	7
99-TT-189	0.424	11	66	0.01	7766	0.02	0.89	0.01	0.2	<4	48	<2	39	<2	<1	1
99-TT-190	0.305	5	470	0.17	3885	0.07	1.77	0.06	0.62	<4	19	<2	6	3	1	3
99-TT-191	0.117	<2	32	1.01	1372	0.01	0.31	0.01	0.04	<4	5	<2	12	<2	<1	1

Table 3—Lower detection limits of analytical data for rock samples from the Santa Renia Fields and Beaver Peak 7-1/2 minute quadrangles, Nevada.

[ppm, parts per million; wt. percent, weight percent]

U.S. Mineral Laboratories, Inc. (USML, partial digestion, see text) (ppm)

Ag	0.015	Hg	0.1
As	1.	Mo	0.1
Au	0.0005	Pb	0.25
Bi	0.25	Sb	0.25
Cd	0.1	Se	1.
Cu	0.05	Te	0.5
Ga	0.5	Tl	0.5
		Zn	1.

Acme Analytical Laboratories, Inc. (Acme, total digestion, see text)

Ag	0.5 ppm	Ni	2.0 ppm
Al	0.01 wt. percent	P	0.002 wt. percent
As	5. ppm	Pb	5. ppm
Au	4. ppm	Sb	5. ppm
Ba	1. ppm	Sc	1. ppm
Be	1. ppm	Sn	2. ppm
Bi	5. ppm	Sr	2. ppm
Ca	0.01 wt percent	Th	2. ppm
Cd	0.4 ppm	Ti	0.01 wt. percent
Co	2. ppm	U	10. ppm
Cr	2. ppm	V	2. ppm
Cu	2. ppm	W	4. ppm
Fe	0.01 wt. percent	Y	2. ppm
K	0.01 wt. percent	Zn	2. ppm
La	2. ppm	Zr	2. ppm
Mg	0.01 wt. percent		
Mn	5. ppm		
Mo	2. ppm		
Na	0.01 wt. percent		
Nb	2. ppm		

TABLE 4—ANALYTICAL DATA FOR 15 ELEMENTS FROM 72 ROCKS FROM THE BOULDER CREEK AREA (SAMPLE GROUP 3) OF THE BEAVER PEAK QUADRANGLE, NEV.

[ppb, parts per billion; ppm, parts per million; minus sign (-), less than value shown; N.A., not available; N.D., not determined; partial, analysis by partial digestion methods (see text)]

Sample	UTM-Easting	UTM-Northing	Description	Au ppb partial	Ag ppm partial	As ppm partial	Sb ppm partial	Hg ppb partial	Cu ppm partial	Pb ppm partial	Zn ppm partial	Mo ppm partial	Bi ppm partial	Te ppm partial	Tl ppm partial	Ga ppm partial	Se ppm partial	Cd ppm partial
B-97-1	554,800	4,548,910	N.A.	8	-0.1	-3	-2	81	163.8	7.3	48	-0.5	-1	-2	-0.5	N.D.	N.D.	N.D.
B-97-2	554,854	4,549,295	N.A.	-2	-0.1	-3	-2	48	110.6	2.9	18.1	-0.5	-1	-2	-0.5	N.D.	N.D.	N.D.
B-97-3	554,904	4,549,126	N.A.	4	0.2	-3	-2	888	190.4	8	45.2	3.6	-1	-2	-0.5	N.D.	N.D.	N.D.
B-97-4	555,012	4,549,122	N.A.	-2	0.2	-3	-2	186	196	6.2	80.1	3.1	-1	-2	-0.5	N.D.	N.D.	N.D.
B-97-5	555,140	4,549,300	N.A.	-2	-0.1	-3	-2	77	119.7	4.8	5.1	-0.5	-1	-2	-0.5	N.D.	N.D.	N.D.
B-97-6	556,053	4,549,950	N.A.	-2	-0.1	-3	-2	86	176.8	2.2	8	-0.5	-1	-2	-0.5	N.D.	N.D.	N.D.
B-97-7	555,864	4,549,925	N.A.	-2	-0.1	-3	-2	50	226.9	5.9	14	0.7	-1	-2	-0.5	N.D.	N.D.	N.D.
B-97-8	555,749	4,549,931	N.A.	4	0.1	-3	-2	35	254.2	7.5	9.6	3.6	-1	-2	-0.5	N.D.	N.D.	N.D.
B-97-9	555,661	4,550,014	N.A.	-2	-0.1	-3	-2	86	285.2	3.4	5.9	-0.5	-1	-2	-0.5	N.D.	N.D.	N.D.
B-97-10	555,566	4,550,029	N.A.	10	0.1	-3	-2	127	294.5	6.8	13	4	-1	-2	-0.5	N.D.	N.D.	N.D.
B-97-11	555,397	4,550,122	N.A.	-2	-0.1	-3	-2	103	207.2	7	9	3.9	-1	-2	-0.5	N.D.	N.D.	N.D.
B-97-12	555,329	4,550,206	N.A.	-2	-0.1	-3	-2	55	156.7	1.9	4.5	0.6	-1	-2	-0.5	N.D.	N.D.	N.D.
K-97-36	555,067	4,550,277	N.A.	2	-0.1	-3	-2	70	135	3.8	5	2.1	-1	-2	-0.5	N.D.	N.D.	N.D.
K-97-37	555,132	4,550,254	N.A.	-2	-0.1	-3	-2	60	135.3	3.6	4.9	-0.5	-1	-2	-0.5	N.D.	N.D.	N.D.
K-97-36	555,301	4,550,199	N.A.	-2	-0.1	-3	-2	53	161.3	3.4	2.2	-0.5	-1	-2	-0.5	N.D.	N.D.	N.D.
K-97-69	555,276	4,547,863	Ovq brx, FeOx, brx foliation 342 deg x vert	2	-0.1	-3	-2	85	120.1	4.4	47.3	6.6	-1	-2	-0.5	N.D.	N.D.	N.D.
K-97-70	555,888	4,547,590	Ov as brx, goeth + green FeOx	25	-0.1	19	-2	300	139.4	6.1	59.9	13.1	-1	-2	-0.5	N.D.	N.D.	N.D.
K-97-74	555,095	4,548,465	dike, lathy feldspar, porous + wk FeOx	3	-0.1	-3	-2	327	33.5	5.5	7	6.8	-1	-2	0.5	N.D.	N.D.	N.D.
K-97-75	555,103	4,548,685	Ovq brx, in fault zone, str FeOx	3	-0.1	-3	-2	55	112.6	2.7	31.6	0.6	-1	-2	-0.5	N.D.	N.D.	N.D.
K-97-76	555,165	4,548,247	Ovq, sanded, brown-yellow goeth+lim FeOx, tr mm clear Q vnlts	-2	-0.1	3	-2	55	144.1	3	73.6	3	-1	-2	-0.5	N.D.	N.D.	N.D.
K-97-77	555,158	4,548,183	Ovq brx, bleached, silicif fault gouge, FeOx	-2	-0.1	-3	-2	82	165.6	3.4	228.8	8.4	-1	-2	-0.5	N.D.	N.D.	N.D.
K-97-78	555,198	4,548,057	dike, feldspar porphyry, white argil alt, yellow FeOx, jarosite in vugs	-2	-0.1	-3	-2	-10	50.7	18.1	16.8	11.7	-1	-2	2.3	N.D.	N.D.	N.D.
K-97-79	555,235	4,548,074	Ovq brx, brown gossanous FeOx, footwall of K-97-78 dike	-2	-0.1	83	-2	136	157.5	7.7	149.5	16.6	-1	-2	-0.5	N.D.	N.D.	N.D.
K-97-80	555,324	4,547,966	Pol, hem + lim gouge in str altered (argil??) zone	3	-0.1	3	-2	164	170.5	6.3	16.3	9.4	-1	-2	1.1	N.D.	N.D.	N.D.
K-97-81	554,490	4,548,680	Pol, brx, FeOx as goeth + lim	-2	-0.1	-3	-2	245	155.2	4.2	165.5	9.6	-1	-2	-0.5	N.D.	N.D.	N.D.
102350	554,810	4,545,475	green chert, str brx w/ lim+hem+jarosite, liesegang band	21	-0.2	8	-5	477	51	11	19	8	-5	N.D.	N.D.	N.D.	N.D.	N.D.
102351	554,900	4,546,250	green chert, str FeOx and local clay alt of fault gouge	10	0.4	56	14	1610	243	26	56	17	-5	N.D.	N.D.	N.D.	N.D.	N.D.
102352	555,040	4,546,825	FeOx "sponge" rock w/ matrix of clear Q vnlts, tr silicif	8	0.4	40	5	236	102	4	497	13	-5	N.D.	N.D.	N.D.	N.D.	N.D.
102353	557,450	4,546,425	chert-mudst brx, str limonite, gossanous	7	-0.2	14	-5	92	125	3	2565	9	-5	N.D.	N.D.	N.D.	N.D.	N.D.
102354	557,440	4,546,360	chert-mudst brx, str limonite, gossanous	8	-0.2	16	-5	121	79	-2	1876	33	-5	N.D.	N.D.	N.D.	N.D.	N.D.
102355	557,150	4,546,300	Pol ss + cong, silicified + mod FeOx	74	-0.2	5	-5	110	16	6	11	4	-5	N.D.	N.D.	N.D.	N.D.	N.D.
102356	557,125	4,546,575	Pol, str FeOx gouge, silicified	-5	-0.2	12	-5	78	13	-2	91	2	-5	N.D.	N.D.	N.D.	N.D.	N.D.
102357	554,550	4,544,220	green-gray thick bed chert brx, red hematite stain,	3	-0.1	12	3	59	206.5	10.8	7.2	16.9	-1	0.2	1.6	N.D.	N.D.	N.D.
102358	554,530	4,544,410	chert brx, str FeOx as lim + goeth, tr hematite	10	-0.1	24	3	171	194.5	8.6	33	37.1	-1	0.1	-0.5	N.D.	N.D.	N.D.
102359	554,350	4,545,200	chert brx, FeOx as mod goeth + tr lim, mod milky Q vnlts	6	0.2	16	4	100	187.2	4	33.8	16	-1	0.1	-0.5	N.D.	N.D.	N.D.
102360	554,910	4,545,450	chert brx, str FeoX brx matrix, rock flour actually	4	-0.1	7	3	179	234.6	4.2	22.1	12	-1	0.1	-0.5	N.D.	N.D.	N.D.
102361	555,310	4,545,315	chert brx, bleached, str yellow FeOx	25	1	7	5	238	287.8	6.8	52.2	18.3	-1	0.2	-0.5	N.D.	N.D.	N.D.
102362	555,430	4,545,540	chert brx, bleached, str yellow FeOx	73	-0.1	3	2	169	233.7	5.8	8.1	7.6	-1	0.1	-0.5	N.D.	N.D.	N.D.
102363	555,590	4,545,915	green chert brx, v str hematite gouge zones	14	-0.1	4	3	118	163.5	6.9	25.1	12	-1	-0.1	-0.5	N.D.	N.D.	N.D.
102364	555,740	4,546,040	black ch brx, w/ FeOx fracs + local yellow FeOx brx matrix	5	0.2	6	3	246	194.6	5.9	5.3	10.7	-1	-0.1	2.2	N.D.	N.D.	N.D.
102365	555,650	4,545,360	green and gray chert, brx, bleached	8	-0.1	14	4	201	255.6	5.3	127.7	9.1	-1	-0.1	-0.5	N.D.	N.D.	N.D.
102366	555,675	4,545,410	chert brx, liesegang band, bleached, FeOx lim + hem	55	0.2	15	5	364	223.6	8.4	21.9	33.5	-1	0.2	-0.5	N.D.	N.D.	N.D.
102367	556,000	4,545,520	chert, liesegang band, local clay alt brx	58	0.4	23	5	329	265.7	10.3	112.2	23.9	-1	-0.1	-0.5	N.D.	N.D.	N.D.
102368	556,675	4,545,000	chert, total brx, str yellow FeOx + minor hem + goeth	19	-0.1	9	2	159	226.2	5.3	26.4	7.3	-1	-0.1	1.2	N.D.	N.D.	N.D.
102369	556,800	4,545,075	chert, str brx, tr liesegang band	8	-0.1	1	2	144	187	4	7.5	3.4	-1	-0.1	-0.5	N.D.	N.D.	N.D.
102370	557,420	4,544,825	chert, str brx, tr liesegang band	8	-0.1	9	2	140	186.8	4.8	590	21.7	-1	-0.1	-0.5	N.D.	N.D.	N.D.
102371	557,830	4,544,850	green ch brx, local white Q vn frags in brx, local str FeOx	6	-0.1	10	3	220	256	5.7	25.1	5.2	-1	0.1	-0.5	N.D.	N.D.	N.D.
102372	559,830	4,545,620	black carb siltstone, tan weathered, liesegang band bedding	3	0.4	2	2	96	27.4	2.9	66.9	2.6	-1	-0.1	-0.5	N.D.	N.D.	N.D.
102381	528,972	4,579,671	felsic volc, wk silicif, local str FeOx + minor clay alt	4	-0.1	17	2	92	80.3	3.1	12.4	2	13.7	0.5	-0.5	N.D.	N.D.	N.D.
102382	554,120	4,542,520	green-gray chert, str FeOx fracs-brx, FeOx as goethite	1.27	0.161	5.77	1.2	105	251	5.46	61.8	3.62	0.111	0.034	0.194	1.06	0.4	0.414
102363	554,210	4,545,450	green-gray ch, brx, tr to mod FeOx on fracs	1.57	0.0224	1.52	0.445	42	277	2.74	9.68	1.83	0.109	0	0.12	0.969	0.073	0.068
102384	554,130	4,545,870	green-gray ch, brx, tr to mod FeOx on fracs, bleached, hem stain	1.52	0.025	2.66	0.638	51	283	4.09	15.2	2.13	0.038	0	0.069	0.614	0.45	0.23
102385	554,030	4,546,110	green-gray ch, brx, str FeOx goeth on fracs, bleached, hem stain	2.2	0.0331	1.63	0.613	42	290	3.02	7.12	2.01	0	0	0.061	0.04	0	0.096
102386	553,730	4,546,490	Ds(?) ch, tr argil alt on str foliations, tr to mod FeOx	1.53	0.0259	2	0.589	51	255	4.31	12.8	2.71	0.146	0.019	0.091	0.817	0.667	0.198
102387	553,840	4,546,690	chert brx, white, total reXTLIzation, w/ clear Q micro vnlts	1.4	0.0259	1.58	0.551	3	392	1.86	4.34	3.15	0.088	0	0.049	0.715	0	0.054
102366	554,040	4,546,920	chert brx, white, total reXTLization, w/ clear Q micro vnlts, FeOx	1.68	0.0243	2.21	0.665	50	301	3.92	11.3	2.39	0.096	0.036	0.032	0.609	0.22	0.168
102389	554,300	4,546,910	chert brx, white, total reXTLization, w/ clear Q micro vnlts, FeOx	1.39	0.0276	2.76	0.691	176	231	3.07	8.47	3.41	0	0	0.075	0.287	0.311	0.052
102390	554,550	4,546,860	green-gray ch, str FeOx fractures	1.7	0.0216	1.62	0.703	36	270	6.4	3.61	2.31	0.129	0	0.09	1.21	0.303	0.055
102391	554,850	4,546,860	Pol ss + cong, silicified + str FeOx as lim + goeth	1.63	0.069	6.1	2.21	203	23.5	6.72	129	3.37	0.027	0.051	1.06	0.482	3.57	0.875
102392	554,760	4,546,570	Pol ss + cong, bleached, str FeOx, near spring seep	4.7	0.0495	11.5	1.74	183	40.9	10.8	13.3	4.5	0.103	0.033	0.586	1.13	5.24	0.248
102393	554,580	4,546,640	huge brx fault zone o.c., str FeOx and clay in brx matrix	1.71	0.0127	27.5	0.673	23	30.3	3.06	207	2.95	0.09	0.088	0.051	0.425	0.039	1.78
102394	553,530	4,547,730	silty ch, wk argil alt	1.5	0.0163	0.93	0.284	35	13.7	2.29	11	0.947	0	0.007	0.103	0.516	0.132	0.11
102395	553,270	4,546,560	Ds or Se??, siltstone + ch, gossanous FeOx brx	1.63	0.0106	4.72	1.02	91	36.8	3.23	143	4.31	0.101	0.109	0.067	1.61	0.393	0.689
102396	553,050	4,546,600	bold green-brown ch, FeOx str on fracs and voids, wk argil alt	1.31	0.0125	1.1	0.222	14	12.4	1.6	10.3	1.9	0.093	0.044	0.065	0.649	0.139	0.065
102397	552,760	4,546,560	ch, white bleached, reXTLized, str foliated	1.5	0.0142	1.31	0.246	15	8.49	1.23	8.98	1.36	0.072	0.034	0.089	0.22	0.022	0.149
102398	552,510	4,546,660	thick bed gray ch, local sulfide clots, red hematite stained, PK ch??	8.22	0.0163	1.41	0.189	36	43.9	1.63	45.5	2.07	0.137	0.059	0.262	1.67	0	0.241
102399	556,300	4,545,400	ch brx, FeOx, liesegang banded	12.2	0.172	13	5.21	249	39.1	8.25	8.18	8.78	0	0.041	0.232	0.934	14.4	0.099
102400	555,900	4,544,960	Pol (Stralheam) ss + pebble cong, total FeOx	3.03	0.184	16.2	4.81	472	70.3	21.6	94.8	5.76	0.12	0.058	0.199	1.17	8.32	4.25
12746	554,820	4,549,040	silic Ovq brx, 2nd Q druse on fracs	2.24	0.0457	8.04	0.803	33	29.3	3.3	34.9	4.18	0.043	0.077	0	0.595	0.35	0.332

Table 4

Sample	UTM—Easting	UTM—Northing	Description	Au	Ag	As	Sb	Hg	Cu	Pb	Zn	Mo	Bi	Te	Tl	Ga	Se	Cd
				ppb	ppm	ppm	ppm	ppm	ppm	ppm	ppm	ppm	ppm	ppm	ppm	ppm	ppm	ppm
				partial	partial	partial	partial	partial	partial	partial	partial	partial	partial	partial	partial	partial	partial	partial
12747	552,020	4,544,970	greenish gray chert, tr FeOx on fracs	0 805	0 0292	4 43	0 563	43	30 5	4 38	19 5	4.63	0 133	0.102	0.081	1.45	0.224	0.092
12748	552,310	4,545,090	grn-gray ch, multistage clear lo milky Q vnlts	3.52	0 126	2 58	1 03	60	29.9	2.53	46 6	5.08	0.052	0 046	0.099	0 532	0.558	0.494
12749	552,660	4,545,230	gray, brown FeOx chert, tr sulfides + Q druse in cav	0.896	0.0415	2.17	0 579	69	32.9	2 92	6 57	4	0.103	0.076	0 096	0.758	0.167	0.073
12750	552,940	4,545,360	bedded barite, gossanous FeOx + barite vnlts	3 89	0 175	6 31	1.2	250	71.3	6 44	104	6.49	0 082	0.132	0.184	0.512	0.462	1.08
12751	553,050	4,545,330	black ch brx, str FeOx, local gossanous patches	2 57	0.118	17	3.09	252	108	5 3	1297	21.3	0.029	0.164	0.127	0.738	9 7	0.572
12752	553,310	4,545,380	chert brx, v str FeOx, locally bleached white	0 776	0.0161	5 92	0 499	16	46 8	3 37	840	7 67	0 092	0 129	0.049	0 806	0 248	7.35
12753	553,500	4,545,350	green chert, wk frac FeOx + minor brx	1 07	0.053	6.19	1.11	105	28 7	6.61	51	6.26	0.114	0 116	0 073	0.753	1.09	0.526
12754	553,440	4,545,250	chert, gossanous FeOx brx matrix, lim + goeth	4 21	0.105	19 2	1.72	298	43 4	5 53	415	12.3	0.066	0 125	0.037	0 541	0.307	2 59
12755	552,110	4,545,370	brown FeOx ch, tr milky Q vnlts, local reXTLized matrix	4.86	0 109	2 51	0 658	42	15 9	2 5	14.1	3.98	0.052	0 089	0.065	0 517	0.623	0.092

TABLE 5—NUMBER AND NUMERICAL VALUE OF SUBSTITUTIONS FOR INDETERMINATE ANALYSES IN TABLES 1, 2, AND 4.

[--, not applicable; N.D., not determined; ppm, parts per million; wt. percent, weight percent]

		Table 1		Table 2		Table 4	
Element	Digestion (see text)	Nunber of substitutions	Value of substitution	Number of substitutions	Value of substitution	Number of substitutions	Value of substitution
Ag	Partial	None	--	None	--	37	0.05 ppm
As	Partial	None	--	None	--	18	1.5 ppm
Au	Partial	24	0.0001 ppm	14	0.0001 ppm	13	0.0001 ppm
Bi	Partial	None	--	None	--	48	0.014 ppm
Cd	Partial	None	--	None	--	None	--
Cu	Partial	None	--	None	--	None	--
Ga	Partial	6	0.0035 ppm	None	--	None	--
Hg	Partial	None	--	2	0.008 ppm	None	--
Mo	Partial	None	--	None	--	7	0.25 ppm
Pb	Partial	None	--	None	--	1	1.0 ppm
Sb	Partial	None	--	None	--	26	1.0 ppm
Se	Partial	5	0.001 ppm	6	0.001 ppm	2	0.011 ppm
Te	Partial	None	--	None	--	36	0.0035 ppm
Tl	Partial	None	--	None	--	33	0.018 ppm
Zn	Partial	None	--	None	--	None	--
Mo	Total	12	1 ppm	7	1 ppm	N.D.	--
Cu	Total	None	--	None	--	N.D.	--
Pb	Total	42	2.5 ppm	36	2.5 ppm	N.D.	--
Zn	Total	None	--	None	--	N.D.	--
Ag	Total	59	0.25 ppm	47	0.25 ppm	N.D.	--
Ni	Total	None	--	None	--	N.D.	--
Co	Total	14	1.0 ppm	1	1.0 ppm	N.D.	--
Mn	Total	None	--	None	--	N.D.	--
Fe	Total	None	--	None	--	N.D.	--
As	Total	46	2.5 ppm	26	2.5 ppm	N.D.	--
U	Total	113	5.0 ppm	91	5.0 ppm	N.D.	--
Au	Total	115	2.0 ppm	91	2.0 ppm	N.D.	--
Th	Total	11	1.0 ppm	22	1.0 ppm	N.D.	--
Sr	Total	None	--	None	--	N.D.	--
Cd	Total	97	0.2 ppm	57	0.2 ppm	N.D.	--
Sb	Total	101	2.5 ppm	70	2.5 ppm	N.D.	--
Bi	Total	115	2.5 ppm	81	2.5 ppm	N.D.	--
V	Total	None	--	None	--	N.D.	--
Ca	Total	None	--	None	--	N.D.	--
P	Total	None	--	None	--	N.D.	--
La	Total	None	--	1	1.0 ppm	N.D.	--
Cr	Total	None	--	None	--	N.D.	--
Mg	Total	None	--	None	--	N.D.	--
Ba	Total	None	--	None	--	N.D.	--
Ti	Total	None	--	None	--	N.D.	--
Al	Total	None	--	None	--	N.D.	--
Na	Total	2	0.005 wt. Percent	None	--	N.D.	--
K	Total	None	--	None	--	N.D.	--
W	Total	113	2.0 ppm	91	2.0 ppm	N.D.	--
Zr	Total	None	--	None	--	N.D.	--
Sn	Total	6	1.0 ppm	90	1.0 ppm	N.D.	--
Y	Total	1	1.0 ppm	None	--	N.D.	--
Nb	Total	11	1.0 ppm	19	1.0 ppm	N.D.	--
Be	Total	39	0.5 ppm	61	0.5 ppm	N.D.	--
Sc	Total	16	0.5 ppm	3	0.5 ppm	N.D.	--

Table 6—Summary statistics for rock analyses along traverse AA' (table 1) in the Santa Renia Fields and Beaver Peak quadrangles, Nev. Log ppm (parts per million) except for Fe, Ca, P, Mg, Ti, Al, Na, and K which are log weight percent.
[partial, analyses by partial digestion techniques; total, analyses by total digestion techniques (see text)]

	log Ag-partial	log As-partial	log Au-partial	log Bi-partial	log Cd-partial	Cu-partial	log Ga-partial	log Hg-partial	log Mo-partial	log Pb-partial	log Sb-partial	log Se-partial	log Te-partial	log Tl-partial
Mean	-.939	.522	-3.178	-.732	-.842	1.195	-.385	-.997	.453	.539	-.132	-.259	-.852	-.599
Std. Dev.	.485	.523	.647	.120	.498	.302	.562	.446	.325	.326	.367	.908	.159	.288
Std. Error	.045	.049	.060	.011	.048	.026	.052	.042	.030	.030	.034	.085	.015	.027
Count	115	115	115	115	115	115	115	115	115	115	115	115	115	115
Minimum	-1.745	-.493	-4.000	-.955	-1.878	.483	-2.155	-2.301	-.268	-.101	-.870	-3.000	-1.481	-1.721
Maximum	.748	2.097	-1.745	-.385	.860	2.111	.922	.393	1.188	1.279	1.064	1.422	-.474	.204
# Missing	0	0	0	0	0	0	0	0	0	0	0	0	0	0
Variance	.235	.274	.418	.014	.248	.091	.316	.199	.105	.106	.135	.825	.025	.083
Coef. Var.	-.518	1.002	-.204	-.164	-.591	.252	-1.541	-.447	.716	.604	-2.778	-3.502	-.188	-.480
Range	2.493	2.590	2.255	.570	2.536	1.828	3.077	2.694	1.455	1.380	1.934	4.422	1.008	1.925
Sum	-107.958	80.084	-365.439	-84.157	-96.870	137.430	-41.947	-114.641	52.141	81.974	-15.190	-29.830	-98.023	-68.886
Sum Squares	128.141	82.611	1208.949	63.227	109.822	174.815	51.319	136.928	35.854	45.487	17.358	101.787	86.427	50.893
Geom. Mean	•	•	•	•	•	1.155	•	•	•	•	•	•	•	•
Harm. Mean	•	•	•	•	•	1.112	•	•	•	•	•	•	•	•
Skewness	.780	.786	.382	.867	.411	.192	-.115	.108	-.026	.425	.290	-1.240	-.589	-1.026
Kurtosis	.301	.356	-1.024	.838	.006	.197	.416	.881	-.293	-.202	.070	2.010	1.822	3.676
Median	-1.038	.412	-3.301	-.757	-.845	1.204	-.368	-1.013	.452	.489	-.108	-.148	-.842	-.599
IQR	.658	.835	1.132	.122	.774	.383	.609	.517	.449	.348	.534	.913	.181	.289
Mode	-1.337	.228	-4.000	•	-1.260	1.068	-1.301	•	•	•	.167	-3.000	-1.013	-.526
10% Tr. Mean	-.977	.478	-3.214	-.742	-.865	1.191	-.365	-.997	.458	.523	-.139	-.158	-.849	-.585
MAD	.324	.336	.602	.081	.394	.194	.292	.259	.219	.185	.260	.482	.097	.149

	log Zn-partial	log Mo-total	Cu-total	log Pb-total	log Zn-total	log Ag-total	log Ni-total	log Co-total	log Mn-total	log Fe-total	log As-total	log U-total	log Au-total	log Th-total	log Sr-total	log Cd-total
Mean	1.114	.570	1.283	.762	1.337	-.277	1.171	.447	1.913	.029	.773	.707	.301	.498	1.952	-.596
Std. Dev.	.572	.321	.296	.332	.474	.413	.218	.269	.382	.269	.420	.059	0.000	.330	.384	.267
Std. Error	.053	.030	.028	.031	.044	.038	.020	.025	.036	.025	.039	.005	0.000	.031	.034	.025
Count	115	115	115	115	115	115	115	115	115	115	115	115	115	115	115	115
Minimum	.217	0.000	.477	.398	.802	-.802	.699	0.000	1.380	-.481	.398	.699	.301	0.000	1.301	-.699
Maximum	3.017	1.322	2.140	1.431	3.014	.966	2.326	1.342	2.989	1.022	2.137	1.204	.301	1.491	3.038	.857
# Missing	0	0	0	0	0	0	0	0	0	0	0	0	0	0	0	0
Variance	.327	.103	.088	.110	.225	.170	.047	.072	.146	.073	.176	.003	0.000	.109	.133	.071
Coef. Var.	.514	.564	.231	.438	.355	-1.490	.186	.801	.200	9.402	.543	.083	0.000	.662	.187	-.447
Range	2.800	1.322	1.663	1.033	2.412	1.571	1.627	1.342	1.809	1.503	1.739	.505	0.000	1.491	1.737	1.556
Sum	128.112	65.584	147.489	87.597	153.717	-31.834	134.666	51.419	220.009	3.294	88.876	81.287	34.618	57.221	224.472	-68.783
Sum Squares	180.024	49.185	199.136	79.270	231.121	28.211	183.095	31.219	437.533	8.364	88.780	57.622	10.421	40.856	453.283	49.278
Geom. Mean	.953	•	1.248	.689	1.257	•	1.153	•	1.880	•	.878	.705	.301	•	1.921	•
Harm. Mean	.784	•	1.205	.823	1.181	•	1.135	•	1.851	•	.803	.704	.301	•	1.892	•
Skewness	.481	.044	.048	.373	.698	1.137	1.370	.396	1.217	1.433	1.158	7.608	•	.972	.945	2.978
Kurtosis	.026	-.545	.330	-1.011	.418	.400	5.688	.284	.373	2.108	.861	56.957	•	.628	.381	9.252
Median	1.097	.602	1.301	.776	1.255	-.602	1.178	.477	1.756	-.060	.699	.699	.301	.477	1.845	-.899
IQR	.931	.477	.352	.591	.699	.505	.237	.301	.479	.236	.558	0.000	0.000	.301	.405	0.000
Mode	•	.301	1.382	.398	.845	-.602	1.000	.301	•	-.114	.398	.699	.301	.301	•	-.899
10% Tr. Mean	1.087	.571	1.282	.733	1.306	-.348	1.158	.440	1.858	-.006	.708	.699	.301	.471	1.914	-.672
MAD	.467	.243	.187	.380	.358	0.000	.125	.176	.122	.110	.301	0.000	0.000	.176	.173	0.000

Table 6—cont'd.

	log Sb-total	log Bi-total	log V-total	log Ca-total	log P-total	log La-total	log Cr-total	log Mg-total	log Ba-total	log Ti-total
Mean	.440	398	1.750	-.770	-1.413	1.017	2 221	-.784	3.099	-1.172
Std Dev.	.117	0.000	.440	698	.445	.312	237	571	.345	326
Std. Error	.011	0 000	041	.065	.041	.029	.022	053	032	.030
Count	115	115	115	115	115	115	115	115	115	115
Minimum	.398	.398	.699	-1.523	-2.222	477	1 398	-1.699	2 121	-2 000
Maximum	1.000	.398	3.001	1.140	- 024	1.944	2.709	.946	3 949	-.229
# Missing	0	0	0	0	0	0	0	0	0	0
Variance	.014	0.000	.194	.487	.198	097	.056	.326	.119	106
Coef. Var.	.265	0.000	.252	- 907	- 315	306	.107	- 726	.111	-.278
Range	.602	0.000	2.302	2.662	2.198	1.467	1.311	2.645	1 829	1 771
Sum	50.595	45.763	201.198	-88.505	-162.507	116.975	255.453	-90.180	356.331	-134.827
Sum Squares	23.813	18.211	374.113	123.678	252.207	130.049	573.865	107.828	1117 646	170.207
Geom. Mean	.429	.398	1.689	•	•	.974	2.207	•	3.079	•
Harm. Mean	.422	.398	1 621	•	•	.935	2 191	•	3.058	•
Skewness	2.655	•	-.012	1.175	.802	.949	-1.182	1.009	-.197	.310
Kurtosis	6.129	•	.150	210	.494	.323	2.041	.946	.274	.179
Median	.398	398	1.740	-1.097	-1.495	.954	2.260	-.886	3.093	-1.222
IQR	0.000	0.000	.523	.857	.531	.301	.210	.450	.397	.387
Mode	.398	.398	1.653	-1.222	-1.824	.845	•	-.921	•	-1.222
10% Tr. Mean	.408	.398	1.756	-.873	-1.448	.987	2.246	-.836	3 108	-1.184
MAD	0.000	0.000	.268	.243	.275	.176	.105	211	192	.176

	log Al-total	log Na-total	log K-total	log W-total	log Zr-total	log Sn-total	log Y-total	log Nb-total	log Be-total	log Sc-total
Mean	.085	-1.305	-.268	307	1.407	.018	.839	.502	-.043	.310
Std Dev.	362	.536	.346	.046	.344	.083	.375	337	.230	.327
Std. Error	.034	.050	.032	.004	.032	.008	035	.031	.021	.030
Count	115	115	115	115	115	115	115	115	115	115
Minimum	- 699	-2.301	-1.155	.301	.602	0.000	0.000	0.000	-.301	-.301
Maximum	.957	.057	.585	.699	2.352	.602	1.580	1.362	.477	1.176
# Missing	0	0	0	0	0	0	0	0	0	0
Variance	131	.288	.119	.002	.118	.007	.140	.113	.053	107
Coef. Var.	4.241	-.411	-1.291	151	.245	4.505	.447	.670	-5.393	1.055
Range	1.656	2.358	1.740	.398	1.750	.602	1.580	1.362	778	1.477
Sum	9.813	-150.032	-30.783	35.317	161.785	2.107	96.461	57.732	-4.913	35.619
Sum Squares	15.768	226.532	21.853	11.091	241.093	.816	96.923	41.896	6.261	23.195
Geom. Mean	•	•	•	.305	1.368	•	•	•	•	•
Harm. Mean	•	•	•	.304	1 330	•	•	•	•	•
Skewness	.205	1.003	-.162	7.601	.968	4.873	.446	1.040	.621	-.428
Kurtosis	.185	.666	-.014	56.809	.901	25.206	-.618	.707	-.181	-.198
Median	.090	-1.398	-.244	.301	1.322	0.000	.776	.477	0.000	.301
IQR	.360	.301	.373	0.000	.314	0.000	.477	.301	.301	.176
Mode	•	-1 398	-.398	.301	•	0.000	.477	.301	0.000	.301
10% Tr. Mean	.078	-1.359	-.261	.301	1.368	0.000	.821	.470	-.068	.322
MAD	.166	.125	.188	0.000	.155	0.000	.301	.176	0.000	.176

Table 7—Summary statistics for 78 rocks analyzed in the Boulder Creek area (Group 3, table 4) of the Beaver Peak quadrangle, Nev.

[All values are log parts per million of analyses by partial digestion methods (see text). Black dot, not determined]

	log Au	log Ag	log As	log Sb	log Hg	log Cu	log Pb	log Zn	log Mo	log Bi	log Te	log Tl	log Ga	log Se	log Cd
Mean	-2.472	-1.217	.626	.106	-1.014	2.016	.678	1.499	.613	-1.596	-1.858	-1.290	-.178	-.487	-.525
Std. Dev.	.525	.392	.492	.362	.455	.421	.317	.673	.545	.386	.698	.597	.309	.821	.614
Std. Error	.059	.044	.056	.041	.051	.048	.036	.076	.062	.044	.083	.071	.056	.150	.112
Count	78	78	78	78	78	78	78	78	78	78	71	71	30	30	30
Minimum	-3.110	-1.975	-.032	-.724	-2.523	.929	0.000	.342	-.602	-1.854	-2.456	-1.745	-1.398	-1.959	-1.284
Maximum	-1.131	0.000	1.919	1.190	.207	2.593	2.185	3.409	1.569	-.821	-.699	.362	.223	1.158	.866
# Missing	0	0	0	0	0	0	0	0	0	0	7	7	48	48	48
Variance	.275	.153	.242	.131	.207	.178	.101	.453	.297	.149	.487	.356	.096	.675	.377
Coef. Var.	-.212	-.322	.786	3.429	-.448	.209	.468	.449	.889	-.242	-.376	-.463	-1.737	-1.687	-1.170
Range	1.979	1.975	1.951	1.914	2.730	1.664	2.185	3.067	2.171	1.033	1.757	2.106	1.621	3.117	2.150
Sum	-192.777	-94.899	48.855	8.242	-79.097	157.265	52.887	116.915	47.817	-124.495	-131.940	-91.589	-5.341	-14.601	-15.747
Sum Squares	497.648	127.278	49.245	10.978	96.122	330.758	43.616	210.135	52.200	210.175	279.289	143.092	3.725	26.669	19.211
Geom. Mean	•	•	•	•	•	1.965	•	1.356	•	•	•	•	•	•	•
Harm. Mean	•	•	•	•	•	1.905	•	1.218	•	•	•	•	•	•	•
Skewness	.857	.711	.624	.590	-.442	-.823	1.302	.794	-.721	.945	.420	1.262	-2.063	.073	.649
Kurtosis	-.101	.566	-.728	.815	1.316	-.497	5.531	.165	.150	-.920	-1.632	.754	6.240	-.159	-.589
Median	-2.556	-1.301	.467	0.000	-1.009	2.193	.662	1.372	.628	-1.854	-2.456	-1.745	-.139	-.482	-.628
IQR	.874	.301	.885	.301	.596	.716	.342	.949	.610	.673	1.386	.721	.312	.651	.874
Mode	-3.000	-1.301	.176	0.000	•	•	•	•	-.602	-1.854	-2.456	-1.745	•	-1.959	-1.036
10% Tr. Mean	-2.534	-1.237	.581	.091	-.998	2.060	.665	1.437	.658	-1.646	-1.918	-1.407	-.139	-.491	-.580
MAD	.444	.060	.291	.169	.284	.214	.170	.449	.320	0.000	0.000	0.000	.148	.301	.408

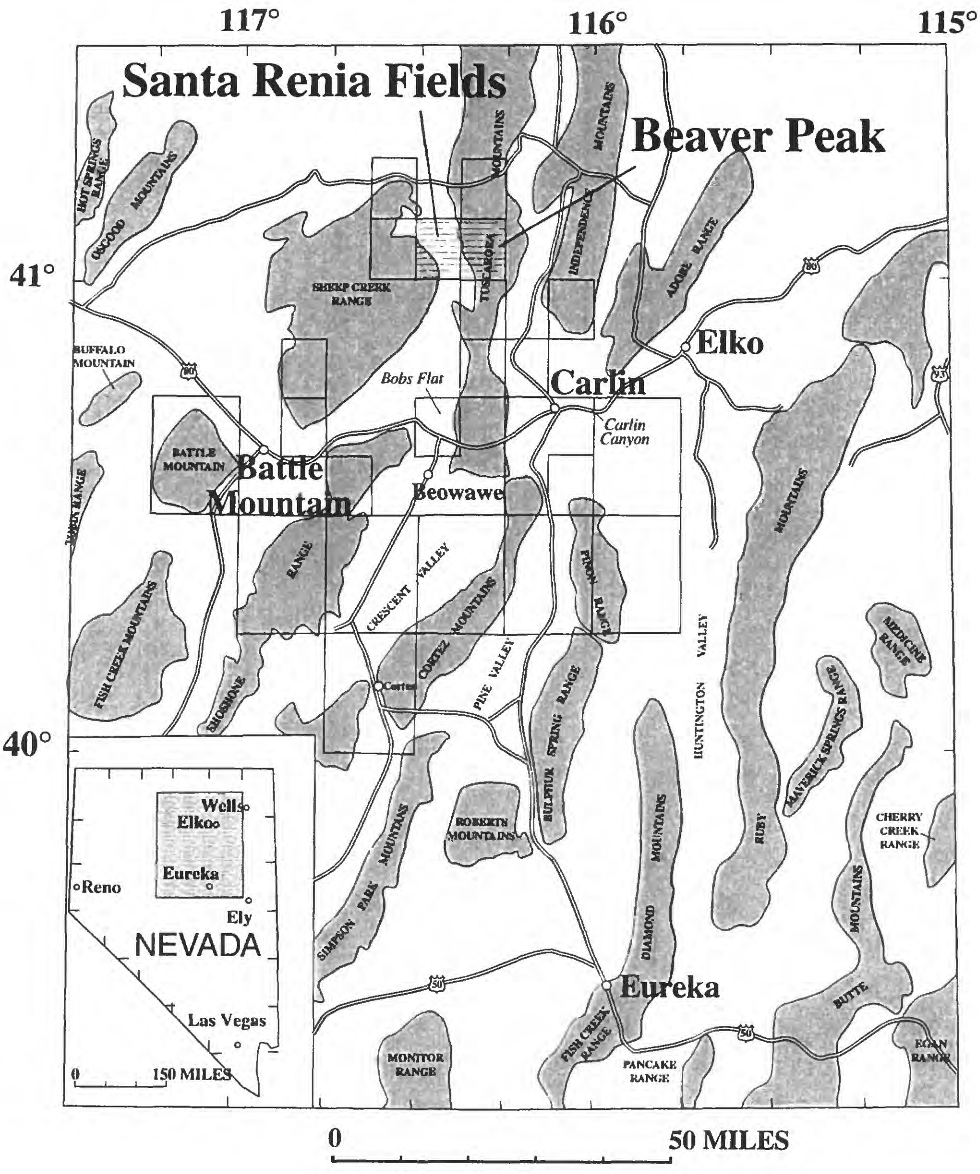

Figure 1—Index map of north-central Nevada showing locations of Santa Renia Fields and Beaver Peak 7–1/2 minute quadrangles. Outline of other nearby quadrangles also shown.

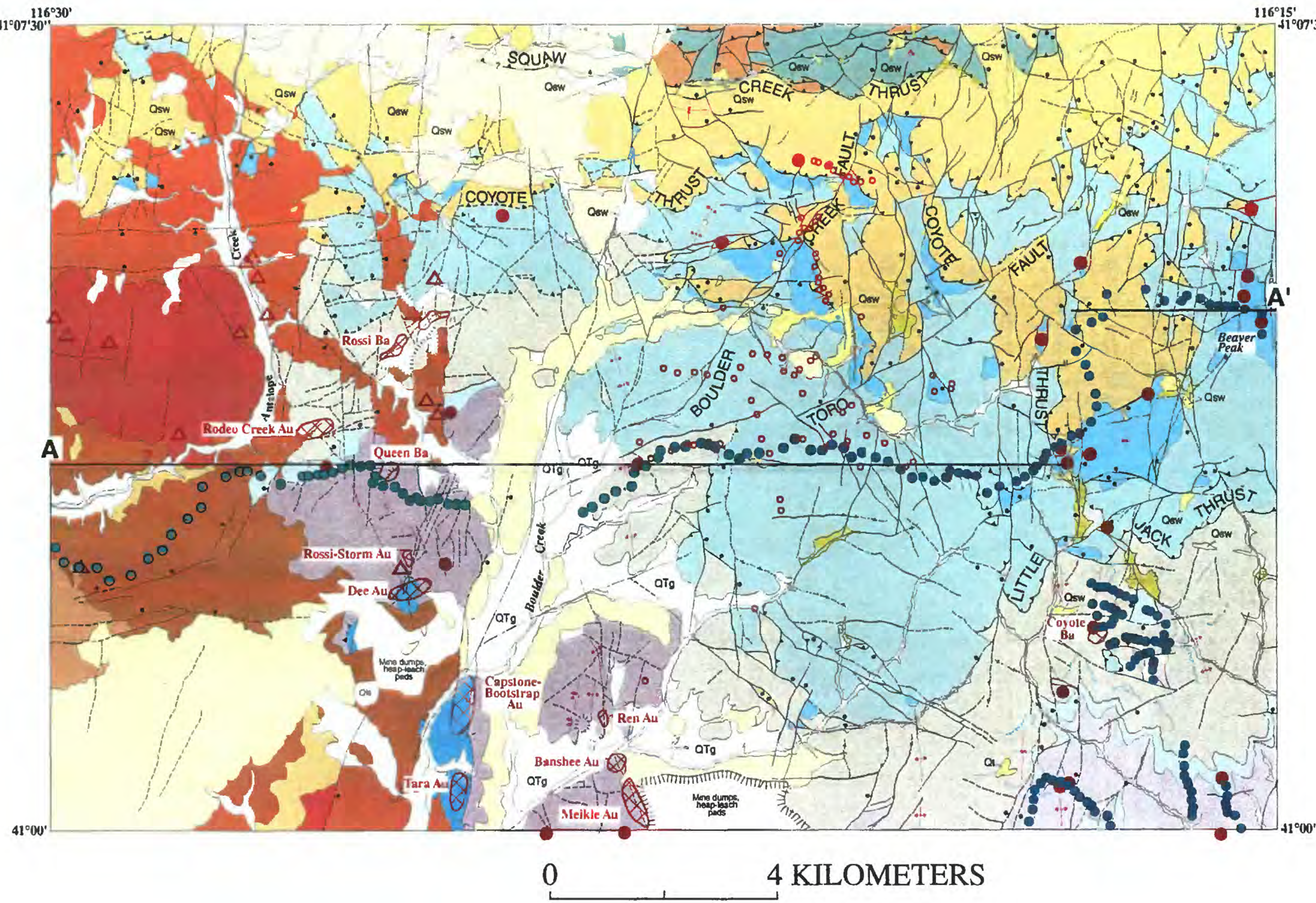

Figure 2. Geologic sketch map of the Santa Renia Fields and Beaver Peak 7–1/2 minute quadrangles, Nev., showing localities of three groups of analyzed rocks. Santa Renia Fields geology (west half of figure), modified from T.G. Theodore, J.K. Cluer, and S.C. Finney (unpub data, 2000) and Barrick Gold Corp. (unpub. data, 2000); Beaver Peak geology (east half of figure) modified from T.G. Theodore, B.C. Moring, A.K. Armstrong, A.G. Harris, and S.C. Finney (unpub. data, 2000).

Figure 2—Cont'd.

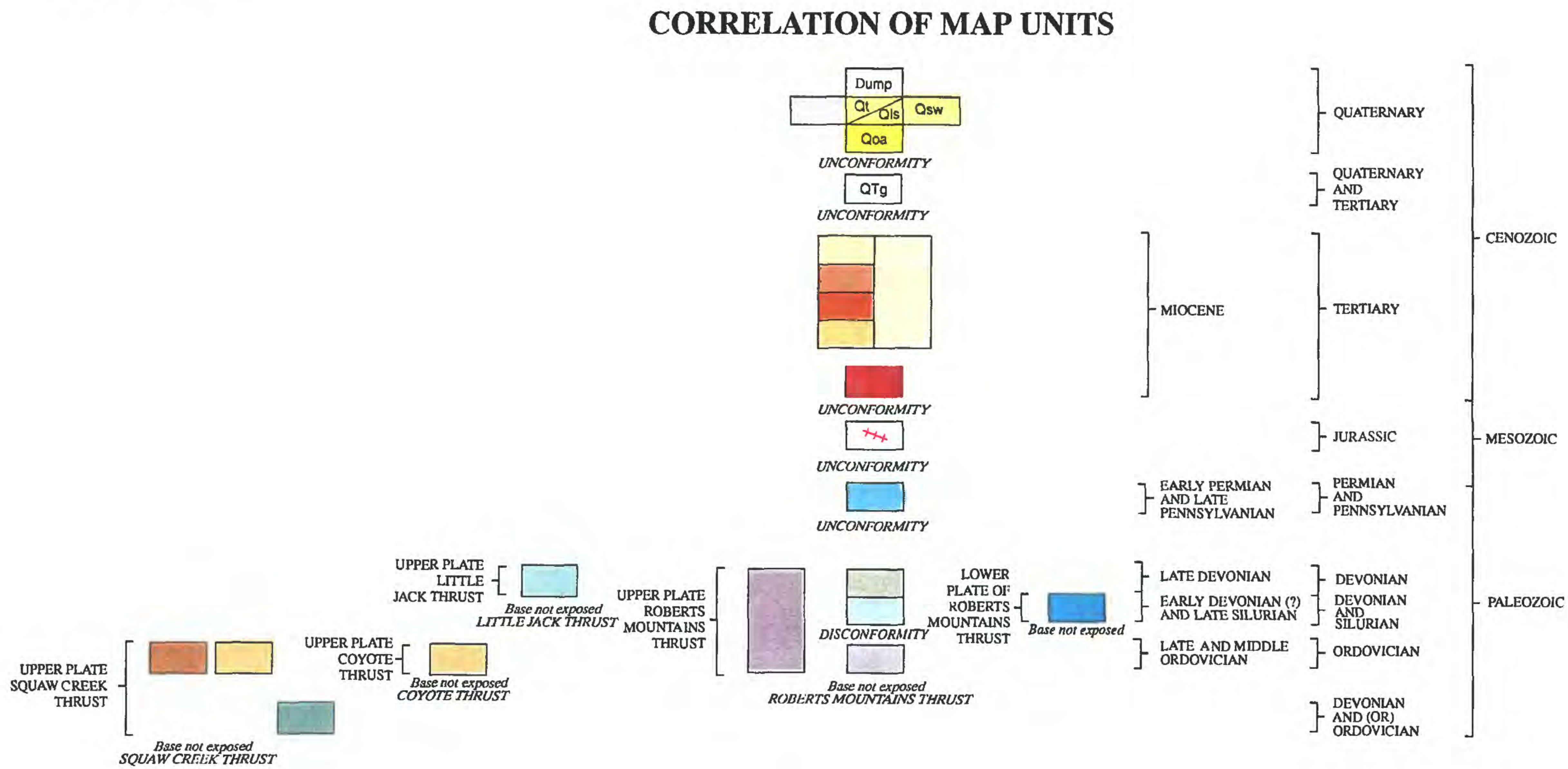

Figure 2—cont'd.

DESCRIPTION OF MAP UNITS

Dump **Waste dumps and tailings ponds (Quaternary)**—Outer limit of dumps and tailings ponds in general area of Newmont Gold Mining Company and Barrick Gold Corporation mining facilities as of late 1998 near Meikle Mine and as of early 2000 near Dee Mine

Younger alluvium and fanglomerate deposits (Quaternary)—Unconsolidated gravel and sand deposits. Includes some fanglomeratic deposits near lower reaches of major drainages near southern boundary of east part of area

Qt Qls **Talus deposits and (or) landslide deposits (Qls) (Quaternary)**

Qsw **Slope-wash deposits (Quaternary)**

Qoa **Older alluvium (Quaternary)**

QTg **Gravel deposits (Quaternary and Tertiary)**

Carlin Formation of Regnier (1960) (Miocene)—In this area includes:

Fanglomerate deposits, unconsolidated

Silts and sands, mostly unconsolidated

Silts and sands, mostly unconsolidated, sedimentary breccia, and abundant air-fall tuff (15.1 to 14.4 Ma, Fleck and others, 1998)

Tuff, partly welded, and minor silts and sands, mostly unconsolidated

Undivided

Porphyritic rhyolite and vitrophyre (north of Antelope Creek) and peralkaline rhyolite (west of Boulder Creek) (Miocene)—Same as informally named Craig rhyolite of Bartlett and others (1991). Approximately 15.1 Ma (Fleck and others, 1998)

Altered dikes (Jurassic?)—East of Boulder Creek fault, intensely clay-altered felsite dikes including monzonite and alkali granite facies comprised either of stubby intergrown laths of clay-clouded plagioclase and K–feldspar or mostly K–feldspar. Weather yellowish white and contain buff- to ochre-colored iron-oxide stains. Poorly exposed in two isolated exposures where dikes are emplaced into pebbly conglomerate of lower strata of Strathearn Formation. Pebbly conglomerate in immediate area of dikes, as well as along a narrow zone elongate to N. 30° E., shows presence of microveins including quartz, chlorite, and yellowish iron-oxide minerals—possibly including jarosite—that replace sulfide minerals. Chlorite also forms mm-scale halos around microveins. Dikes are probably correlative with greater than 147–Ma informally named Arturo dike in the Dee Mine (Theodore and others, 1998). In general area of Queen, Rossi, and Tara Mines, many clay-altered dikes show microfabrics suggestive of spessartite lamprophyre

Strathearn Formation of Dott (1955) (Permian and Pennsylvanian)—Generally highly resistant, thick, drab gray brown to reddish brown ledges or rubble strewn slopes of mostly chert-pebble-conglomerate make up foreland clastic deposits in this area—derived, in part, from reactivated highlands of Antler orogeny of Roberts and others (1958). Crops out in numerous discontinuous bodies, where underlying rocks primarily are Devonian chert mélange unit in upper plate of Little Jack thrust. Basal part of formation also includes onlap relations with Devonian Slaven Chert in lower plate of Little Jack thrust. Near base commonly includes chert pebble conglomerate as much as 200 m thick, some including interbedded highly fusulinid-rich lenses of peloidal grainstone. Basal strata overlain by as much as 30 m of gray to light gray limestone, and approximately 300 m of dolomitic siltstone, including grains of K–feldspar, near top of sequence where best exposed near Beaver Peak. Matrix of chert pebble conglomerate includes abundant variably rounded monocrystalline quartz grains and quartzarenite fragments derived from underlying quartzarenite of Middle Ordovician Vinini Formation in upper plate of Coyote thrust. Upper parts of formation also onlap quartzarenite of Vinini Formation in upper plate of Coyote thrust

Upper plate of Squaw Creek thrust—This tectonic package of rocks, considered to have an imbricate structural relation with underlying packages, consists of a number of structural blocks whose bedding attitudes are oriented at high angles to underlying, largely homoclinal, quartzarenite that makes up lower plate. In this area includes:

Siltstone unit of Vinini Formation of Merriam and Anderson (1942) (Ordovician)—Poorly exposed, light gray to gray-brown, mostly siliceous feldspathic siltstone. Includes some size-specific rounding of larger detrital grains of quartz. Angular grains of K–feldspar make up as much as approximately 25 volume percent of rock. Unit also includes some olive green chert, brown shale, and fine-grained sandstone

Figure 2—"Description of map units" (cont'd.)

Quartzarenite of Vinini Formation of Merriam and Anderson (1942) (Ordovician)—Small, isolated exposures of quartzarenite near north-central border of area above projected trace of Squaw Creek thrust.

Chert, undivided (Devonian and (or) Ordovician)—Generally poorly exposed, light gray to dark gray, well-bedded chert. Narrow carbonaceous seams present along parting surfaces of bedding, and some chert microbrecciated during diagenesis and further cemented by infilling of additional chert

Upper plate of Coyote thrust—Coyote thrust emplaced during late Late Pennsylvanian and middle Early Permian. Thrust plate as much as approximately 800 m thick to the north-northwest of Beaver Peak, but thins dramatically to the west where the plate is approximately 150 m thick near the northwest corner of the Santa Renia Fields quadrangle. In this area includes:

Quartzarenite of Vinini Formation of Merriam and Anderson (1942) (Ordovician)— Resistant moderately rounded ridges of mostly massive orange-brown- to drab ochre-brown-weathering quartzarenite. Quartzarenite typically mature and made up of medium-grained, well-sorted fabrics of monocrystalline quartz grains showing size-specific rounding. Includes sparse thin interbeds of green to olive green chert, and other chert possibly caught up along unmapped minor steeply-dipping normal faults. Near northwest corner of area includes green and black, thin discontinuous beds of chert that apparently increase in overall abundance downsection and to the northwest. Locally, quartzarenite includes poorly exposed, interbedded gray brown siltstone, fine-grained quartzarenite, and black shaly chert. Unit includes sedimentary and tectonic breccia, latter shows recrystallization of angular quartz matrix among well-rounded quartz grains. Locally dense concentration of planar quartz veins. Gray brown micrite (as much as 1 m thick), in fault sliver east of Boulder Creek, is interbedded with rusty-brick-red weathering siltstone and contains juvenile conodonts that are Caradocian (middle Middle to middle Late Ordovician) (Anita Harris, written commun., 1998; Theodore and others, 1998). Shale in green chert interbedded with quartzarenite approximately 30 m above trace of Coyote thrust near northwest corner of quadrangle, west of Boulder Creek, include *Cryptograptus schaeferi*, *Glossograptus* sp., *Nemagraptus* sp., (?)*Leptograptus*, and *Pseudoclimacograptus* sp. that are uppermost Middle Ordovician (Stanley C. Finney, written commun., 1997; Theodore and others, 1998). Quartzarenite commonly is intensely recrystallized to white sucrose hornfels near Coyote thrust. Hornfels near thrust locally contains abundant brick-red iron-oxide minerals and breccia. Quartzarenite intensely lineated, in places including widespread slickensides, within 10 m of trace of Coyote thrust. Base of formation not exposed

Upper plate of Little Jack thrust—Little Jack thrust inferred to be imbricate structure related to Coyote thrust. Best exposures of Little Jack thrust with underlying unit are northwest and northeast of abandoned Coyote barite mine. In this area includes:

Chert mélange unit of Slaven Chert of Gilluly and Gates (1965) (Devonian)—Commonly ridge-forming rubbly exposures that include chaotic depositional and intensely deformed tectonic fabrics. Unit typically weathers green gray with locally moderate amounts of yellow brown iron oxide. One of more striking features of unit is absence of continuous bedding surfaces and presence of structurally transposed lithologic layering that yields flat-shaped chips whose shapes are controlled by closely spaced foliation surfaces. Sequences dominated by somewhat more argillaceous chert and shale locally have highly contorted lithologic layering, including presence of numerous slip surfaces on individual outcrops and, and such sequences yield broad areas of light gray to tannish gray debris-covered colluvial slopes. Some sequences are intensely rodded. Generally, variably-colored mm– to cm–sized, angular to ovoid chert fragments set in either a chert matrix or ductile argillaceous matrix—some fragments have fabrics suggestive of soft-sediment deformation features. Fragmental nature of unit persists down to microscopic scale. Overall tectonostratigraphic thickness of unit quite variable, but roughly as much as 1,400 m thick near north edge of area in general area of Toro fault. Near trace of Little Jack thrust, includes some sequences, as much as 50 to 60 m thick, of mottled gray-green-weathering well-bedded chert probably incorporated structurally into the Little Jack allochthon from underlying unit. Also near Little Jack thrust, rocks are exceptionally altered to clay(s) and other brown, ochre brown, and green brown iron-oxide minerals. Unit presumably correlative with Late Devonian sedimentological breccia and barite breccia unit of Slaven Chert in Shoshone Range (C.T. Wrucke, oral commun., 1999) on the basis of Devonian conodonts in limestone interbed in northwest part of area (Theodore and others, 1998)

Upper plate of Roberts Mountains thrust—In this area includes:

Siliceous rocks, undivided (Devonian, Silurian, and (or) Ordovician)—Mostly black Ordovician chert and shale in general area of Queen and Dee Mines, but includes undivided Slaven Chert. Silurian Elder Sandstone of Gilluly and Gates (1965), and Ordovician chert, shale, and siltstone near Ren and Meikle Mines

Slaven Chert of Gilluly and Gates (1965) (Devonian)—Generally resistant ridge-forming, homoclinal sequence of commonly north-dipping, relatively thin, gray to black chert beds in rhythmically-stratified sequences having mostly 2 to 4 cm between parting surfaces. Rocks characterized by planar bedding surfaces that weather typically to 2– to 5–cm-wide angular fragments. In places, formation is tightly folded along numerous outcrop-scale fold axes that verge mostly towards the south. Formation is approximately 700 m thick north of Little Jack Creek where Little Jack thrust forms upper contact. Near southwest corner of quadrangle, includes narrow fault slivers of chert mélange unit. Formation near base locally includes 25– to 30–cm-wide beds of buff-weathering gray dolostone that is interbedded with brown to brownish black chert containing abundant 1.5– to 2.0–cm-wide compaction structures, as well as rip-up

Figure 2 "Description of map units" (cont'd.)

mud clasts and other soft-sediment deformation features. Spar dolostone contains abundant regularly-sized ooids, approximately 0.1 to 0.3 mm wide. Conodonts obtained from locality near apparent base of formation and near southeast corner of quadrangle include faunule indicative of Lower *Palmatolepsis rhenana* Subzone (early late Frasnian) (Late Devonian) (Anita G. Harris, written commun., 1999). Palmatolepid-polygnathid biofacies indicates outer shelf or deeper water depositional setting. Well-exposed base of formation near southeast corner of area also shows gradational contact with underlying Silurian Elder Sandstone across approximately 10 m of stratigraphic section

Elder Sandstone of Gilluly and Gates (1965) (Silurian)—Slope-forming, generally olive gray-green, dolomitic and calcareous siltstone and dark gray shale that weather to various shades of brown and gray brown. Thickness of formation is approximately 150 m. Forms recessive part of well-exposed homoclinal sequence of formations dipping at shallow angles to north near southeast corner of area where ridgelines are held up by thick strata of overlying Slaven Chert. Locally also includes some interbeds of chert as well as prominent sequence of chert near base probably correlative with Early Silurian (Llandoverian) Cherry Spring chert of Noble and others (1997) in the northern Adobe Range. Laminae in siltstone are defined by mm-sized, discontinuous, wispy layers that show some weakly developed crossbeds. Siltstone commonly includes 0.03– to 0.04–mm-wide (medium to coarse silt) angular detrital grains of quartz, K–feldspar (roughly 10 to 15 volume percent), white mica, biotite (white mica >> biotite), and opaque minerals. In places, siltstone is partly recrystallized to spar silty dolostone and dolomite is ferroan. Locality near southeast corner of area approximately from middle of well exposed section through formation, yielded more than 30 shale chips with contained graptolites—many chips contain several graptolite specimens (S. C. Finney, written commun., 1998). The graptolite fauna consist of two species: *Bohemograptus bohemicus* and *Saetograptus willowensis*, a fauna reported by Berry and Murphy (1975) from the middle of the Silurian Roberts Mountains Formation in central Nevada. The fauna is characteristic of the *B. bohemicus* Zone of the Late Ludlovian (early Late Silurian)

Chert and shale unit of Vinini Formation of Merriam and Anderson (1942) (Ordovician)—Mostly dark gray to black shale and chert, including some argillite, that crop out near southeast corner of area and comprise basal formation of homoclinal sequence of formations that dip shallowly (10 to 15°) to north. Strata generally slope forming, poorly exposed, and typically include evidence of outcrop-scale structural disruption such as crumpled bedding and presence of cleavage. Locally includes thin (approximately 0.5 m) laminated gray micrite, that weathers light gray to buff gray near top of strata. Gray micrite interbedded with black chert. Some black micrite, barren of conodonts, immediately below contact with overlying siltstone of Elder Sandstone, shows no evidence of structural disruption. Collection of conodonts obtained from locality at 7,220–ft elevation on ridgetop, long. 116°17'30", approximately 600 m north of south border of quadrangle, can be no younger than early Ashgillian (late Late Ordovician) or older than late early Caradocian (early Late Ordovician) (Anita G. Harris, written commun., 1999). Two other nearby localities north of Little Jack Creek in Rodeo Creek NE 7–1/2 minute quadrangle, approximately 1.1 km southwest of southeast corner of area and at approximately 6,000–ft elevation, contain graptolite faunas indicating correlation with the Middle Ordovician *Hustedeograptus teretiusculus* Zone (Zone 10 of Berry, 1960) (Stanley C. Finney, written commun., 1998). Unit also correlates with the lower part of Upper Member of Vinini Formation at type locality at Vinini Creek, Roberts Mountains, approximately 125 km to south

Lower plate of Roberts Mountains thrust—In this area includes:

Lower plate rocks, undivided (Devonian, Silurian, and Ordovician)—Includes mostly massive gray micrite and oolitic packstone of Silurian and Devonian Roberts Mountains Formation of Merriam and Anderson (1942) at Dee Mine, mostly thin-bedded siliceous argillite and micritic limestone of Devonian Rodeo Creek unit near Dee Mine, and small exposures of quartz-dolomitic wackestone of Ordovician Hansen Creek Formation near Capstone-Bootstrap Mine

Contact

High-angle fault—Bar and ball on downdropped block. Long-dashed where approximately located; short-dashed where inferred; dotted where concealed

Thrust fault—Sawteeth on upper plate. Long-dashed where approximately located; short dashed where inferred dotted where concealed

Fossil locality

Ar–Ar sample

Locality of analyzed rock sample (sample Groups 1 and 2, see text)

Locality of analyzed rock sample (Group 3, see text)

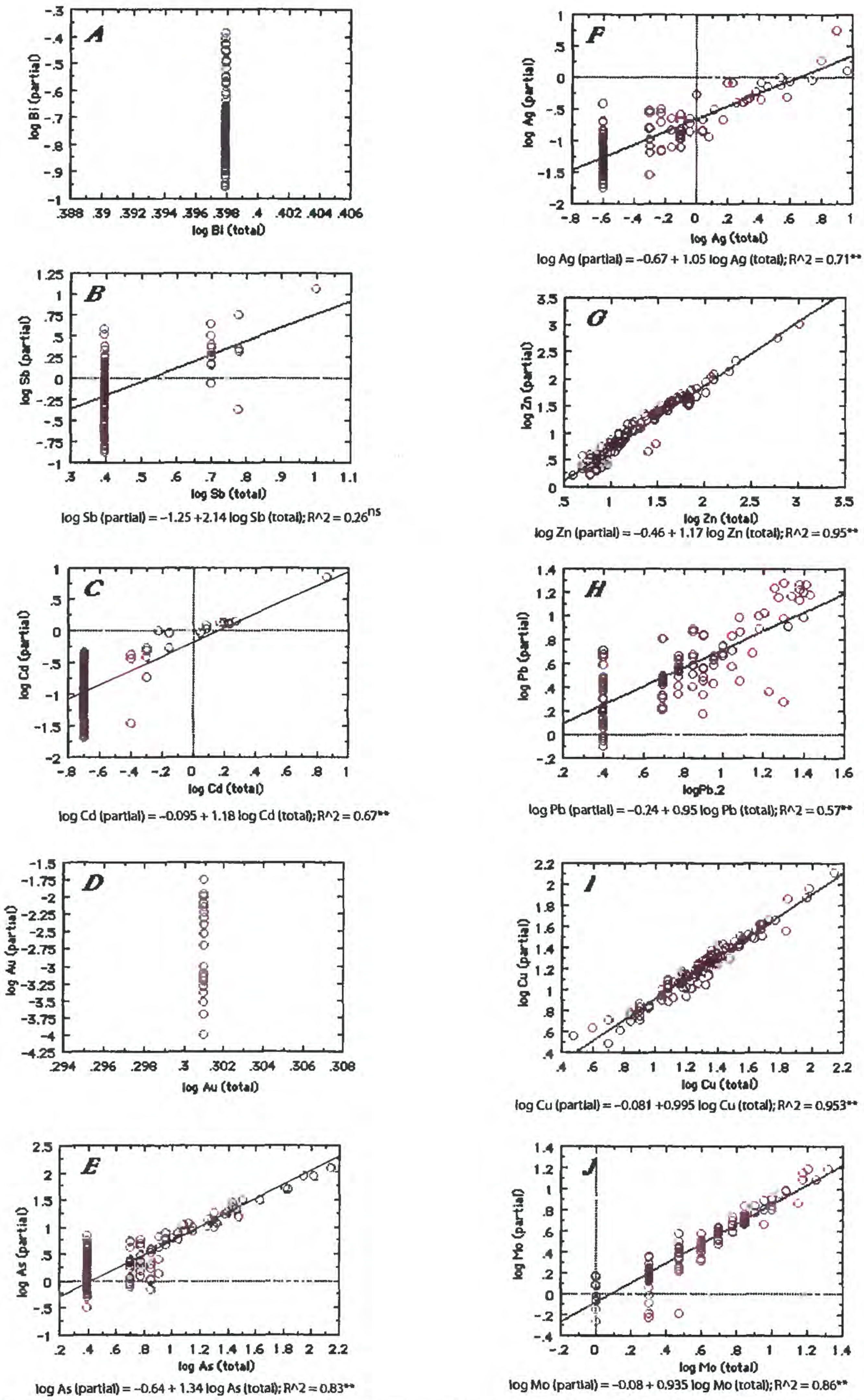

Figure 3—Diagrams showing analytical results, in logarithms to the base 10, of partial digestions versus total digestions for Bi (*A*), Sb (*B*), Cd (*C*), Au (*D*), As (*E*), Ag (*F*), Zn (*G*), Pb (*H*), Cu (*I*), and Mo (*J*) in 115 rocks (Group 1, see text) from an approximately east-west profile across the Santa Renia Fields and Beaver Peak quadrangles, Nev. Data from table 1. ns, not significant at the 5 % level; **, significant at the 1 % level.

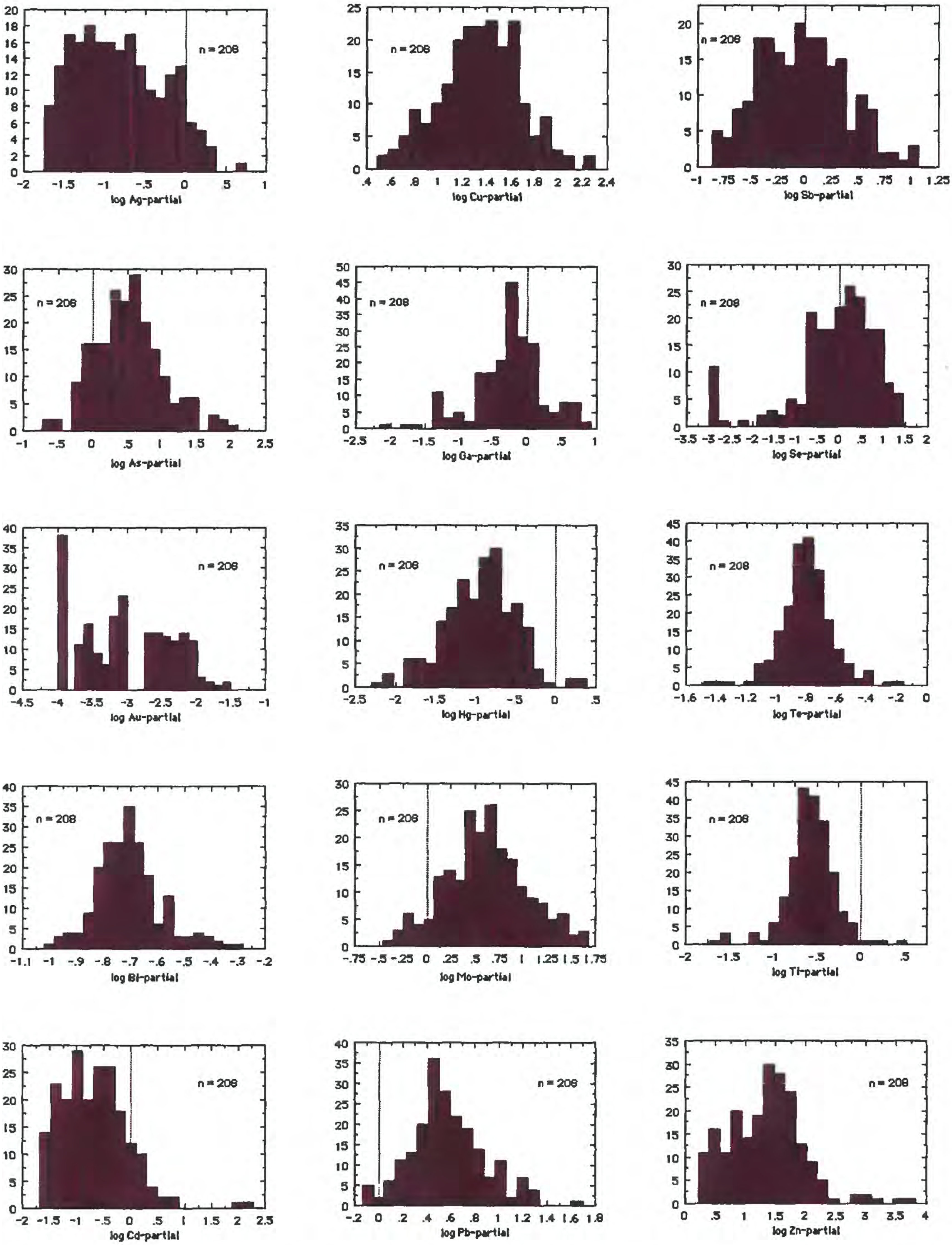

Figure 4—Log-frequency distribution of elements from analyses of 208 rocks that comprise sample Groups 1 and 2 (see text) in the Santa Renia Fields and Beaver Peak quadrangles, Nev. Partial, partial digestion techniques; total, total digestion techniques.

Figure 4—cont'd.

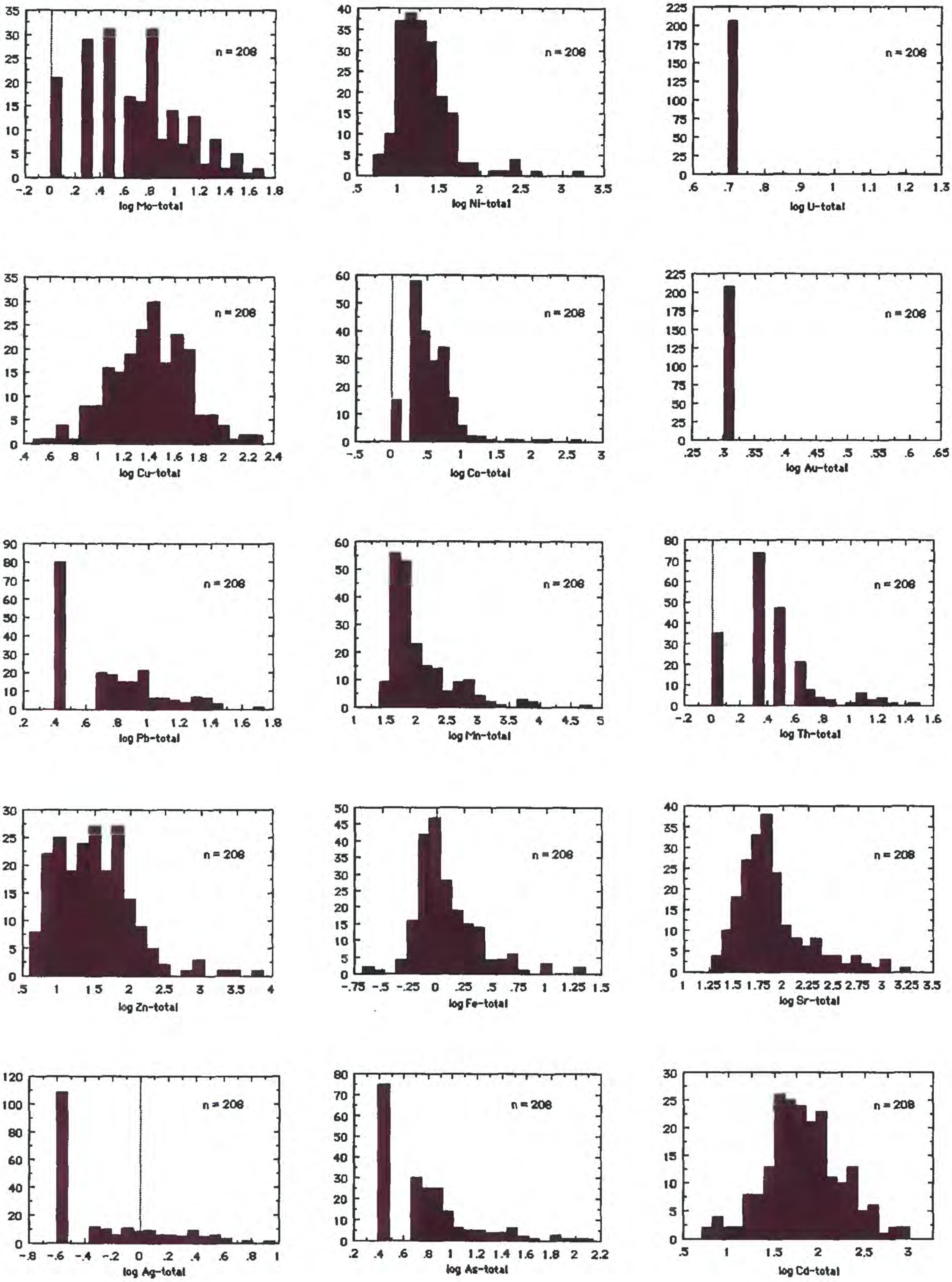

Figure 4—cont'd.

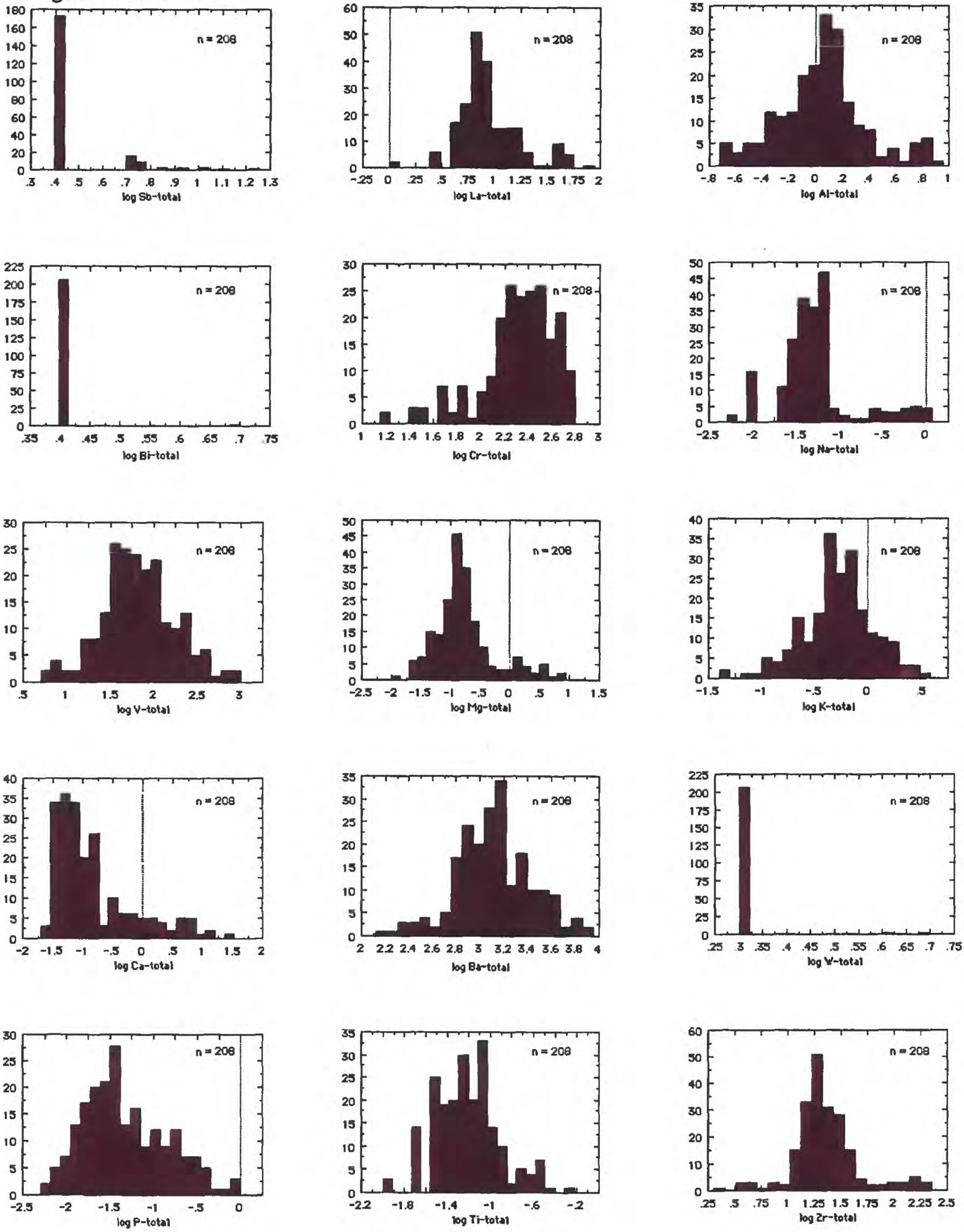

Figure 4—cont'd.

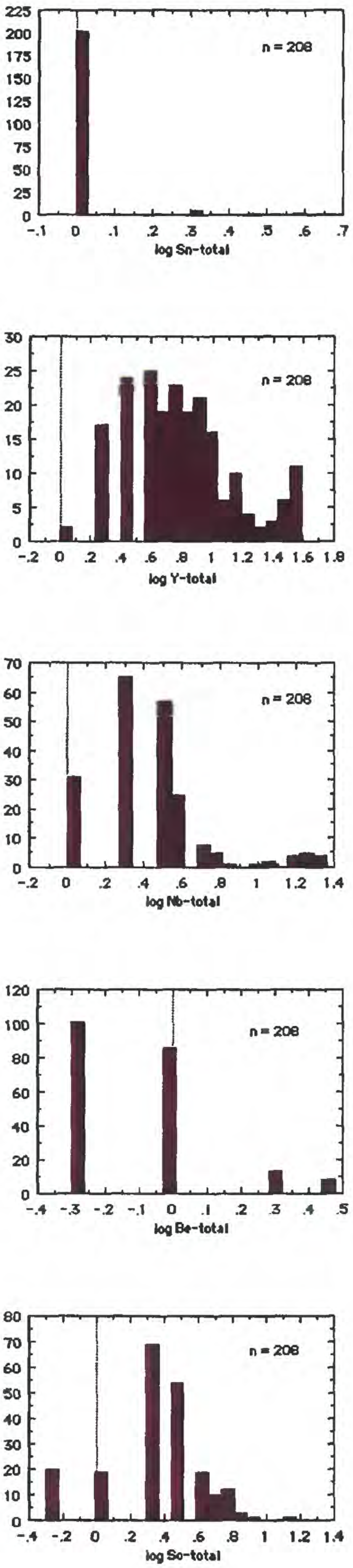

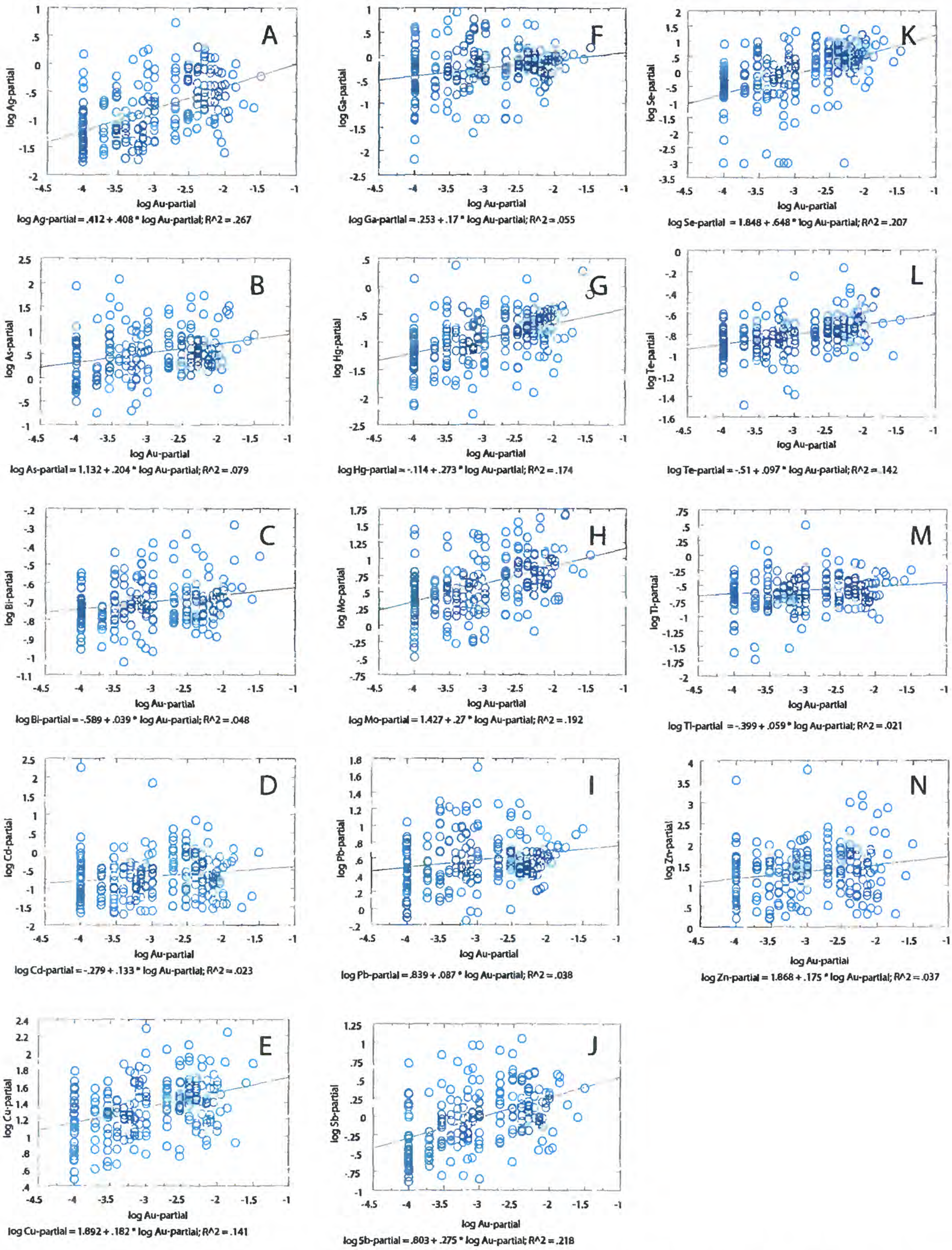

Figure 5—Plots showing log Au (ppm) versus log Ag (ppm), log As (ppm), log Bi (ppm), log Cd (ppm), log Cu (ppm), log Ga (ppm), log Hg (ppm), log Mo (ppm), log Pb (ppm), log Sb (ppm), log Se (ppm), log Te (ppm), log Tl (ppm), and log Zn (ppm) for combined sample Groups 1 and 2 (see text) .

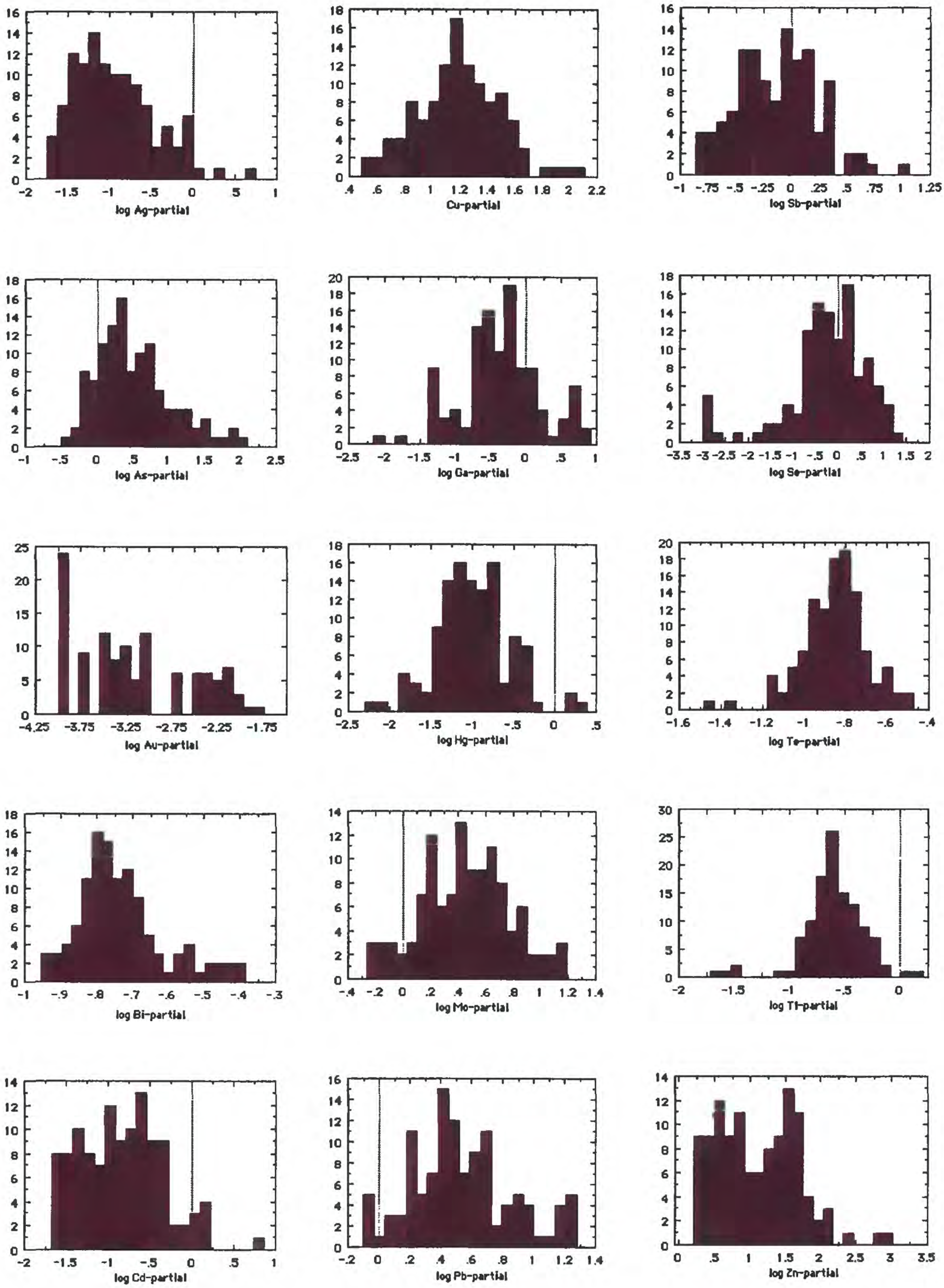

Figure 6—Log-frequency distribution of elements from analyses of 115 rocks that comprise sample Group 1 collected along traverse AA' in the Santa Renia Fields and Beaver Peak quadrangles, Nev. Partial, partial digestion techniques; total, total digestion techniques.

Figure 6—cont'd.

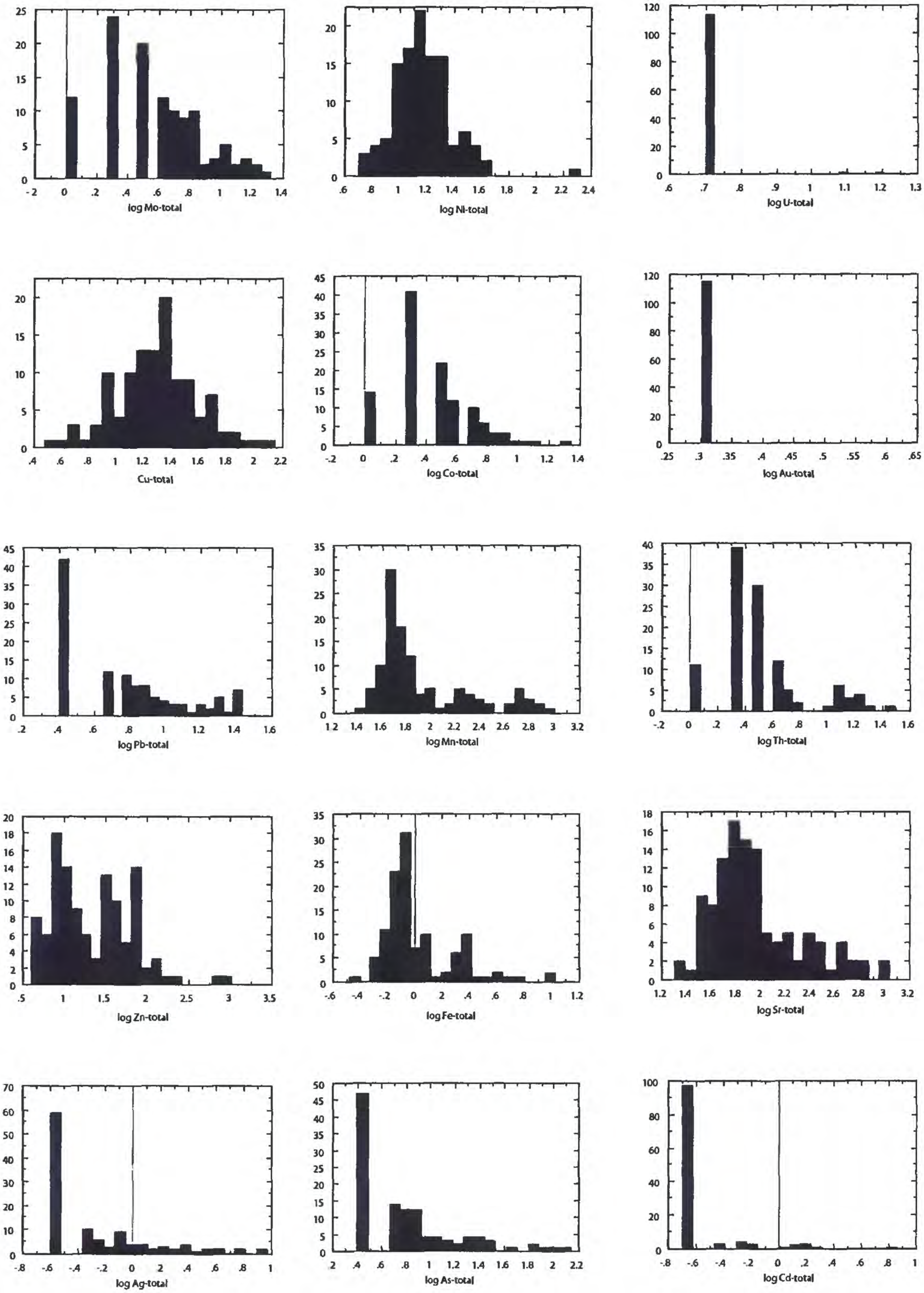

Figure 6—cont'd.

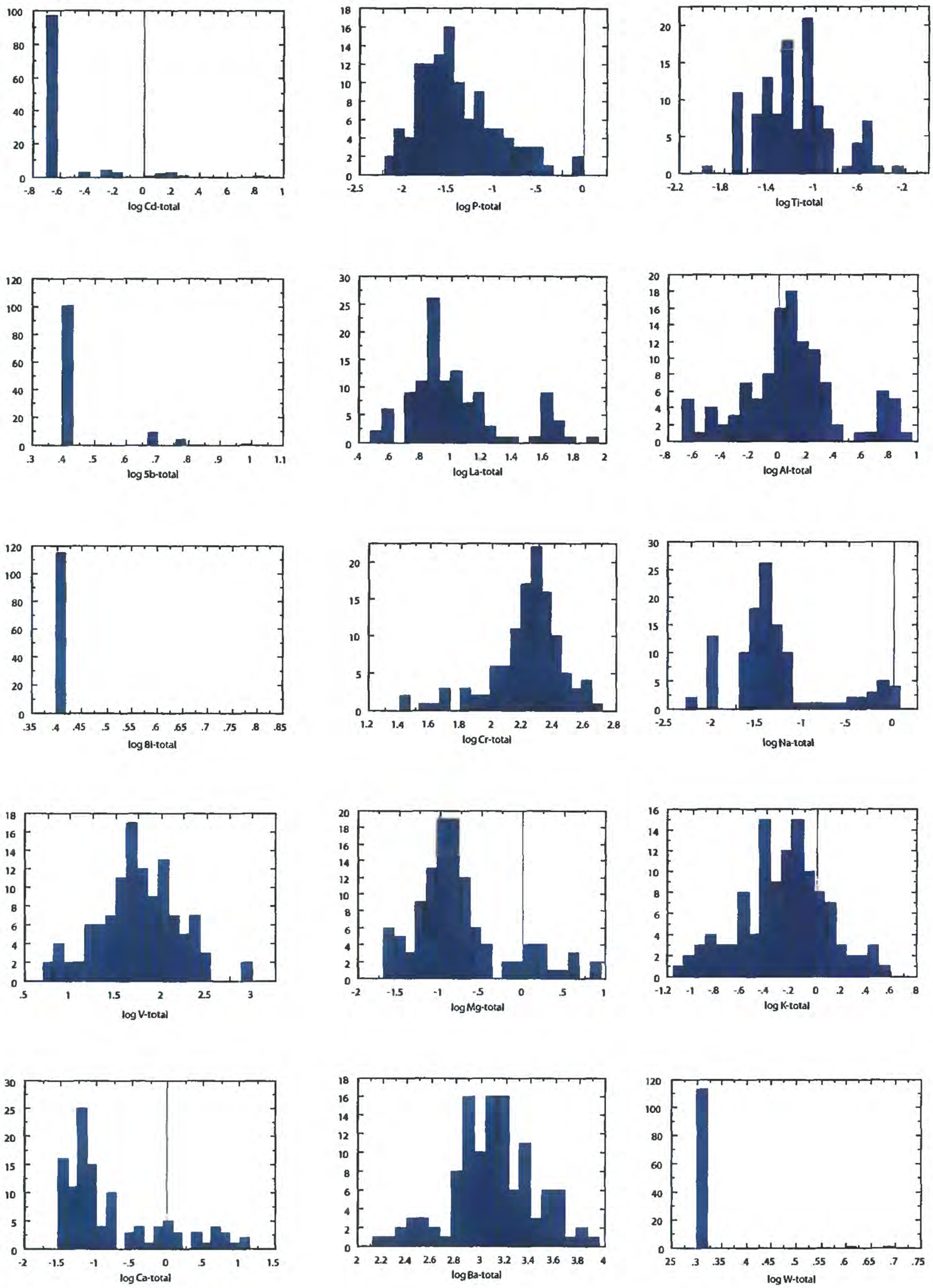

Figure 6—cont'd.

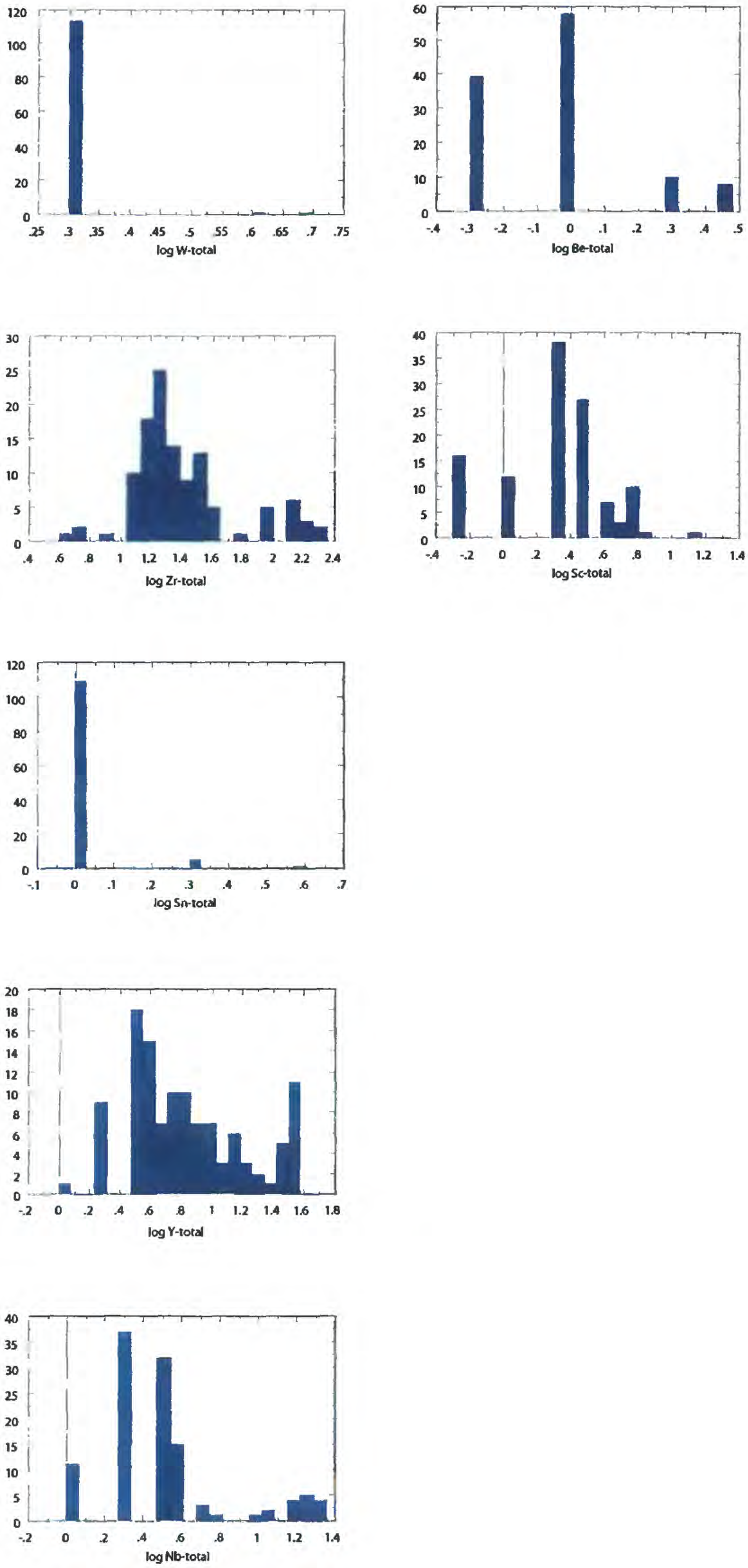

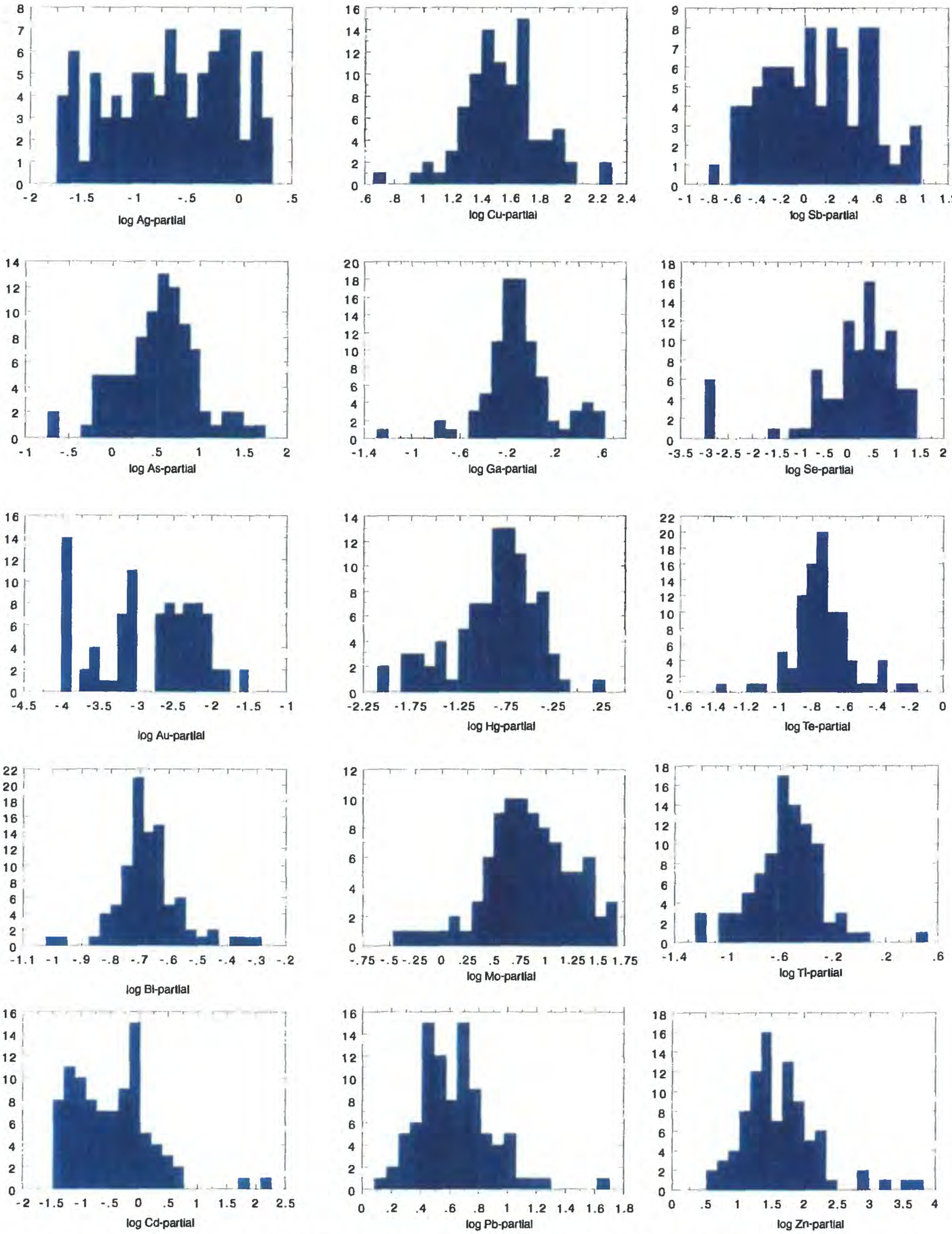

Figure 7—Log-frequency distribution of elements from analyses of 93 rocks that comprise sample Group 2 collected in southeast part of the Beaver Peak quadrangle, Nev. Includes 14 rocks from Coyote barite mine. Log ppm except for Fe, Ca, P, Mg, Ti, Al, Na, and K which are log weight percent.

Figure 7—cont'd.

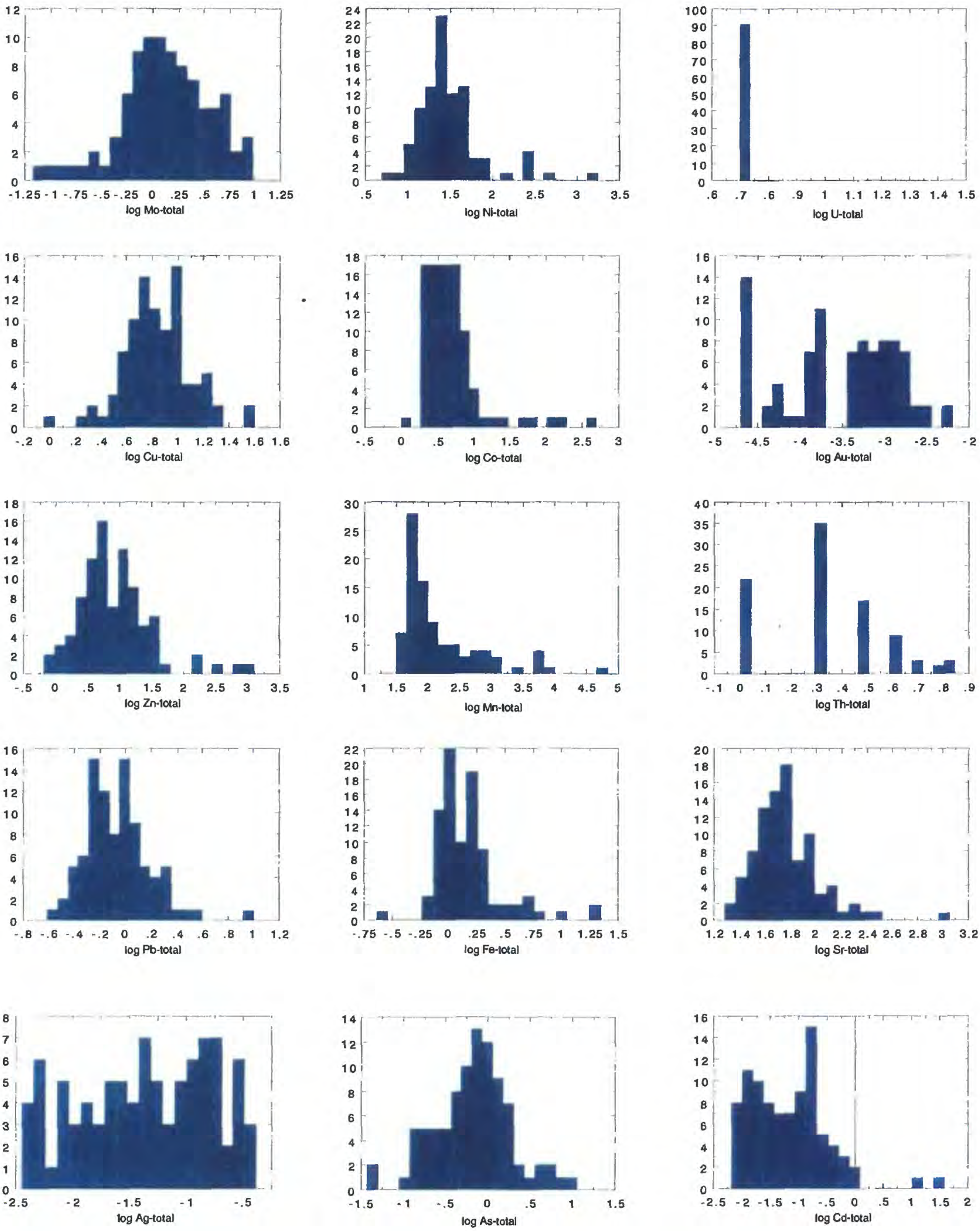

Figure 7—cont'd

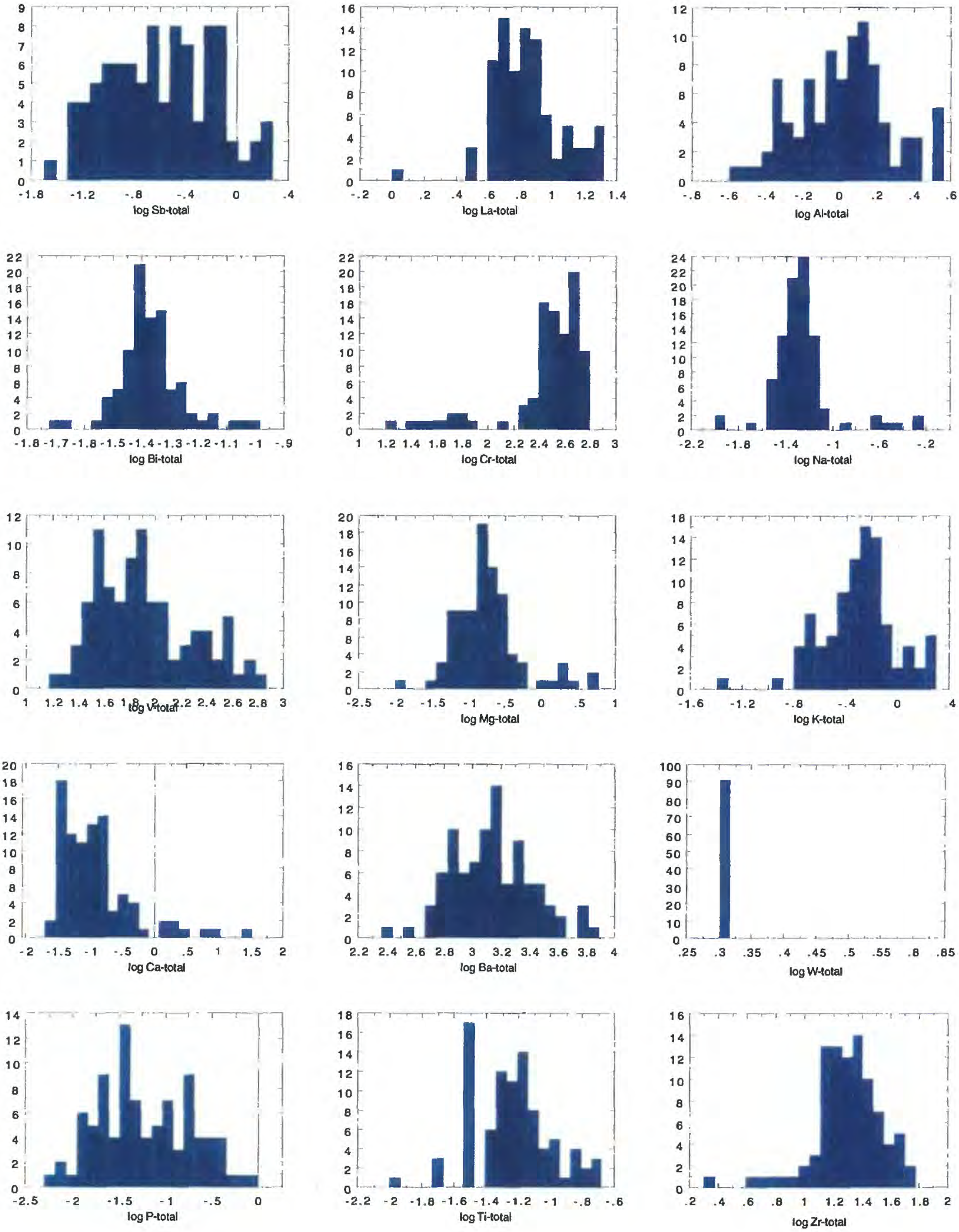

Figure 7—cont'd.

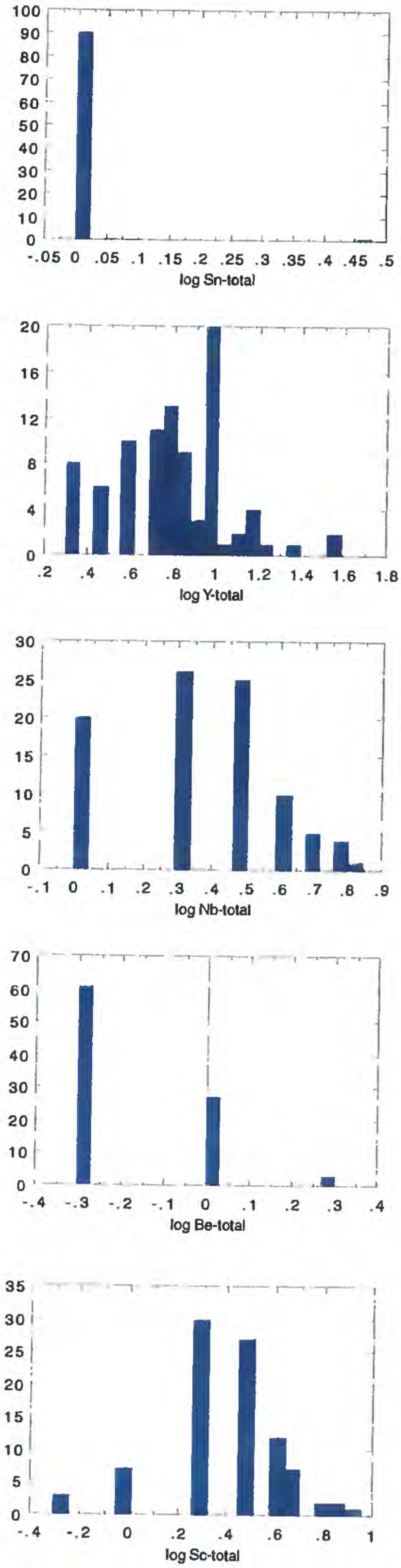

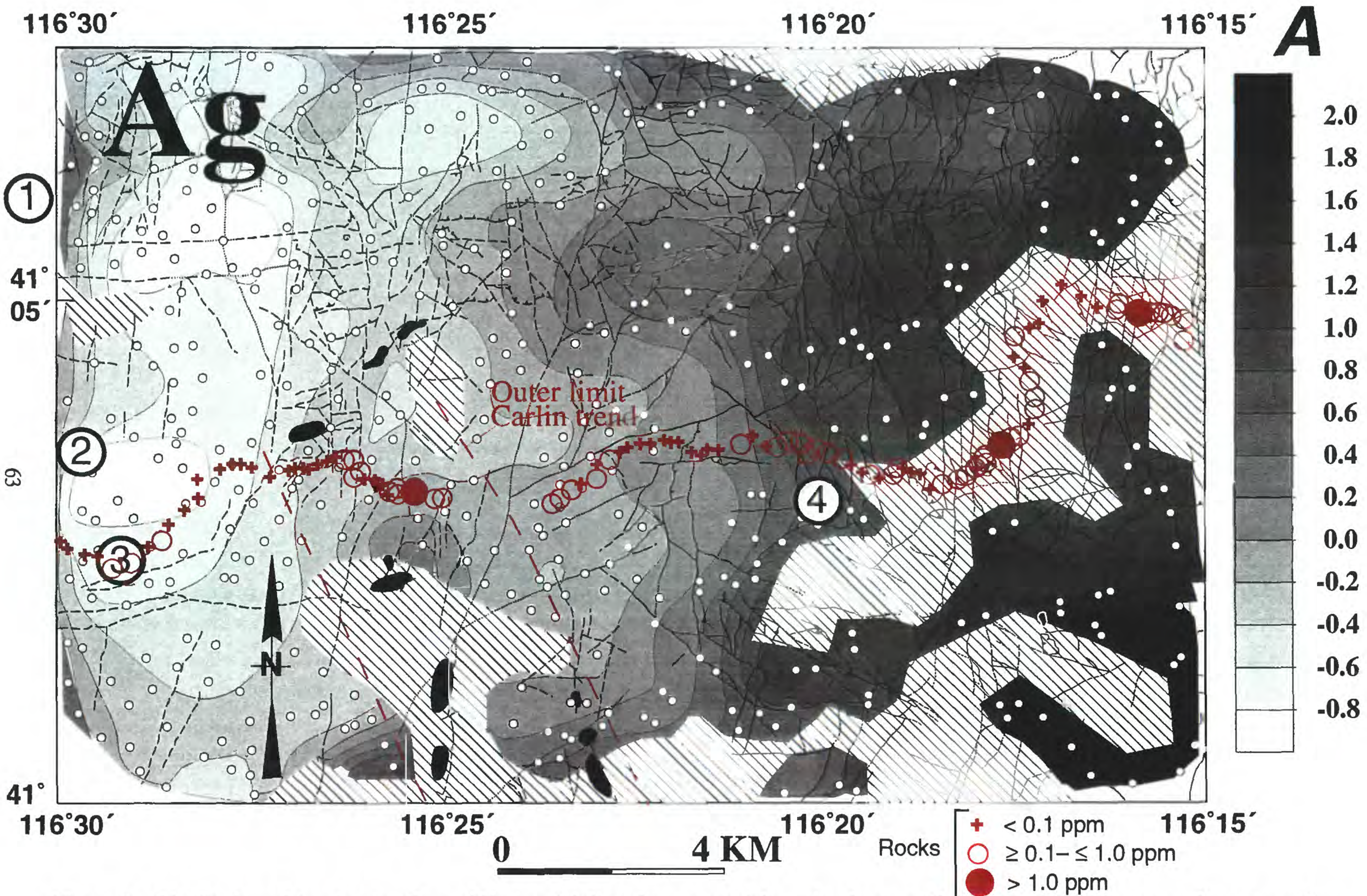

Figure 8—Distribution of Ag, As, Au, Cu, and Zn (partial digestion, see text) in rocks along profile compared with stream-sediment samples from Santa Renia Fields and Beaver Peak quadrangles, Nev. Contours of stream-sediment data in various shades of gray showing normalized standard deviations (modified from Theodore and others, 1999). Areas shown in hachured pattern not contoured because of presence of surface disturbance and (or) steep prominent ridges. Small open circles, stream-sediment sample localities; numbered large open circles, areas of significant silica veins (see text); filled black areas, Au deposits and barite deposits (see fig. 2).

Figure 8—cont'd.

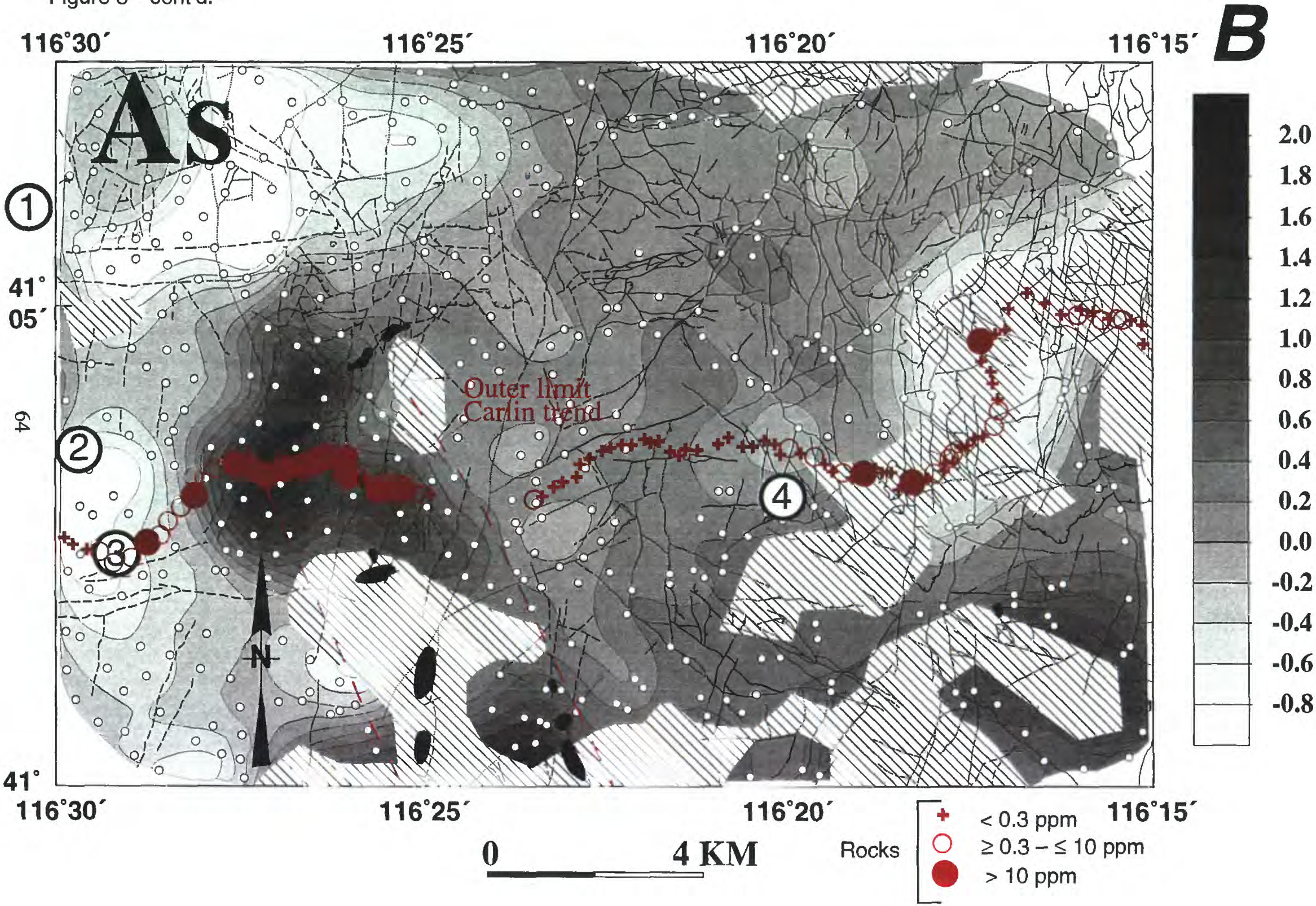

Figure 8—cont'd.

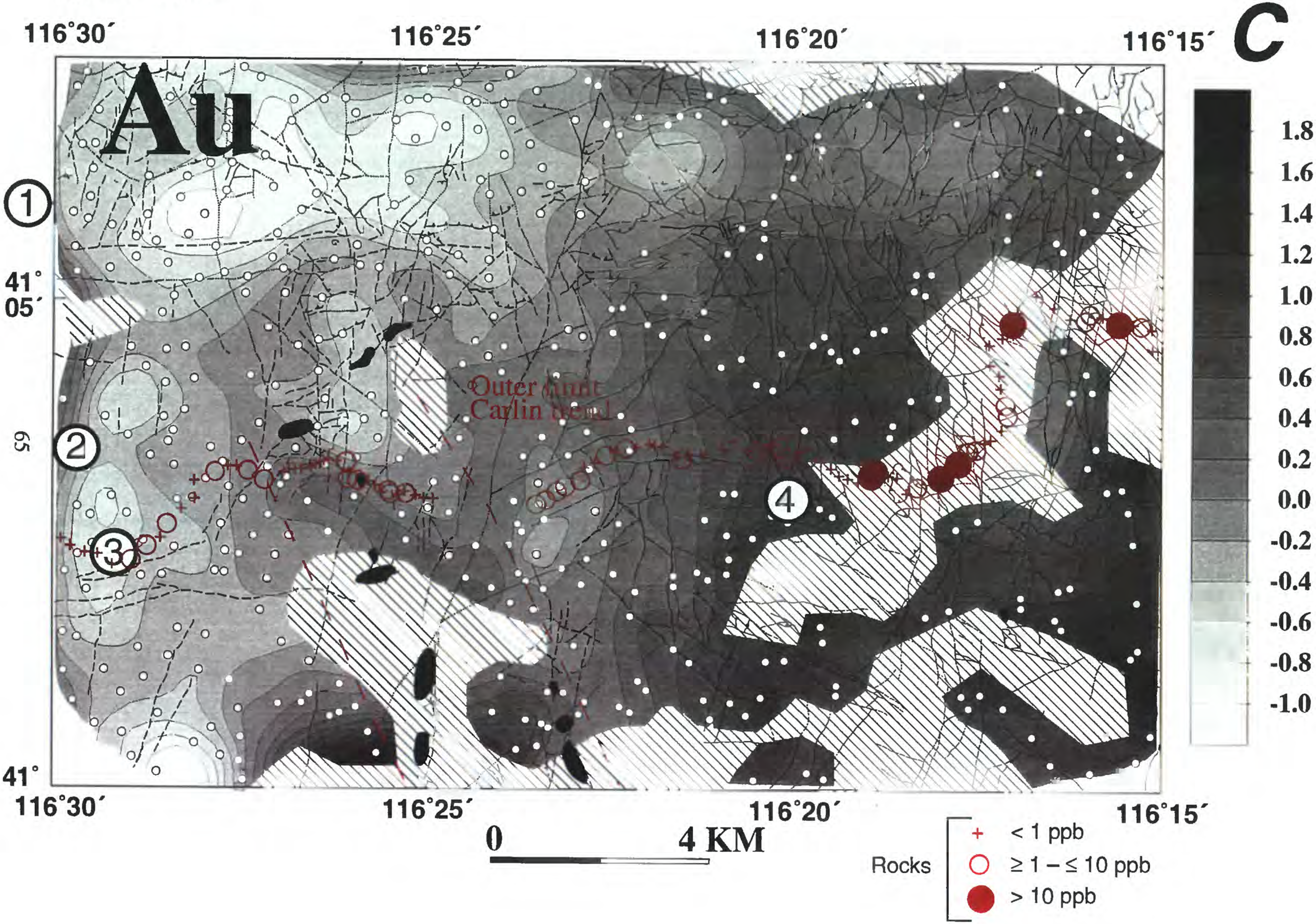

Figure 8—cont'd.

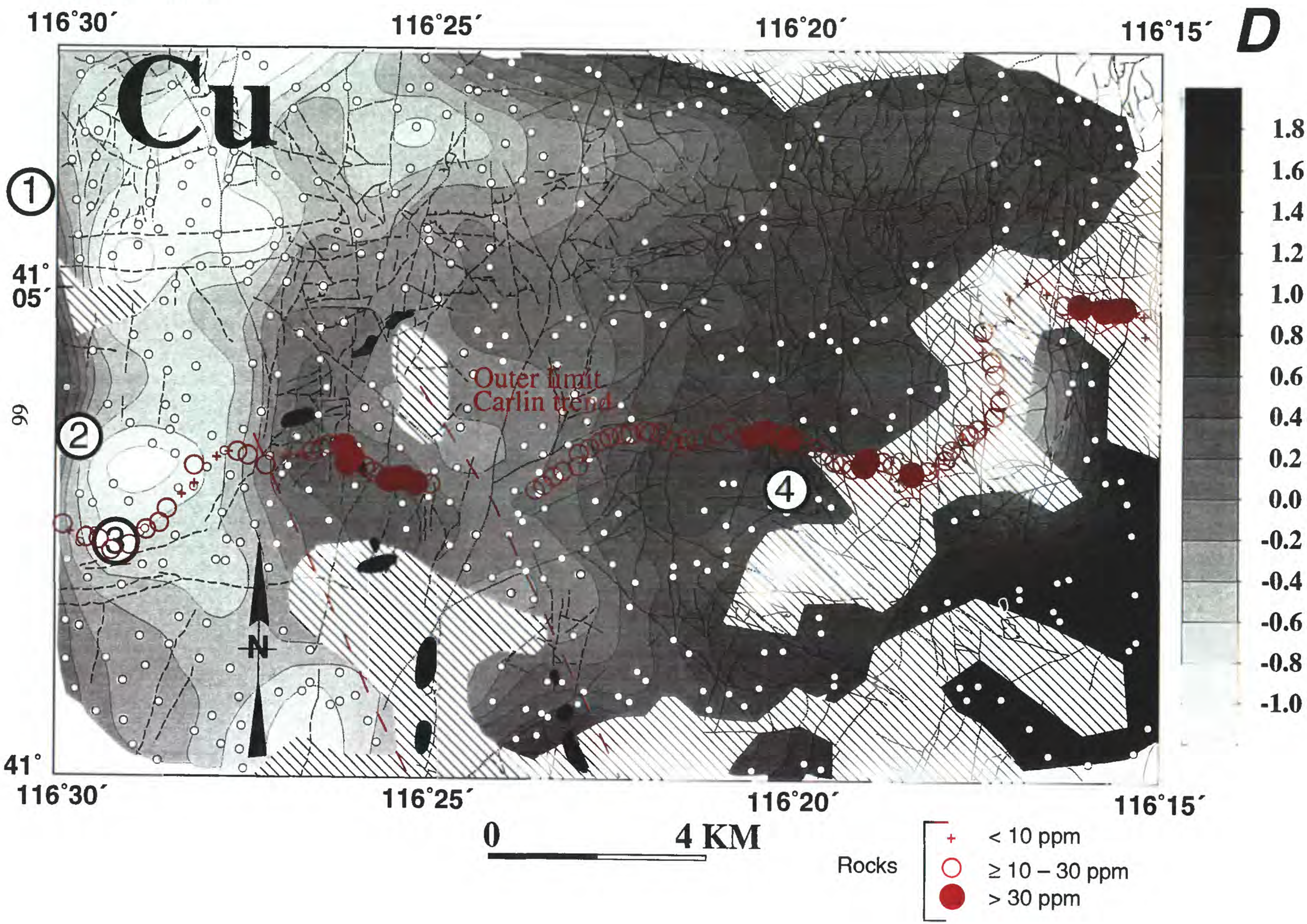

Figure 8—cont'd.

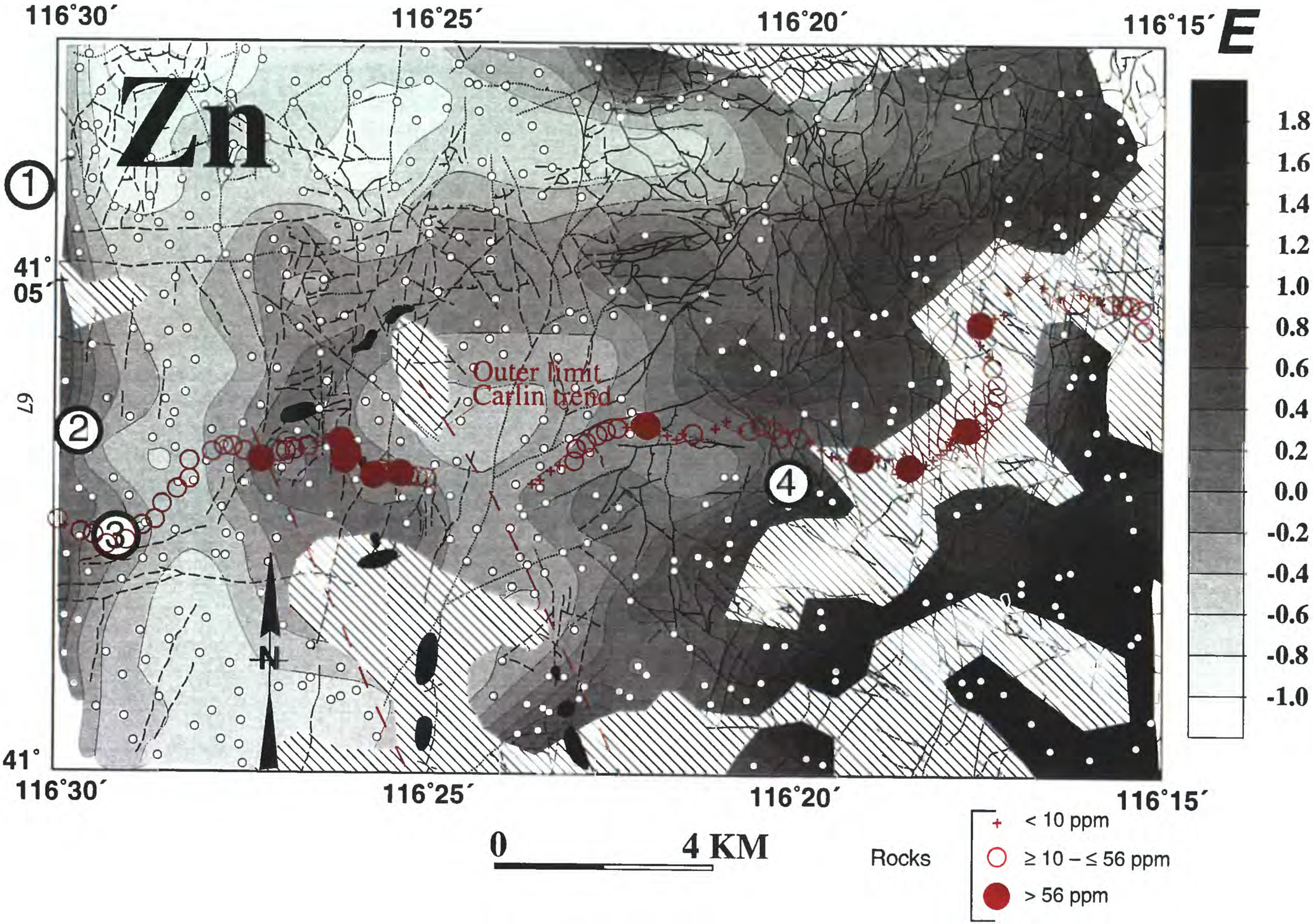

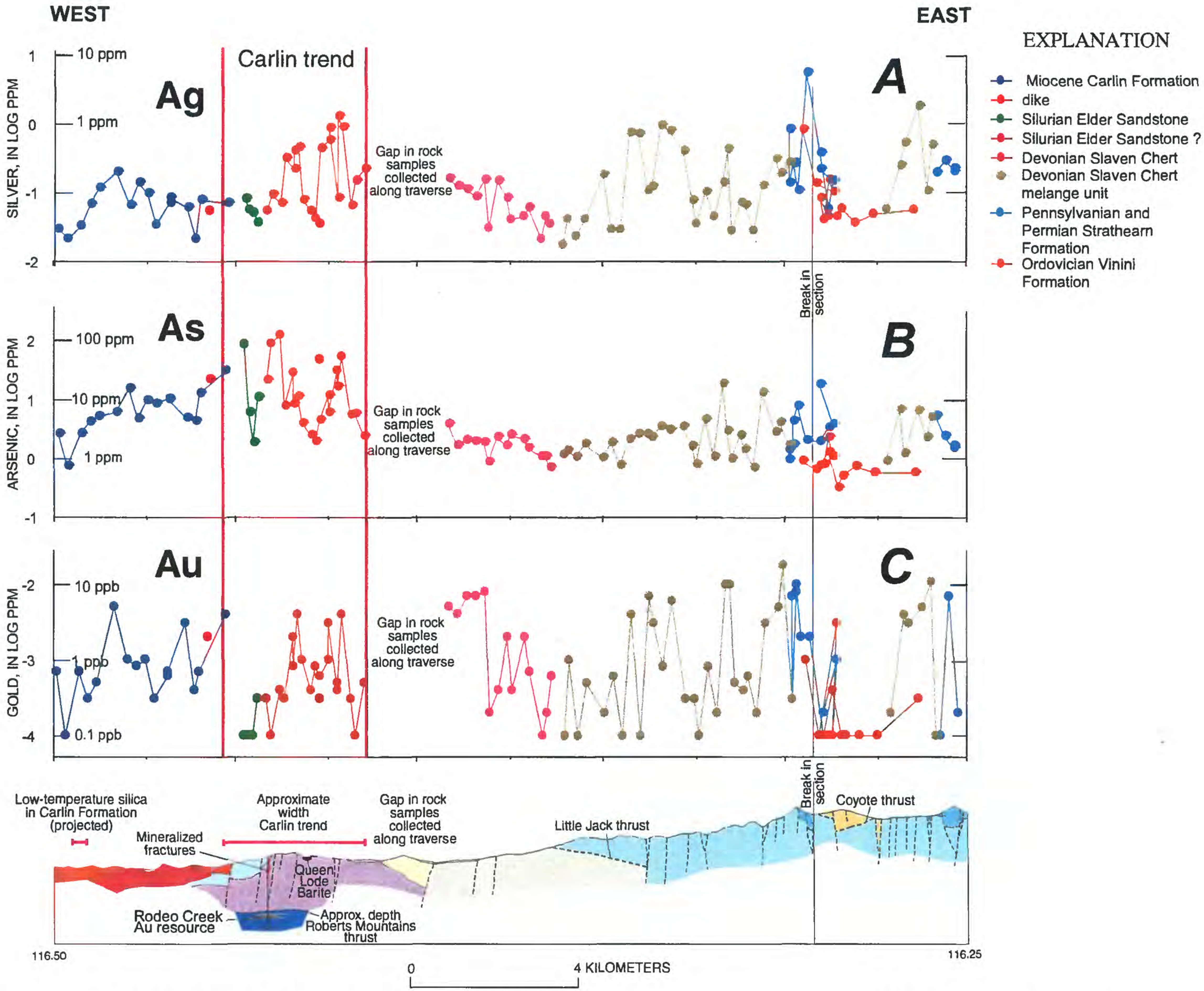

Figure 9—Abundances of Ag, As, Au, Bi, Cd, Cu, Hg, Mo, Pb, Sb, Se, Te, Tl and Zn in rock versus distance projected to profile AA'. See figure 2 for locations of profile AA' and samples analyzed. Data from table 1 (see text).

Figure 9—cont'd.

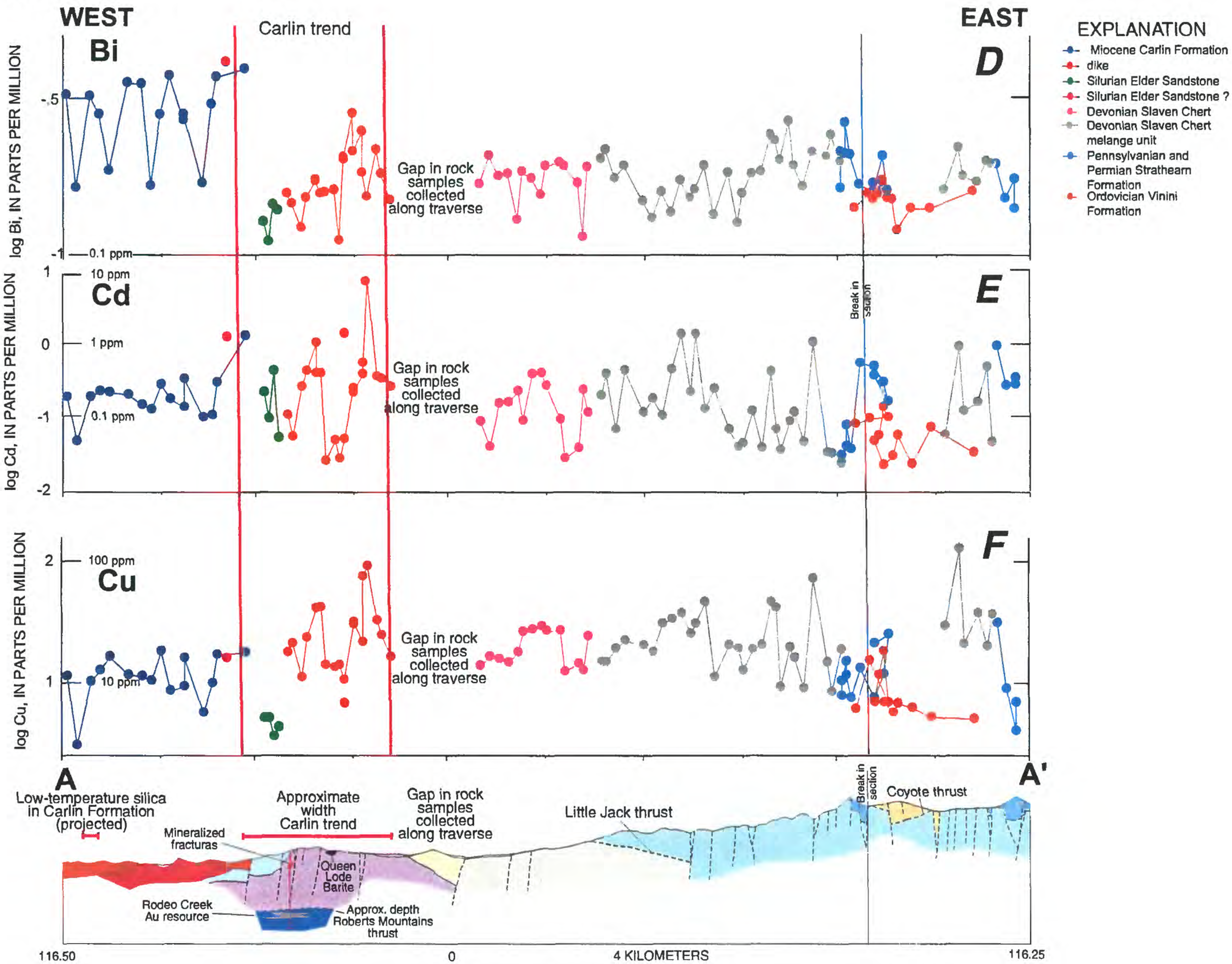

Figure 9—cont'd.

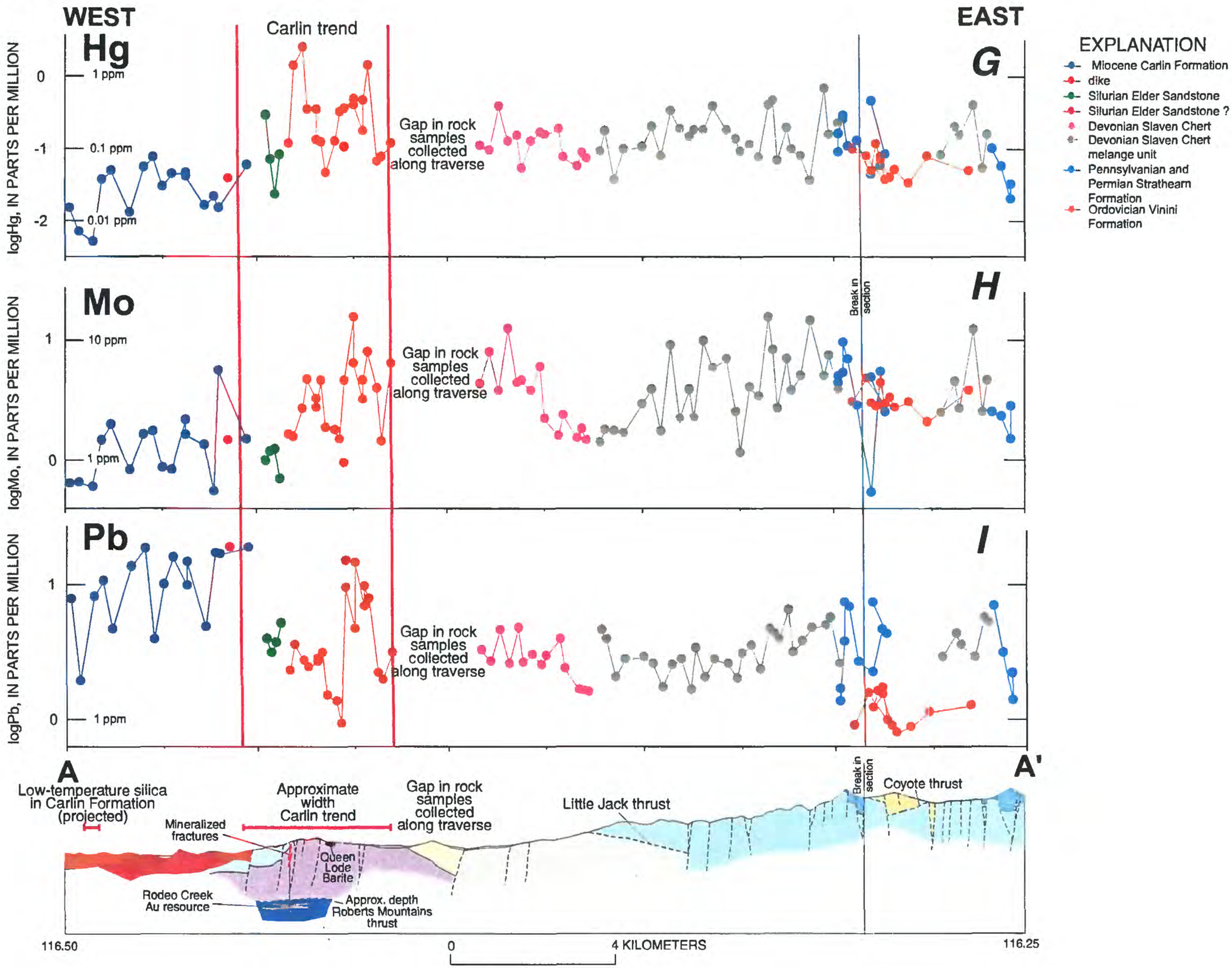

Figure 9—cont'd.

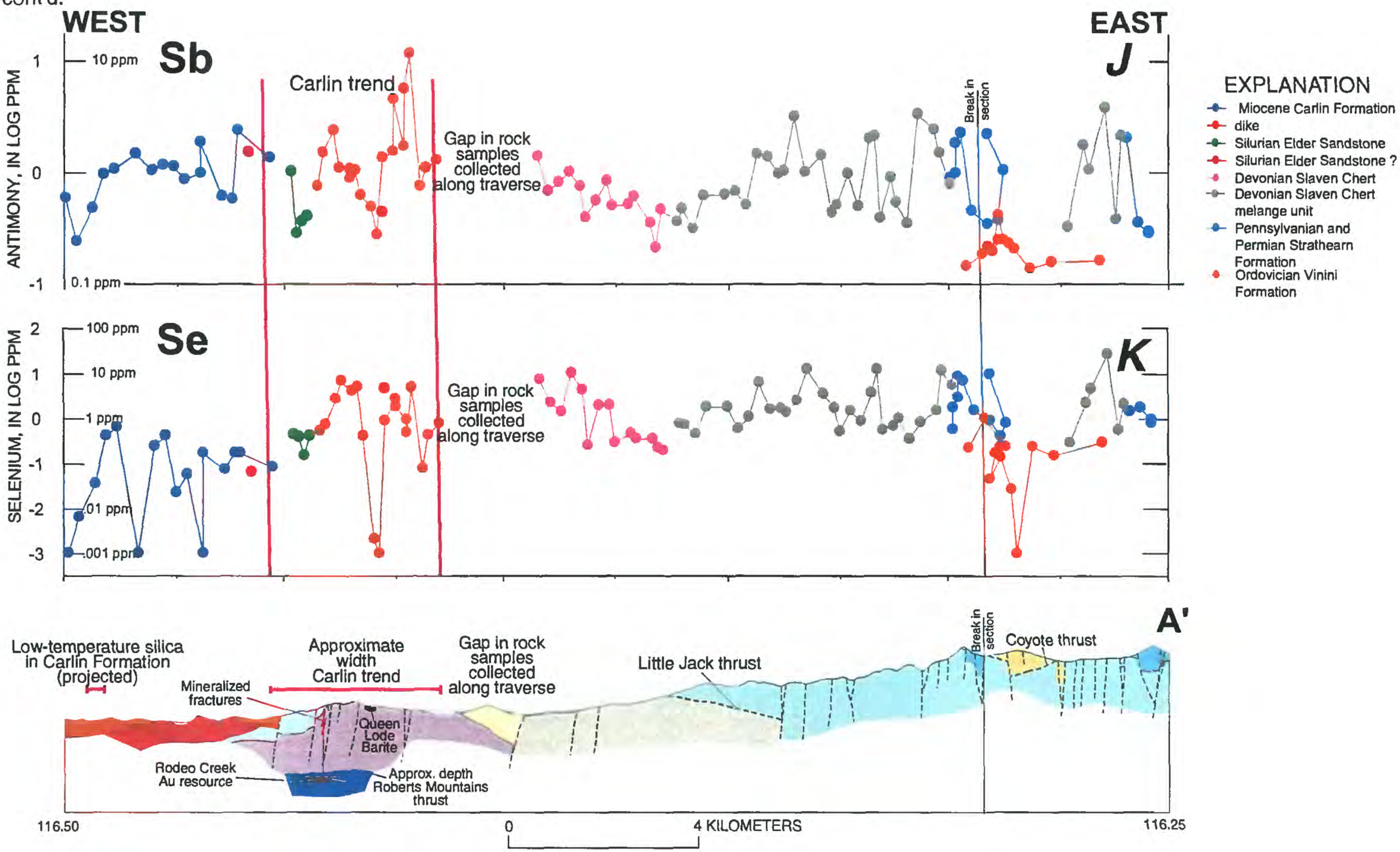

Figure 9–cont'd.

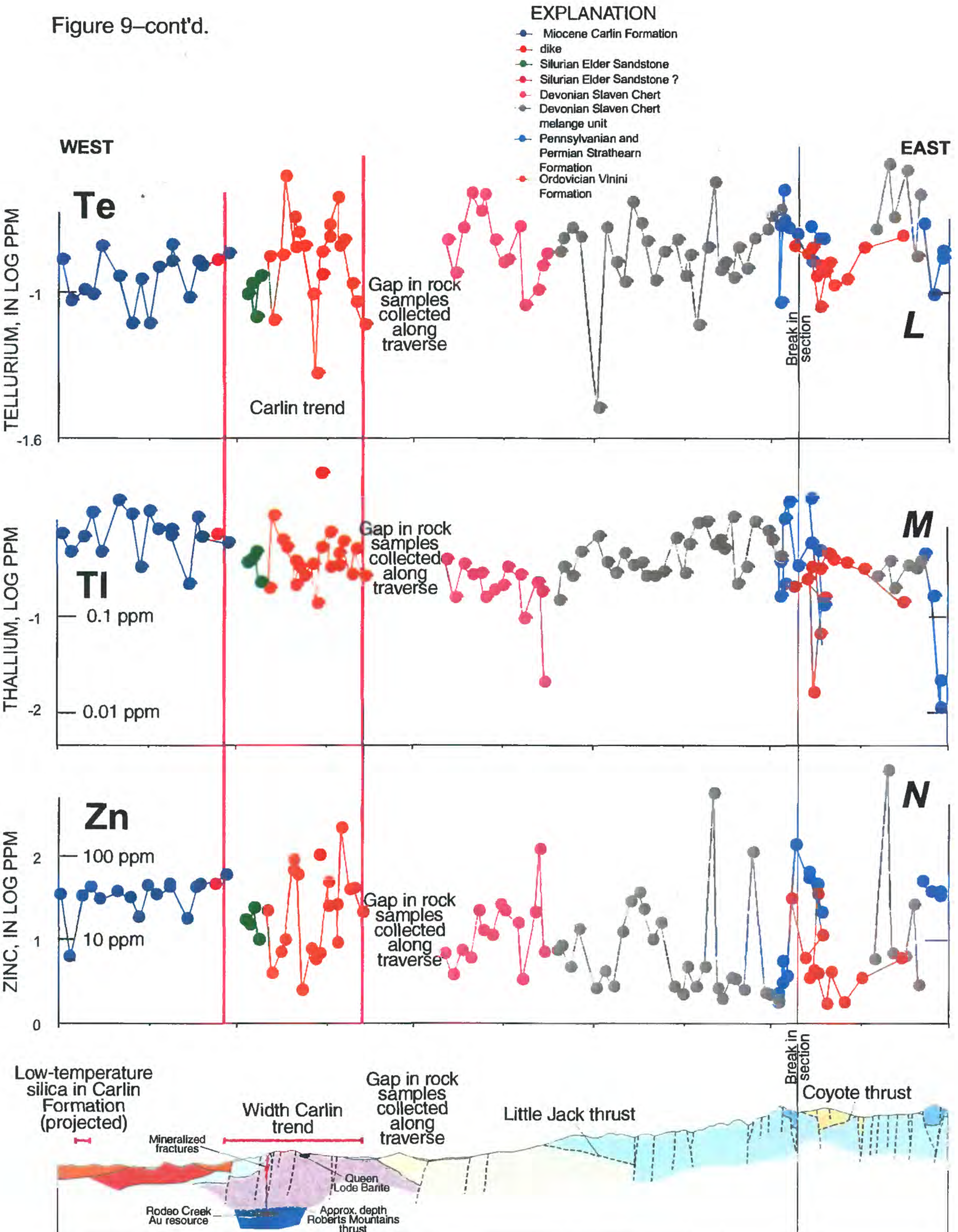

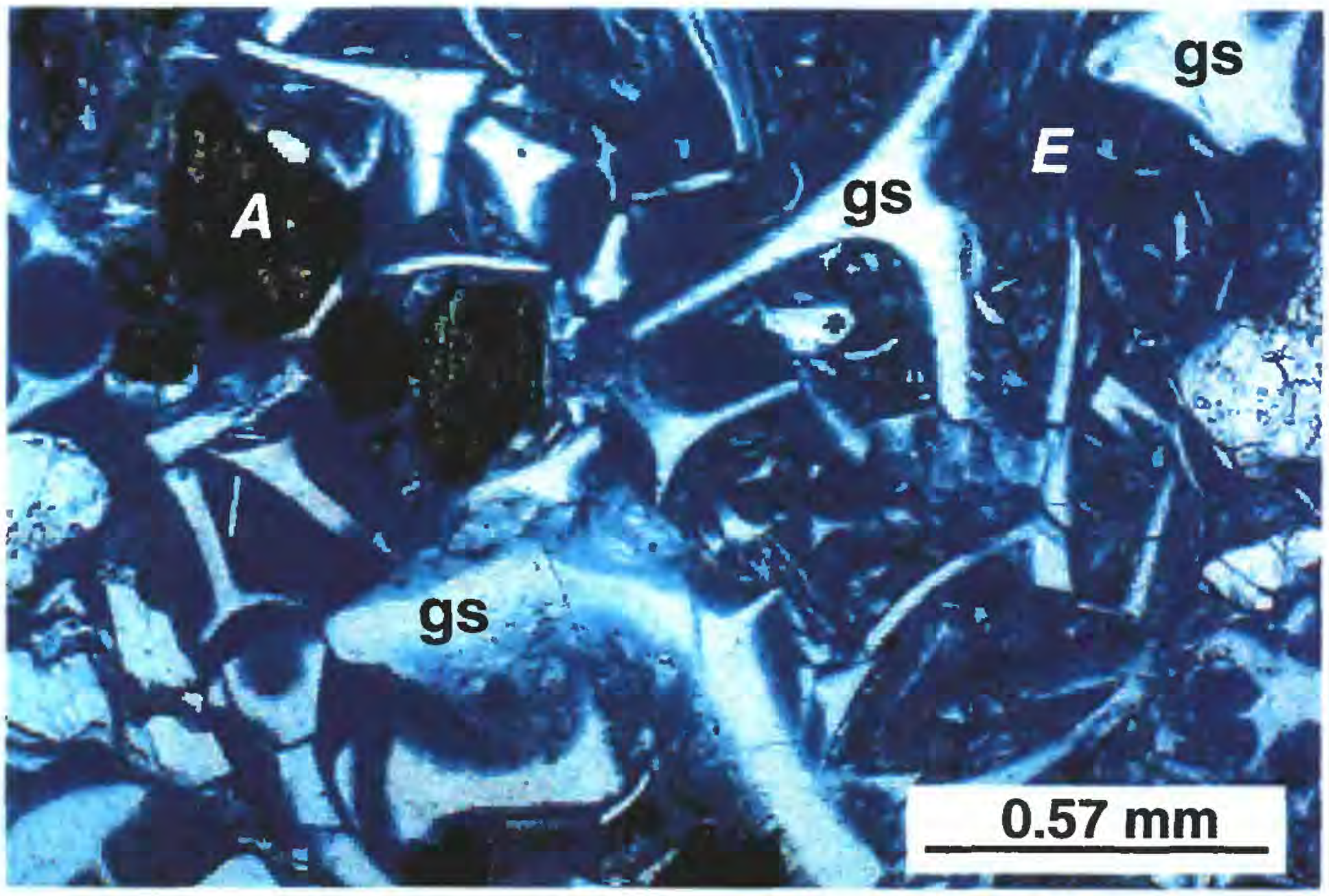

Figure 10—Photomicrograph of air-fall tuff in Miocene Carlin Formation, Santa Renia Fields quadrangle, Nev. Plane-polarized light; gs, glass shard; *A*, abrasive contaminant; *E*, hole filled with blue-stained epoxy.

Figure 11—Chalcedonic vein cutting Miocene Carlin Formation near west end of profile AA' (fig. 2) in Santa Renia Fields quadrangle, Nev.

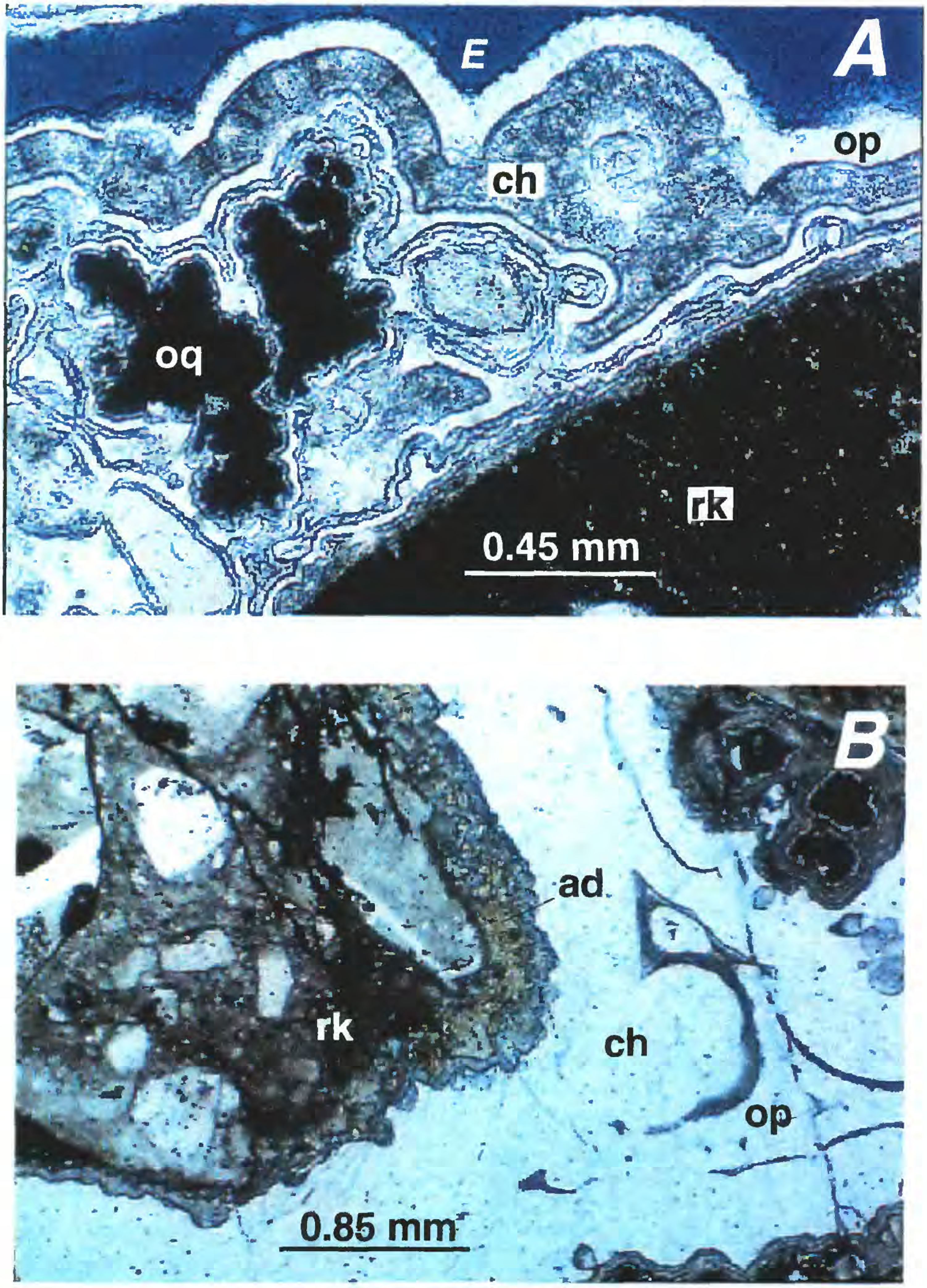

Figure 12—Photomicrographs of chalcedonic veins cutting Miocene Carlin Formation near west end of profile AA' (fig. 2) in Santa Renia Fields quadrangle, Nev. Plane-polarized light; ch, chalcedonic quartz; op, opal; ad, adularia; rk, rock fragments; *E*, hole filled with blue-stained epoxy. *A*, Colloform aggregate of opal encrusted on chalcedonic quartz with enclosed opaque mineral. *B*, Chalcedonic quartz with adularia.

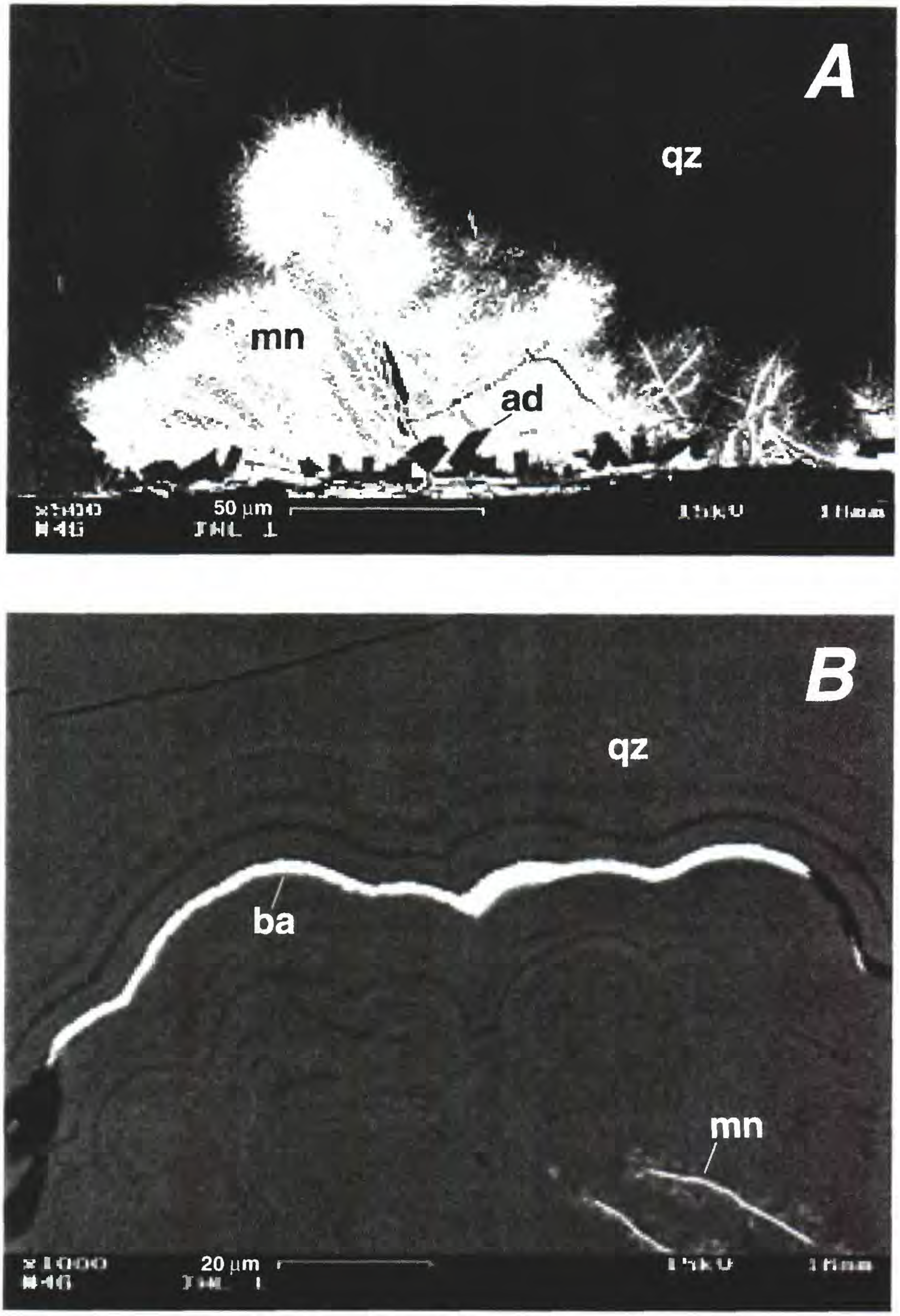

Figure 13—Back-scattered scanning electron images of mineral admixtures in chalcedonic quartz (qz) that cuts Miocene Carlin Formation near west edge of Santa Renia Fields quadrangle, Nev. *A*, dendritic manganese oxide (mn) and crystals of adularia (ad) in chalcedonic quartz; *B*, conformable lamina of barite in colloform chalcedonic quartz .

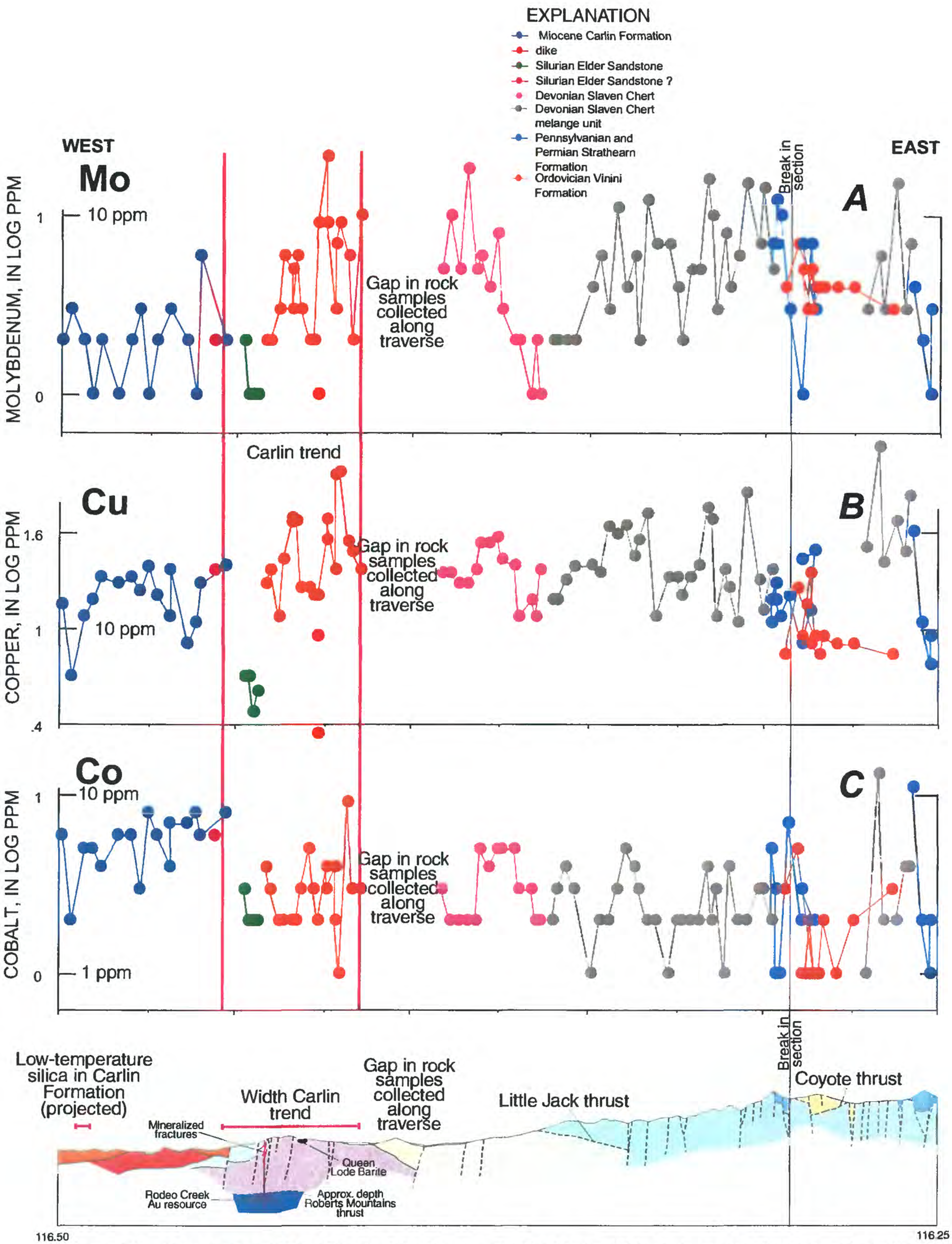

Figure 14—Abundances of Mo, Cu, Co, Mn, Zn, Ag, Fe, Th, U, As, Ni in rock versus distance projected to profile AA'. See figure 2 for locations of profile AA' and samples analyzed. Data (total digestion) from table 1(see text).

Figure 14—cont'd.

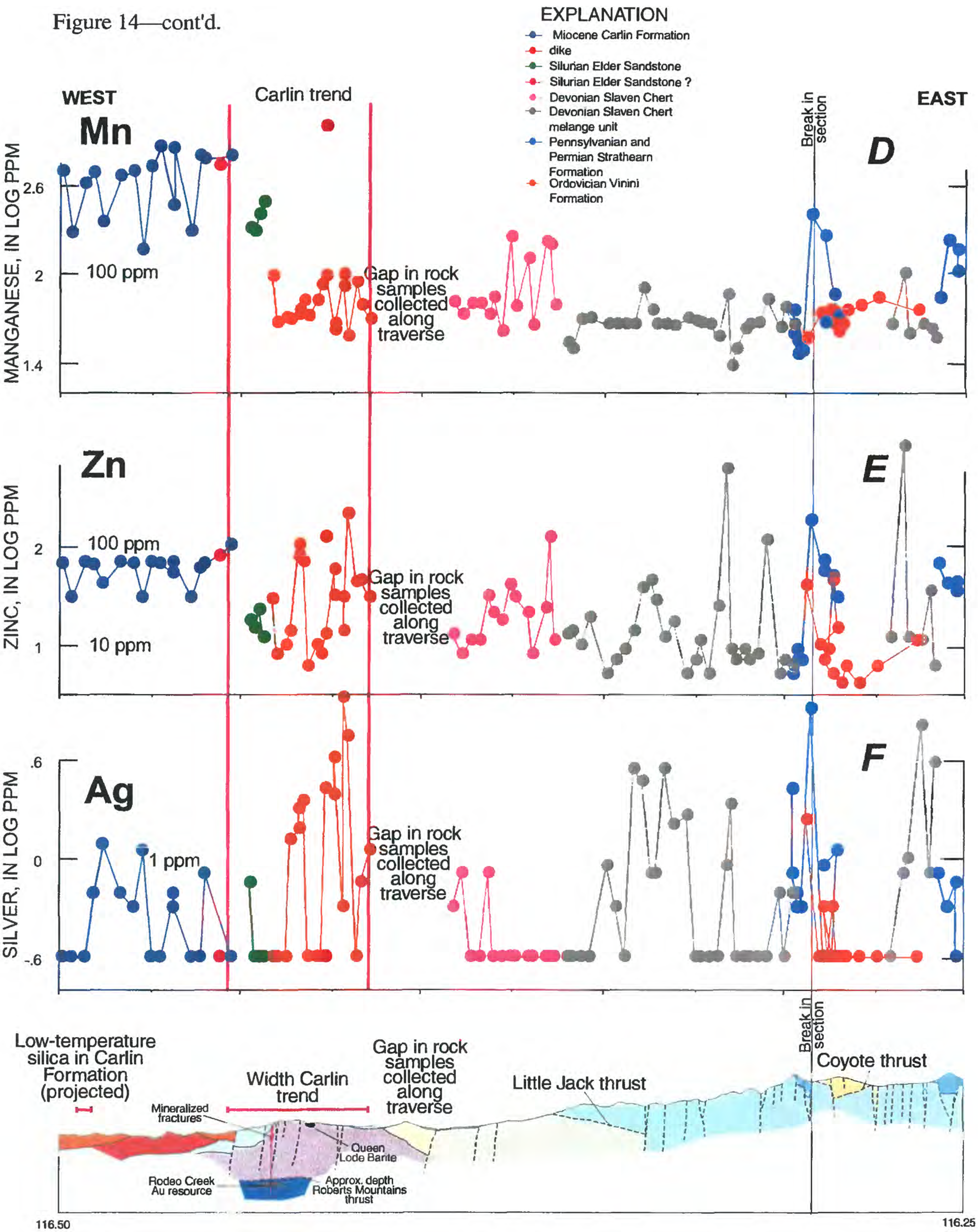

Figure 14—cont'd.

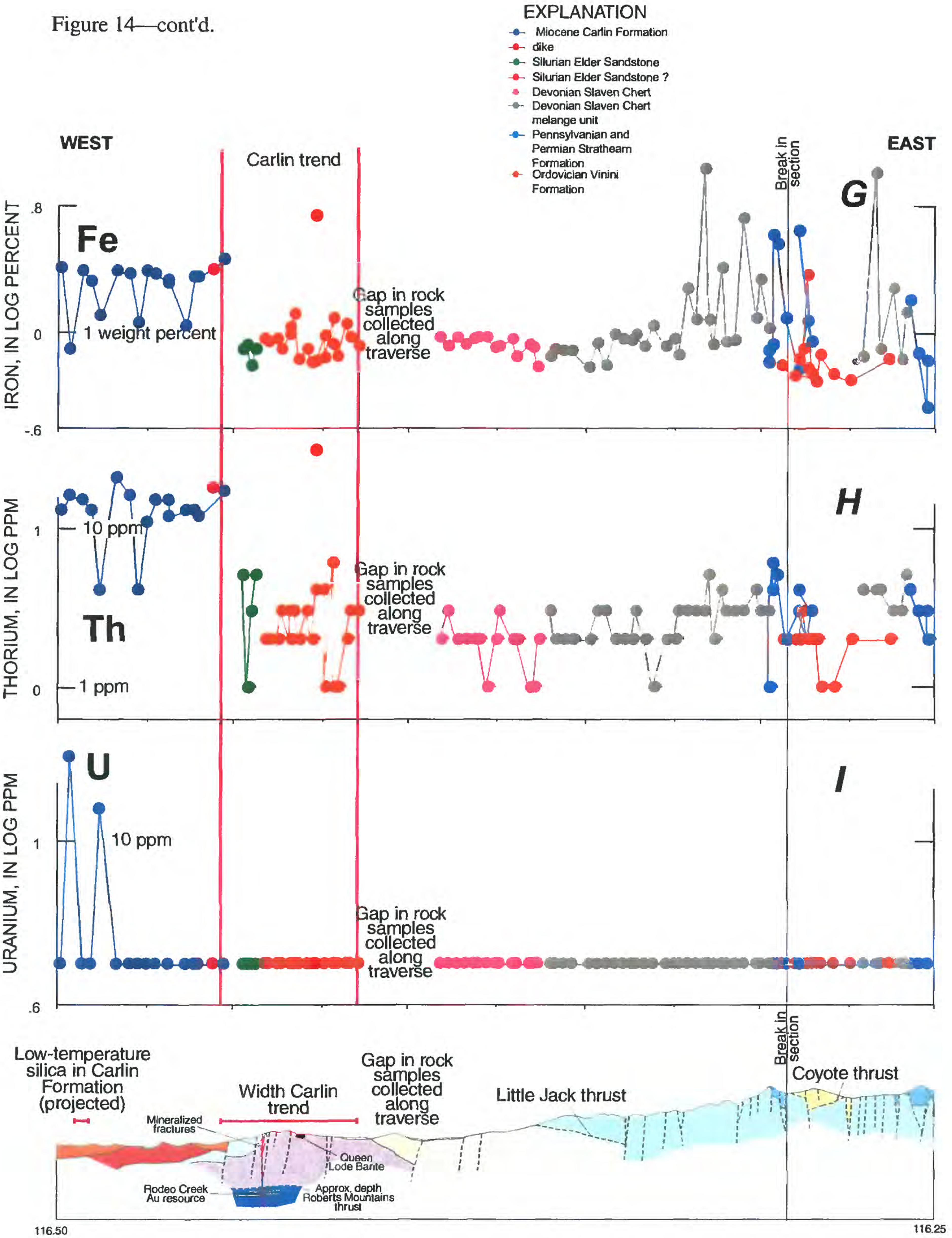

Figure 14—cont'd.

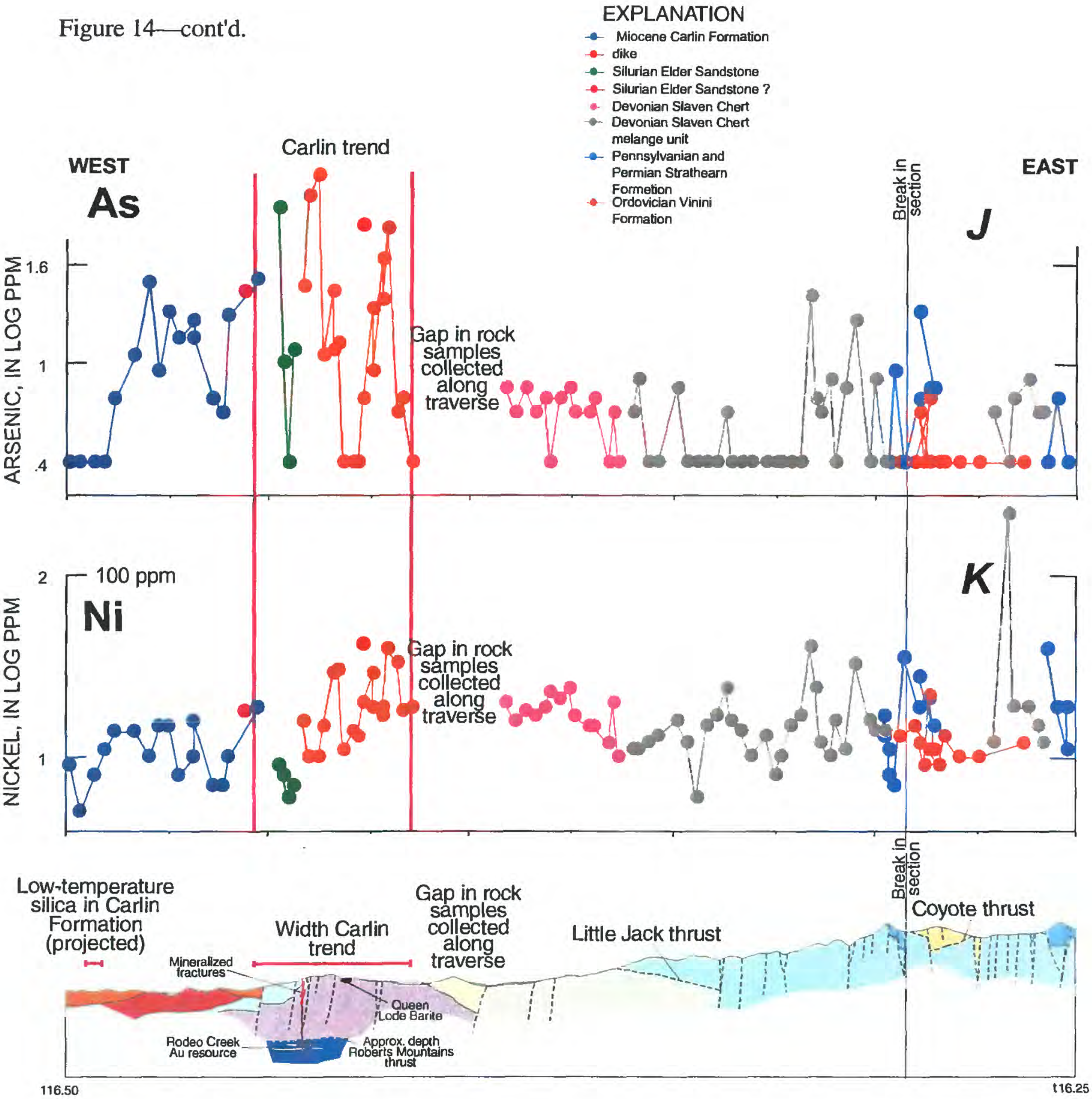

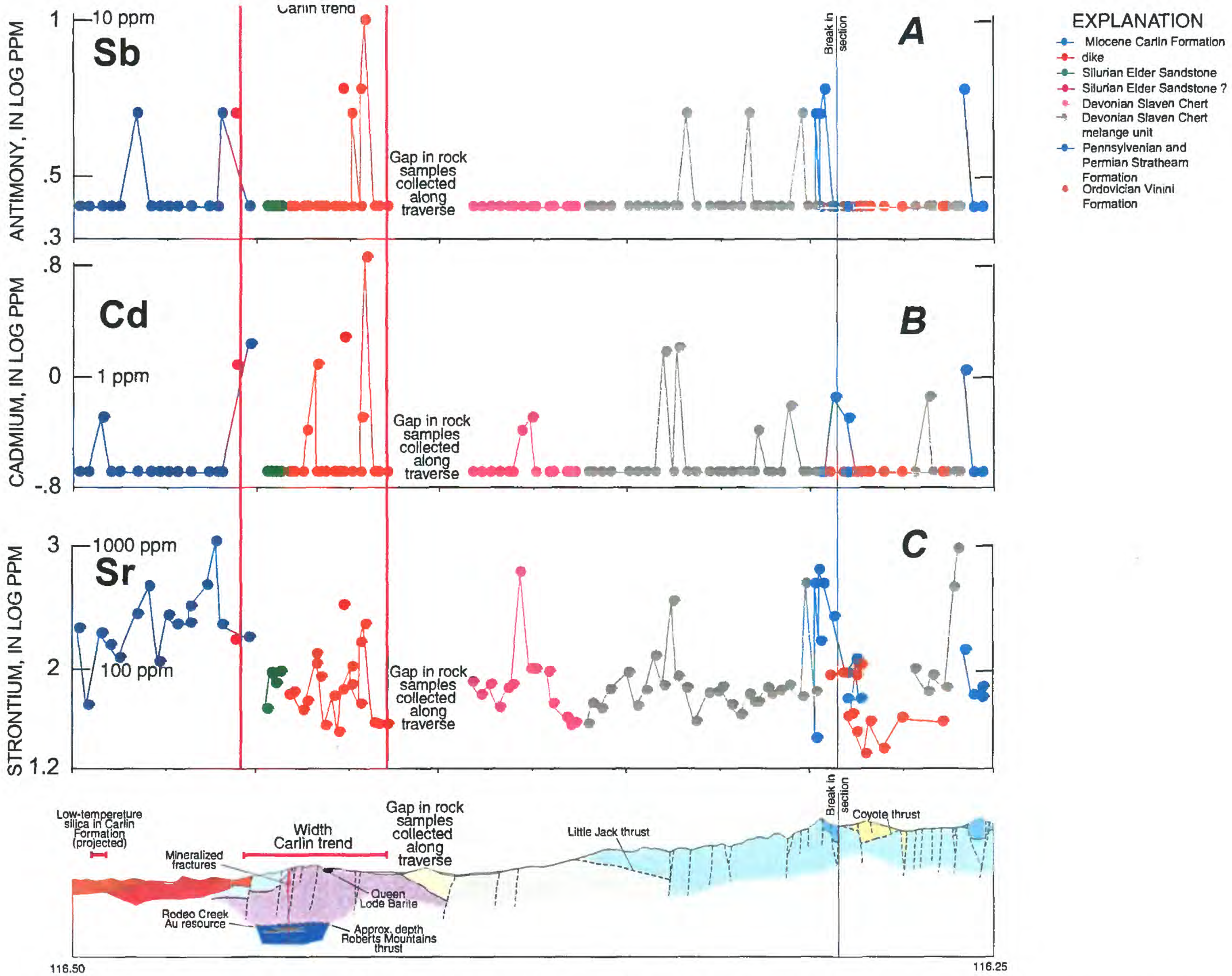

Figure 15—Abundances of Sb, Cd, Sr, V, Ca, P, La, Cr, Mg, Ba, Al, Na, K, W, Zr, Sn, Y, Nb, Be, and Sc in rock versus distance projected to profile AA'. See figure 2 for locations of profile AA' and samples analyzed. Data (total digestion) from table 1 (see text). Explanation for geologic cross section same as figure 2.

Figure 15—cont'd.

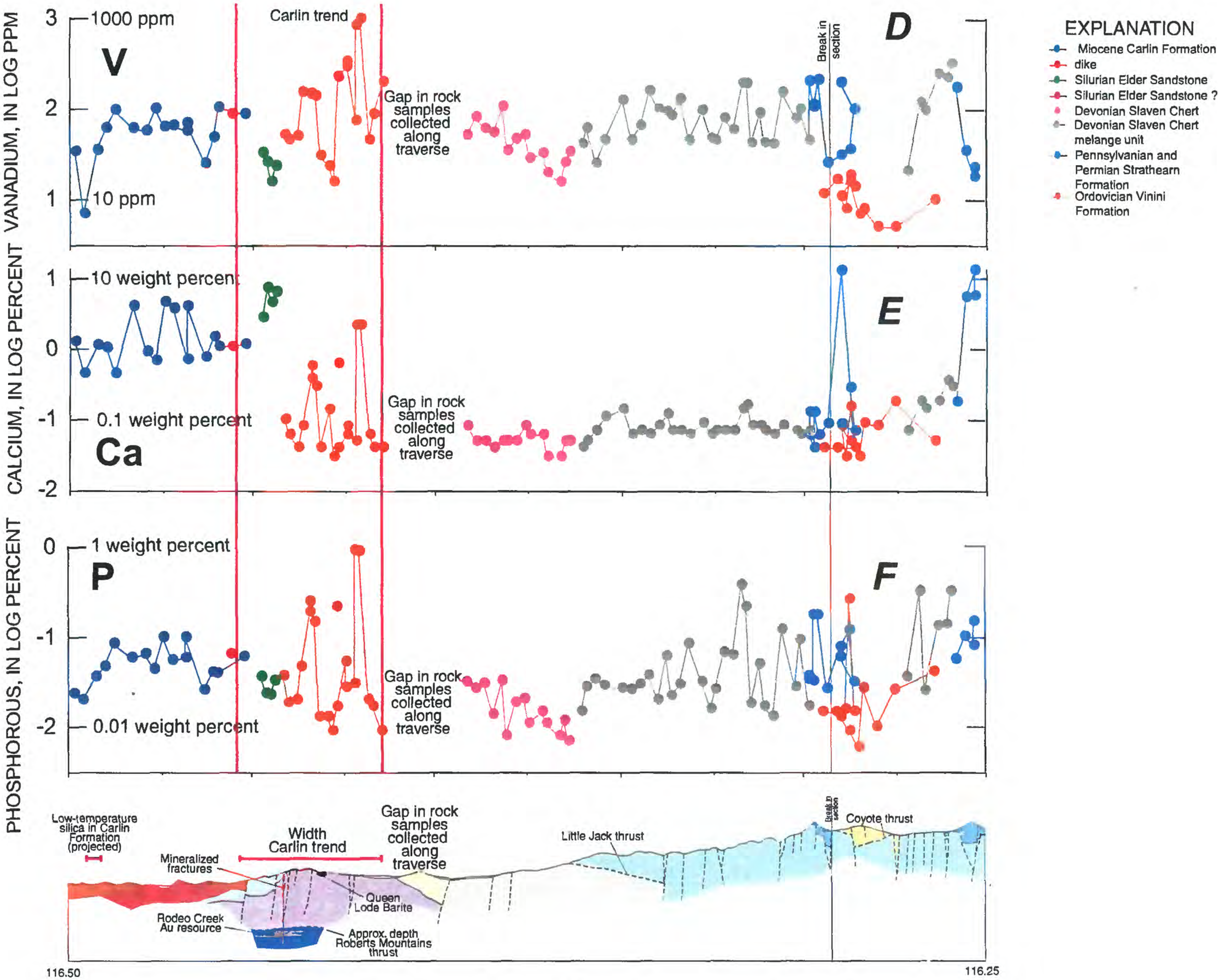

Figure 15—cont'd.

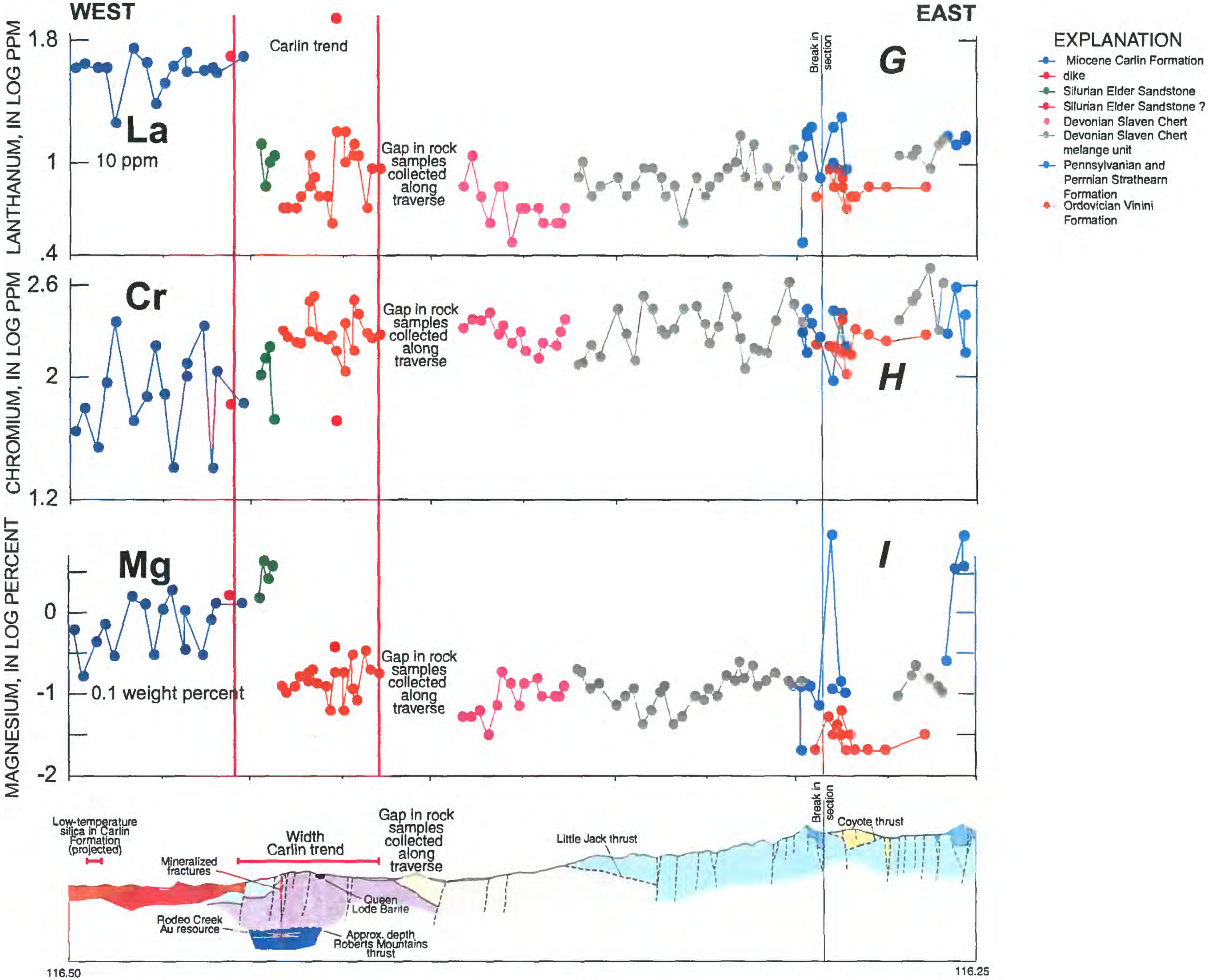

Figure 15—cont'd.

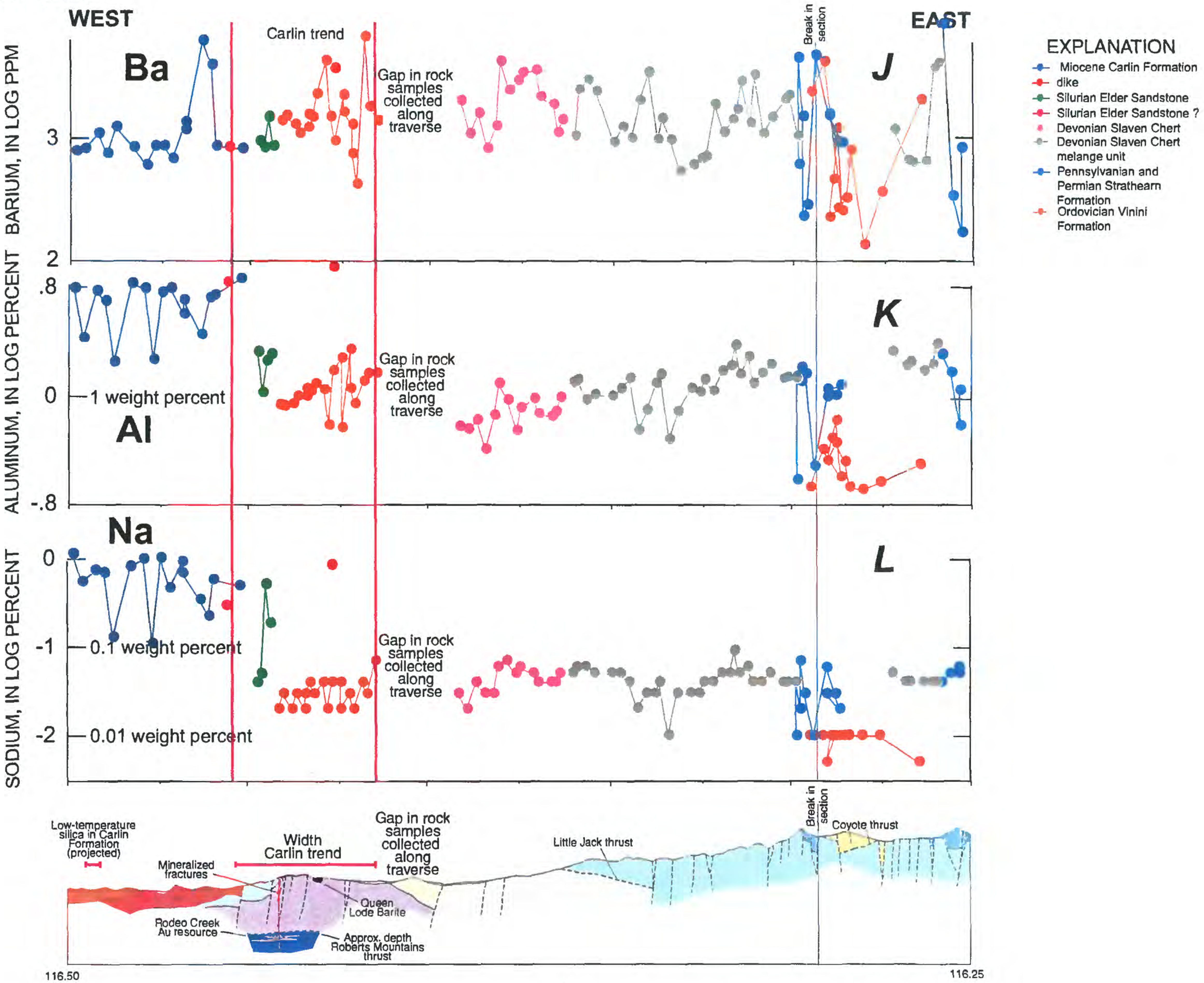

Figure 15—cont'd.

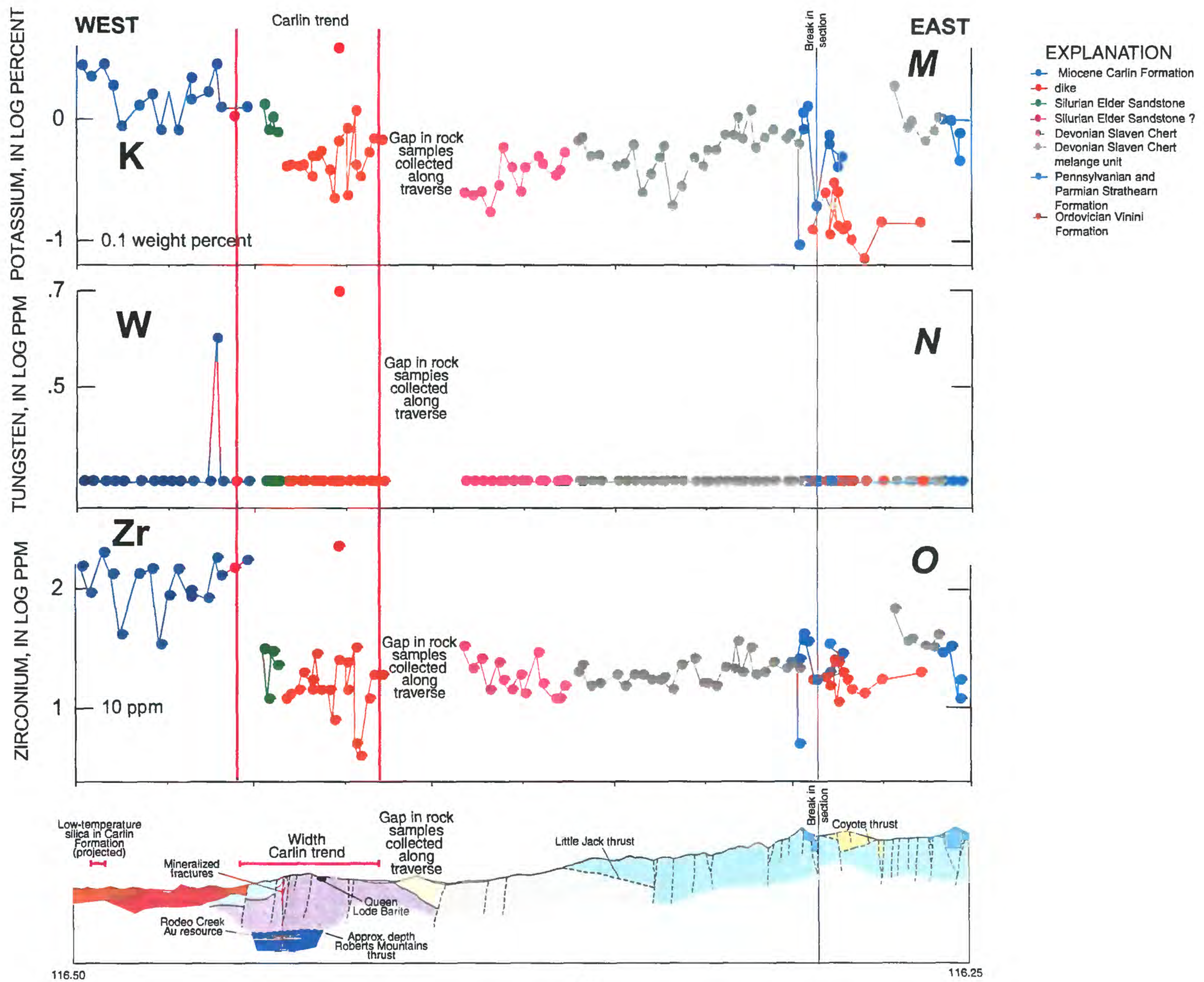

Figure 15—cont'd.

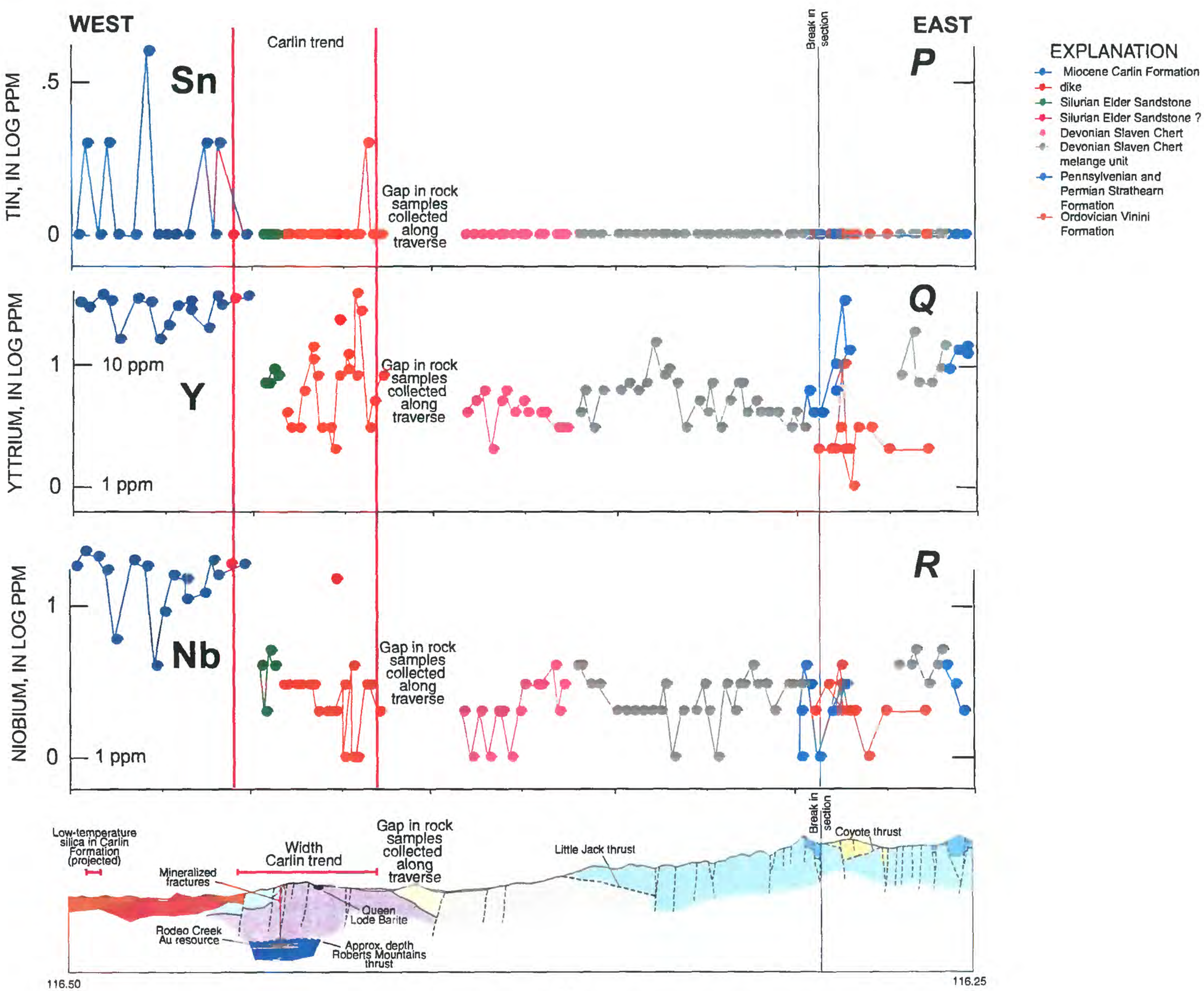

Figure 15—cont'd.

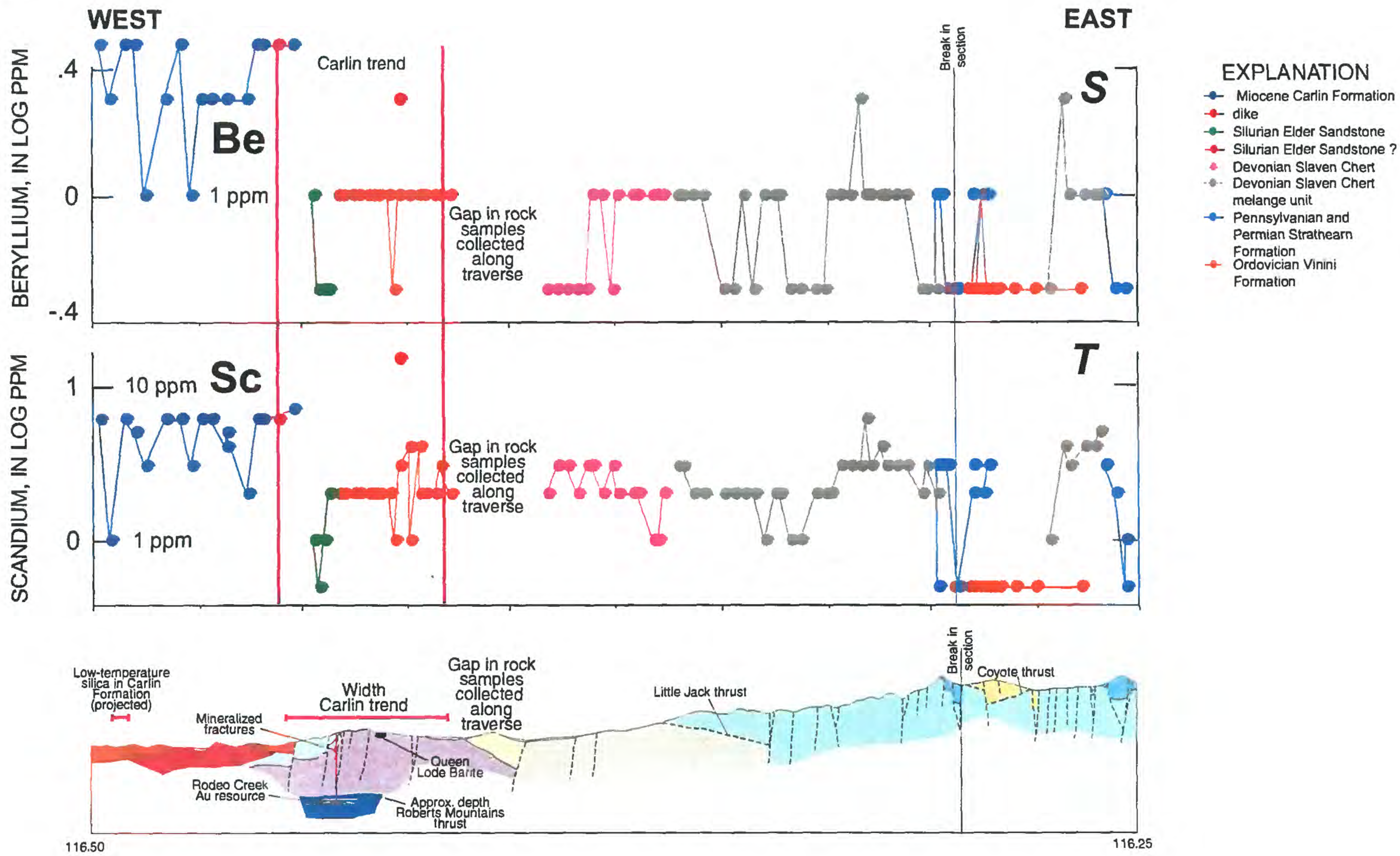

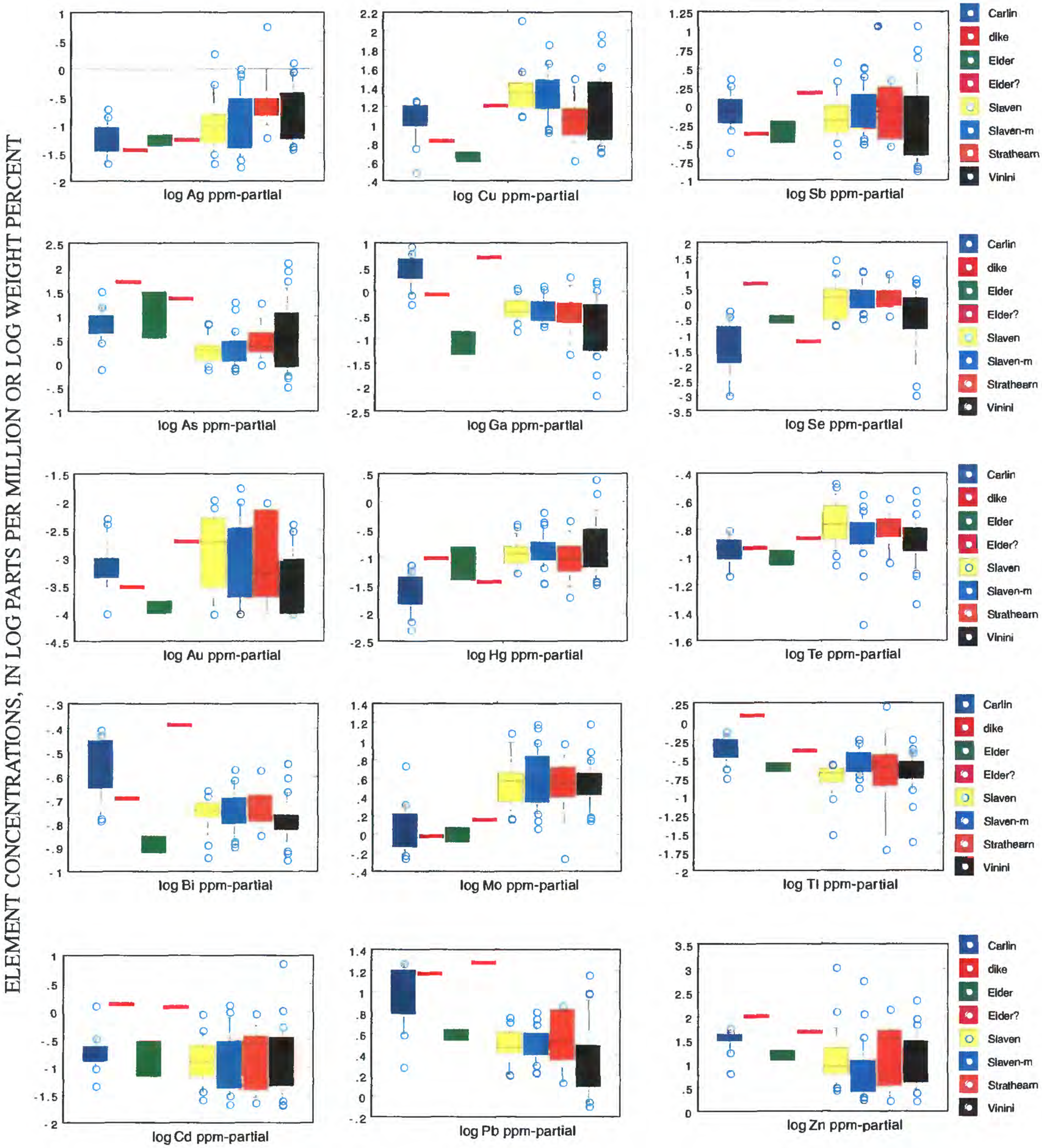

Figure 16—Box plots showing element concentrations for 115 samples grouped by major rock type along east-west profile AA' across the Santa Renia Fields and Beaver Peak quadrangles, Nev. Carlin, Miocene Carlin Formation; dike, single sample of altered dike along Carlin trend of Au deposits; Elder, Silurian and Devonian Elder Sandstone; Elder?, single sample provisionally assigned to Elder Sandstone (see text); Slaven, well-bedded Devonian Slaven Chert; Slaven-m, mélange unit of Slaven Chert; Strathearn, Pennsylvanian and Permian Strathearn Formation; Vinini, Ordovician Vinini Formation, includes chert and shale unit and quartzarenite unit.

Figure 16—cont'd.

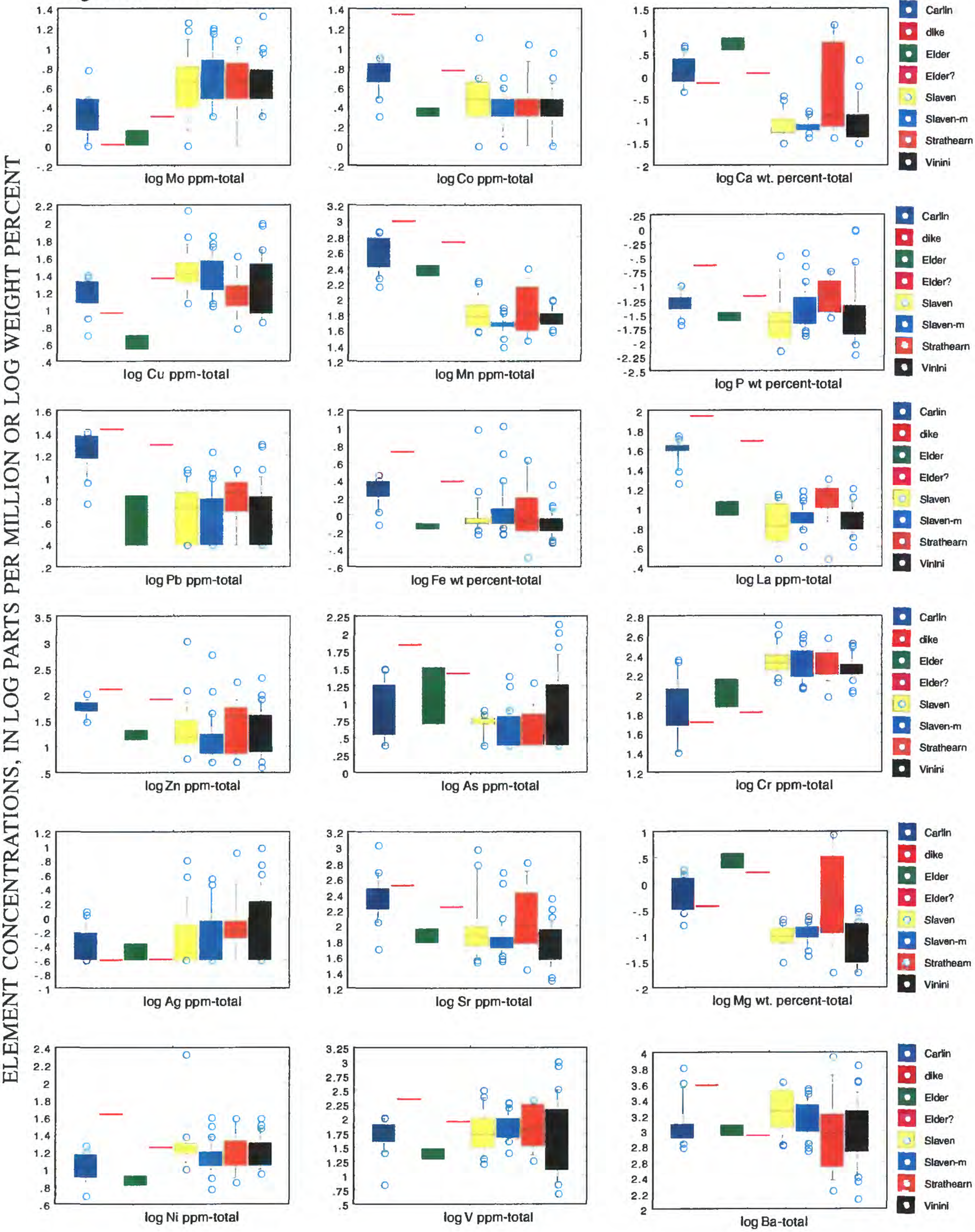

Figure 16—cont'd.

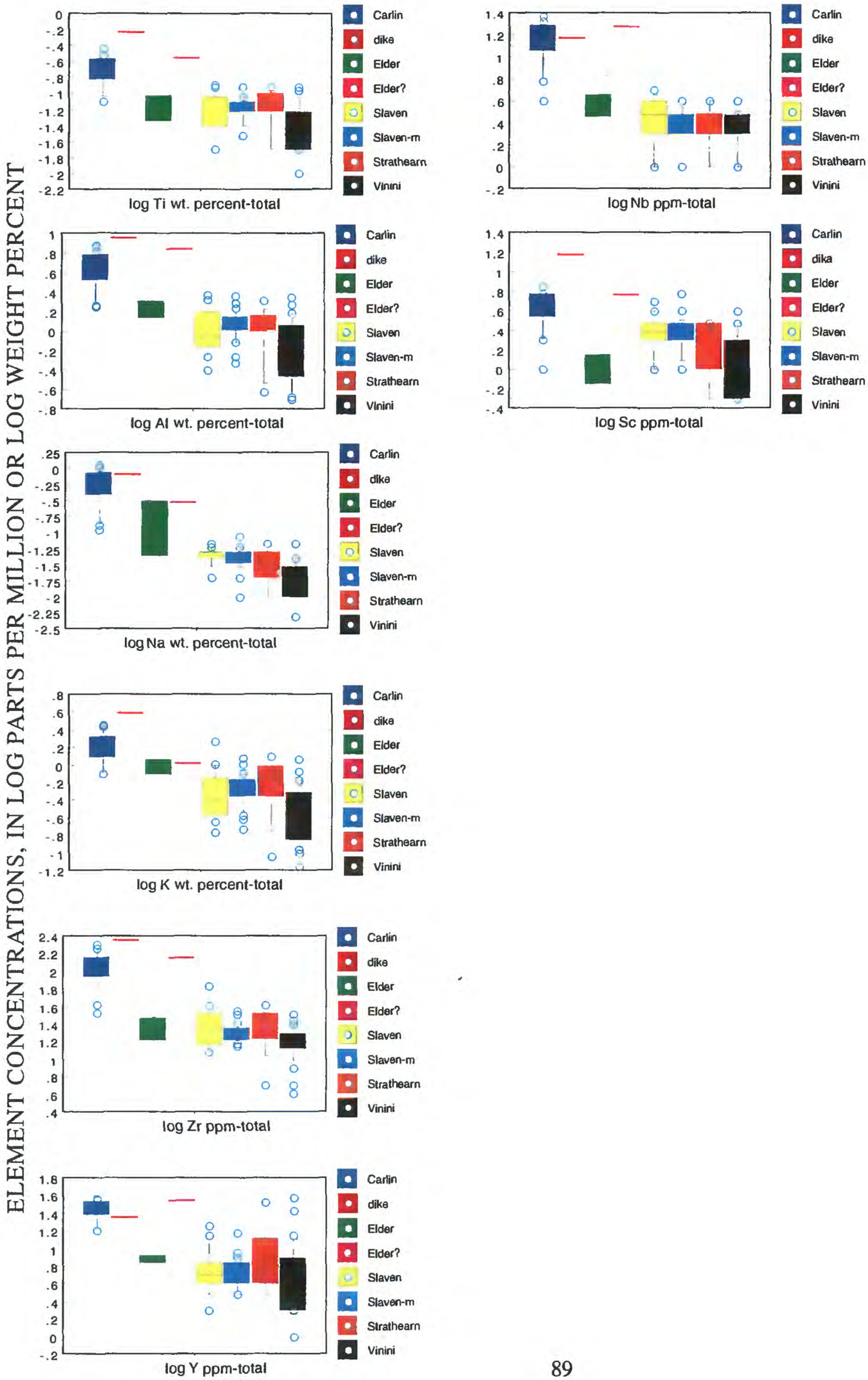

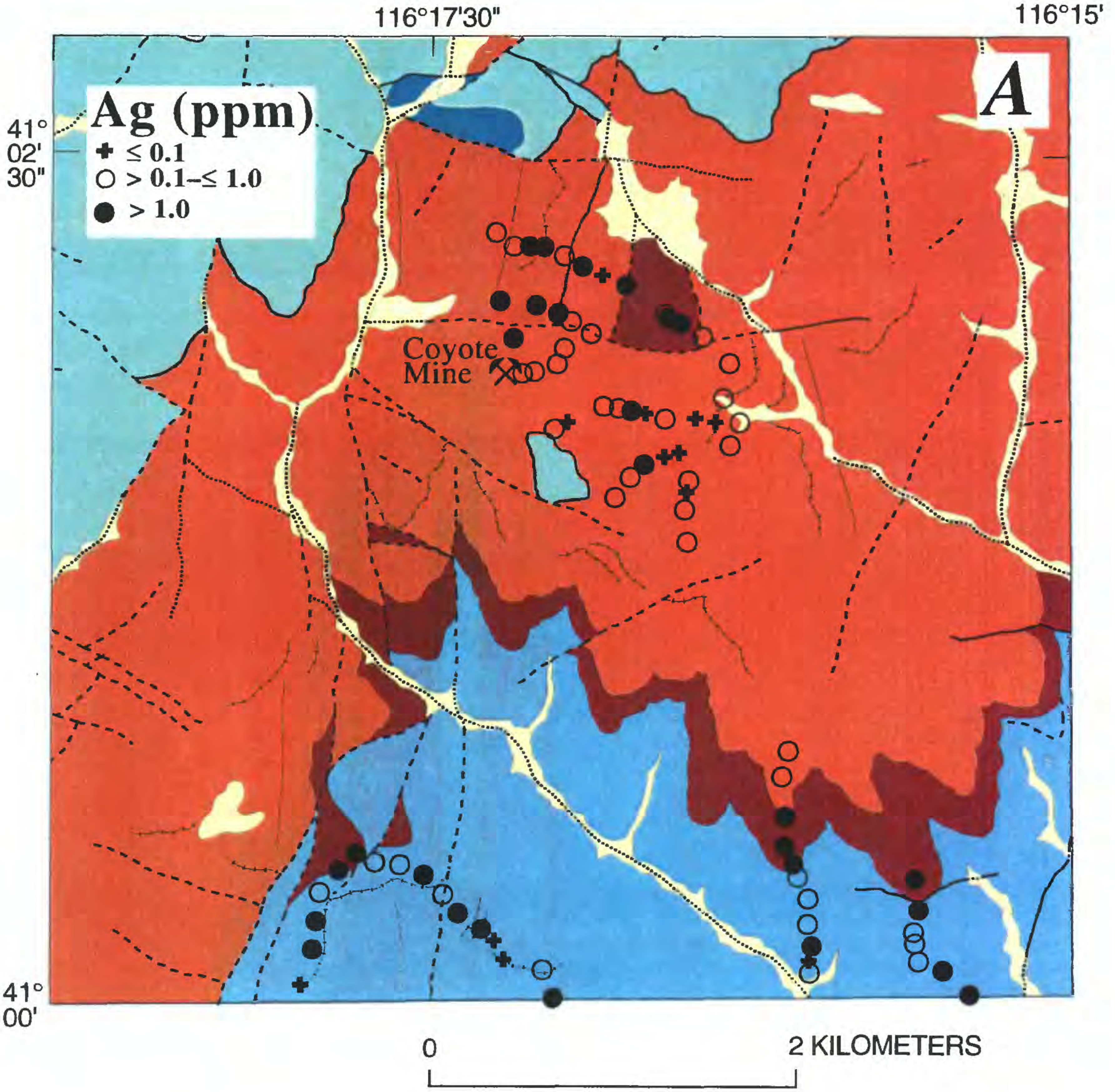

Figure 17—Distribution of 15 elements in 79 rocks analyzed by partial digestion methods in general area of Coyote barite mine in southeast part of Beaver Peak quadrangle, Nev. See figure 2 for explanation of simplified geologic sketch map. Class intervals of element concentrations determined from appropriate breaks in log-frequency histograms (fig. 7) of the 79 samples plus 14 samples analyzed from the Coyote barite mine.

Figure 17—cont'd.

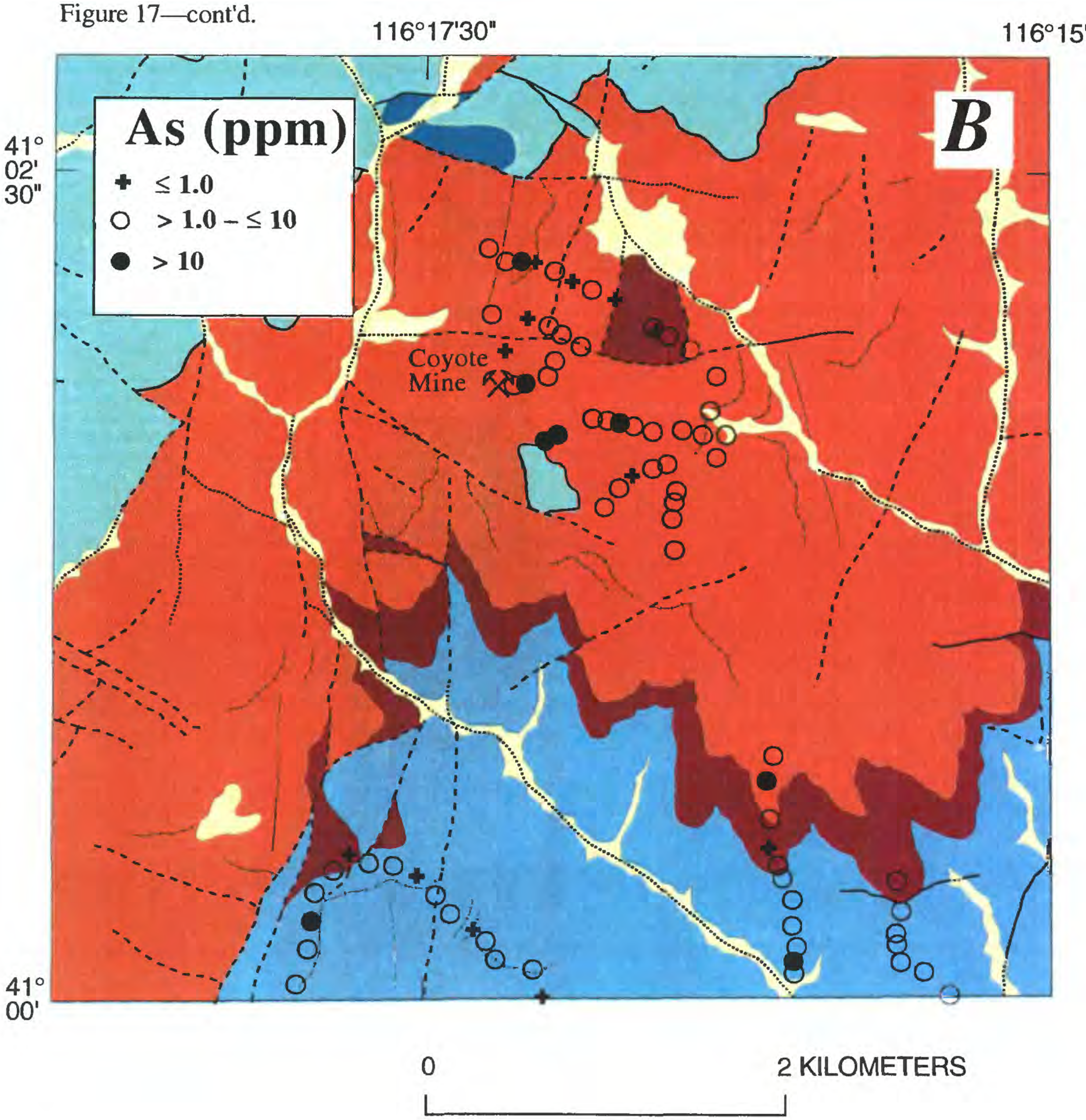

Figure 17—cont'd.

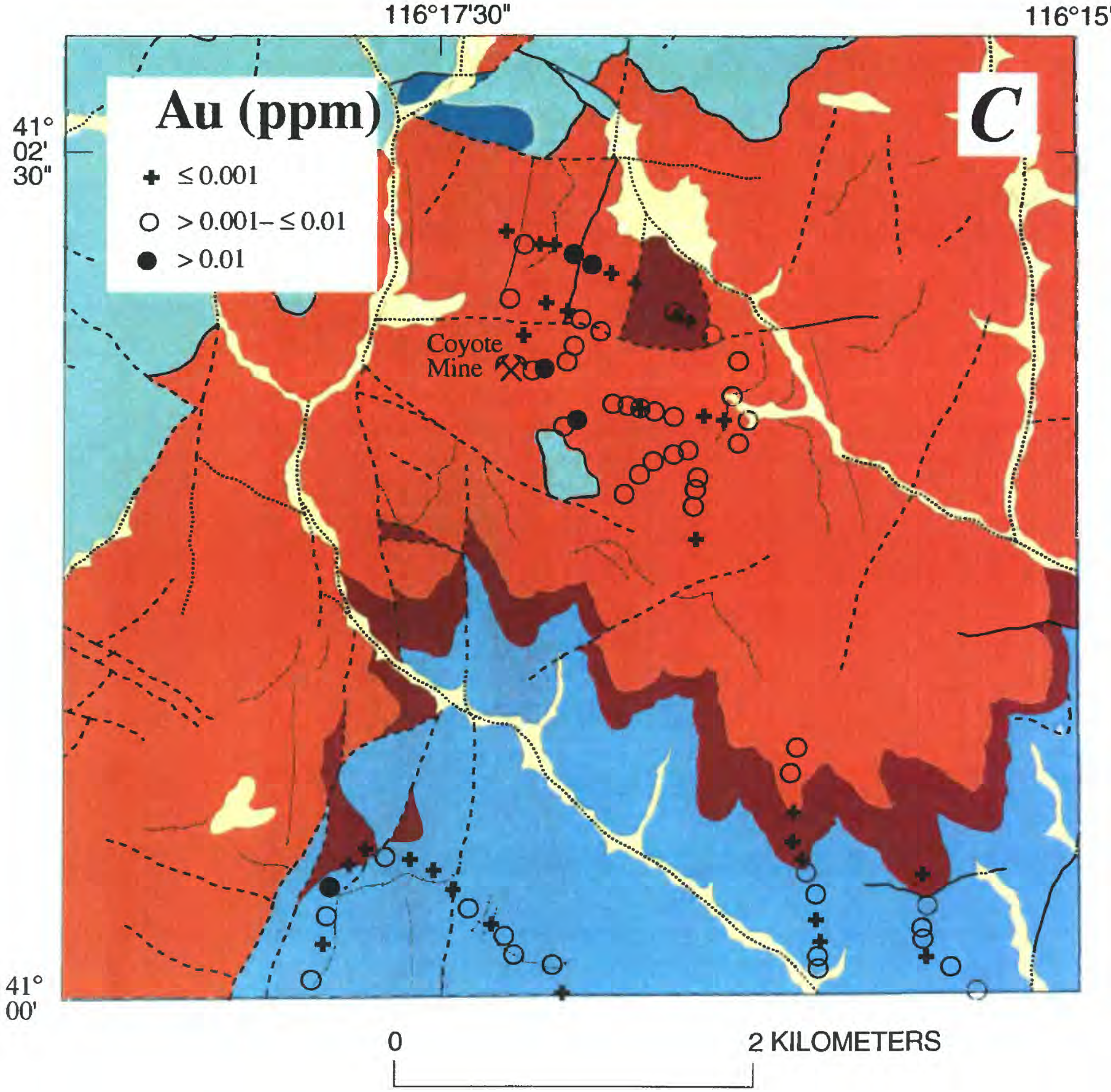

Figure 17—cont'd.

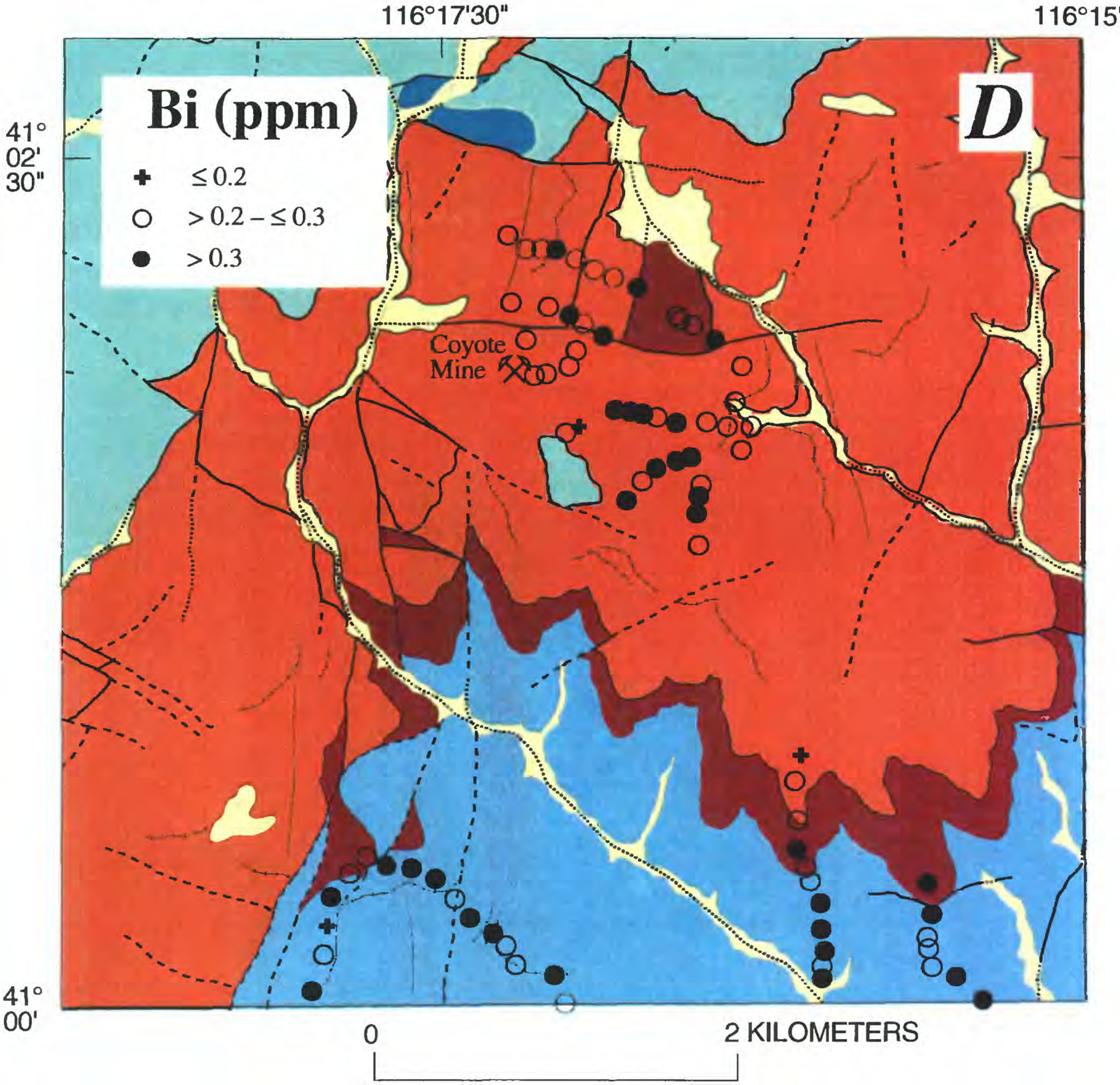

Figure 17—cont'd.

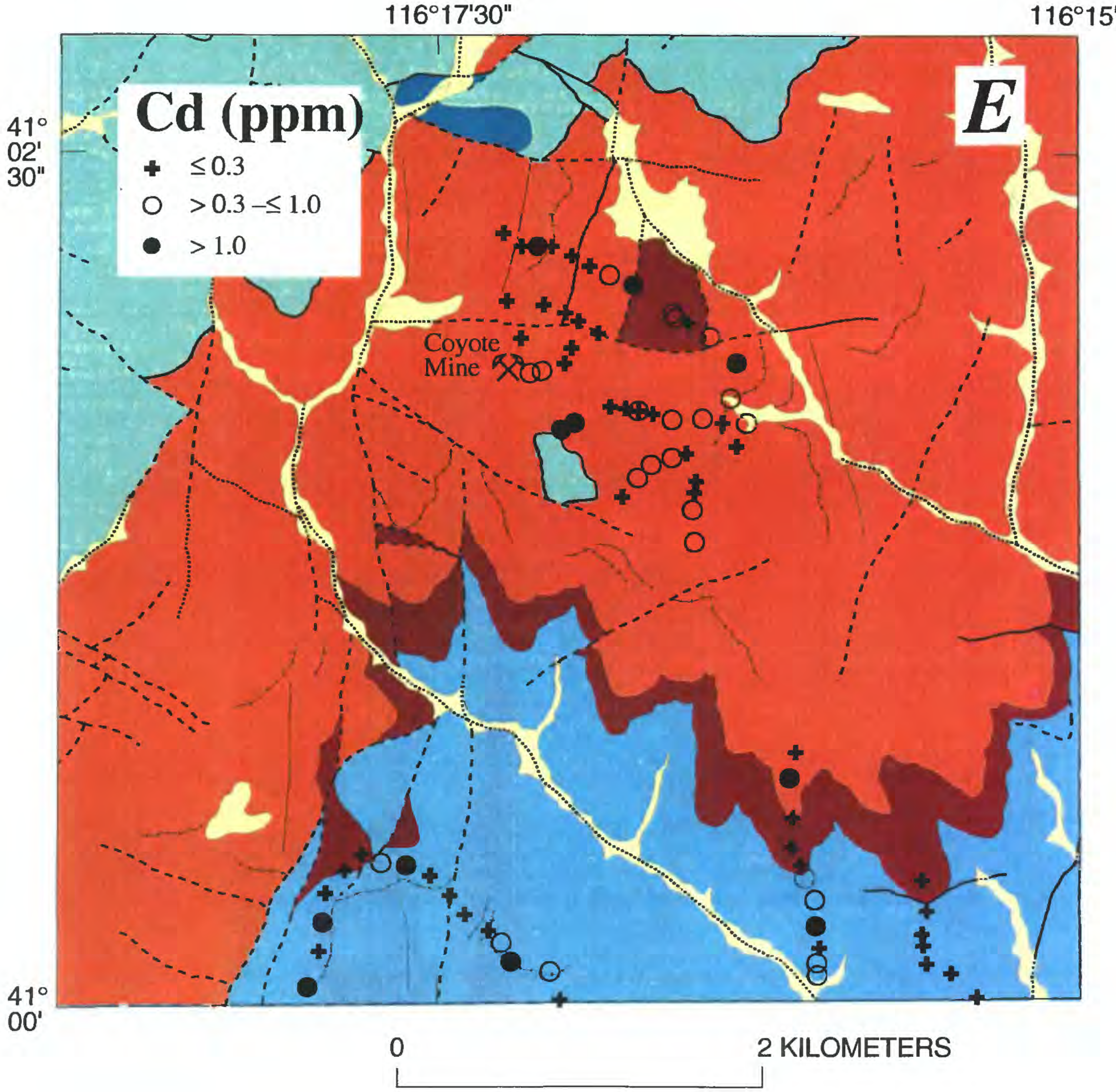

Figure 17—cont'd.

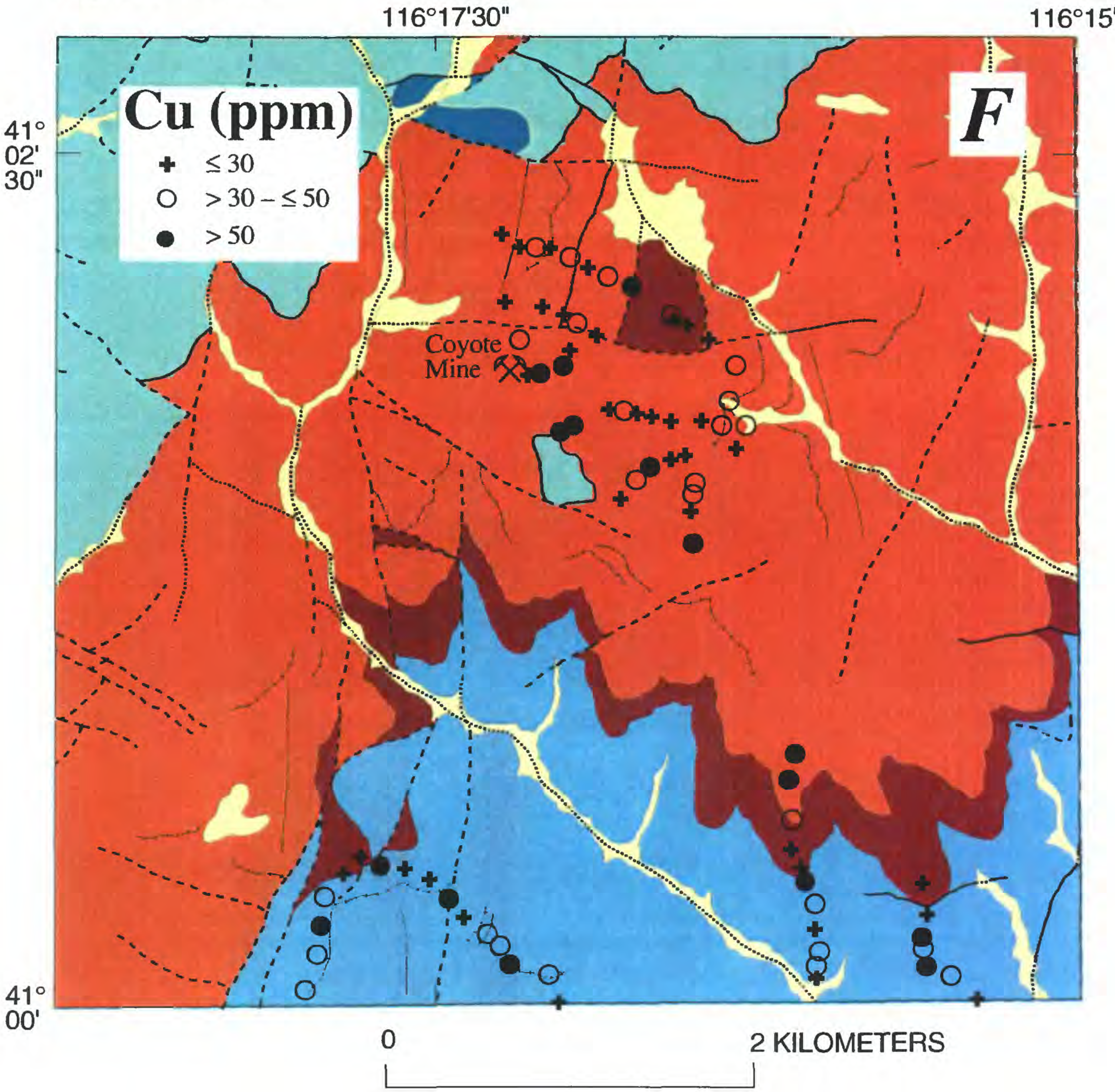

Figure 17—cont'd.

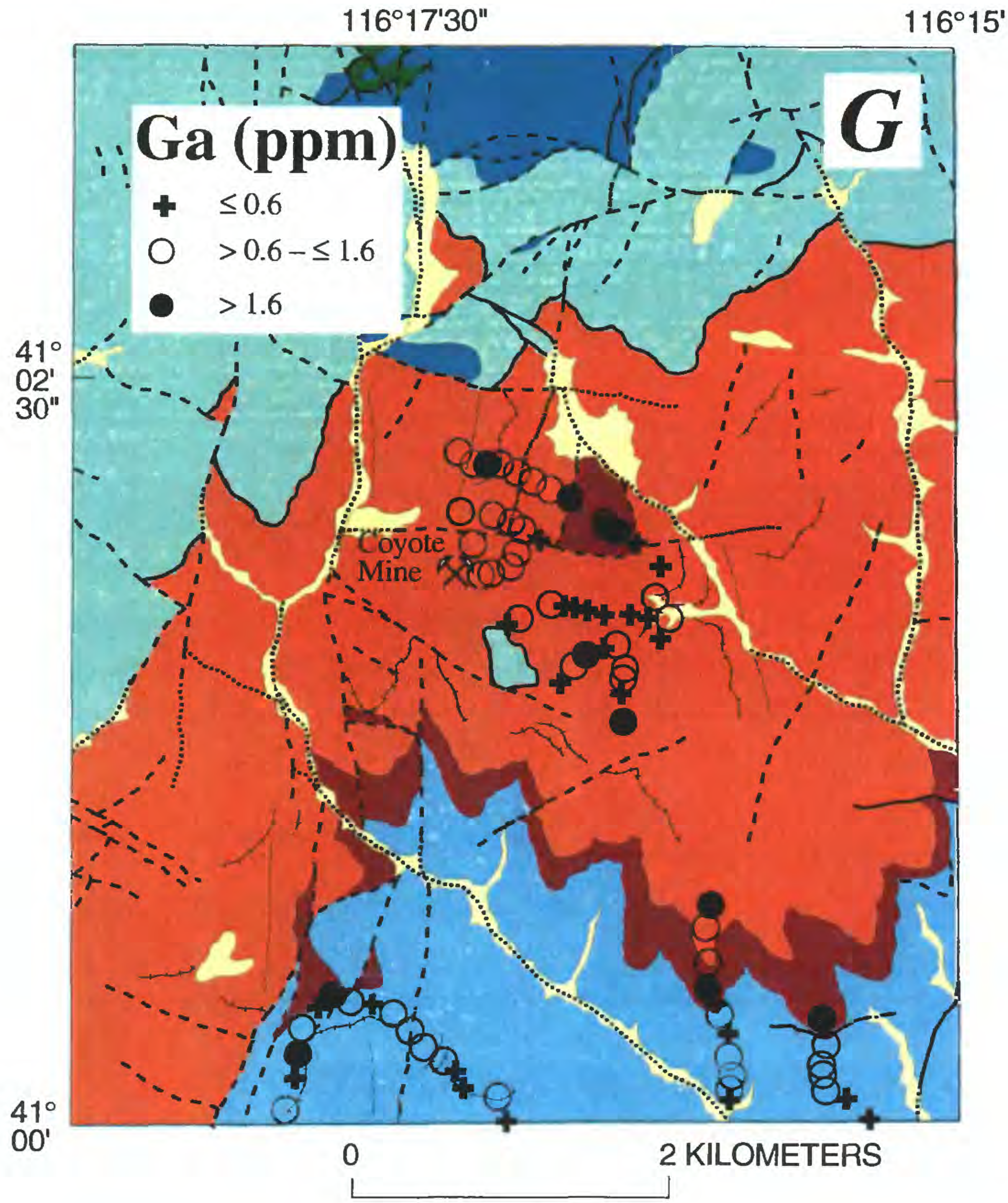

Figure 17—cont'd.

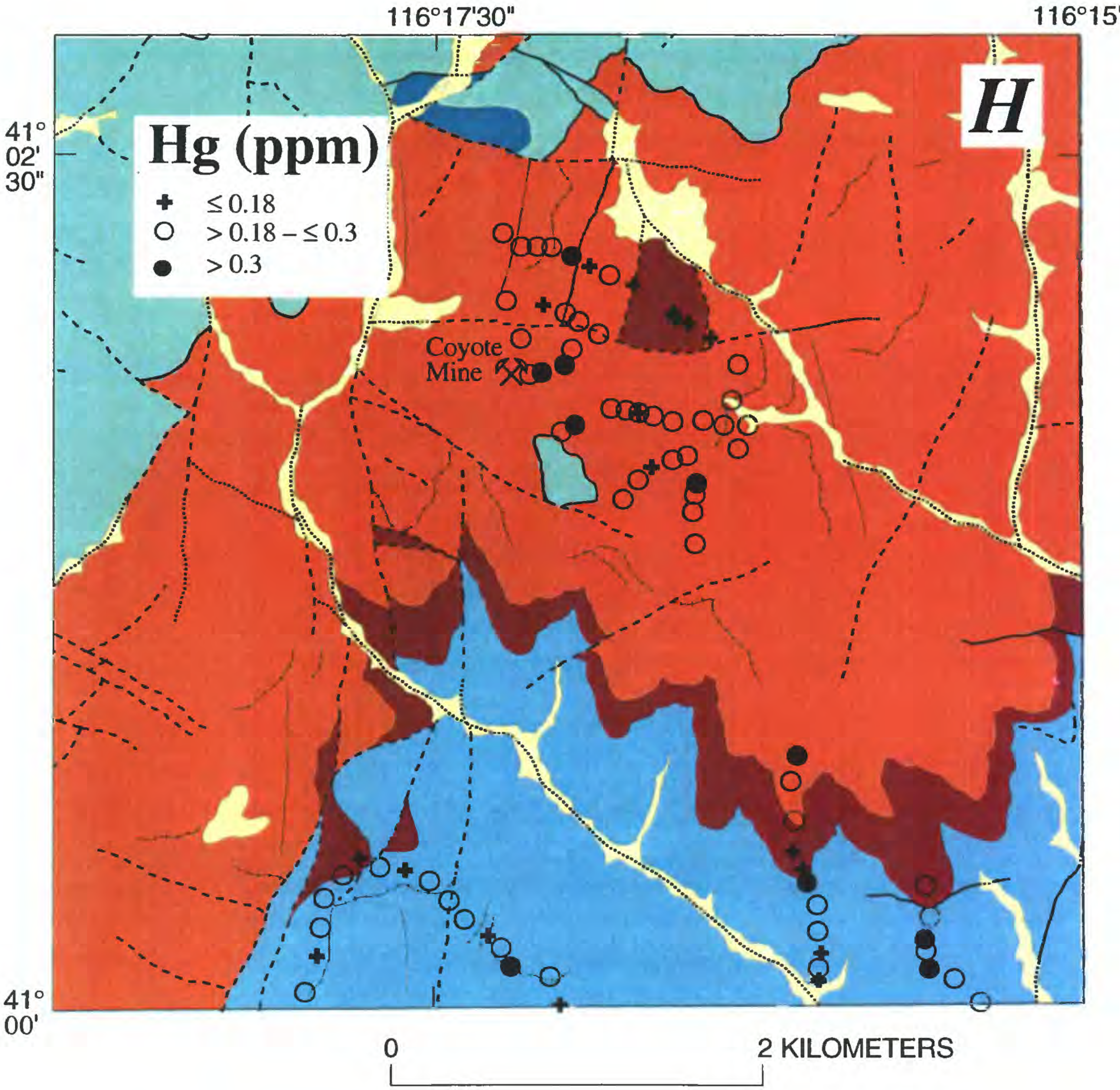

Figure 17—cont'd.

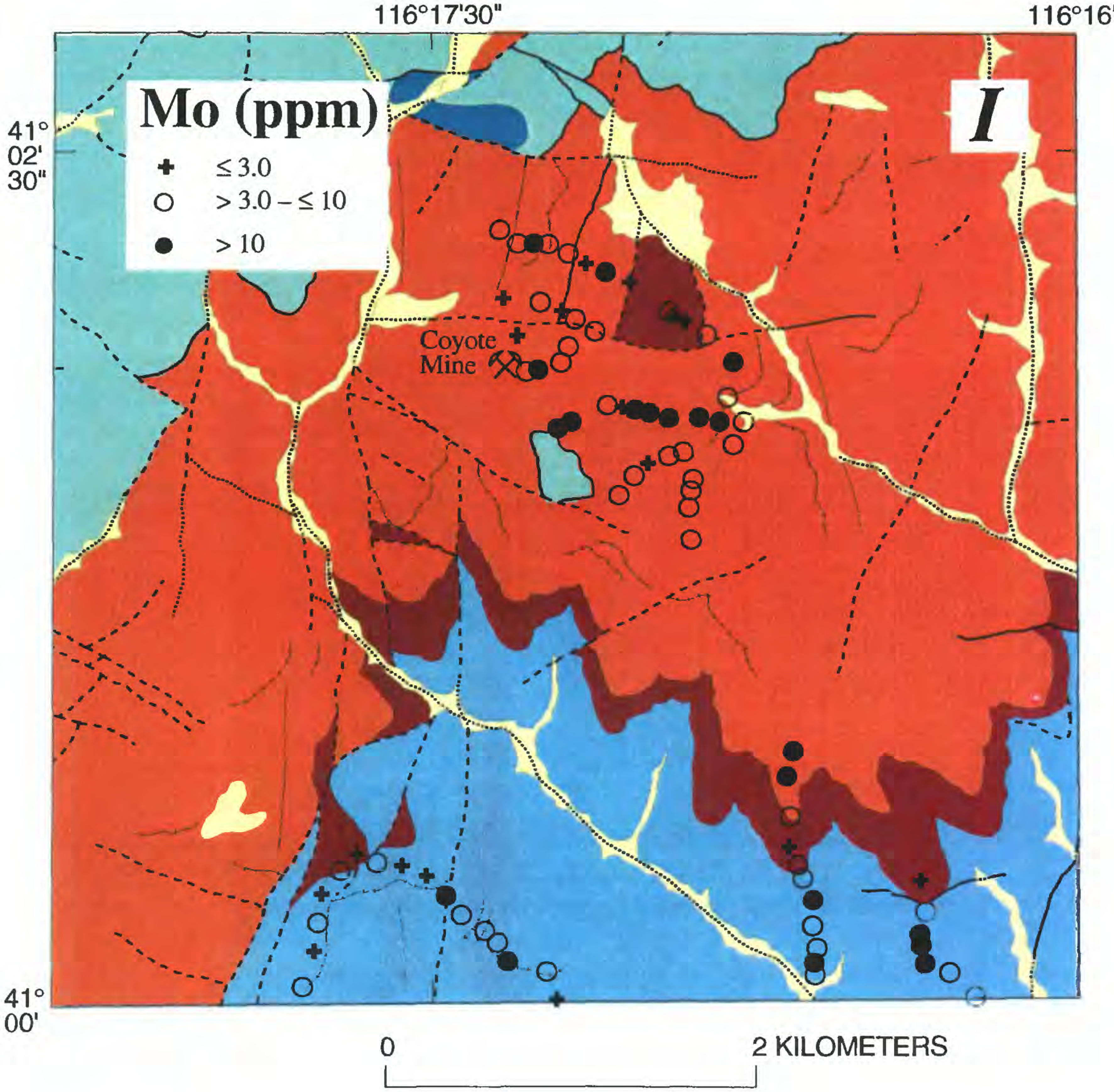

Figure 17—cont'd.

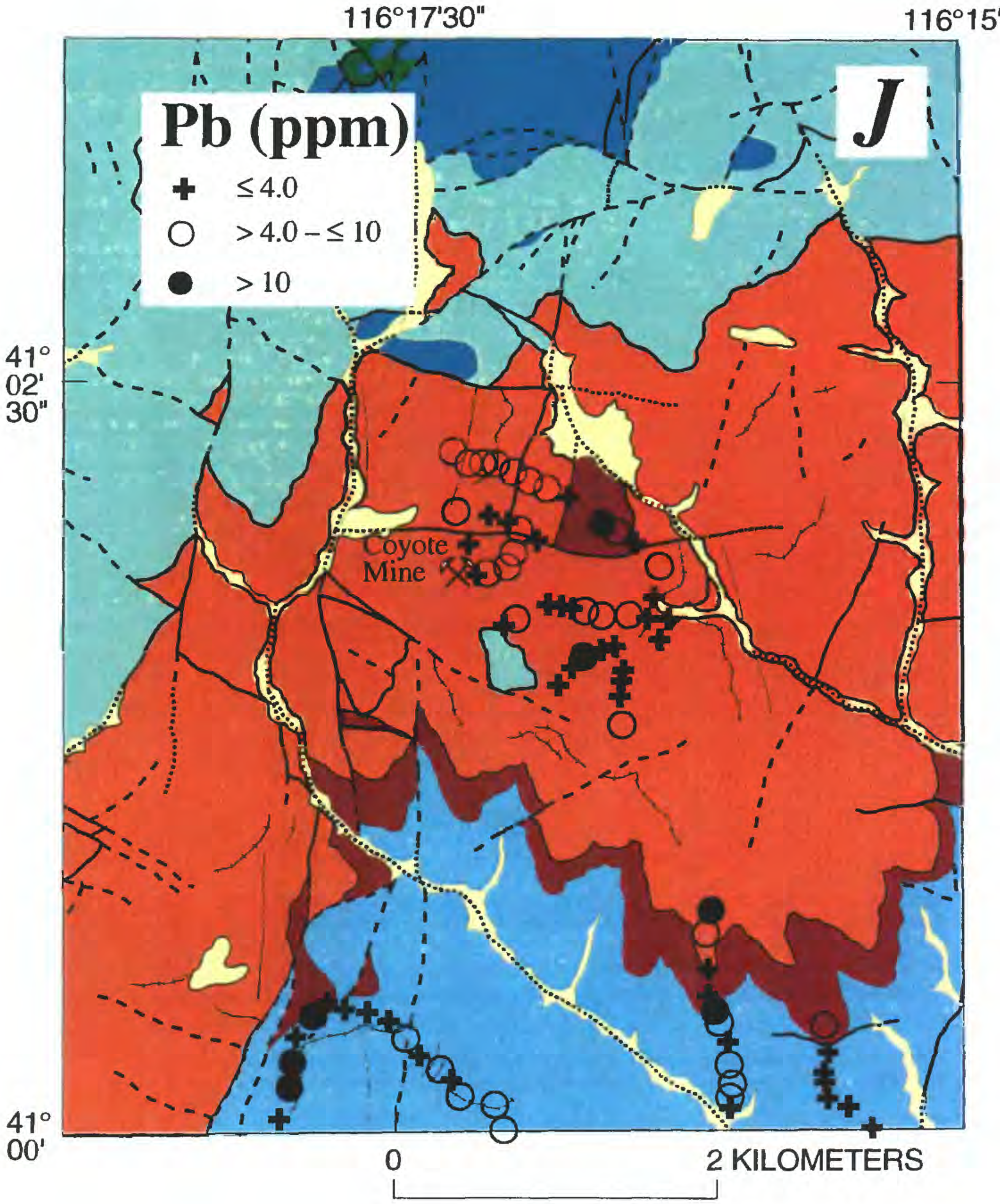

Figure 17—cont'd.

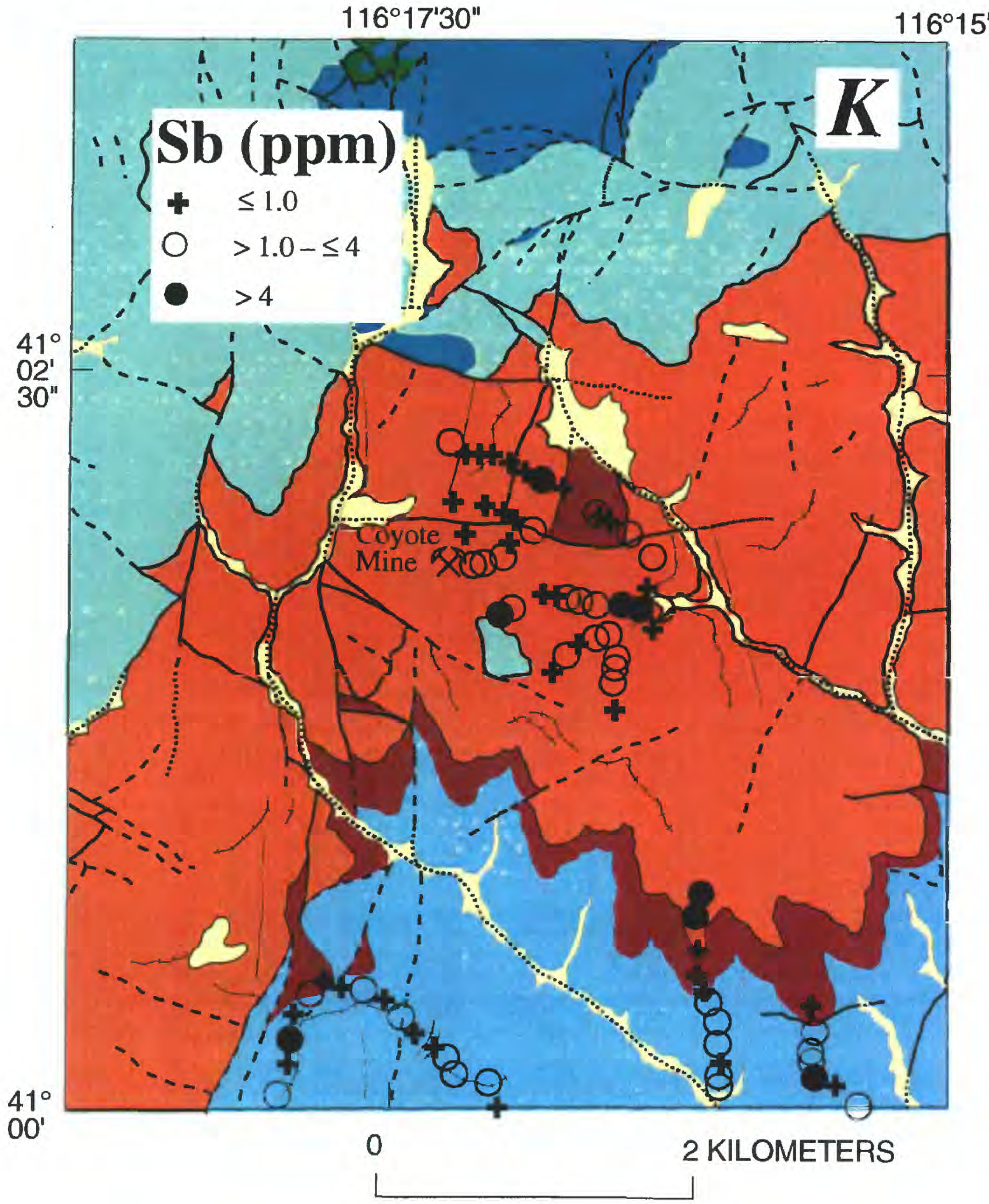

Figure 17—cont'd.

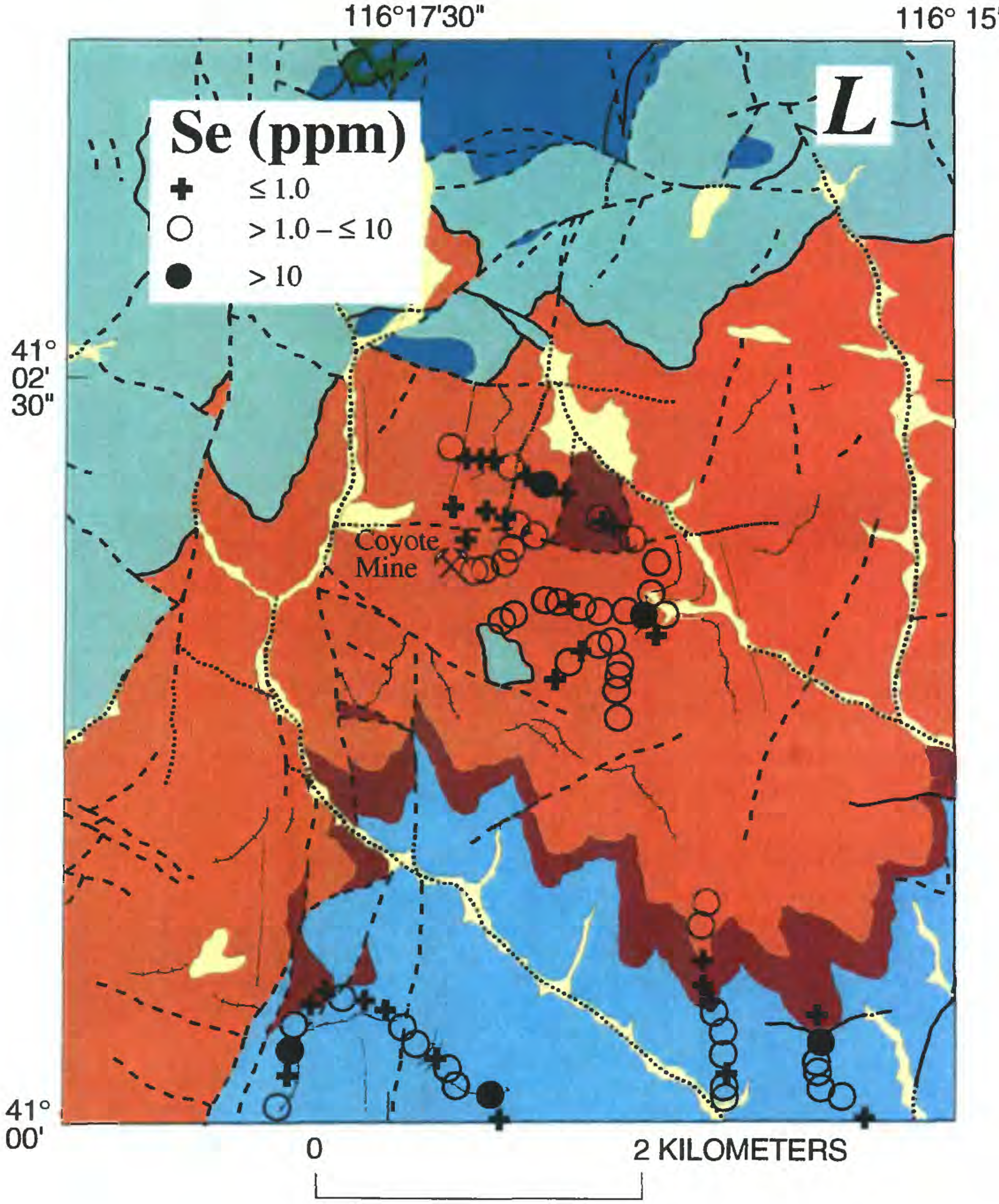

Figure 17—cont'd.

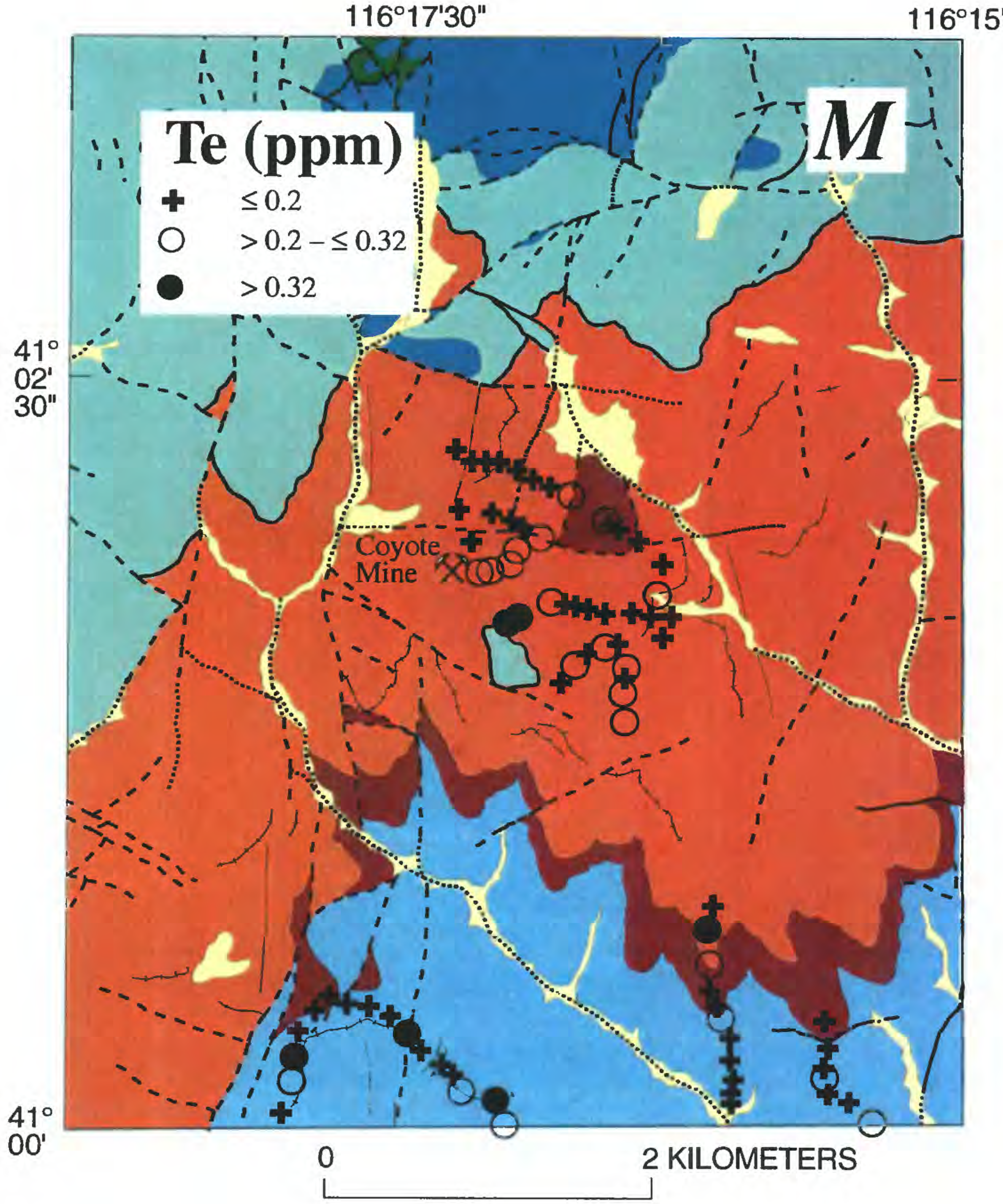

Figure 17—cont'd.

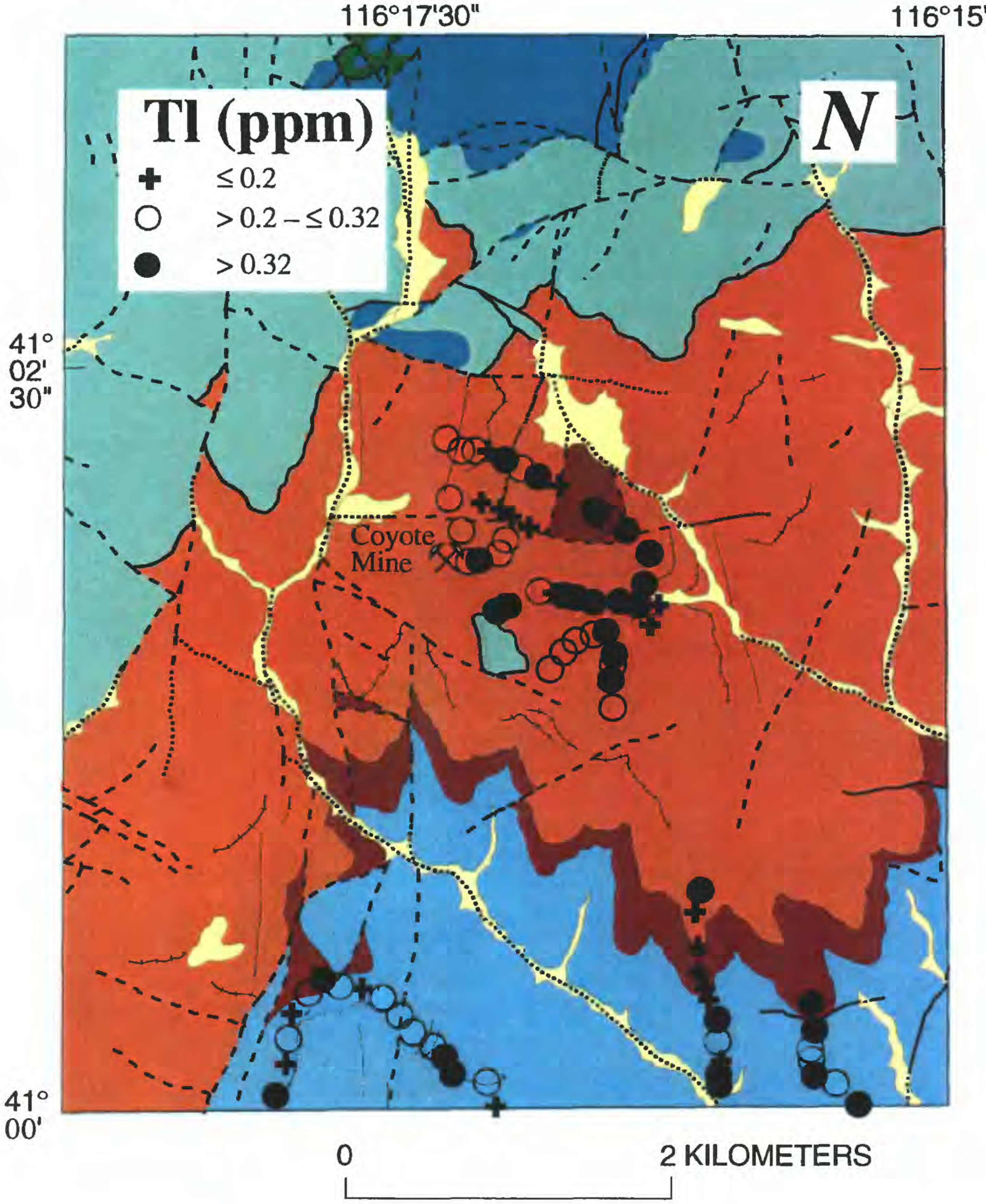

Figure 17—cont'd.

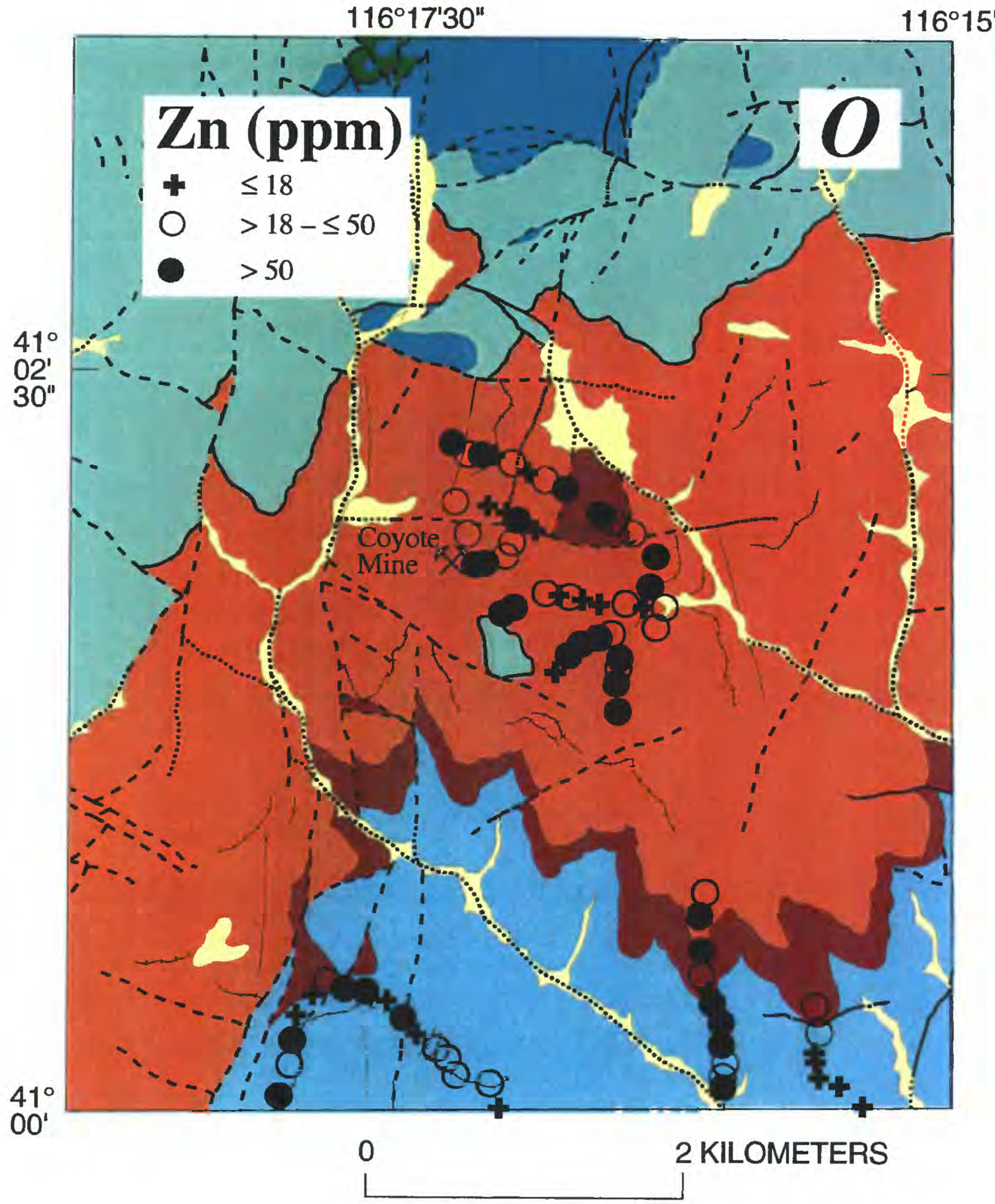

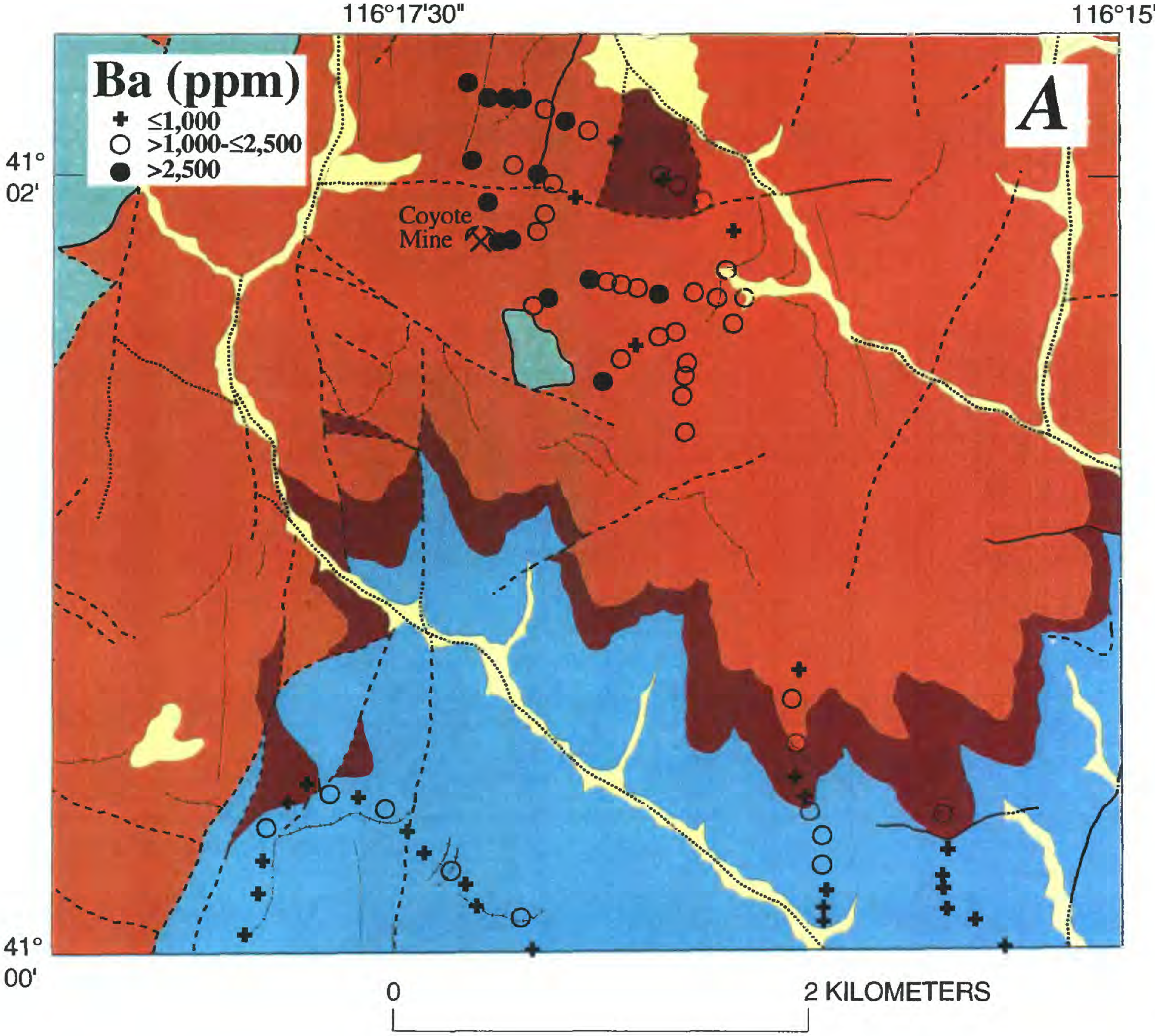

Figure 18—Distribution of seven elements (Ba, Sr, P, V, P, Cr, La and Nb) analyzed by total digestion methods in 79 rocks in general area of Coyote barite mine near southeast corner of Beaver Peak quadrangle, Nev. See figure 2 for explanation of geology.

Figure 18—cont'd.

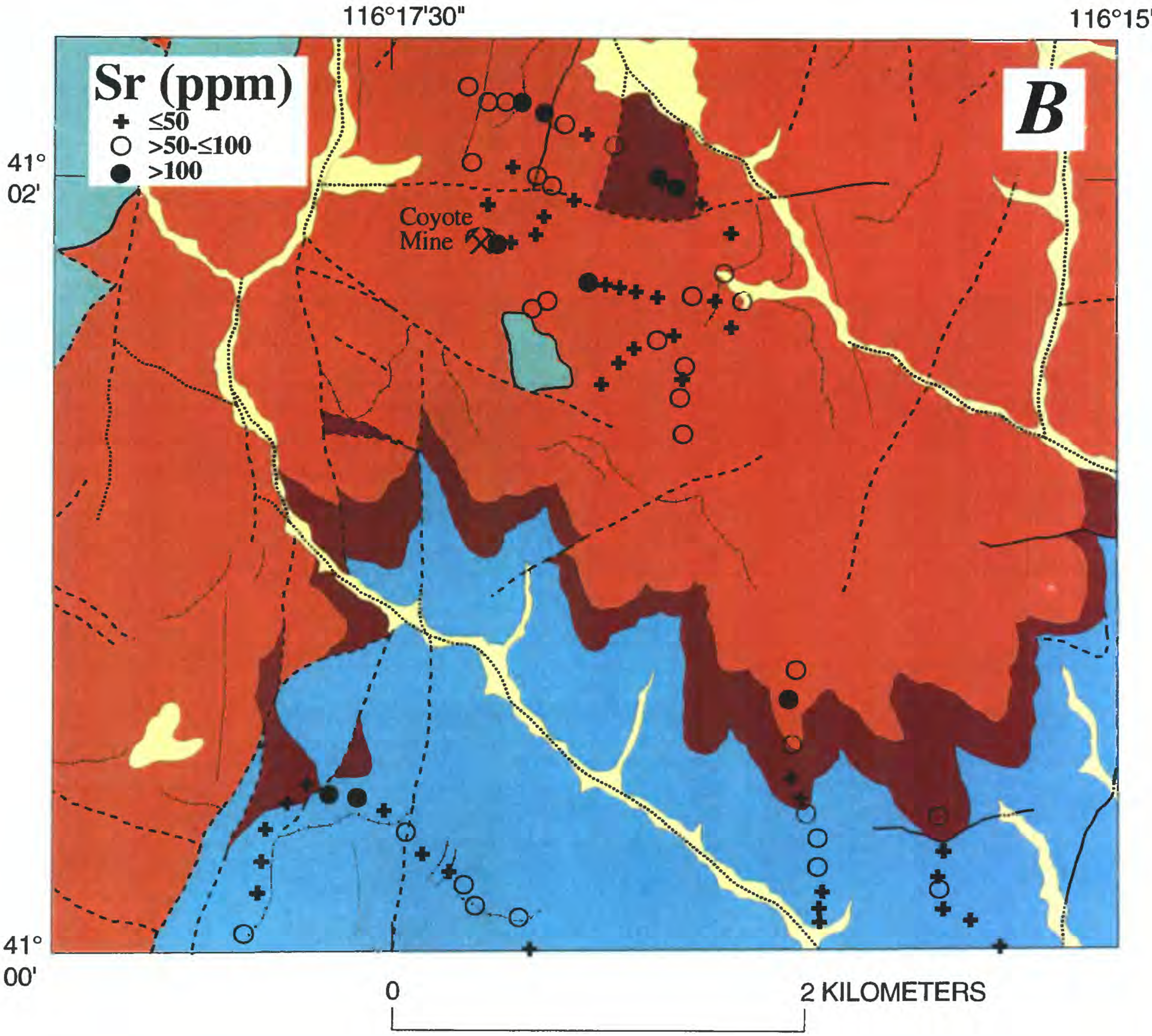

Figure 18—cont'd.

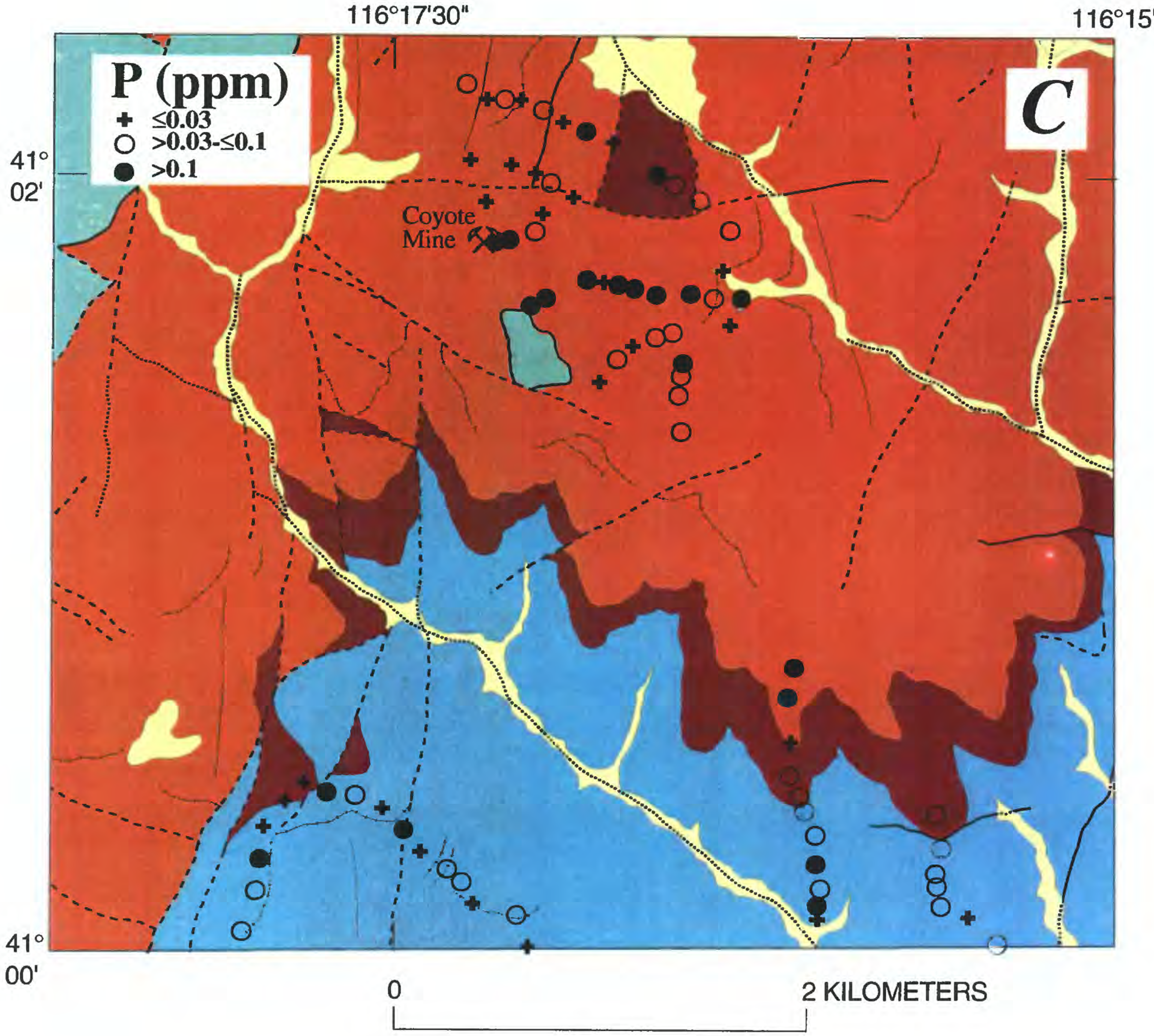

Figure 18—cont'd.

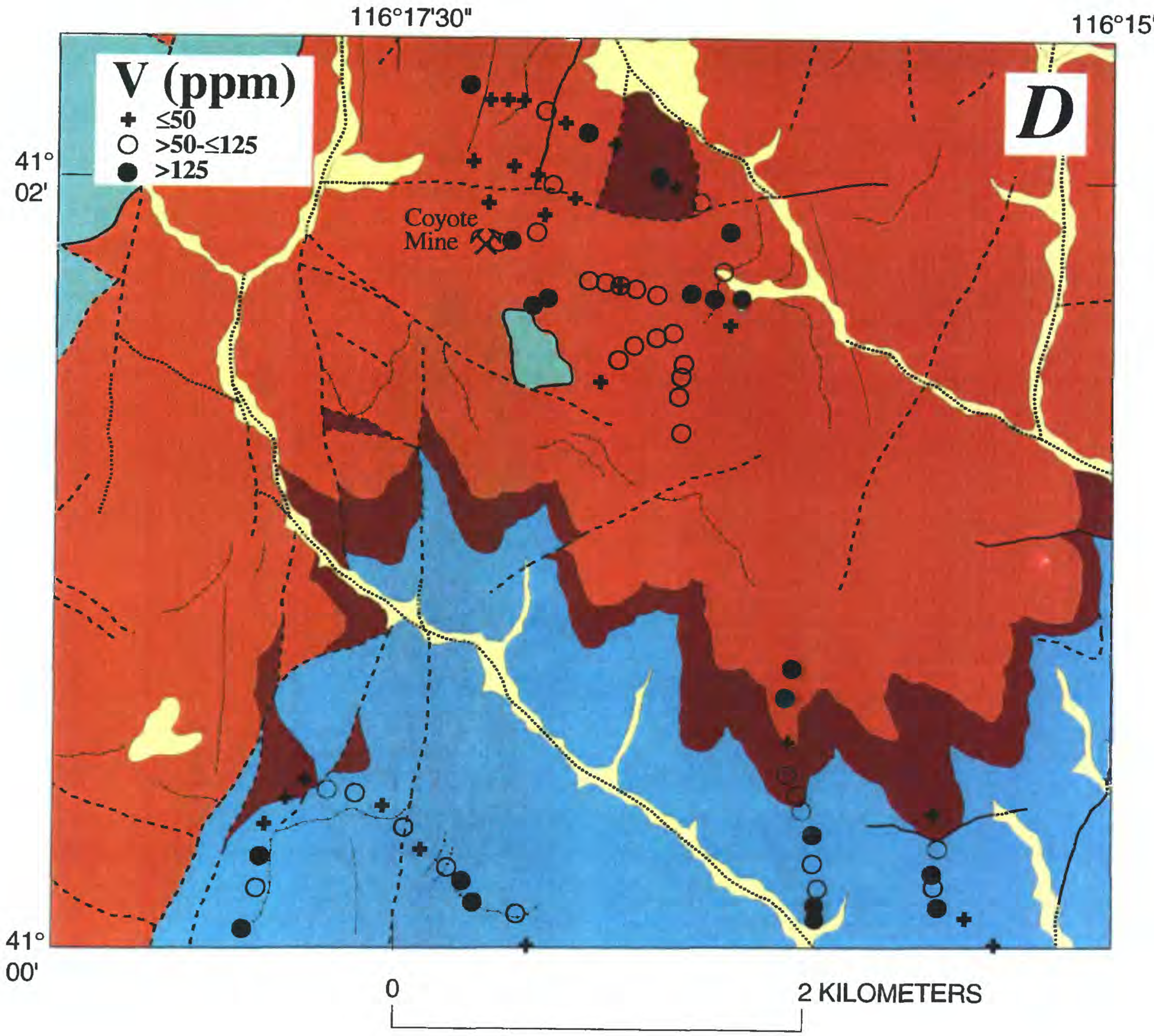

Figure 18—cont'd.

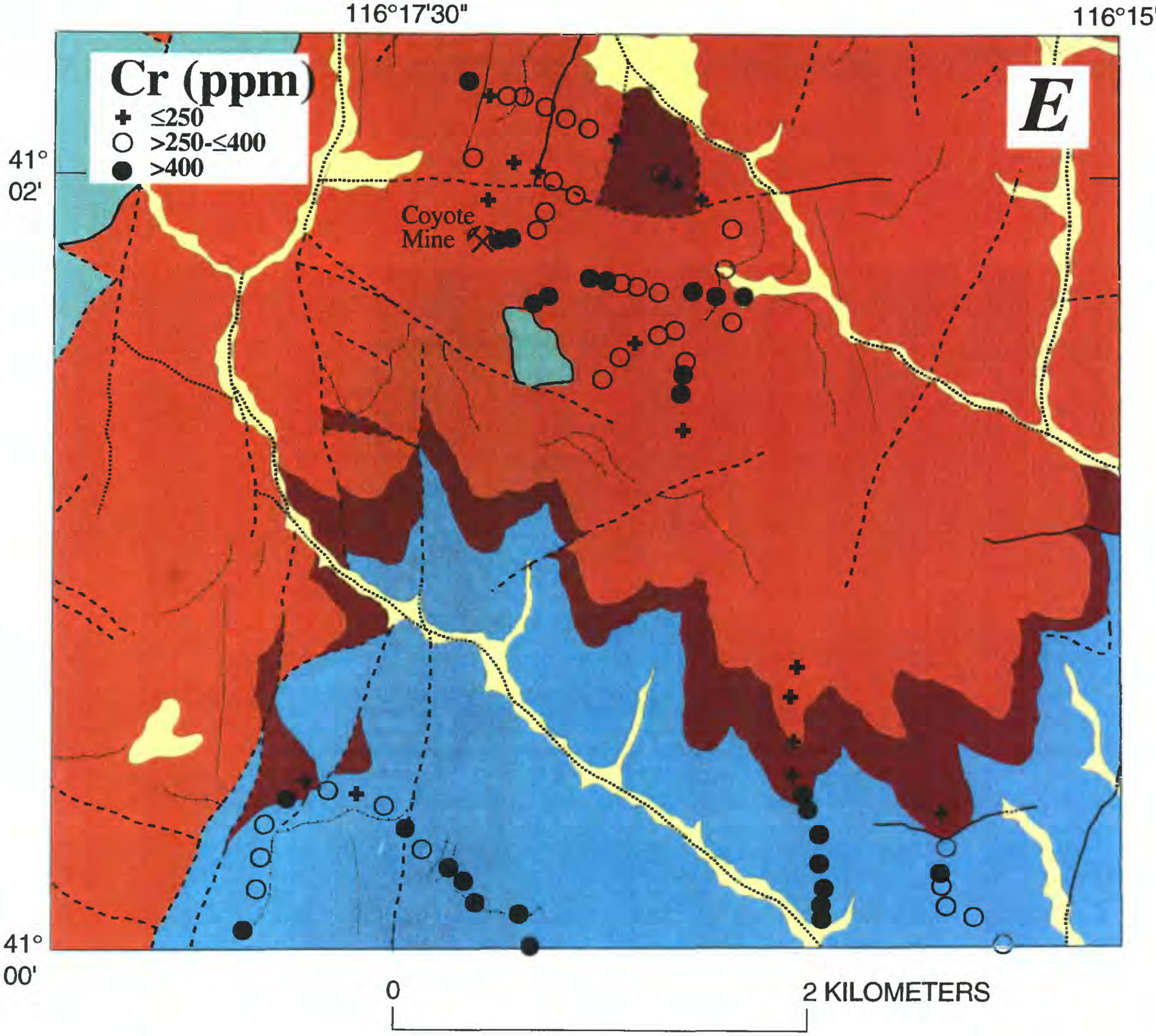

Figure 18—cont'd.

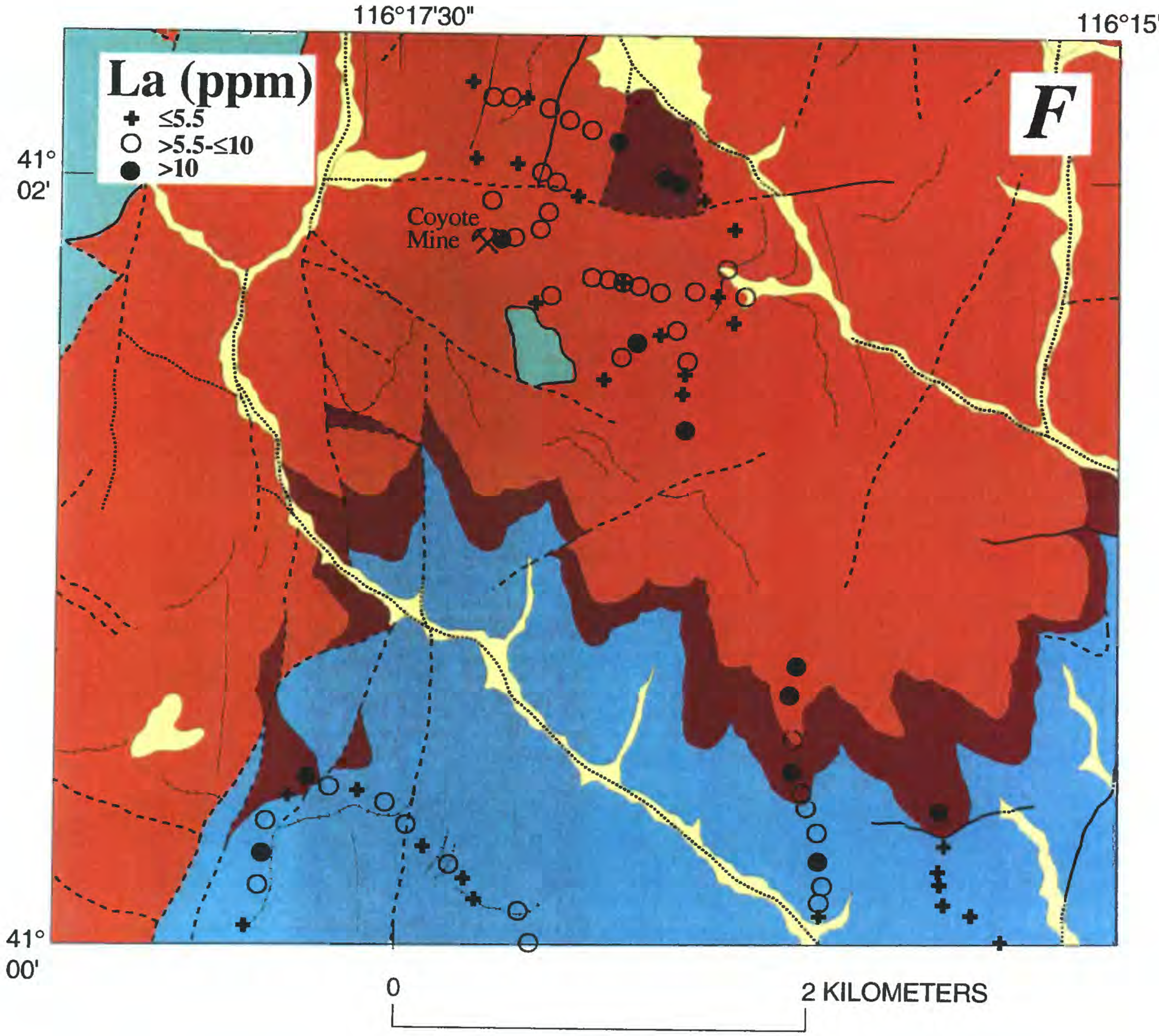

Figure 18—cont'd.

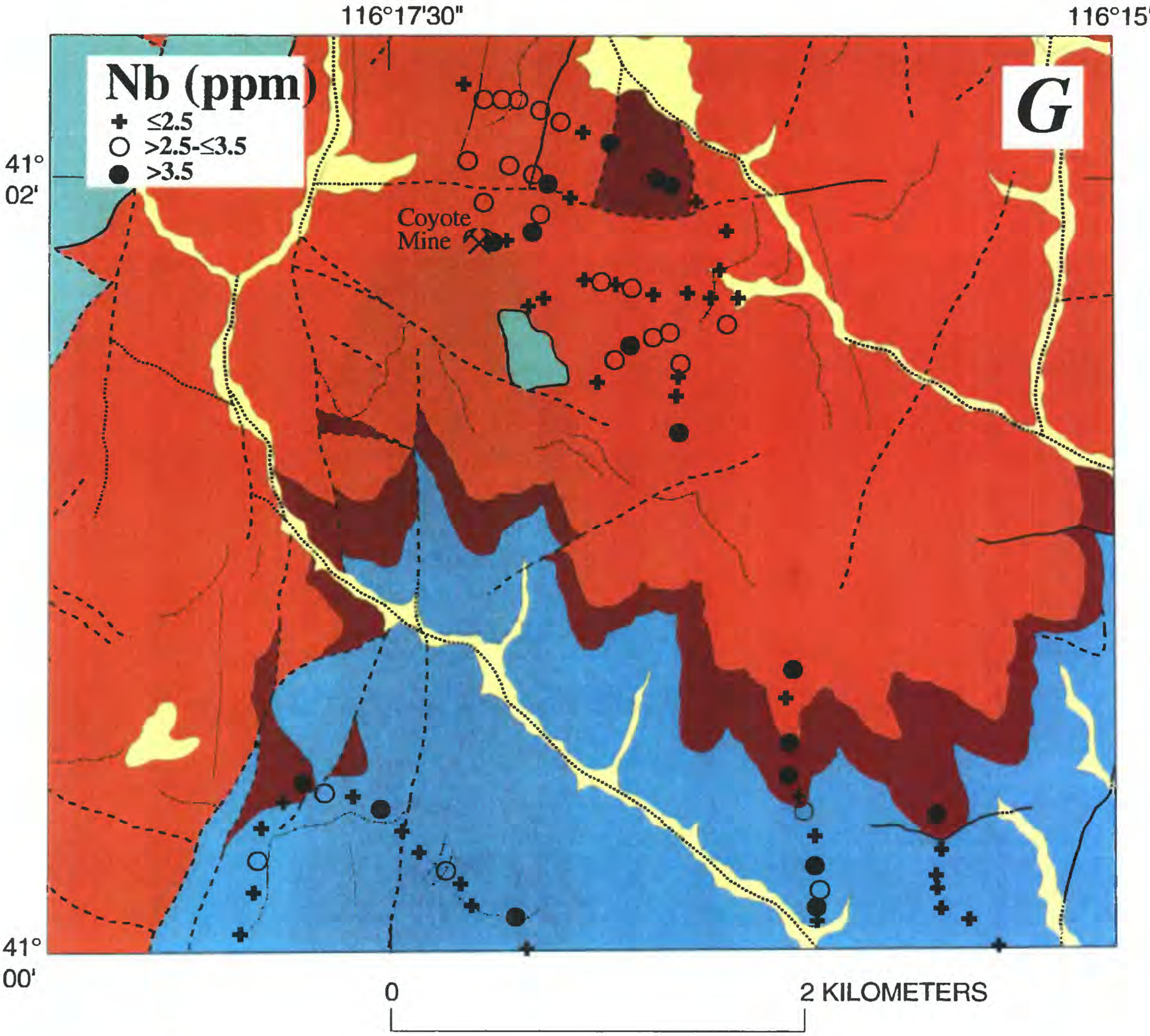

Figure 19—General view of the open pit at the Coyote barite deposit, looking northwest, in the southern part of the Beaver Peak quadrangle, Nev. White dots show locations of four analyzed samples (99-TT-124; 99-TT-189 to -191). White dashed line indicates approximate front boundary of the barite lode.

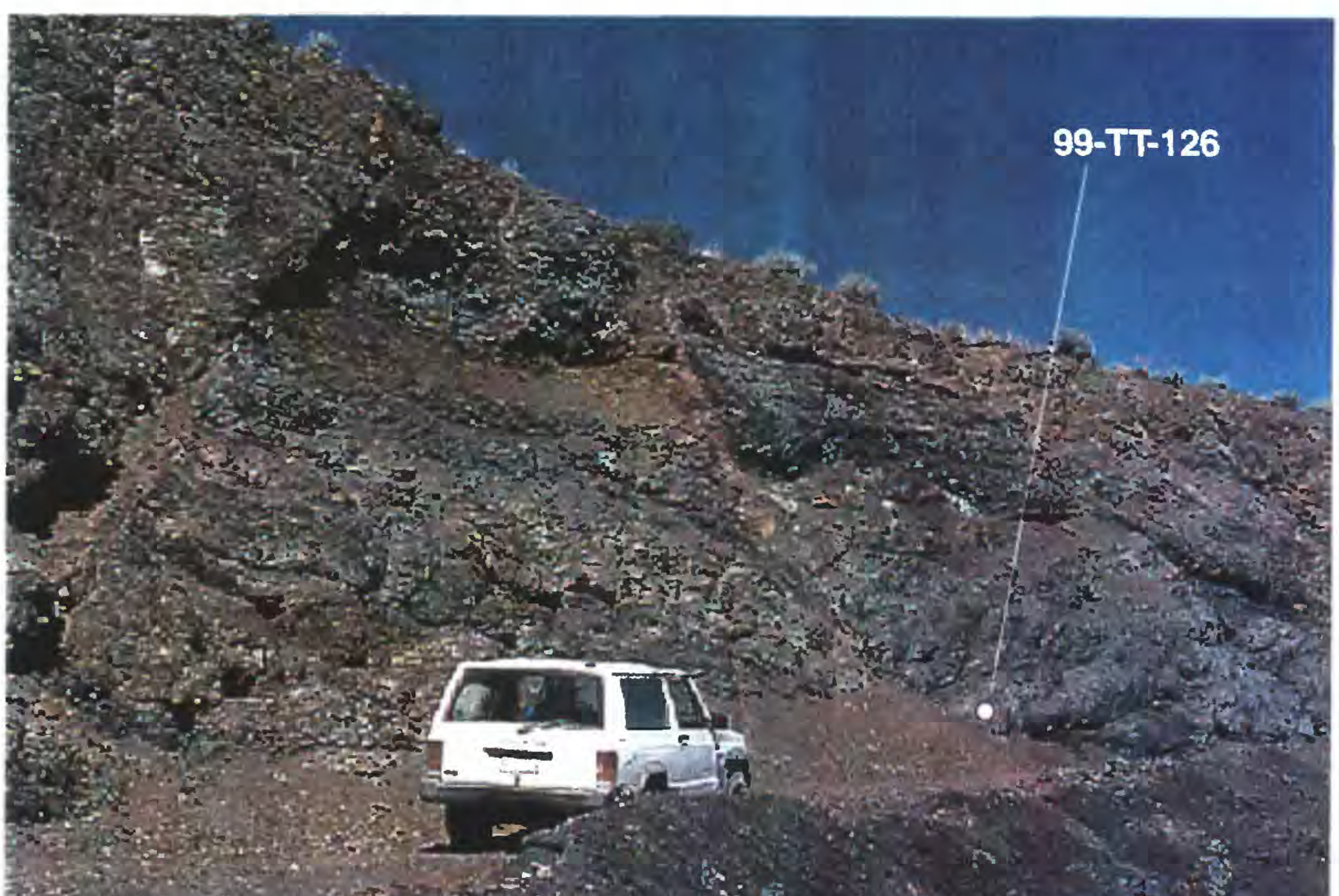

Figure 20—Structure of the upper bench of the Coyote open pit, looking west-northwest, detail of part of figure 21, southern part of the Beaver Peak quadrangle, Nev. White dot shows location of sample 99-TT-126.

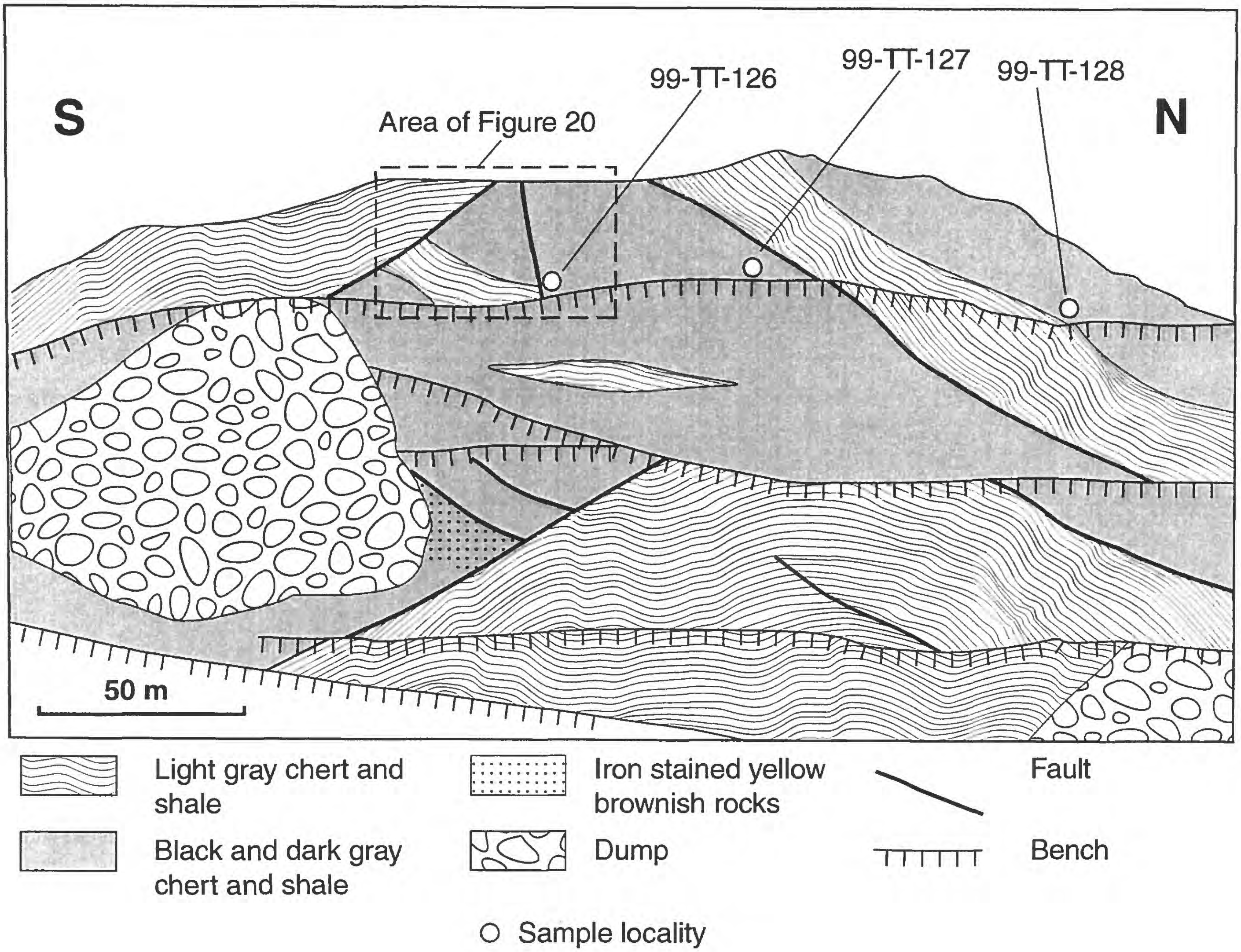

Figure 21—Southern part of the open pit at the Coyote barite deposit, looking west, in the southeast part of the Beaver Peak quadrangle, Nev. White dots show locations of three analyzed samples (99-TT-126 to -128).

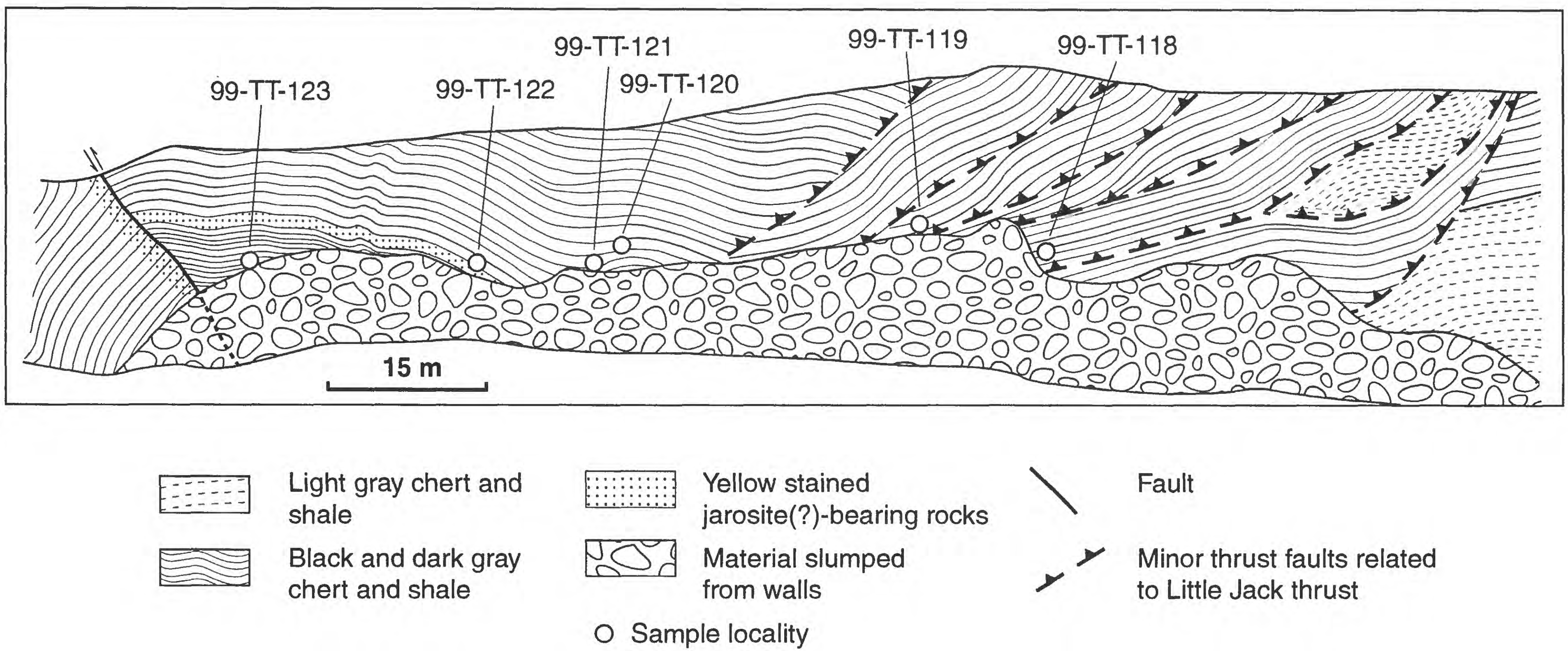

Figure 22—View around perimeter of the northern end of lowermost bench of open pit at the Coyote barite deposit, looking north, in the southern part of the Beaver Peak quadrangle, Nev. White dots show locations of six analyzed samples (sample nos. 99-TT-118 to -123, table 2).

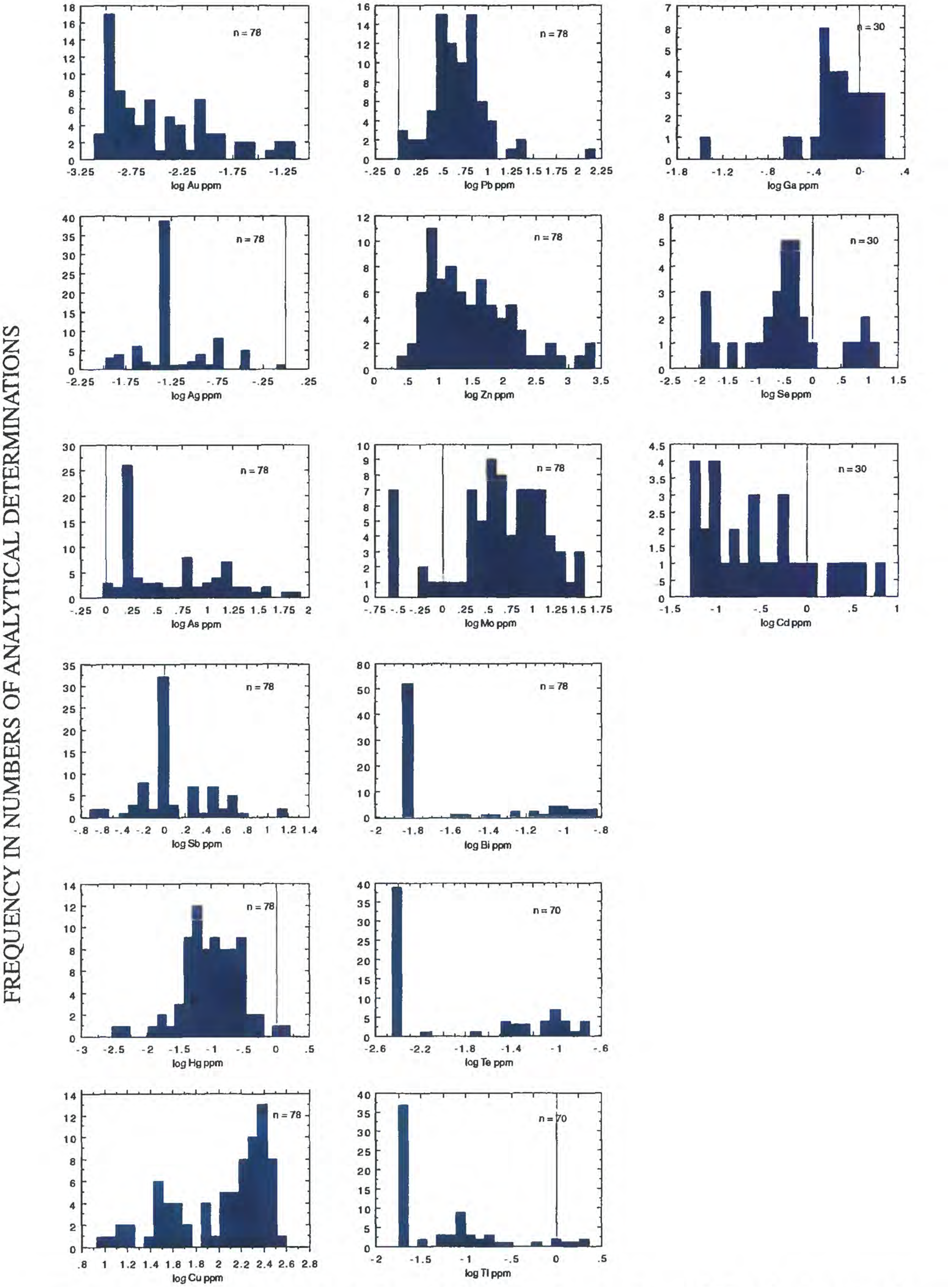

Figure 23—Log-frequency distribution of 15 elements from analyses of 78 rocks that comprise sample Group 3 (see text) near Boulder Creek in the Beaver Peak quadrangle, Nev. All analyses by partial digestion techniques; n, number of analytical determinations.

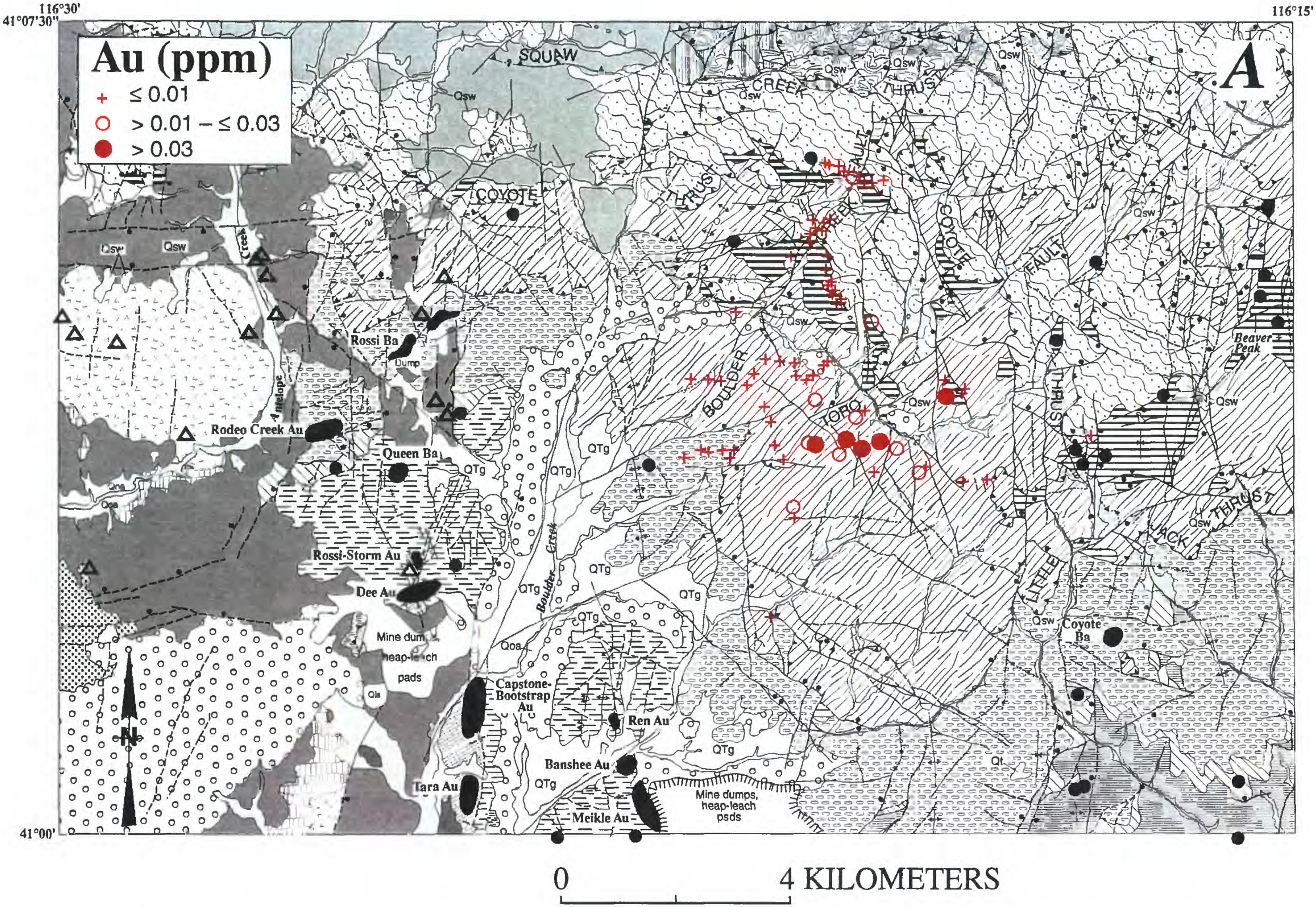

Figure 24—Geologic sketch map of the Santa Renia Fields and Beaver Peak 7–1/2 minute quadrangles, Nev., showing element concentrations in Group 3 samples (see text). Geology modified from figure 2. ***A***, Au; ***B***, Ag; ***C***, As; ***D***, Sb; ***E***, Hg; ***F***, Cu; ***G***, Pb; ***H***, Zn; ***I***, Mo; ***J***, Bi.

Figure 24—cont'd.

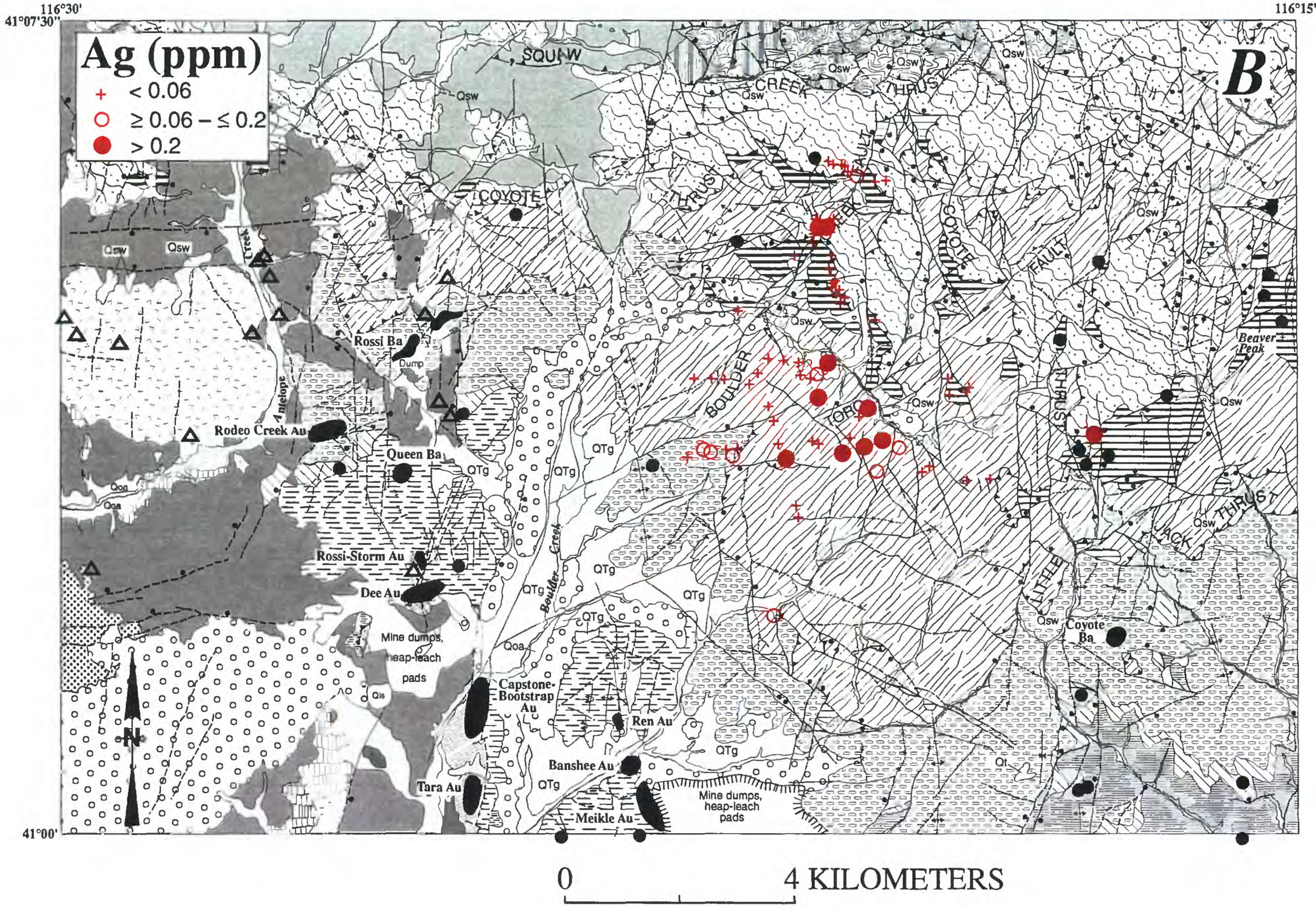

Figure 24—cont'd.

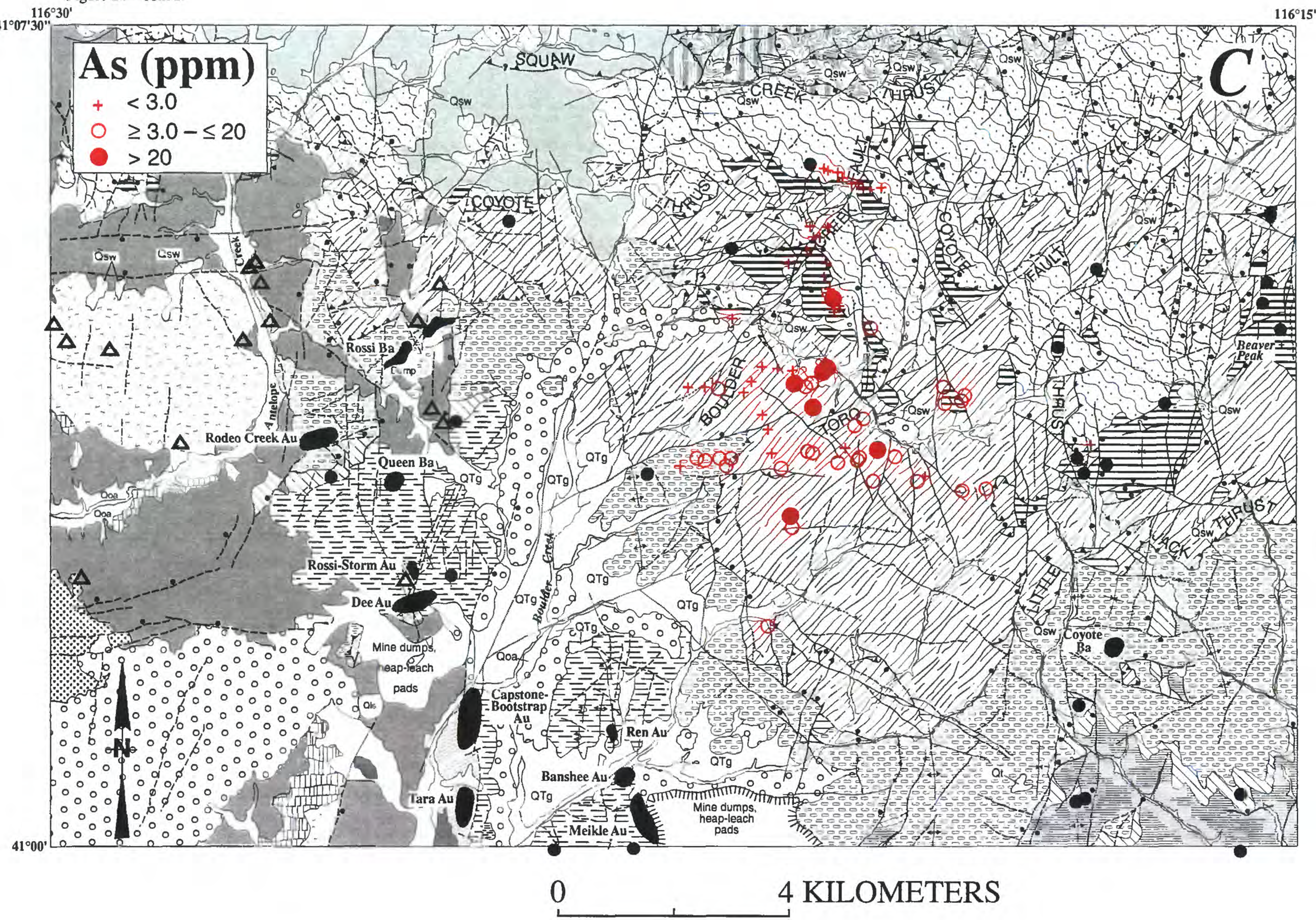

Figure 24—cont'd.

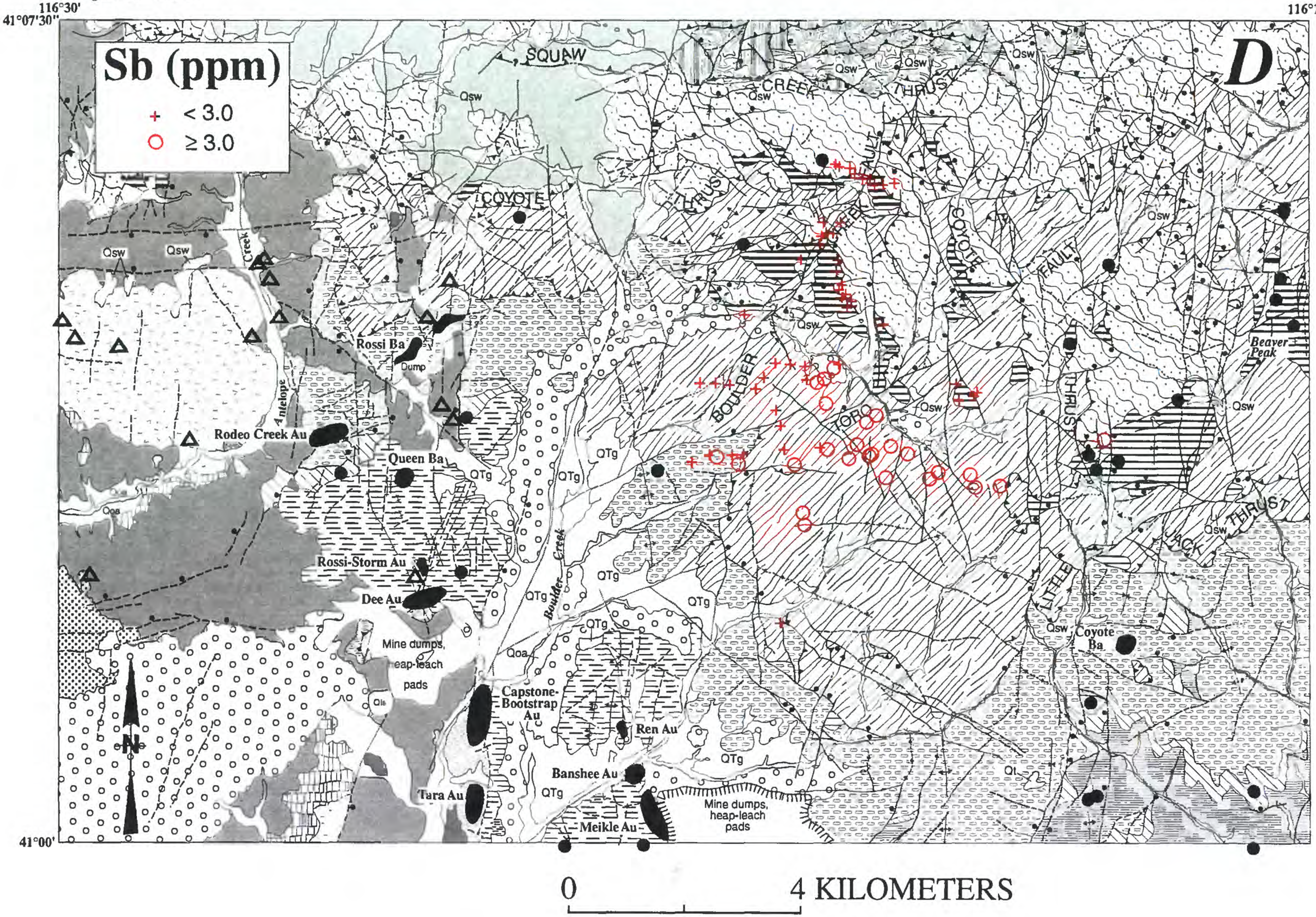

Figure 24—cont'd.

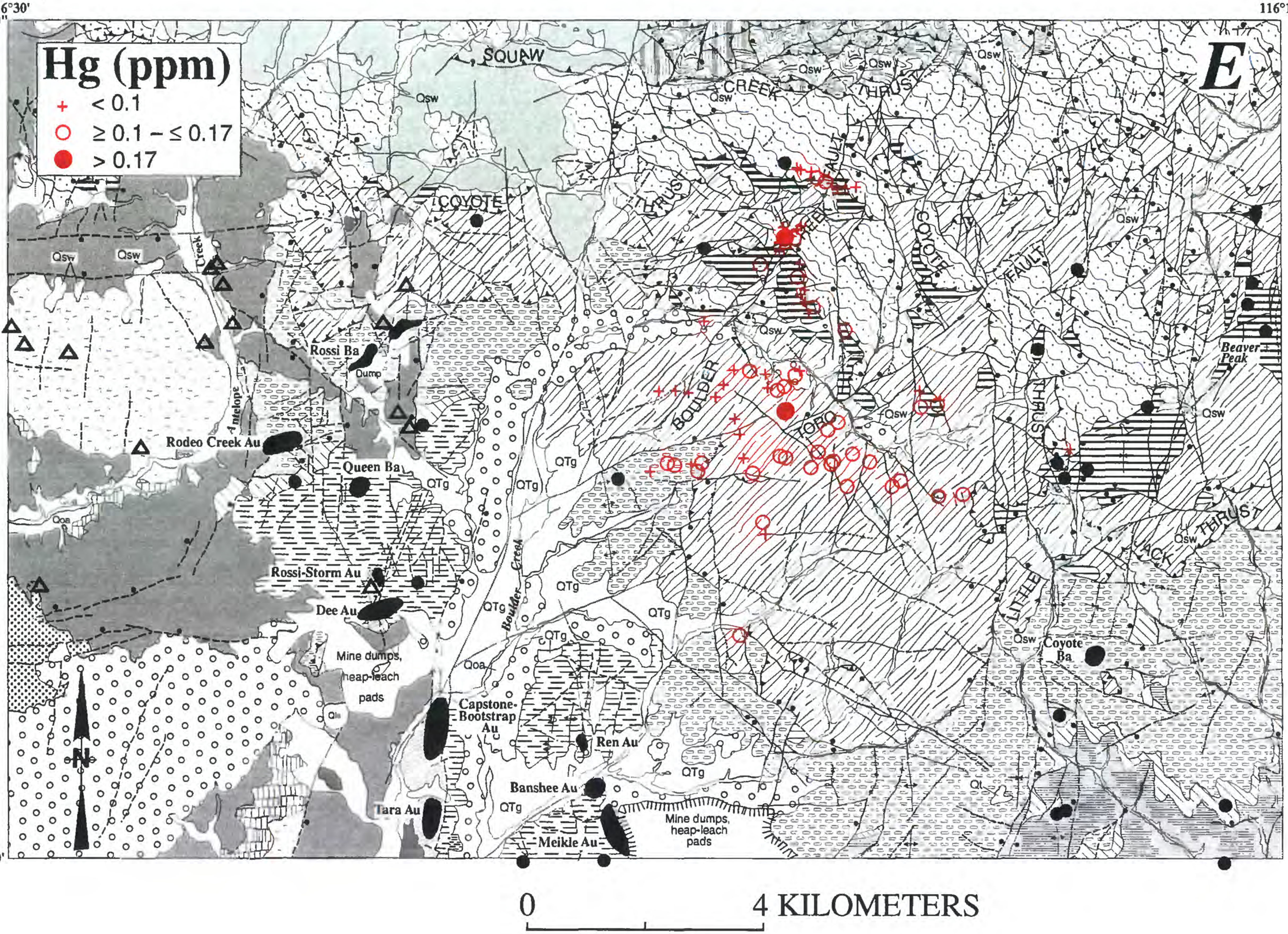

Figure 24—cont'd.

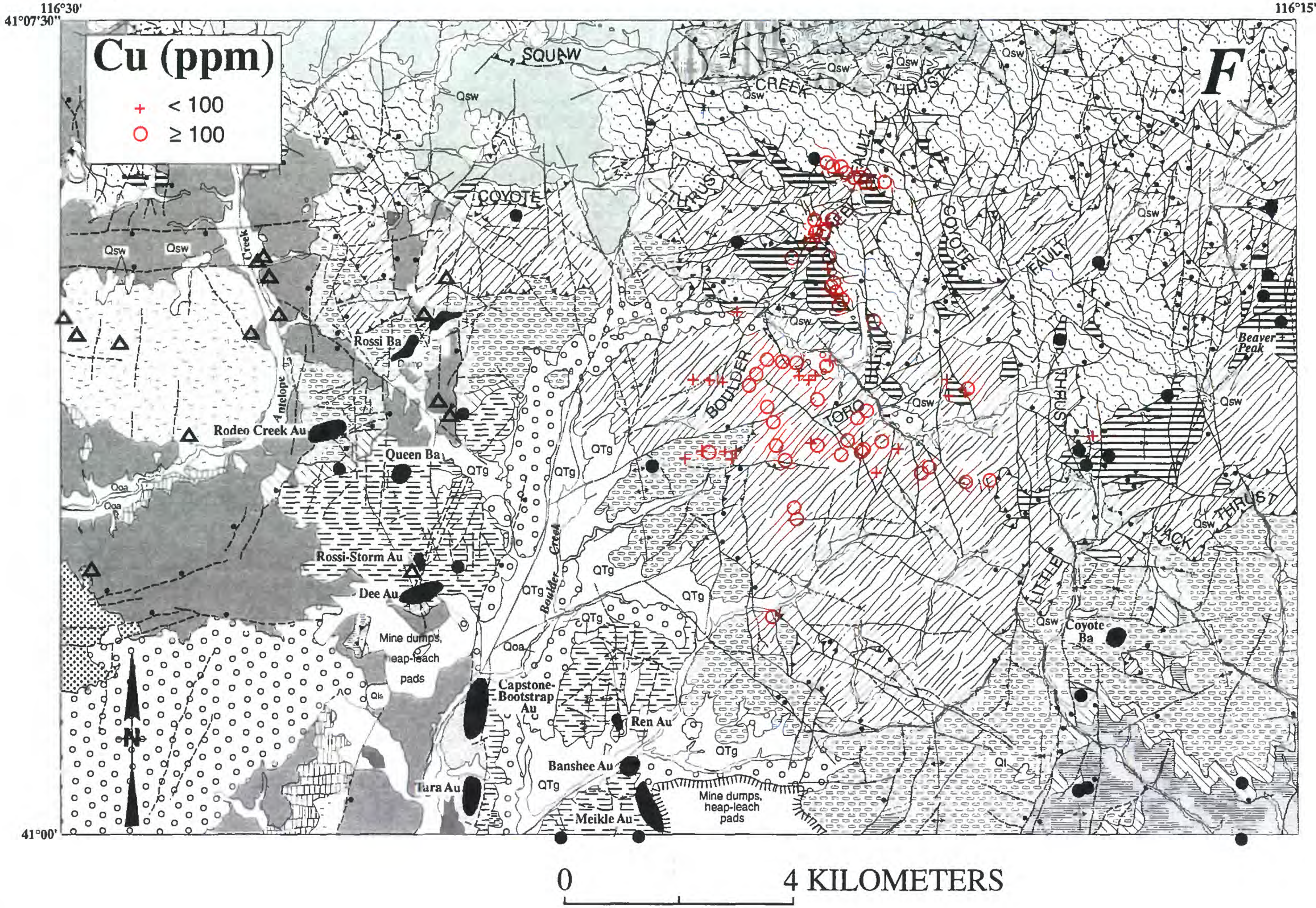

Figure 24—cont'd.

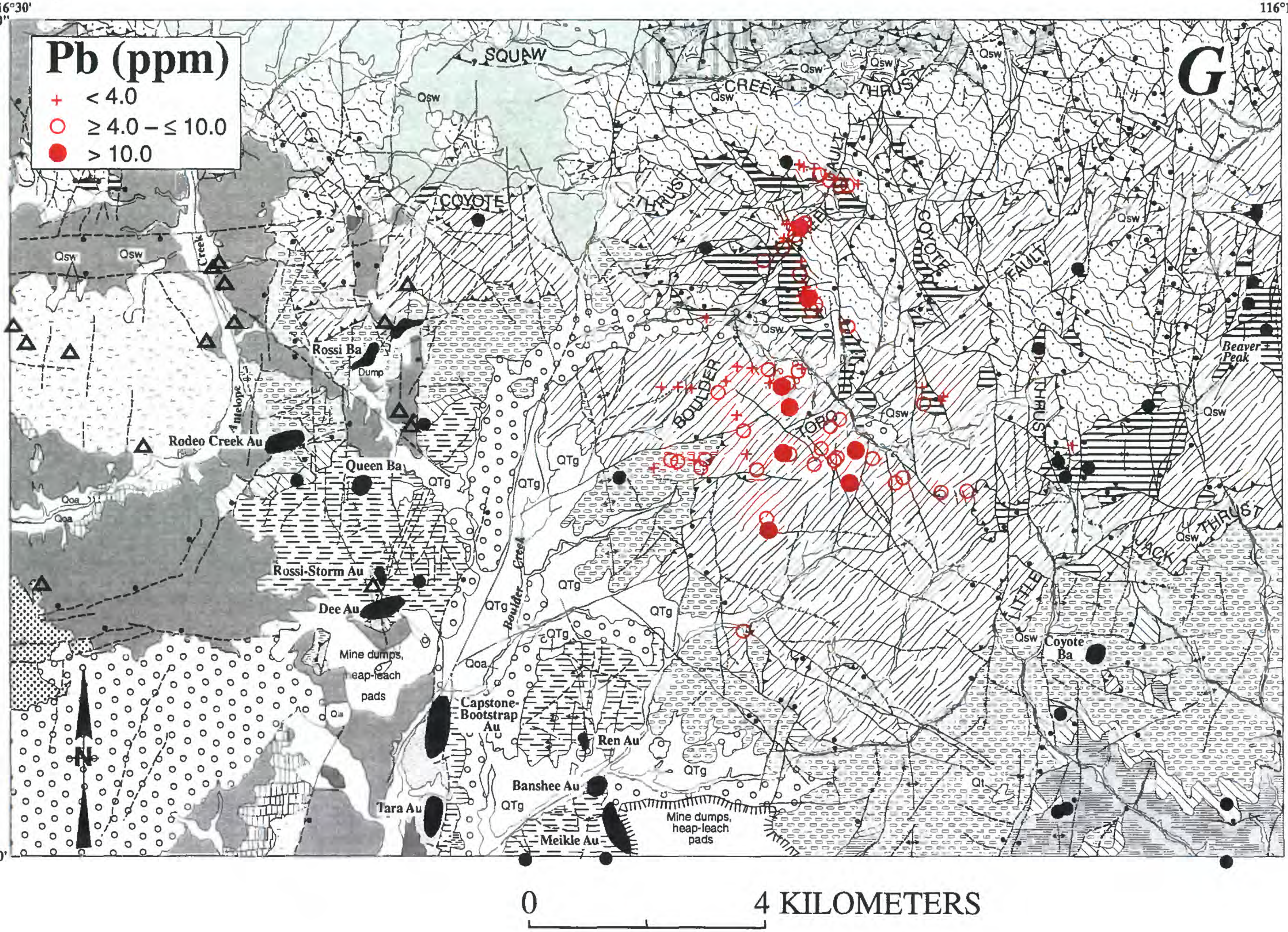

Figure 24—cont'd.

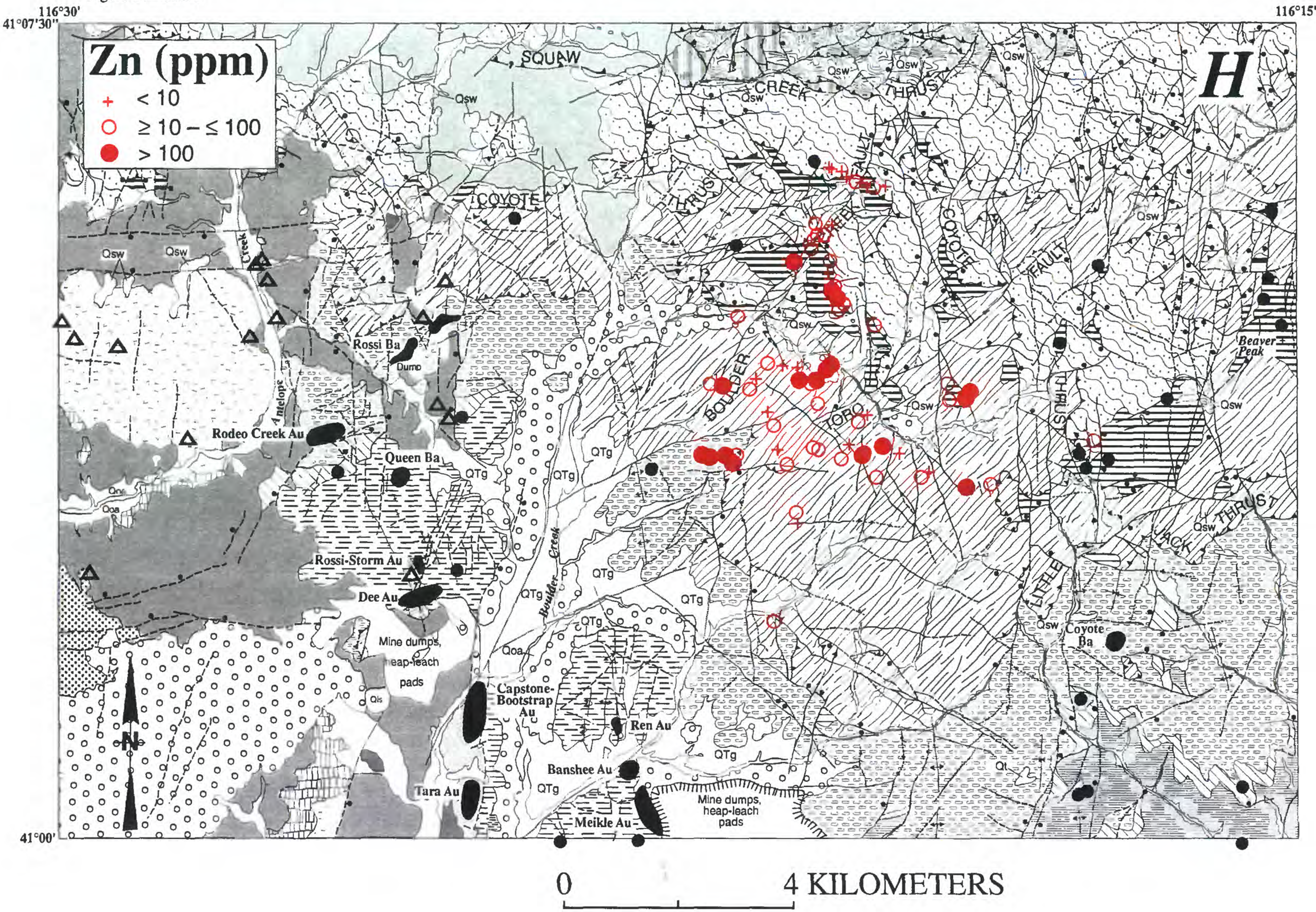

Figure 24—cont'd.

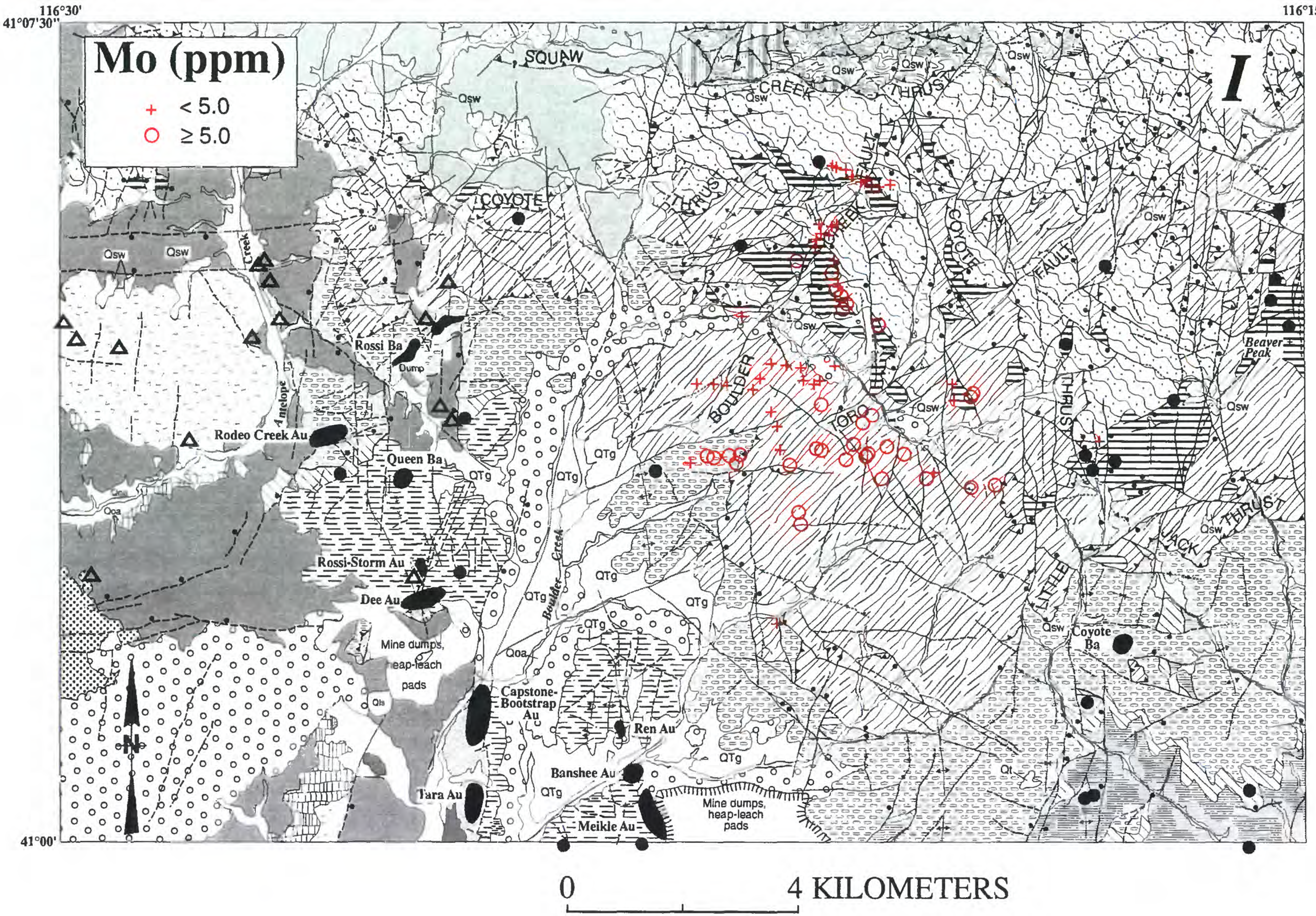

Figure 24—cont'd.